THEORETICAL AND EXPERIMENTAL STUDY OF INTERNAL AND ANNULAR FLOW INDUCED INSTABILITIES OF CYLINDRICAL SHELLS

By

ABDALLAH EL CHEBAIR

Department of Mechanical Engineering
McGill University
Montreal, Quebec, Canada

Under the supervision of
Dr. M.P. Paidoussis and Dr. A.K. Misra

Submitted to the Faculty of Graduate Studies
and Research of McGill University
in partial fulfillment of the requirements
for the degree of
Doctor of Philosophy

ISBN 0-315-48492-6

ABSTRACT

This Thesis investigates theoretically and experimentally the dynamical behaviour and the stability of a cylindrical shell coaxially located in a rigid cylindrical pipe and subjected to internal or annular flow.

In the theoretical study, the fluid flow in the inner shell and the annulus is assumed to be viscous and incompressible. The fluid forces consist of two parts: (i) steady viscous forces representing the effects of upstream pressurization of the flow (to overcome frictional pressure drop) and skin friction on the shell surface, which are determined using turbulent fully-developed boundary layer theory; (ii) unsteady viscous forces which are derived by means of linearized Navier-Stokes equations. Shell motions are described by a modification of Flugge's shell equations. Two methods of solution are employed to formulate the problem:

1. Fourier transform technique;
2. travelling wave solution.

In the first method, the shell could be clamped or pinned at both ends; while in the second method, the shell is simply supported at both ends. The objectives are to investigate the effects of unsteady viscous forces on the dynamical behaviour and stability of the system in the presence and absence of steady forces.

Calculations have been conducted with a steel shell conveying water with different gap-to-radius ratios $g/a_1 = 1/10$ and $1/100$.

First, the system is subjected to unsteady viscous forces only. The results are compared to those of inviscid theory. It is found that, for internal flow and annular flow with large g/a_i, the effects of viscosity on the stability of the system are insignificant; however, for the smaller gap ($g/a_i = 1/100$), those effects are more pronounced, rendering the system more stable. When both steady and unsteady viscous forces are applied, the results are quite different from the previous case. For internal flow, the system becomes more stable; while for annular flow, the system loses stability at much lower velocities for both gap-systems. In the annular flow case, the loss of stability depends only on the steady viscous forces for the parameters considered. The unsteady forces affect only the frequency of the system before it becomes unstable.

In the experimental study, the flow is only annular and the fluid is air. The flexible shell is made of silicone rubber and the outer cylinder is made of plexiglas. The shell could be clamped at both ends or clamped at one end and free at the other. For the clamped-clamped shell, the system loses stability by divergence (buckling) as predicted by linear theory. However, coupled-mode flutter was never observed experimentally. Clamped-free shells, on the other hand, lose stability by flutter.

SOMMAIRE

Cette thèse presente une étude théorique et expérimentale de la dynamique et de la stabilité d'une coque cylindrique localisée d'une façon coaxial dans un cylindre rigide et soumise à un écoulement interne ou annulaire.

Dans l'étude théorique, l'écoulement de fluide à l'interieur de la coque ou dans l'espace annulaire est considéré visqueux et incompressible. Les forces du fluide consistent en deux parties: (i) les forces visqueuses stationnaires representant les effets de pressurisation de fluide nécessaire pour compenser les pertes de charge, ainsi que la force de frottement pariétal; (ii) les forces visqueuses instationnaires étant basées sur la théorie linearisée des équations de Navier-Stokes. Les déplacements de la coque sont décrits par les équations modifiées des coques minces de Flugge. Deux méthodes de solution sont utilisées pour formuler le problème:

1. technique de transformation de Fourier
2. solution avec des ondes mobiles.

Dans la première méthode, la coque peut être encastrée ou simplement supportée aux deux extrémités; tandis que dans l'autre méthode, la coque est simplement supportée aux deux extrémités.

L'objectif est d'examiner les effets de forces visqueuses instationnaires sur le comportement dynamique et la stabilité du système dans la présence ou l'absence des forces permanentes.

Les calculs sont effectués pour une coque d'acier soumise à un écoulement d'eau avec différents rapports d'espace annulaire par rayon au rayon g/a_i = 1/10 et 1/100.

Premièrement, le système est soumi aux forces visqueuses instationnaires seules. On trouve que, pour l'écoulement interne et annulaire et pour $g/a_i = 1/10$, les effets de la viscosité du fluide sur la stabilité du système sont négligeables. Pourtant, pour le petit espacement de $g/a_i = 1/100$, ces effets sont plus prononcés, rendant le système plus stable. Lorsque les deux forces visqueuses stationnaires et instationnaires sont appliquées, les résultats sont tout à fait differents du cas précédent. Pour l'écoulement interne, le système devient plus stable; tandis que pour l'écoulement annulaire, le système perd sa stabilité à des vitesses moins élevées que celles du cas précédent. Dans l'écoulement annulaire, la perte de stabilité depend uniquement des forces visqueuses stationnaires. Les forces visqueuses instationnaires influent seulement les fréquences du système avant qu'il devienne instable.

Dans l'étude expérimentale, l'écoulement est seulement annulaire et l'air est utilisé comme fluide. La coque est faite de caoutchouc et le cylindre rigide est fait de plastique. La coque peut être encastrée aux deux extrémités ou encastrée à une extrémité et libre à l'autre. Pour la coque encastrée aux deux extrémités, le système perd sa stabilité par flambage comme prédit par la théorie linéarisée. Cependant, l'instabilité oscillatoire (flottement) en modes conjugués n'a jamais été observée expérimentalement. Pour la coque encastrée à une extrémité et libre à l'autre, le système perd sa stabilité par flottement.

ACKNOWLEDGEMENTS

The author would like to express his appreciation for the help and encouragement of Professors M.P. Paidoussis and A.K. Misra throughout the course of this work.

Many thanks are also given to Mary Fiorilli for her patience and her excellent typing job.

TABLE OF CONTENTS

NOMENCLATURE

(r,θ,x)	Cylindrical coordinates

ORDINARY SYMBOLS

a_i	Inner shell radius
a_o	Inner radius of the outer rigid cylinder
D_h	Hydraulic diameter
E	Young's modulus of elasticity
f_i	Friction factor for the internal flow
f_o	Friction factor for the annular flow
h	Shell thickness
k_s	$h^2/12a_i^2$
k	Axial wave number.(travelling wave solution)
L	Length of the flexible portion of the shell
m	Axial mode number (Fourier transform method)
n	Circumferential mode number
P	Steady fluid pressure
p'	Unsteady fluid pressure
p	Total pressure
q_1, q_2 and q_3	Steady viscous forces
q_x, q_θ and q_r	Unsteady viscous forces in the (x,θ,r) directions
r_m	Radius of maximum velocity for the annular flow
Re	Reynolds number
t	Time
U_i	Steady internal flow

U_o	Steady annular flow
U_{avi}	Averaged velocity for internal flow
U_{avo}	Averaged velocity for annular flow
$U_{\delta i}$	Steady internal flow velocity at δ
$U_{\delta o}$	Steady annular flow velocity at δ
$\bar{V}$	Velocity vector
V_x, V_θ, V_r	Components of the velocity in the (x,θ,r) directions
$u, v, w,$	Shell displacement in the (x,θ,r) directions

GREEK LETTERS

α	Fourier transform variable
β	$(\frac{i\omega}{\upsilon} - k^2)^{1/2}$ for travelling wave solution $(\frac{i\omega}{\upsilon} - \alpha^2)^{1/2}$ for Fourier transform method
ϵ_i	a_i/L
ϵ_o	a_o/L
ϵ_r	a_o/a_i
ζ	x/L
η	$\dfrac{\rho_i a_i}{\rho_s h}$
u	$\text{u} = \left[\dfrac{E}{\rho_s(1-\upsilon_s^2)}\right]^{1/2}$
Λ	$\dfrac{Eh}{(1-\upsilon_s^2)}$
μ_i	Dynamic viscosity of internal fluid
μ_o	Dynamic viscosity of annular fluid

ν_i	Kinematic viscosity for inner fluid
ν_o	Kinematic viscosity for annular fluid
ν_s	Poisson's ratio of the shell
ξ_i	$\frac{UL}{\nu_i}$
ξ_o	$\frac{UL}{\nu_o}$
ξ_r	$\frac{\xi_o}{\xi_i}$
ρ_i	Density of internal fluid
ρ_o	Density of annular fluid
ϕ	Velocity potential of flow perturbation
ψ	Velocity perturbation vector
Ω	Circular frequency of motion (rad/s)

CHAPTER I

INTRODUCTION

The dynamical behaviour and stability of cylindrical structures subjected to, or containing flowing fluid have been studied quite extensively. Interest in this field started with the observation of bending vibrations of the Trans-Arabian pipeline, in the early 1950's (see Ashley and Haviland [1]). For the last three decades, however, research into the dynamics of pipes and shells containing flowing fluid has been given additional attention due to the development of nuclear power plants. Historical reviews may be found in references [2-4].

In presenting the bibliography, three types of flow are considered: internal, external and annular. For each case, the stability of beam-type cylinders is considered first, followed by the stability of shells.

1.1 INTERNAL FLOW

The stability of a straight pipe with simply-supported ends conveying fluid was first investigated by Feodos'ev [5], Housner [6] and Niordson [7]. Using different methods, they arrived at the same conclusion: the system's natural frequencies are reduced as the flow velocity is increased. However, at sufficiently high flow velocities, the system is subjected to buckling (divergence), in which the tube buckles essentially like a column subject to compressive axial loading.

In a more general work, Paidoussis and Issid [8,9] studied the dynamical behaviour of pipes conveying fluid with both ends supported - either pinned or clamped. They reported that according to linear theory, the system is not only subject to divergence (buckling) but also to coupled-mode flutter at higher flow velocities. In physical terms, this is expected to be so, because the system is conservative gyroscopic and the presence of Coriolis terms could in fact cause coupled-mode flutter instabilities [10]. However, by nonlinear analysis, Holmes [11] showed that a pipe supported at both ends cannot flutter.

The theoretical predictions for buckling have been confirmed experimentally by Naguleswaran and Williams [12], Liu and Mote [13] and, more recently, by Jendrzejczyk and Chen [14]. However, coupled-mode flutter has never been observed experimentally.

The stability of a cantilevered tube conveying fluid was first studied by Benjamin [15,16]. He considered the case of articulated tubes conveying fluid, and found that cantilevered tubes develop oscillatory instability (flutter) due to their non-conservative nature. These findings were later confirmed both theoretically and experimentally by Gregory and Paidoussis [17,18].

In the research described so far, the cylinder was considered as a beam, and only the oscillation in the flexural beam modes was studied. However, the instabilities associated with very thin pipes conveying fluid are more of the shell-type, rather than the beam-type. Paidoussis and Denise [19,20], were the first to observe this phenomenon while experimenting with thin cantilevered tubes conveying air. They demonstrated that, if the cantilever is sufficiently short (so that it remains stable with respect to the flexural instability to fairly high flow), a shell-type instability occurs spontaneously above a certain critical flow velocity: the cantilever vibrates in the second circumferential mode of a circular cylindrical shell ($n = 2$).

The subject was studied theoretically and experimentally [20], both for clamped-clamped and cantilevered shells. The theoretical model described shell motions by means of Flugge's equations, and the fluid forces were obtained by linearized potential flow theory. The same types of instabilities described in the beam theory for thicker pipes still hold for the shell theory; except that they are of course associated with shell modes, as mentioned earlier. Thus, for a shell supported at both ends, the system loses stability first by divergence, followed by coupled-mode flutter. It is important to mention that, in contrast to the pipe problem, only flutter was observed experimentally.

In the case of a cantilevered shell, both theory and experiment showed that, the system is only subject to single-mode flutter.

The topic was later studied by Weaver and Unny [21] and Shayo and Ellen [22], in the case of simply supported shells, and by Weaver and Myklatun [23], in the case of clamped-clamped shells. They have all found the same type of instabilities described earlier [20]. The problem was also studied by Pham and Misra [24], with special attention to the effect of a superimposed linearly varying or constant axial loading on the shell.

The fluidelastic instabilities referred to above rarely materialize in practice, because the critical flow velocities associated with the instabilities are extremely high and seldom encountered. Nevertheless, this work has found physiological applications in the study of flutter and collapse of respiratory passages [25-27].

1.2 EXTERNAL FLOW

As in the case of internal flow, extensive research has been done on the dynamics of cylindrical structures subjected to external axial flow. Paidoussis [28-29] was the first to study the dynamical behaviour of flexible cylinders in an axial flow. Using the slender-body approximation, he showed that, cylinders with both ends supported lose stability by divergence and, at higher flow velocities, by coupled mode flutter.

In a separate work, Paidoussis [30] showed that if the flow about the cylinder is confined, by a conduit or by adjacent structures, then the instabilities occur at lower flow velocities due to the increase in the virtual mass. The effect of slenderness of the cylinder and compressibility of the fluid was later studied by Paidoussis and Ostoja-Starzewski [31]. Interestingly, compressibility was found to have an insignificant effect on the stability of the cylinder (for slender cylinders).

Chen [32] was the first to study the dynamics of arrays of parallel cylinders in dense fluid. He showed that the instabilities occur at much lower flow velocities than for a single flexible cylinder. This is so, because of the increase in the virtual mass associated with the fluid-dynamic coupling.

The stability of clusters of cylinders in axial flow and the sequence of instabilities as the flow velocity is increased were examined thoroughly, both theoretically and experimentally by Paidoussis [33]. Theory and experiment were found to be in good agreement, and similar conclusions as in Ref. [32] were obtained.

In parallel to the work on dynamics of cylinders in axial flow, extensive research has been done on the effect of external axial flow on the dynamics and stability of cylindrical shells. Both supersonic and subsonic flows were considered. A review on this topic may be found in a work of Dowell [34]. These studies are applicable in the aeronautical field and, accordingly, they are concerned with flutter in very high speed compressible flow. The dynamical behaviour of the system is similar to that of a shell with internal flow; nevertheless, the two cases cannot be directly compared. Among the numerous outstanding published papers, the work by Dowell and Widnall on the formulation of the generalized aerodynamic forces by means of Fourier transform techniques should be specially noted [35], as this work is adaptable for the problem considered in this Thesis.

1.3 ANNULAR FLOW

So far we have discussed the instabilities associated with internal and external flows. For these types of flows, the velocities at which instabilities occur are very high. Hence, they are of limited practical concern, despite their very considerable fundamental appeal. The case of annular flow is quite different; many failures associated with this type of flow have been reported. A review of Practical Problems is given in Ref. [2].

The case of a rigid cylindrical body, hinged at one point and coaxially positioned in a flow-carrying duct, was studied by Hobson [36]. He showed that, as the flow velocity is increased in the annulus, the negative fluid-dynamic damping overcomes the mechanical damping, which results in oscillatory instabilities in the system. Mateescu and Paidoussis [37] investigated this problem further. In their inviscid analysis, they showed that the position of the hinge affects strongly the stability of the system.

They identified a critical location of the hinge; downstream of that location, the system becomes unstable and the associated flow velocity decreases as the hinge is moved further downstream. Paidoussis and Mateescu extended their theory to take into account viscous effects [38]. It was found that the viscous effects stabilize the system, becoming more important as the annulus becomes narrower.

The dynamical behaviour of coaxial shells with *still* fluid in the annulus has also been studied fairly thoroughly, the main interest in these studies being the coupling of the shells, especially where the annular fluid is a liquid. In such cases the hydrodynamic or added mass, for sufficiently narrow annuli can be several times the mass of the shell, which obviously exerts a strong influence on the eigenfrequencies of the system and results in a very strong coupling. Krajcinovic [39], Au-Yang [40], Brown and Lieb [41] are among those who have studied this problem. In different manners, they reached the same conclusion: that the effect of the added mass is to give a reduction in the natural frequencies of the system.

In all the above studies of coaxial shells, the fluid is assumed to be inviscid. Some studies have taken fluid viscosity into account. Chen, Wambsganss and Jendrzejczyk [42] studied analytically and experimentally the vibration of a cylindrical rod in a viscous fluid enclosed by a rigid concentric shell. They found that, for a fixed rod diameter and kinematic viscosity, both the added mass and damping coefficient increase as the annular gap decreases. Yeh and Chen [43] have developed a remarkable method to take into account the viscosity effect for this type of systems. Particular attention may be given to this work, since it can be adapted for the problem at hand. The system was modeled as two coaxial shells separated by a viscous fluid. Flugge's shell equations of motion and the linearized Navier-Stokes equations for viscous fluid were employed. A travelling-wave type solution was assumed for shell and fluid. The natural frequencies, mode shapes and modal damping ratios of the coupled modes were then calculated. It was found that the effect of fluid viscosity on the system natural frequencies is negligibly small in most practical systems. However, fluid viscosity contributes significantly to the modal damping. For a coupled shell system, the viscous effects are mostly pronounced for the out-of-phase modes than that of the in-phase modes.

Here it should be emphasized that the work discussed in the foregoing on coaxial shells [39-43] involved quiescent fluid in the annulus.

The problem of shells containing swirling annular flow has been studied extensively [44], because of its application to aircraft engines. In contrast, the study of the dynamics and stability of cylindrical structures subjected to straight annular flow has only recently begun. Chen [45] studied the dynamics of a rod-shell system conveying fluid. He showed that the natural frequencies and critical flow velocity of the coupled rod-fluid-shell are smaller than those of an isolated rod subjected to axial flow.

Recently the stability of shells subjected to straight annular flow has been studied [46-48]. A historical literature review may be found in Ref. [47]. It is found that, in general, for reasonably narrow annuli, a shell subjected to a straight annular flow, which is the topic of the present work, loses stability at much lower flow velocities than when it is subjected to internal flow [47] — an effect which becomes even more pronounced when the annulus is made up of two coaxial shells, instead of having a rigid outer containment pipe. The instabilities predicted were similar to those of shells with internal flow: divergence (buckling), followed by coupled-mode flutter.

Weppelink [46] formulated the problem of two coaxial cylinders, only the inner one of which is flexible (cantilevered or clamped-clamped), conveying incompressible fluid inside the shell and in the annulus; shell motions were described by the Morley - Koiter shell equation, and the fluid forces were determined by linearized potential flow theory.

Paidoussis, Misra and Chan [47,48] also conducted a study on this topic. They considered the case of two coaxial shells. At first they neglected the viscous fluid effects [47]. The inviscid terms in the equations were derived from potential flow theory and the aerodynamic forces were formulated using an integral transform technique. Shell motion was described by Flugge's equations. The rationale for neglecting viscous effects was that they would principally induce steady-state, time-mean axial and radial loads, the effects of which are qualitatively well known. Incidentally, this argument is precisely valid for tubular beams conveying fluid; as shown by Benjamin [15,16] for fully developed turbulent flow, the viscous effects are negligible in the following sense: the terms in the equation of motion arising from pressure drop in the fluid are completely cancelled out by those produced by surface traction forces on the beam due to fluid friction, so that the analysis may be conducted as if the fluid were effectively inviscid. However, this is not true for cylindrical shells.

For this reason, Paidoussis, Misra and Chan [48] extended their inviscid theory to include the viscous effects. They only took into account the steady time-dependent viscous terms and neglected the unsteady ones. Flugge's shell equations had to be modified to incorporate the stresses and strains caused by the viscous forces. The flow was assumed to be fully developed and the viscous forces were derived based on a work by Laufer [49]. It was found that among the steady viscous terms, the dominant one is associated with the pressurization of the upstream end of the annulus (or, equivalently depressurization of the downstream end) to overcome frictional pressure drop; depending on the internal pressure in the inner shell, pressurization can have a strong effect on stability as compared to inviscid theory.

In contrast to the unsteady forces in the inviscid theory, the effect of unsteady viscous forces in axial flow have not been given attention. One reason for this could be the complexity of the problem (cf. Ref. [38]), in particular the handling of the boundary condition at a moving wall.

To the author's knowledge, the effects of both steady and unsteady viscous forces together, on the stability of coaxial shells subjected to flow in the annulus have never been studied. Similarly, the effect of annular flow on cylindrical shells has never been experimentally investigated.

1.4 OBJECTIVES

This Thesis presents a theoretical and an experimental investigation of the effects of axial flow on a cylindrical shell coaxially located within a cylindrical rigid pipe. In the theory, the flow could be internal or annular and the effects of the steady and unsteady viscous forces are investigated. For the experiment, the flow is only annular.

The unsteady aerodynamic or hydrodynamic forces are formulated using two different methods:

(i) the first one is based on an integral Transform technique [47]. This method is very costly in computation; since the aerodynamic forces are frequency-dependent, an iteration method is needed to study the stability and the integration has to be performed for each frequency;

(ii) the second method is based on a travelling-wave type solution, and is more practical for the cases considered, with the computation cost reduced enormously.

In the first method, the shell is assumed to be clamped or pinned at both ends to identical but rigid cylinders of infinite length. In the second method, the shell is essentially of infinite length, with periodic supports at intervals equal to the length of the shell being considered; the supports are of the pinned type. The flow is assumed to be turbulent and fully developed. The steady viscous forces are taken into account in both methods.

The structure of this Thesis is as follows. In Chapter II, ~~the~~ problem is formulated. The shell motion is described by the modified Flugge equations derived in Ref. [48]. The unsteady viscous forces are derived from the Navier-Stokes equations. They are linearized with the aid of the assumption of small perturbations.

In Chapter III, the derivation of the first method of solution is completed. Galerkin's technique is employed in the solution of the equations of motion, and the integral transform technique is used for obtaining the generalized fluid forces.

In Chapter IV, the derivation of the second method is completed. The travelling wave method is employed in the solution of the equations of motion, and in obtaining the generalized fluid forces. The derivation of inviscid theory using the travelling-wave method is incorporated in this Chapter to facilitate the comparison between viscous and inviscid theory.

In Chapter V, the theoretical results obtained for the clamped-clamped and pinned-pinned shells are discussed and compared with those from the inviscid theory.

In Chapter VI, the experimental apparatus and measurement techniques are discussed, and in Chapter VII the experimental results are compared with the theoretical ones.

Finally in Chapter VIII, the conclusions are given, along with some suggestions for further work.

CHAPTER II

FORMULATION OF THE PROBLEM

2.1 DESCRIPTION OF THE SYSTEM

The system consists of a flexible cylindrical shell of length L, coaxially located in a rigid cylindrical pipe (Fig. 1). The shell is assumed to be thin, elastic and isotropic. The geometric configuration and the material properties of the system are denoted by: shell radius a_i, shell thickness h, shell length L, Young's modulus of elasticity of the shell E, density of the shell ρ_s, Poisson's ratio ν_s and inner radius of the outer rigid cylinder a_o.

The displacements of the middle surface of the shell, with respect to its undeformed position, are represented by the cylindrical coordinates (x,θ,r). The x-axis coincides with the common axis of the shell and the outer cylinder. The displacements are denoted by $u(x,\theta,t)$, $v(x,\theta,t)$ and $w(x,\theta,t)$ in the axial, circumferential and radial directions, respectively. The displacements are assumed to be sufficiently small, so that linear shell theory can be applied in this study.

In deriving the unsteady forces, two methods of solution are considered: (i) a Fourier transform technique, and (ii) a travelling wave-type solution. In the first method, the shell is assumed to be clamped or simply-supported at both ends, while for the second method only a simply-supported case is considered. Also, for the Fourier transform method, the shell is assumed to be connected at either end to semi-infinite rigid tubes of the same radii and wall thicknesses, so that the perturbations originating in the flexible shell could be considered to vanish at the "inlet" and "outlet" of the rigid cylinders — for analytical convenience.

The system could be subjected to inner and annular axial flow. The fluid is assumed to be incompressible, and the flow is fully-developed turbulent. The flow velocities are denoted by U_i and U_o. The two fluids, generally considered to be different, have densities ρ_i and ρ_o, and dynamic viscosities μ_i and μ_o; the subscripts i and o refer to internal and annular flow, respectively.

The fluid forces exerted on the system are of two types:

(i) Steady viscous forces as derived in Ref. [48], for instance. They consist of the static pressure required to drive the viscous fluid through the cylinders and the surface frictional force in the axial direction. The steady viscous forces are called basic loads and are responsible for pre-stressing the shell. They will induce the basic stresses which also ~~determine~~ the steady deformation of the shell due to the mean flow.

(ii) Unsteady viscous forces which consist of the time-dependent fluid forces. These forces are viewed as additional loads. The unsteady forces produce the additional stresses and the additional displacements. The derivation of these forces and the study of their effects on the stability of the system represent a major part of this Thesis.

2.2 EQUATIONS OF MOTION

The equilibrium of the shell, subject to the total stress system, has been derived in Ref. [48]. The shell was assumed to be pre-stressed by the following basic loads:

(i) a constant axial force per unit area

$$\bar{P}_x = B_f; \qquad (2.1)$$

7

(ii) an axially symmetric normal pressure

$$\bar{P}_r = -(C_f x + D_f) \tag{2.2}$$

In these relationships B_f, C_f and D_f are related to the pressure drop of the viscous fluid as it flows in the inner shell or in the annulus.

The associated axial and hoop stress resultants were shown [48] to be

$$\bar{N}_x = B_f(\frac{1}{2} L - x) - \upsilon_s a_i (\frac{1}{2} LC_f + D_f), \tag{2.3}$$

$$\bar{N}_\theta = -a_i (C_f x + D_f). \tag{2.4}$$

In addition to these stress resultants, there are the stresses associated with shell deformations, which are coupled to the unsteady viscous perturbations. The dynamic equilibrium of the shell, subject to the total stress system is governed by the following equations of motion:

$$u'' + \frac{1-\upsilon_s}{2} u^{\circ\circ} + \frac{1+\upsilon_s}{2} v'^{\circ} + \upsilon_s w' + k_s \left[\frac{1-\upsilon_s}{2} u^{\circ\circ} - w''' + \frac{1-\upsilon_s}{2} w'^{\circ\circ} \right] + q_1 u'' + q_2 (v^\circ + w) + q_3 (u^{\circ\circ} - w') = \gamma \left[\frac{\partial^2 u}{\partial t^2} - \frac{q_x}{\rho_s h} \right], \tag{2.5}$$

$$\frac{1+\upsilon_s}{2} u'^{\circ} + v^{\circ\circ} + \frac{1-\upsilon_s}{2} v'' + w^\circ + k_s \left[\frac{3}{2} (1 - \upsilon_s) v'' - \frac{3-\upsilon_s}{2} w''^{\circ} \right] + q_1 v'' + q_3 (v^{\circ\circ} + w^\circ) = \gamma \left[\frac{\partial^2 v}{\partial t^2} - \frac{q_\theta}{\rho_s h} \right], \tag{2.6}$$

$$\upsilon_s u' + v^\circ + w + k_s \left[\frac{1-\upsilon_s}{2} u'^{\circ\circ} - u''' - \frac{3-\upsilon_s}{2} v''^{\circ} + \nabla^4 w + 2w^{\circ\circ} + w \right] - q_1 w'' - q_3 (u' - v^\circ + w^{\circ\circ}) = -\gamma \left[\frac{\partial^2 w}{\partial t^2} - \frac{q_r}{\rho_s h} \right], \tag{2.7}$$

where $\quad (\ )' = a_i \dfrac{\partial}{\partial x}, \quad (\ )^\circ = \dfrac{\partial}{\partial \theta},$

$$k_s = \frac{1}{12} (h/a_i)^2, \quad \gamma = \rho_s \frac{a_i^2 (1 - \upsilon_s^2)}{E}, \tag{2.8}$$

$$\nabla^2 = a_i^2 (\partial^2/\partial x^2) + (\partial^2/\partial \theta^2),$$

$$q_1 = \left[(1 - \nu_s^2)/Eh \right] \overline{N}_x \ , \quad q_2 = \left[a_i(1 - \nu_s^2)/Eh \right] \overline{P}_x \ ,$$

$$q_3 = \left[a_i(1 - \nu_s^2)/Eh \right] \overline{P}_r \ ,$$

with $\overline{P}_x$, $\overline{P}_r$ and $\overline{N}_x$ given by equations (2.1)-(2.3). A complete derivation of q_1, q_2 and q_3 is given in Appendix A. In equations (2.5)- (2.7), q_r, q_θ and q_x are the unsteady viscous forces per unit area of the middle surface of the shell, in the radial, circumferential and axial directions, respectively. They are given by

$$\begin{aligned} q_r &= \tau'_{rri}|_{r=a_i} - \tau'_{rro}|_{r=a_i} \ , \\ q_\theta &= \tau'_{r\theta i}|_{r=a_i} - \tau'_{r\theta o}|_{r=a_i} \ , \\ q_x &= \tau'_{rxi}|_{r=a_i} - \tau'_{rxo}|_{r=a_i} \ , \end{aligned} \tag{2.9}$$

where τ'_{rr}, $\tau'_{r\theta}$ and τ'_{rx} are the unsteady fluid stresses, in the radial, circumferential and axial directions, respectively.

2.3 DERIVATION OF THE FLUID FORCES

The following analysis is applicable for both internal and annular flow. The flow is unsteady and has been assumed to be imcompressible and viscous. The flow velocity may be expressed as follows:

$$\overline{V} = \overline{\nabla}\phi + \overline{\nabla}\times\overline{\psi} + \overline{U}(r) \ , \tag{2.10}$$

where $\phi(x,\theta,r,t)$ is a scalar potential and $\overline{\psi}(x,\theta,r,t)$ is a velocity perturbation vector, so that $\overline{\nabla}\phi$ and $\overline{\nabla}\times\overline{\psi}$ are the unsteady parts of the velocity, representing the perturbed state. U(r) is the steady part, the mean flow velocity in the axial direction. (This decomposition of the flow velocity has been introduced for convenience in the manipulations that follow in the analysis; it is the result of several attempts to analyze the system, and was found to be the most suitable.)

The velocity component in the axial, circumferential and radial directions are given, respectively, by:

$$V_x = U(r) + \frac{\partial \phi}{\partial x} + \frac{\psi_\theta}{r} + \frac{\partial \psi_\theta}{\partial r} - \frac{1}{r}\frac{\partial \psi_r}{\partial \theta} \, , \tag{2.11}$$

$$V_\theta = \frac{1}{r}\frac{\partial \phi}{\partial \theta} + \frac{\partial \psi_r}{\partial x} - \frac{\partial \psi_x}{\partial r} \, , \tag{2.12}$$

$$V_r = \frac{\partial \phi}{\partial r} + \frac{1}{r}\frac{\partial \psi_x}{\partial \theta} - \frac{\partial \psi_\theta}{\partial x} \, , \tag{2.13}$$

where $\psi_x(x,\theta,r,t)$, $\psi_\theta(x,\theta,r,t)$ and $\psi_r(x,\theta,r,t)$ are the components of $\bar{\psi}(x,\theta,r,t)$ in the axial, circumferential and radial directions, respectively.

Similarly, the pressure is defined by

$$p(x,\theta,r,t) = P_o(x,r) + p'(x,\theta,r,t), \tag{2.14}$$

where P_o is the steady pressure, and p' is the perturbation pressure.

The fluid stresses are defined as:

$$\tau_{rx}(x,\theta,r,t) = \bar{\tau}_{rx}(x,r) + \tau'_{rx}(x,\theta,r,t) \, , \tag{2.15}$$

$$\tau_{r\theta}(x,\theta,r,t) = \bar{\tau}_{r\theta}(x,r) + \tau'_{r\theta}(x,\theta,r,t) \, ; \tag{2.16}$$

$$\tau_{rr}(x,\theta,r,t) = \bar{\tau}_{rr}(x,r) + \tau'_{rr}(x,\theta,r,t) \, , \tag{2.17}$$

where $\bar{\tau}_{rx}$, $\bar{\tau}_{r\theta}$, $\bar{\tau}_{rr}$ are the steady stresses in the axial, circumferential and radial directions, respectively, and the primed quantities are the corresponding unsteady components. The fluid stresses are related to the flow velocities as follows:

$$\tau_{rx} = \mu \left[\frac{\partial V_r}{\partial x} + \frac{\partial V_x}{\partial r} \right] , \tag{2.18}$$

$$\tau_{r\theta} = \mu \left[r \frac{\partial}{\partial r} \left(\frac{V_\theta}{r} \right) + \frac{1}{r} \frac{\partial V_r}{\partial \theta} \right] , \tag{2.19}$$

$$\tau_{rr} = -p + 2\mu \frac{\partial V_r}{\partial r} , \tag{2.20}$$

where μ is the dynamic viscosity of the fluid.

Substituting equations (2.11)-(2.14) into equations (2.18)-(2.20), this leads to the terms for steady and unsteady stresses

$$\bar{\tau}_{rx} = \mu \frac{dU}{dr} , \tag{2.21}$$

$$\bar{\tau}_{r\theta} = 0 , \tag{2.22}$$

$$\bar{\tau}_{rr} = - P_o , \tag{2.23}$$

$$\tau'_{rx} = \mu \left[2 \frac{\partial^2 \phi}{\partial x \partial r} + \frac{1}{r} \frac{\partial^2 \psi_x}{\partial x \partial \theta} - \frac{\partial^2 \psi_\theta}{\partial x^2} - \frac{\psi_\theta}{r^2} + \frac{1}{r} \frac{\partial \psi_\theta}{\partial r} + \frac{\partial^2 \psi_\theta}{\partial r^2} + \frac{1}{r^2} \frac{\partial \psi_r}{\partial \theta} - \frac{1}{r} \frac{\partial^2 \psi_r}{\partial \theta \partial r} \right] , \tag{2.24}$$

$$\tau'_{r\theta} = \mu \left[\frac{-2}{r^2} \frac{\partial \phi}{\partial \theta} + \frac{2}{r} \frac{\partial^2 \phi}{\partial \theta \partial r} + \frac{1}{r} \frac{\partial \psi_x}{\partial r} - \frac{\partial^2 \psi_x}{\partial r^2} + \frac{1}{r^2} \frac{\partial^2 \psi_x}{\partial \theta^2} - \frac{1}{r} \frac{\partial^2 \psi_\theta}{\partial \theta \partial x} + \frac{\partial^2 \psi_r}{\partial x \partial r} - \frac{1}{r} \frac{\partial \psi_r}{\partial x} \right] \tag{2.25}$$

$$\tau'_{rr} = - p' + 2\mu \left(\frac{\partial^2 \phi}{\partial r^2} - \frac{1}{r^2} \frac{\partial \psi_x}{\partial \theta} + \frac{1}{r} \frac{\partial^2 \psi_x}{\partial \theta \partial r} - \frac{\partial^2 \psi_\theta}{\partial x \partial r} \right) . \tag{2.26}$$

2.3.1 Derivation of the pressure perturbation

The continuity equation for incompressible fluid is given by:

$$\bar{\nabla} \cdot \bar{V} = 0. \tag{2.27}$$

Substituting equation (2.10) into equation (2.27) leads to the Laplacian equation

$$\nabla^2 \phi = 0. \tag{2.28}$$

The Navier-Stokes equation governing the viscous flow is as follows:

$$\rho \left[\frac{\partial \bar{V}}{\partial t} + \left(\bar{V} \cdot \bar{\nabla} \right) \bar{V} \right] = - \bar{\nabla} p + \mu \nabla^2 \bar{V}. \tag{2.29}$$

Substituting for $\bar{V}$ and p given by equations (2.10) and (2.14), respectively and assuming a small disturbance, the above equation may be linearized by dropping second order terms, i.e.,

$$\rho \left[\frac{\partial}{\partial t} \left(\bar{\nabla}\phi + \bar{\nabla} \times \bar{\psi} \right) + \left\{ \left(\bar{\nabla}\phi + \bar{\nabla} \times \bar{\psi} \right) \cdot \bar{\nabla} \right\} \bar{U} + \left(\bar{U} \cdot \bar{\nabla} \right) \bar{U} + \left(\bar{U} \cdot \bar{\nabla} \right) \left(\bar{\nabla}\phi + \bar{\nabla} \times \bar{\psi} \right) \right] = - \bar{\nabla} p' - \bar{\nabla} P_o + \mu \nabla^2 \left[\bar{\nabla}\phi + \bar{\nabla} \times \bar{\psi} \right] + \mu \nabla^2 \bar{U}. \tag{2.30}$$

Also, the Navier-Stokes equation is clearly valid for the steady viscous flow; hence we must have

$$\rho \left(\bar{U} \cdot \bar{\nabla} \right) \bar{U} = - \bar{\nabla} P_o + \mu \nabla^2 \bar{U}. \tag{2.31}$$

Subtracting equation (2.31) from equation (2.30), and using equation (2.28), leads to

$$\rho \left[\frac{\partial}{\partial t} \left(\bar{\nabla}\phi + \bar{\nabla} \times \bar{\psi} \right) + \left\{ \left(\bar{\nabla}\phi + \bar{\nabla} \times \bar{\psi} \right) \cdot \bar{\nabla} \right\} \bar{U} + \left(\bar{U} \cdot \bar{\nabla} \right) \left(\bar{\nabla}\phi + \bar{\nabla} \times \bar{\psi} \right) \right] = - \bar{\nabla} p' + \mu \nabla^2 \left(\bar{\nabla} \times \bar{\psi} \right) \tag{2.32}$$

Equation (2.32) may be written in the cylindrical coordinates, which results in having three equations and four unknowns ψ_x, ψ_θ, ψ_r and p'. (Note that ϕ

is known from the solution of equation (2.28)). The reason for the presence of an extra unknown is as follows. The three velocity perturbation components V_x, V_θ, V_r that are the primary unknowns have been expressed in terms of the four new variables ϕ, ψ_x, ψ_θ, ψ_r in equations (2.11)-(2.13) giving rise to an extra variable. Obviously these four variables cannot be independent. In order to resolve this difficulty, a constraint is introduced as follows:

$$\rho \left[\frac{\partial}{\partial t} \left(\overline{\nabla} \times \overline{\psi} \right) \right] = \mu \, \nabla^2 \left(\overline{\nabla} \times \overline{\psi} \right) \quad . \tag{2.33}$$

This chosen equation of constraint is a vector equation, which adds three (not one) additional equations. This in fact is overspecifying the mathematical problem; however, as will be seen later, two of the added equations will reduce to a single one, due to the choice of the assumed solution for ψ_r and ψ_θ, which finally results in having three equations and three unknowns ϕ, ψ_r, ψ_x.

Now subtracting equation (2.33) from equation (2.32) one obtains

$$\rho \left[\frac{\partial}{\partial t} \; \overline{\nabla}\phi + \left\{ \left(\overline{\nabla}\phi + \overline{\nabla} \times \overline{\psi} \right) \cdot \overline{\nabla} \right\} \overline{U} + \left(\overline{U} \cdot \overline{\nabla} \right) \left(\overline{\nabla}\phi + \overline{\nabla} \times \overline{\psi} \right) \right] = - \overline{\nabla} p' . \tag{2.34}$$

The constraint given by (2.33) may be justified as follows. Basically the vector potential $\overline{\psi}$ was introduced to represent the viscous perturbations. Then, it is possible to derive these velocity perturbations separately as in equation (2.33), and include their effects on the dynamic pressure as in equation (2.34). In the absence of $\overline{\psi}$, equations (2.33) and (2.34) will reduce to potential flow theory. This justification may not be the best in mathematical terms, but it is based on physical grounds. Equation (2.33) may now be rewritten as

$$\bar{\nabla}\times\left[\rho\frac{\partial\bar{\psi}}{\partial t}-\mu\nabla^2\bar{\psi}\right]=0. \tag{2.35}$$

A proof of the above transformation is given in Appendix B.

A solution for equation (2.35) is

$$\rho\frac{\partial\bar{\psi}}{\partial t}=\mu\nabla^2\bar{\psi}\,; \tag{2.36}$$

it recognized here that equation (2.36) is not a general solution for equation (2.35); it is rather a particular one. This equation may be rewritten in cylindrical coordinates as follows:

$$\rho\frac{\partial\psi_x}{\partial t}=\mu\left(\frac{\partial^2\psi_x}{\partial r^2}+\frac{1}{r}\frac{\partial\psi_x}{\partial r}+\frac{1}{r^2}\frac{\partial^2\psi_x}{\partial\theta^2}+\frac{\partial^2\psi_x}{\partial x^2}\right), \tag{2.37}$$

$$\rho\frac{\partial\psi_\theta}{\partial t}=\mu\left(\frac{\partial^2\psi_\theta}{\partial r^2}+\frac{1}{r}\frac{\partial\psi_\theta}{\partial r}+\frac{1}{r^2}\frac{\partial^2\psi_\theta}{\partial\theta^2}+\frac{\partial^2\psi_\theta}{\partial x^2}-\frac{\psi_\theta}{r^2}+\frac{2}{r^2}\frac{\partial\psi_r}{\partial\theta}\right), \tag{2.38}$$

$$\rho\frac{\partial\psi_r}{\partial t}=\mu\left(\frac{\partial^2\psi_r}{\partial r^2}+\frac{1}{r}\frac{\partial\psi_r}{\partial r}+\frac{1}{r^2}\frac{\partial^2\psi_r}{\partial\theta^2}+\frac{\partial^2\psi_r}{\partial x^2}-\frac{\psi_r}{r^2}-\frac{2}{r^2}\frac{\partial\psi_\theta}{\partial\theta}\right). \tag{2.39}$$

Having determined ψ_r, ψ_θ, ψ_x and ϕ, the pressure perturbation p' may be obtained from equation (2.34). It is convenient now to write equation (2.34) in the (x,θ,r) directions, i.e.,

$$\rho\left[\frac{\partial}{\partial t}\left(\frac{\partial\phi}{\partial x}\right)+U\frac{\partial}{\partial x}\left(\frac{\partial\phi}{\partial x}\right)+U\frac{\partial}{\partial x}\left(\frac{\psi_\theta}{r}+\frac{\partial\psi_\theta}{\partial r}-\frac{1}{r}\frac{\partial\psi_r}{\partial\theta}\right)\right.$$
$$\left.+\left(\frac{\partial\phi}{\partial r}+\frac{1}{r}\frac{\partial\psi_x}{\partial\theta}-\frac{\partial\psi_\theta}{\partial x}\right)\frac{dU}{dr}\right]=-\frac{\partial p'}{\partial x}, \tag{2.40}$$

$$\rho\left[\frac{\partial}{\partial t}\left(\frac{1}{r}\frac{\partial\phi}{\partial\theta}\right)+U\frac{\partial}{\partial x}\left(\frac{1}{r}\frac{\partial\phi}{\partial\theta}\right)+U\frac{\partial}{\partial x}\left(\frac{\partial\psi_r}{\partial x}-\frac{\partial\psi_x}{\partial r}\right)\right]=-\frac{1}{r}\frac{\partial p'}{\partial\theta}, \tag{2.41}$$

$$\rho\left[\frac{\partial}{\partial t}\left(\frac{\partial\phi}{\partial r}\right)+U\frac{\partial}{\partial x}\left(\frac{\partial\phi}{\partial r}\right)+U\frac{\partial}{\partial x}\left(\frac{1}{r}\frac{\partial\psi_x}{\partial\theta}-\frac{\partial\psi_\theta}{\partial x}\right)\right]=-\frac{\partial p'}{\partial r}. \tag{2.42}$$

Any of the above equations can be used for calculating the pressure perturbation p'; however, the compatibility of the three equations is discussed in Chapter V.

2.4 BOUNDARY CONDITIONS

The velocity of the fluid at the wall must be equal to the velocity of the shell. Thus, the boundary conditions in the (x,θ,r) directions may be expressed as:

$$\frac{\partial \phi}{\partial x} + \frac{\psi_\theta}{r} + \frac{\partial \psi_\theta}{\partial r} - \frac{1}{r}\frac{\partial \psi_r}{\partial \theta} = \frac{Du}{Dt}, \tag{2.43}$$

$$\frac{1}{r}\frac{\partial \phi}{\partial \theta} + \frac{\partial \psi_r}{\partial x} - \frac{\partial \psi_x}{\partial r} = \frac{Dv}{Dt}, \tag{2.44}$$

$$\frac{\partial \phi}{\partial r} + \frac{1}{r}\frac{\partial \psi_x}{\partial \theta} - \frac{\partial \psi_\theta}{\partial x} = \frac{Dw}{Dt}, \tag{2.45}$$

where

$$\frac{D}{Dt} = \frac{\partial}{\partial t} + U\frac{\partial}{\partial x}, \tag{2.46}$$

and U is the mean flow velocity at the moving wall.

It is understood that, in the viscous theory, the no-slip condition on the wall must be applied. This requires that the mean flow velocity U at the wall be equal to zero. However, in this study, we have faced a problem in applying the no-slip condition at the moving wall. To understand the physical nature of this problem, it is helpful to present the potential (inviscid) flow theory first.

2.4.1 Potential Flow Theory

In inviscid theory [47], the impermeability condition is always used to describe the boundary condition: the velocity perturbation at the wall is equal to the substantial derivative of the shell deformation in the radial direction. If $\frac{\partial \phi}{\partial r}$ represents the velocity perturbation in the radial direction, and w represents the shell deformation in the same direction, then the impermeability condition could be represented by:

$$\frac{\partial \phi}{\partial r}\Big|_{r=a_i} = \frac{\partial w}{\partial t} + U_c\frac{\partial w}{\partial x}, \tag{2.47}$$

where U_c is a constant flow velocity.

The pressure perturbation obtained from potential flow theory is given by

$$p' = -\rho \left[\frac{\partial \phi}{\partial t} + U_c \frac{\partial \phi}{\partial x} \right] . \qquad (2.48)$$

The solution for ϕ, can be represented by a Bessel function; solving for the pressure term, one can obtain the following expression:

$$p' = -\rho \left[\frac{\partial^2 w}{\partial t^2} + 2U_c \frac{\partial^2 w}{\partial x \partial t} + U_c^2 \frac{\partial^2 w}{\partial x^2} \right] \times I(n,\lambda), \qquad (2.49)$$

where I is a functional of Bessel functions, depending on the circumferential wave number n and the axial one λ, and ρ is the density of the fluid. The various terms may be identified sequentially, as the inertia force, a Coriolis term, and a centrifugal term.

2.4.2 Present Theory

It is understood from potential flow theory that, when the shell deforms, the flow induces three types of forces, inertia, Coriolis and centrifugal. The centrifugal forces are velocity-squared dependent.

In the viscous theory (present theory), if the no-slip condition is applied at the moving wall, the centrifugal forces do not appear any more. That disagrees with the physical behaviour of the system, because buckling instabilities do not occur in the absence of centrifugal forces; (this was confirmed by simple calculations using potential flow theory, in which the centrifugal forces were artificially suppressed).

Mateescu [53] dealt with this type of problem when studying the stability of a shell conveying viscous fluid. She considered the case of a developing inner flow and was able to divide the flow into two regions:

(i) an inviscid flow in the core of the shell;

(ii) a viscous flow close to the wall (at a distance equal to the boundary layer thickness).

To overcome the problem presented earlier, the boundary condition was applied at the edge of the boundary layer thickness where the mean flow velocity is equal to U_c, rather than at the wall, where it would be equal to zero.

Ventres [54], in studying the effect of boundary layer on the shear flow, has applied the boundary condition at the edge of the viscous sub-layer, again to overcome the difficulty discussed here.

The method derived by Mateescu [53], cannot be incorporated in the present work, since the flow is assumed to be fully developed. Nevertheless, the effect of the mean flow velocity is incorporated at the boundary, by two different methods.

Method 1.

In this method, a slip condition is permitted at the moving wall; a mean velocity was assumed to exist which is averaged (over the flow area) and lumped at the wall. The averaging for this mean velocity was done as follows:

(i) for internal flow

$$U_{avi} = \int_0^{a_i} \frac{2\,U(r)\,r\,dr}{a_i^2} \; ; \tag{2.50}$$

(ii) for the annular flow

$$U_{avo} = \int_{a_i}^{r_m} \frac{2\,U(r)\,r\,dr}{(r_m^2 - a_i^2)} \; ; \tag{2.51}$$

where r_m is the radial position at which the maximum flow velocity occurs; r_m is evaluated in Appendix A. In these equations, U_{avi} denotes the average velocity for internal flow, and U_{avo} denotes the average flow velocity in the annulus.

Method 2.

In this method, the boundary condition is applied at a distance δ from the wall, which is equal to the shell deformation in the radial direction. The associated flow velocity is described in power-law form:

(i) for internal flow

$$U_{\delta i} = U_{maxi} \left(\frac{\delta}{a_i} \right)^{1/s} ; \tag{2.52}$$

(ii) for annular flow

$$U_{\delta o} = U_{maxo} \left(\frac{\delta}{r_m - a_i} \right)^{1/s} . \tag{2.53}$$

where r_m and s are taken from the steady case, the values of which are given in Appendices A and D, respectively.

The effect of varying δ on the stability of the system is investigated and presented later in the discussion.

It is important to mention here that, although extensive research has been done to develop these two methods for handling the boundary conditions, there might yet be different and better methods to resolve this dilemma. Nevertheless, with the best information currently available to the author, these two methods are thought to represent reasonable and convenient ways to arrive at a solution to the problem at hand.

The two regions of the fluid are now considered. A subscript "i" is used to denote the internal region while "o" is used for the annular region. For the internal region, in view of the above analysis, we have

$$\nabla^2 \phi_i = 0 , \tag{2.54}$$

and

$$\rho_i \frac{\partial \bar{\psi}_i}{\partial t} = \mu_i \nabla^2 \bar{\psi}_i . \tag{2.55}$$

These equations are subjected to the following boundary conditions

$$\left(\frac{\partial \phi_i}{\partial x} + \frac{\psi_{\theta i}}{r} + \frac{\partial \psi_{\theta i}}{\partial r} - \frac{1}{r} \frac{\partial \psi_{ri}}{\partial \theta} \right) \Bigg|_{r=a_i-\delta} = \frac{\partial u}{\partial t} + U_{\delta i} \frac{\partial u}{\partial x} , \tag{2.56}$$

$$\left(\frac{1}{r} \frac{\partial \phi_i}{\partial \theta} + \frac{\partial \psi_{ri}}{\partial x} - \frac{\partial \psi_{xi}}{\partial r} \right) \Bigg|_{r=a_i-\delta} = \frac{\partial v}{\partial t} + U_{\delta i} \frac{\partial v}{\partial x} , \tag{2.57}$$

$$\left(\frac{\partial \phi_i}{\partial r} + \frac{1}{r} \frac{\partial \psi_{xi}}{\partial \theta} - \frac{\partial \psi_{\theta i}}{\partial x} \right) \Bigg|_{r=a_i-\delta} = \frac{\partial w}{\partial t} + U_{\delta i} \frac{\partial w}{\partial x} , \tag{2.58}$$

$$\text{for} \quad 0 \le x \le L ;$$

The left-hand side in each of the equations (2.56)-(2.58) is equal to 0 for $x < 0$ and $x > L$. Equations (2.56), (2.57) and (2.58) are in the axial, circumferential and radial direction, respectively.

Similarly, the equations governing the velocity perturbations in the annular region are

$$\nabla^2 \phi_o = 0 , \tag{2.59}$$

and

$$\rho_o \frac{\partial \bar{\psi}_o}{\partial t} = \mu_o \nabla^2 \bar{\psi}_o . \tag{2.60}$$

The associated boundary conditions are

$$\left(\frac{\partial \phi_o}{\partial x} + \frac{\psi_{\theta o}}{r} + \frac{\partial \psi_{\theta o}}{\partial r} - \frac{1}{r} \frac{\partial \psi_{ro}}{\partial \theta} \right) \Bigg|_{r=a_i+\delta} = \frac{\partial u}{\partial t} + U_{\delta o} \frac{\partial u}{\partial x} , \tag{2.61}$$

$$\left(\frac{1}{r} \frac{\partial \phi}{\partial \theta} + \frac{\partial \psi_{ro}}{\partial x} - \frac{\partial \psi_{xo}}{\partial r} \right) \Bigg|_{r=a_i+\delta} = \frac{\partial v}{\partial t} + U_{\delta o} \frac{\partial v}{\partial x} , \tag{2.62}$$

$$\left(\frac{\partial \phi_o}{\partial r} + \frac{1}{r} \frac{\partial \psi_{xo}}{\partial \theta} - \frac{\partial \psi_{\theta o}}{\partial x} \right) \Bigg|_{r=a_i+\delta} = \frac{\partial w}{\partial t} + U_{\delta o} \frac{\partial w}{\partial x} , \tag{2.63}$$

and

$$\left(\frac{\partial \phi_o}{\partial x} + \frac{\psi_{\theta o}}{r} + \frac{\partial \psi_{\theta o}}{\partial r} - \frac{1}{r} \frac{\partial \psi_{ro}}{\partial \theta} \right) \Bigg|_{r=a_o} = 0 , \tag{2.64}$$

$$\left(\frac{1}{r} \frac{\partial \phi_o}{\partial \theta} + \frac{\partial \psi_{ro}}{\partial x} - \frac{\partial \psi_{xo}}{\partial r} \right) \Bigg|_{r=a_o} = 0 , \tag{2.65}$$

$$\left(\frac{\partial \phi_o}{\partial r} + \frac{1}{r} \frac{\partial \psi_{xo}}{\partial \theta} - \frac{\partial \psi_{\theta o}}{\partial x} \right) \Bigg|_{r=a_o} = 0 . \tag{2.66}$$

for $0 \le x \le L$;

and equal to zero for $x < 0$ and $x > L$.

The above boundary conditions are given according to the variable δ method (method 2). However, for the first method, equations (2.54)-(2.66) are still applicable but δ is set equal to zero while $U_{\delta i}$ and $U_{\delta o}$ are replaced by U_{avi} and U_{avo}, respectively.

CHAPTER III

METHOD OF SOLUTION I:

FOURIER TRANSFORM METHOD

In this chapter, clamped-clamped and pinned-pinned shells are considered. The unsteady fluid forces acting on the shell are evaluated using the Fourier transform method. The equations of motion (2.5)-(2.7) are solved using Galerkin's method.

Accordingly, the displacements u, v and w of the mid-surface of the cylindrical shell are expressed as infinite series of the following form:

$$u(x,\theta,r) = \sum_{m=1}^{\infty} A_{mn} \cos n\theta \left[a_i \Phi_m'(x) \right] e^{i\omega t} , \tag{3.1}$$

$$v(x,\theta,r) = \sum_{m=1}^{\infty} B_{mn} \sin n\theta \left[\Phi_m(x) \right] e^{i\omega t} , \tag{3.2}$$

$$w(x,\theta,r) = \sum_{m=1}^{\infty} C_{mn} \cos n\theta \left[\Phi_m(x) \right] e^{i\omega t} , \tag{3.3}$$

here $()'$ stands for $\frac{d(\ )}{dx}$, and A_{mn}, B_{mn}, C_{mn} are arbitrary constant coefficients; m and n are the axial and circumferential wave numbers, respectively; furthermore, $\Phi_m(x)$, $m = 1,2,\ldots$, are the eigenfunctions of a beam having the same boundary conditions as the shell. For a clamped-clamped beam,

$$\Phi_m(x) = \cosh\left(\lambda_m \frac{x}{L}\right) - \cos\left(\lambda_m \frac{x}{L}\right) - \sigma_m \left[\left(\sinh\left(\lambda_m \frac{x}{L}\right) - \sin\left(\lambda_m \frac{x}{L}\right) \right] , \tag{3.4a}$$

where L is the length of the beam; the eigenvalues λ_m and the characteristic constants σ_m are given in Appendix C.

The eigenfunctions for pinned-pinned beam are given by

$$\Phi_m(x) = \sin \frac{m\pi x}{L} \ , \ m = 1,2,\ldots \tag{3.4b}$$

The solution for the perturbation flow velocities are assumed to have the form:

$$\psi_r \ (x,r,\theta,t) = \bar{\psi}_r \ (x,r) \sin n\theta \ e^{i\omega t} \ , \tag{3.5}$$

$$\psi_\theta \ (x,r,\theta,t) = \bar{\psi}_\theta \ (x,r) \cos n\theta \ e^{i\omega t} \ , \tag{3.6}$$

$$\psi_x \ (x,r,\theta,t) = \bar{\psi}_x \ (x,r) \sin n\theta \ e^{i\omega t} \ , \tag{3.7}$$

$$\phi \ (x,r,\theta,t) = \bar{\phi} \ (x,r) \cos n\theta \ e^{i\omega t} \ , \tag{3.8}$$

The inner and annular flow regions are denoted by the subscripts i and o, respectively. The resulting perturbation flow velocity amplitudes $\bar{\psi}_{ri}$, $\bar{\psi}_{\theta i}$, $\bar{\psi}_{xi}$, $\bar{\phi}_i$, $\bar{\psi}_{ro}$, $\bar{\psi}_{\theta o}$, $\bar{\psi}_{xo}$ and $\bar{\phi}_o$ are represented by the inverse Fourier Transforms. For example,

$$\bar{\psi}_{ri}(x,r) = \frac{1}{2\pi} \int_{-\infty}^{\infty} \psi^*_{ri} \ (\alpha,r) e^{-i\alpha x} \, d\alpha \ , \tag{3.9}$$

where α is the transfrom variable, and the transform function is defined as

$$\psi^*_{ri}(\alpha,r) = \int_{-\infty}^{\infty} \bar{\psi}_{ri}(x,r) e^{i\alpha x} \, dx \ . \tag{3.10}$$

All pressure and velocity perturbation terms follow the same representation as in equations (3.9) and (3.10).

3.1 SOLUTION TO THE VELOCITY PERTURBATIONS

The equations governing the velocity perturbations derived in Chapter II are:

$$\nabla^2 \phi = 0 \tag{2.28}$$

and

$$\rho \frac{\partial \psi_x}{\partial t} = \mu \left(\frac{\partial^2 \psi_x}{\partial r^2} + \frac{1}{r} \frac{\partial \psi_x}{\partial r} + \frac{1}{r^2} \frac{\partial^2 \psi_x}{\partial \theta^2} + \frac{\partial^2 \psi_x}{\partial x^2} \right) , \tag{2.37}$$

$$\rho \frac{\partial \psi_\theta}{\partial t} = \mu \left(\frac{\partial^2 \psi_\theta}{\partial r^2} + \frac{1}{r} \frac{\partial \psi_\theta}{\partial r} + \frac{1}{r^2} \frac{\partial^2 \psi_\theta}{\partial \theta^2} + \frac{\partial^2 \psi_\theta}{\partial x^2} - \frac{\psi_\theta}{r^2} + \frac{2}{r^2} \frac{\partial \psi_r}{\partial \theta} \right) , \tag{2.38}$$

$$\rho \frac{\partial \psi_r}{\partial t} = \mu \left(\frac{\partial^2 \psi_r}{\partial r^2} + \frac{1}{r} \frac{\partial \psi_r}{\partial r} + \frac{1}{r^2} \frac{\partial^2 \psi_r}{\partial \theta^2} + \frac{\partial^2 \psi_r}{\partial x^2} - \frac{\psi_r}{r^2} - \frac{2}{r^2} \frac{\partial \psi_\theta}{\partial \theta} \right) . \tag{2.39}$$

Equation (2.28) may be written in terms of cylindrical coordinates,

$$\frac{\partial^2 \phi}{\partial r^2} + \frac{1}{r} \frac{\partial \phi}{\partial r} + \frac{1}{r^2} \frac{\partial^2 \phi}{\partial \theta^2} + \frac{\partial^2 \phi}{\partial x^2} = 0 , \tag{3.11}$$

where it is understood that the above equations are equally valid for the inner and annular regions. Hence, the suffixes i and o are omitted for the time being.

After the assumed solution for ϕ given by (3.8) is substituted into equation (3.11), one obtains

$$\frac{\partial^2 \bar{\phi}}{\partial r^2} + \frac{1}{r} \frac{\partial \bar{\phi}}{\partial r} - \frac{n^2}{r^2} \bar{\phi} + \frac{\partial^2 \bar{\phi}}{\partial x^2} = 0 . \tag{3.12}$$

Taking the Fourier transform of equation (3.12), yields

$$\frac{\partial^2 \phi^*}{\partial r^2} + \frac{1}{r} \frac{\partial \phi^*}{\partial r} - \left(\alpha^2 + \frac{n^2}{r^2} \right) \phi^* = 0 , \tag{3.13}$$

where use has been made of the assumption that

$$\lim_{x\to\pm\infty} \bar{\phi}(x,r) = 0 \quad \text{and} \quad \lim_{x\to\pm\infty} \frac{\partial\bar{\phi}(x,r)}{\partial x} = 0 \ ;$$

thus, it has been assumed that both ends of the shell are connected to rigid cylinders, so the flow perturbation and its derivative will vanish at a great distance away from the flexible portion of the shell.

It is noted that equation (3.13) is in the form of a modified Bessel equation of order n, which has a complete solution of

$$\phi^*(\alpha,r) = C_1(\alpha)\ I_n(\alpha r) + C_2(\alpha)\ K_n(\alpha r) \ , \tag{3.14}$$

where $I_n(\alpha r)$ and $K_n(\alpha r)$ are the nth order modified Bessel functions of the first and second kind, respectively.

By substituting the expanded forms of ψ_r, ψ_θ given by (3.5)-(3.6) into equations (2.38) and (2.39), we obtain

$$i\omega\bar{\psi}_r = \upsilon \left(\frac{\partial^2\bar{\psi}_r}{\partial r^2} + \frac{1}{r}\frac{\partial\bar{\psi}_r}{\partial r} - \frac{n^2}{r^2}\ \bar{\psi}_r + \frac{\partial^2\bar{\psi}_r}{\partial x^2} - \frac{\bar{\psi}_r}{r^2} + \frac{2n}{r^2}\bar{\psi}_\theta \right) , \tag{3.15}$$

and

$$i\omega\bar{\psi}_\theta = \upsilon \left(\frac{\partial^2\bar{\psi}_\theta}{\partial r^2} + \frac{1}{r}\frac{\partial\bar{\psi}_\theta}{\partial r} - \frac{n^2}{r^2}\ \bar{\psi}_\theta + \frac{\partial^2\bar{\psi}_\theta}{\partial x^2} - \frac{\bar{\psi}_\theta}{r^2} + \frac{2n}{r^2}\ \bar{\psi}_r \right) , \tag{3.16}$$

where υ is the kinematic viscosity of the fluid.

Equations (3.15) and (3.16) reduce to one single equation for $\bar{\psi}_r = \pm\ \bar{\psi}_\theta$. By using $\bar{\psi}_r = -\ \bar{\psi}_\theta$, we obtain

$$\frac{\partial^2\bar{\psi}_r}{\partial r^2} + \frac{1}{r}\frac{\partial\bar{\psi}_r}{\partial r} - \left(\frac{i\omega}{\upsilon} + \frac{(n+1)^2}{r^2} \right)\ \bar{\psi}_r + \frac{\partial^2\bar{\psi}_r}{\partial x^2} = 0 \ . \tag{3.17}$$

A similar equation could have been obtained using $\bar{\psi}_r = \bar{\psi}_\theta$; however, the order of the Bessel function would have been different.

Similarly, the assumed form for ψ_x given by (3.7) is substituted into equation (2.37), which leads to the following equation:

$$\frac{\partial^2\bar{\psi}_x}{\partial r^2} + \frac{1}{r}\frac{\partial\bar{\psi}_x}{\partial r} - \left(\frac{i\omega}{\upsilon} + \frac{n^2}{r^2} \right)\ \bar{\psi}_x + \frac{\partial^2\bar{\psi}_x}{\partial x^2} = 0 \ . \tag{3.18}$$

Taking the Fourier transform of equations (3.17) and (3.18), yields

$$\frac{\partial^2 \psi_r{}^*}{\partial r^2} + \frac{1}{r}\frac{\partial \psi_r{}^*}{\partial r} - \left(\frac{i\omega}{\upsilon} + \alpha^2 + \frac{(n+1)^2}{r^2} \right) \psi_r^* = 0 \,, \tag{3.19}$$

and

$$\frac{\partial^2 \psi_x{}^*}{\partial r^2} + \frac{1}{r}\frac{\partial \psi_x{}^*}{\partial r} - \left(\frac{i\omega}{\upsilon} + \alpha^2 + \frac{n^2}{r^2} \right) \psi_x{}^* = 0 \,, \tag{3.20}$$

where use has been made of the fact that

$$\lim_{x\to\pm\infty} \left\{ \psi_x\ (x,r),\ \psi_\theta\ (x,r),\ \psi_r\ (x,r) \right\} = 0 \,,$$

and (3.21)

$$\lim_{x\to\pm\infty} \left\{ \frac{\partial}{\partial x} \left(\psi_r\ (x,r),\ \psi_\theta\ (x,r),\ \psi_x\ (x,r) \right) \right\} = 0 \,,$$

for the same reasons explained earlier with regard to ϕ. Equations (3.19) and (3.20) are modified Bessél equations and admit the following solutions:

$$\psi_x{}^*\ (\alpha,r) = C_3\ (\alpha)\ I_n\ (\beta r) + C_4\ (\alpha)\ K_n\ (\beta r) \,, \tag{3.22}$$

and

$$\psi_r{}^*\ (\alpha,r) = -\psi_\theta{}^* = C_5\ (\alpha)\ I_{n+1}\ (\beta r) + C_6\ (\alpha)\ K_{n+1}\ (\beta r) \,, \tag{3.23}$$

where $I_n(\beta r)$, $K_n(\beta r)$ are nth order modified Bessel functions of the first and second kind, respectively, while $I_{n+1}\ (\beta r)$, $K_{n+1}\ (\beta r)$ are $(n+1)^{th}$ order modified Bessel functions,

and

$$\beta^2 = \left(\frac{i\omega}{\upsilon} + \alpha^2 \right) . \tag{3.24}$$

3.2 SOLUTIONS FOR THE INNER FLOW

The solution for the inner flow may be expressed now by putting a subscript i in the foregoing, i.e.,

$$\phi_i^*(\alpha) = C_{1i}(\alpha)\, I_n(\alpha r) + C_{2i}(\alpha)\, K_n(\alpha r) , \tag{3.25}$$

$$\psi_{xi}^*(\alpha) = C_{3i}(\alpha)\, I_n(\beta_i r) + C_{4i}(\alpha)\, K_n(\beta_i r) , \tag{3.26}$$

$$\psi_{ri}^*(\alpha) = C_{5i}(\alpha)\, I_{n+1}(\beta_i r) + C_{6i}(\alpha)\, K_{n+1}(\beta_i r) . \tag{3.27}$$

Since $K_n(\alpha r)$, $K_n(\beta_i r)$ and $K_{n+1}(\beta_i r)$ become infinitely large at $r \rightarrow 0$, one must have

$$C_{2i}(\alpha) = C_{4i}(\alpha) = C_{6i}(\alpha) = 0;$$

hence, the remaining solutions are

$$\phi_i^*(\alpha) = C_{1i}(\alpha)\, I_n(\alpha r) , \tag{3.28}$$

$$\psi_{xi}^*(\alpha) = C_{3i}(\alpha)\, I_n(\beta_i r) , \tag{3.29}$$

$$\psi_{ri}^*(\alpha) = C_{5i}(\alpha)\, I_{n+1}(\beta_i r) , \tag{3.30}$$

where $C_{1i}(\alpha)$, $C_{3i}(\alpha)$ and $C_{5i}(\alpha)$ are constants to be determined.

3.2.1 Boundary Conditions

For the inner flow, the boundary conditions are given in Chapter II by equations (2.56)-(2.58).

Upon substituting the solutions for ϕ_i, ψ_{xi}, $\psi_{\theta i}$, ψ_{ri}, u, v and w into equations (2.56)-(2.58) and taking the Fourier transform of the resulting equations, one obtains

$$\left(-i\alpha\phi_i^* - \frac{(n+1)}{r}\psi_{ri}^* - \frac{\partial\psi_{ri}^*}{\partial r} \right)_{r=a_i-\delta} = \left(\alpha\omega - \alpha^2 U_{\delta i} \right) a_i \Phi_m^* A_{mn} , \tag{3.31}$$

$$\left(-\frac{n}{r}\phi_i^* - \frac{\partial\psi_{xi}^*}{\partial r} - i\alpha\,\psi_{ri}^* \right)_{r=a_i-\delta} = i \left(\omega - \alpha U_{\delta i} \right) \Phi_m^* B_{mn} , \tag{3.32}$$

$$\left(\frac{\partial\phi_i^*}{\partial r} + \frac{n}{r}\psi_{xi}^* - i\alpha\,\psi_{ri}^* \right)_{r=a_i-\delta} = i \left(\omega - \alpha U_{\delta i} \right) \Phi_m^* C_{mn} , \tag{3.33}$$

where $\Phi_m^*(\alpha)$ is the Fourier transform of $\Phi_m(x)$,

$$\Phi_m^*(\alpha) = \int_{-\infty}^{\infty} \Phi_m(x)\, e^{i\alpha x}\, dx$$

$$= \int_0^L \Phi_m(x)\, e^{i\alpha x}\, dx , \tag{3.34}$$

and

$$\Phi_m(x) = \frac{1}{2\pi} \int_{-\infty}^{\infty} \Phi_m^*(\alpha)\, e^{-i\alpha x}\, d\alpha . \tag{3.35}$$

Since the shell displacements vanish beyond the range $0 \le x \le L$, the integration in equation (3.34) need only be performed from $x = 0$ to $x = L$.

Using the following nondimensional terms

$$\epsilon_i = \frac{a_i - \delta}{L} \simeq \frac{a_i}{L} , \quad \bar{\alpha} = \alpha L , \quad u = \left[\frac{E}{\rho_s(1-\nu_s^2)} \right]^{1/2} ,$$

$$\Omega = \frac{\omega a_i}{u} , \quad \xi_i = \frac{uL}{\nu_i} , \quad \bar{\beta}_i = \beta_i L , \quad \bar{U}_{\delta i} = \frac{U_{\delta i}}{u} .$$

$$\bar{A}_{mn} = \frac{A_{mn}}{L} , \quad \bar{B}_{mn} = \frac{B_{mn}}{L} , \quad \bar{C}_{mn} = \frac{C_{mn}}{L} , \tag{3.36}$$

and substituting the solutions (3.28)-(3.30) into equations (3.31)-(3.33), the boundary conditions may be written in nondomensional form as:

$$-i\bar{\alpha}\epsilon_i\, I_n(\bar{\alpha}\epsilon_i)\, \bar{C}_{1i} - \left[(n+1)\, I_{n+1}(\bar{\beta}_i\epsilon_i) + (\epsilon_i\bar{\beta}_i)\, I'_{n+1}(\bar{\beta}_i\epsilon_i) \right] \bar{C}_{5i}$$

$$= u \left(\epsilon_i\bar{\alpha}\Omega - \epsilon_i^2\, \bar{\alpha}^2 \bar{U}_{\delta i} \right) \Phi_m^* \bar{A}_{mn}, \tag{3.37}$$

$$- n\, I_n(\bar{\alpha}\epsilon_i)\, \bar{C}_{1i} - (\bar{\beta}_i\epsilon_i)\, I_n'(\bar{\beta}_i\epsilon_i)\, \bar{C}_{3i} - i\,\bar{\alpha}\,\epsilon_i\, I_{n+1}(\bar{\beta}_i\epsilon_i)\, \bar{C}_{5i}$$

$$= iU \left(\Omega - \epsilon_i \bar{\alpha}\, \bar{U}_{\delta i} \right) \Phi_m^*\, \bar{B}_{mn}\,, \tag{3.38}$$

$$\epsilon_i \bar{\alpha}\;\; I_n'(\bar{\alpha}\epsilon_i)\, \bar{C}_{1i} + n\, I_n(\bar{\beta}_i\epsilon_i)\, \bar{C}_{3i} \;\; - i\,\bar{\alpha}\,\epsilon_i\, I_{n+1}(\bar{\beta}_i\epsilon_i)\, \bar{C}_{5i}$$

$$= iU \left(\Omega - \epsilon_i \bar{\alpha}\, \bar{U}_{\delta i} \right) \Phi_m^*\, \bar{C}_{mn}\,, \tag{3.39}$$

where

$$I_{n+1}'(\bar{\beta}_i\epsilon_i) = \frac{\partial}{\partial(\bar{\beta}_i\epsilon_i)}\, I_{n+1}(\bar{\beta}_i\epsilon_i)\,,$$

$$I_n'(\bar{\alpha}\epsilon_i) = \frac{\partial}{\partial(\bar{\alpha}\epsilon_i)}\, I_n(\bar{\alpha}\epsilon_i), \tag{3.40}$$

and

$$\bar{C}_{1i} = \frac{C_{1i}}{L}\,,\quad \bar{C}_{3i} = \frac{C_{3i}}{L}\,,\; \bar{C}_{5i} = \frac{C_{5i}}{L}\,. \tag{3.41}$$

3.2.2 Unsteady Fluid Forces for the Inner Flow

The fluid forces for the inner flow are obtained by putting a subscript i in the stress equations described in Chapter II:

$$\tau_{rxi}' = \mu_i \left[2\,\frac{\partial^2\phi_i}{\partial x\partial r} + \frac{1}{r}\,\frac{\partial^2\psi_{xi}}{\partial x\partial\theta} - \frac{\partial^2\psi_{\theta i}}{\partial x^2} - \frac{\psi_{\theta i}}{r^2} + \frac{1}{r}\,\frac{\partial\psi_{\theta i}}{\partial r} + \frac{\partial^2\psi_{\theta i}}{\partial r^2} + \frac{1}{r^2}\,\frac{\partial\psi_{ri}}{\partial\theta} - \frac{1}{r}\,\frac{\partial^2\psi_{ri}}{\partial\theta\partial r} \right], \tag{3.42}$$

$$\tau_{r\theta i}' = \mu_i \left[\frac{-2}{r^2}\,\frac{\partial\phi_i}{\partial\theta} + \frac{2}{r}\,\frac{\partial^2\phi_i}{\partial\theta\partial r} + \frac{1}{r}\,\frac{\partial\psi_{xi}}{\partial r} - \frac{\partial^2\psi_{xi}}{\partial r^2} + \frac{1}{r^2}\,\frac{\partial^2\psi_{xi}}{\partial\theta^2} - \frac{1}{r}\,\frac{\partial^2\psi_{\theta i}}{\partial\theta\partial x} + \frac{\partial^2\psi_{ri}}{\partial x\partial r} - \frac{1}{r}\,\frac{\partial\psi_{ri}}{\partial x} \right], \tag{3.43}$$

$$\tau_{rri}' = - p_i' + 2\mu_i \left(\frac{\partial^2\phi_i}{\partial r^2} - \frac{1}{r^2}\,\frac{\partial\psi_{xi}}{\partial\theta} + \frac{1}{r}\,\frac{\partial^2\psi_{xi}}{\partial\theta\partial r} - \frac{\partial^2\psi_{\theta i}}{\partial x\partial r} \right), \tag{3.44}$$

where τ'_{rxi}, $\tau'_{r\theta i}$, τ'_{rri} and p'_i may be defined as:

$$\tau'_{rxi}(x,r,\theta,t) = \bar{\tau}'_{rxi}(x,r)\cos n\theta\, e^{i\omega t}, \tag{3.45}$$

$$\tau'_{r\theta i}(x,r,\theta,t) = \bar{\tau}'_{r\theta i}(x,r)\sin n\theta\, e^{i\omega t}, \tag{3.46}$$

$$\tau'_{rri}(x,r,\theta,t) = \bar{\tau}'_{rri}(x,r)\cos n\theta\, e^{i\omega t}, \tag{3.47}$$

$$p'_i(x,r,\theta,t) = \bar{p}'_i(x,r)\cos n\theta\, e^{i\omega t}, \tag{3.48}$$

and $\bar{\tau}'_{rxi}$, $\bar{\tau}'_{r\theta i}$, $\bar{\tau}'_{rri}$ and $\bar{p}'_i(x,r)$ would be represented by the inverse Fourier transforms as in equations (3.9) and (3.10).

Upon substituting the solutions for ϕ_i, ψ_{xi}, ψ_{ri}, τ'_{rxi}, $\tau'_{r\theta i}$, τ'_{rri} and p'_i into equations (3.42)-(3.44) and taking the Fourier transform of the resulting equations, then making use of the nondimensional terms, we obtain

$$\tau^*_{rxi} = \frac{\rho_i u}{\xi_i}\left[\begin{array}{l} -2\, i\bar{\alpha}^2 I'_n(\bar{\alpha}\epsilon_i)\,\bar{C}_{1i} - \dfrac{i\bar{\alpha}n}{\epsilon_i} I_n(\bar{\beta}_i\epsilon_i)\,\bar{C}_{3i} \\ + \left[\begin{array}{l} \left\{\dfrac{1}{\epsilon_i^2} + \dfrac{n}{\epsilon_i^2} - \bar{\alpha}^2\right\} I_{n+1}(\bar{\beta}_i\epsilon_i) - \left\{\dfrac{\bar{\beta}_i}{\epsilon_i}(1+n)\right\} I'_{n+1}(\bar{\beta}_i\epsilon_i) \\ - \bar{\beta}_i^2\, I''_{n+1}(\bar{\beta}_i\epsilon_i) \end{array}\right]\bar{C}_{5i} \end{array}\right], \tag{3.49}$$

$$\tau^*_{r\theta i} = \frac{\rho_i u}{\xi_i}\left[\begin{array}{l} \left\{\left(\dfrac{2n}{\epsilon_i^2} I_n(\bar{\alpha}\epsilon_i) - \dfrac{2n}{\epsilon_i}\bar{\alpha}\, I'_n(\bar{\alpha}\epsilon_i)\right)\right\}\bar{C}_{1i} \\ + \left\{-\dfrac{n^2}{\epsilon_i^2} I_n(\bar{\beta}_i\epsilon_i) - \bar{\beta}_i^2 I''_n(\bar{\beta}_i\epsilon_i) + \dfrac{\bar{\beta}_i}{\epsilon_i} I'_n(\bar{\beta}_i\epsilon_i)\right\}\bar{C}_{3i} \\ + \left\{\dfrac{i\bar{\alpha}}{\epsilon_i}(1+n)\, I_{n+1}(\bar{\beta}_i\epsilon_i) - i\bar{\alpha}\,\bar{\beta}_i\, I'_{n+1}(\bar{\beta}_i\epsilon_i)\right\}\bar{C}_{5i} \end{array}\right] \tag{3.50}$$

$$\tau'_{rri} = \rho_i u \left[\left\{ p^{*'}_{1i} + 2\,\frac{\bar{\alpha}^2}{\xi_i}\, I''_n(\bar{\alpha}\epsilon_i) \right\} \bar{C}_{1i} + \left\{ p^{*'}_{2i} + \frac{2}{\xi_i} \left(-\frac{n}{\epsilon_i^2}\, I_n(\bar{\beta}_i \epsilon_i) + \frac{n}{\epsilon_i}\, \bar{\beta}_i\, I'_n(\bar{\beta}_i \epsilon_i) \right) \right\} \bar{C}_{3i} + \left\{ p^{*'}_{3i} + \frac{2}{\xi_i} (-i\bar{\alpha})\, \bar{\beta}_i\, I'_{n+1}(\bar{\beta}_i \epsilon_i) \right\} \bar{C}_{5i} \right], \tag{3.51}$$

where $p^{*'}_{1i}$, $p^{*'}_{2i}$ and $p^{*'}_{3i}$ represent the effect of pressure perturbations on the radial stress τ'_{rri}. The pressure perturbations are evaluated in Appendix D using equations (2.40)-(2.42) derived in Chapter II.

3.3 SOLUTIONS FOR THE ANNULAR FLOW REGION

As in the case of inner flow, the solution for annular flow may be expressed by putting a subscript o, to the pertinent equations obtained in section 3.1. Hence,

$$\phi_o^*(\alpha) = C_{1o}(\alpha)\, I_n(\alpha r) + C_{2o}(\alpha)\, K_n(\alpha r)\ , \tag{3.52}$$

$$\psi_{xo}^*(\alpha) = C_{3o}(\alpha)\, I_n(\beta_o r) + C_{4o}(\alpha)\, K_n(\beta_o r)\ , \tag{3.53}$$

$$\psi_{ro}^*(\alpha) = C_{5o}(\alpha)\, I_{n+1}(\beta_o r) + C_{6o}(\alpha)\, K_{n+1}(\beta_o r) \tag{3.54}$$

where $C_{1o}(\alpha)$, $C_{2o}(\alpha)$, $C_{3o}(\alpha)$, $C_{4o}(\alpha)$, $C_{5o}(\alpha)$ and $C_{6o}(\alpha)$ are determined from boundary conditions (2.61)-(2.66).

3.3.1 Boundary Conditions

We first define the following nondimensional terms:

$$\epsilon_o = \frac{a_o}{L}\ ,\ \xi_o = \frac{uL}{\nu_o}\ ,\ \bar{\beta}_o = \beta_o L\ ,\ \bar{U}_{\delta o} = \frac{U_{\delta o}}{u}\ ,$$

$$\rho_r = \frac{\rho_o}{\rho_i}\ ,\ \bar{C}_{1o} = \frac{C_{1o}}{L}\ ,\ \bar{C}_{2o} = \frac{C_{2o}}{L}\ ,\ \bar{C}_{3o} = \frac{C_{3o}}{L}\ ,$$

$$\bar{C}_{4o} = \frac{C_{4o}}{L}\ ,\ \bar{C}_{5o} = \frac{C_{5o}}{L}\ ,\ \bar{C}_{6o} = \frac{C_{6o}}{L}\ . \tag{3.55}$$

Then, substituting the assumed form of ϕ_o, ψ_{ro}, $\psi_{\theta o}$, ψ_{xo}, u, v and w and taking Fourier Transform of the resulting equations, we obtain at $r = a_i+\delta$:

$$- i\bar{\alpha}\epsilon_i I_n(\bar{\alpha}\epsilon_i)\bar{C}_{1o} - i\bar{\alpha}\epsilon_i K_n(\bar{\alpha}\epsilon_i)\bar{C}_{2o} - \left[(n+1) I_{n+1}(\bar{\beta}_o\epsilon_i) + \epsilon_i\bar{\beta}_o I'_{n+1}(\bar{\beta}_o\epsilon_i)\right]\bar{C}_{5o}$$

$$- \left[(n+1) K_{n+1}(\bar{\beta}_o\epsilon_i) + \epsilon_i\bar{\beta}_o K'_{n+1}(\bar{\beta}_o\epsilon_i)\right]\bar{C}_{6o} = \mathrm{H}\left(\epsilon_i\bar{\alpha}\,\Omega - \epsilon_i^2\bar{\alpha}^2\bar{U}_{\delta o}\right)\Phi_m^*\bar{A}_{mn}, \tag{3.56}$$

$$- n I_n(\bar{\alpha}\epsilon_i)\bar{C}_{1o} - n K_n(\bar{\alpha}\epsilon_i)\bar{C}_{2o} - (\bar{\beta}_o\epsilon_i) I'_n(\bar{\beta}_o\epsilon_i)\bar{C}_{3o} - \bar{\beta}_o\epsilon_i K'_n(\bar{\beta}_o\epsilon_i)\bar{C}_{4o}$$

$$- i\bar{\alpha}\epsilon_i I_{n+1}(\bar{\beta}_o\epsilon_i)\bar{C}_{5o} - i\bar{\alpha}\epsilon_i K_{n+1}(\bar{\beta}_o\epsilon_i)\bar{C}_{6o} = i\mathrm{H}\left(\Omega - \bar{\alpha}\epsilon_i\bar{U}_{\delta o}\right)\Phi_m^*\bar{B}_{mn}, \tag{3.57}$$

$$\epsilon_i\bar{\alpha} I'_n(\bar{\alpha}\epsilon_i)\bar{C}_{1o} + \epsilon_i\bar{\alpha} K'_n(\bar{\alpha}\epsilon_i)\bar{C}_{2o} + n I_n(\bar{\beta}_o\epsilon_i)\bar{C}_{3o} + n K_n(\bar{\beta}_o\epsilon_i)\bar{C}_{4o}$$

$$- i\bar{\alpha}\epsilon_i I_{n+1}(\bar{\beta}_o\epsilon_i)\bar{C}_{5o} - i\bar{\alpha}\epsilon_i K_{n+1}(\bar{\beta}_o\epsilon_i)\bar{C}_{6o} = i\mathrm{H}\left(\Omega - \bar{\alpha}\epsilon_i\bar{U}_{\delta o}\right)\Phi_m^*\bar{C}_{mn}, \tag{3.58}$$

where $$K'_{n+1}(\bar{\beta}_o\epsilon_i) = \frac{\partial}{\partial(\bar{\beta}_o\epsilon_i)} K_n(\bar{\beta}_o\epsilon_i). \tag{3.59}$$

The boundary conditions at $r = a_o$ are given by

$$- i\bar{\alpha}\epsilon_o I_n(\bar{\alpha}\epsilon_o)\bar{C}_{1o} - i\bar{\alpha}\epsilon_o K_n(\bar{\alpha}\epsilon_o)\bar{C}_{2o} - \left[(n+1) I_{n+1}(\bar{\beta}_o\epsilon_o) + \epsilon_o\bar{\beta}_o I'_{n+1}(\bar{\beta}_o\epsilon_o)\right]\bar{C}_{5o}$$

$$- \left[(n+1) K_{n+1}(\bar{\beta}_o\epsilon_o) + \epsilon_o\bar{\beta}_o K'_{n+1}(\bar{\beta}_o\epsilon_o)\right]\bar{C}_{6o} = 0, \tag{3.60}$$

$$- n I_n(\bar{\alpha}\epsilon_o)\bar{C}_{1o} - n K_n(\bar{\alpha}\epsilon_o)\bar{C}_{2o} - (\bar{\beta}_o\epsilon_o) I'_n(\bar{\beta}_o\epsilon_o)\bar{C}_{3o} - \bar{\beta}_o\epsilon_o K'_n(\bar{\beta}_o\epsilon_o)\bar{C}_{4o}$$

$$- i\bar{\alpha}\epsilon_o I_{n+1}(\bar{\beta}_o\epsilon_o)\bar{C}_{5o} - i\bar{\alpha}\epsilon_o K_{n+1}(\bar{\beta}_o\epsilon_o)\bar{C}_{6o} = 0, \tag{3.61}$$

$$\epsilon_o \bar{\alpha}\; I_n'(\bar{\alpha}\epsilon_o)\; \bar{C}_{1o} + \epsilon_o \bar{\alpha}\; K_n'(\bar{\alpha}\epsilon_o)\; \bar{C}_{2o} + n\; I_n(\bar{\beta}_o\epsilon_o)\; \bar{C}_{3o} + n\; K_n(\bar{\beta}_o\epsilon_o)\; \bar{C}_{4o}$$

$$- i\bar{\alpha}\epsilon_o\; I_{n+1}(\bar{\beta}_o\epsilon_o)\; \bar{C}_{5o} - i\bar{\alpha}\epsilon_o\; K_{n+1}(\bar{\beta}_o\epsilon_o)\; \bar{C}_{6o} = 0\;. \tag{3.62}$$

3.3.2 Unsteady Fluid Stresses in the Annular Flow

The fluid forces for the annular flow are obtained by putting a subscript o in the stress equations derived in Chapter II.

$$\tau'_{rxo} = \mu_o \left[2\,\frac{\partial^2\phi_o}{\partial x\partial r} + \frac{1}{r}\,\frac{\partial^2\psi_{xo}}{\partial x\partial\theta} - \frac{\partial^2\psi_{\theta o}}{\partial x^2} - \frac{\psi_{\theta o}}{r^2} + \frac{1}{r}\,\frac{\partial\psi_{\theta o}}{\partial r} + \frac{\partial^2\psi_{\theta o}}{\partial r^2} + \frac{1}{r^2}\,\frac{\partial\psi_{ro}}{\partial\theta} - \frac{1}{r}\,\frac{\partial^2\psi_{ro}}{\partial\theta\partial r} \right]\;, \tag{3.63}$$

$$\tau'_{r\theta o} = \mu_o \left[-\frac{2}{r^2}\,\frac{\partial\phi_o}{\partial\theta} + \frac{2}{r}\,\frac{\partial^2\phi_o}{\partial\theta\partial r} + \frac{1}{r}\,\frac{\partial\psi_{xo}}{\partial r} - \frac{\partial^2\psi_{xo}}{\partial r^2} + \frac{1}{r^2}\,\frac{\partial^2\psi_{xo}}{\partial\theta^2} - \frac{1}{r}\,\frac{\partial^2\psi_{\theta o}}{\partial\theta\partial x} + \frac{\partial^2\psi_{ro}}{\partial x\partial r} - \frac{1}{r}\,\frac{\partial\psi_{ro}}{\partial x} \right] \tag{3.64}$$

$$\tau'_{rro} = -p_o' + 2\mu_o \left(\frac{\partial^2\phi_o}{\partial r^2} - \frac{1}{r^2}\,\frac{\partial\psi_{xo}}{\partial\theta} + \frac{1}{r}\,\frac{\partial^2\psi_{xo}}{\partial\theta\partial r} - \frac{\partial^2\psi_{\theta o}}{\partial x\partial r} \right)\;. \tag{3.65}$$

Using a similar analysis as in the case of inner flow, τ'_{rxo}, $\tau'_{r\theta o}$, τ'_{rro} and p_o' are defined as

$$\tau'_{rxo}(x,r,\theta,t) = \bar{\tau}'_{rxo}(x,r)\cos n\theta\; e^{i\omega t}\;, \tag{3.66}$$

$$\tau'_{r\theta o}(x,r,\theta,t) = \bar{\tau}'_{r\theta o}(x,r)\sin n\theta\; e^{i\omega t}\;, \tag{3.67}$$

$$\tau'_{rro}(x,r,\theta,t) = \bar{\tau}'_{rro}(x,r)\cos n\theta\; e^{i\omega t}\;, \tag{3.68}$$

$$p_o'(x,r,\theta,t) = \bar{p}_o'(x,r)\cos n\theta\; e^{i\omega t}\;, \tag{3.69}$$

where $\bar{\tau}'_{rxo}$, $\bar{\tau}'_{r\theta o}$, $\bar{\tau}'_{rro}$ and $\bar{p}_o'(x,r)$ are represented by the inverse Fourier Transform as in equation (3.9).

Upon substituting the assumed solutions for ϕ_o, ψ_{xo}, ψ_{ro}, τ'_{rxo}, $\tau'_{r\theta o}$, τ'_{rro}, and p_o' into equations (3.63)-(3.65), we obtain

$$\tau^*_{rxo} = \frac{\rho_i \rho_r U}{\xi_o} \left[\begin{aligned} & -2i\,\bar{\alpha}^2\, I_n'(\bar{\alpha}\epsilon_i)\,\bar{C}_{1o} - 2i\,\bar{\alpha}^2\, K_n'(\bar{\alpha}\epsilon_i)\,\bar{C}_{2o} \\ & - \frac{i\bar{\alpha}n}{\epsilon_i} I_n'(\bar{\beta}_o\epsilon_i)\,\bar{C}_{3o} - \frac{i\bar{\alpha}n}{\epsilon_i} K_n'(\bar{\beta}_o\epsilon_i)\,\bar{C}_{4o} \\ & + \left[\begin{aligned} & \left(\frac{1}{\epsilon_i^2} + \frac{n}{\epsilon_i^2} - \bar{\alpha}^2 \right) I_{n+1}(\bar{\beta}_o\epsilon_i) - \frac{\bar{\beta}_o}{\epsilon_i}(1+n)\, I_{n+1}'(\bar{\beta}_o\epsilon_i) \\ & - \bar{\beta}_o^2\, I_{n+1}''(\bar{\beta}_o\epsilon_i) \end{aligned} \right] \bar{C}_{5o} \\ & + \left[\begin{aligned} & \left(\frac{1}{\epsilon_i^2} + \frac{n}{\epsilon_i^2} - \bar{\alpha}^2 \right) K_{n+1}(\bar{\beta}_o\epsilon_i) - \frac{\bar{\beta}_o}{\epsilon_i}(1+n)\, K_{n+1}'(\bar{\beta}_o\epsilon_i) \\ & - \bar{\beta}_o^2\, K_{n+1}''(\bar{\beta}_o\epsilon_i) \end{aligned} \right] \bar{C}_{6o} \end{aligned} \right] \tag{3.70}$$

$$\tau^*_{r\theta o} = \frac{\rho_i \rho_r U}{\xi_o} \left[\begin{aligned} & \left\{ \frac{2n}{\epsilon_i^2} I_n(\bar{\alpha}\epsilon_i) - \frac{2n}{\epsilon_i}\bar{\alpha}\, I_n'(\bar{\alpha}\epsilon_i) \right\} \bar{C}_{1o} \\ & + \left\{ \frac{2n}{\epsilon_i^2} K_n(\bar{\alpha}\epsilon_i) - \frac{2n}{\epsilon_i}\bar{\alpha}\, K_n'(\bar{\alpha}\epsilon_i) \right\} \bar{C}_{2o} \\ & + \left\{ -\frac{n^2}{\epsilon_i^2} I_n(\bar{\beta}_o\epsilon_i) - \bar{\beta}_o^2\, I_n''(\bar{\beta}_o\epsilon_i) + \frac{\bar{\beta}_o}{\epsilon_i} I_n'(\bar{\beta}_o\epsilon_i) \right\} \bar{C}_{3o} \\ & + \left\{ -\frac{n^2}{\epsilon_i^2} K_n(\bar{\beta}_o\epsilon_i) - \bar{\beta}_o^2\, K_n''(\bar{\beta}_o\epsilon_i) + \frac{\bar{\beta}_o}{\epsilon_i} K_n'(\bar{\beta}_o\epsilon_i) \right\} \bar{C}_{4o} \\ & + \left\{ \frac{i\bar{\alpha}}{\epsilon_i}(1+n)\, I_{n+1}(\bar{\beta}_o\epsilon_i) - i\bar{\alpha}\,\bar{\beta}_o\, I_{n+1}'(\bar{\beta}_o\epsilon_i) \right\} \bar{C}_{5o} \\ & + \left\{ \frac{i\bar{\alpha}}{\epsilon_i}(1+n)\, K_{n+1}(\bar{\beta}_o\epsilon_i) - i\bar{\alpha}\,\bar{\beta}_o\, K_{n+1}'(\bar{\beta}_o\epsilon_i) \right\} \bar{C}_{6o} \end{aligned} \right] \tag{3.71}$$

$$\tau^{*}_{rro} = \rho_i \rho_r u \left[\begin{aligned} & \left\{ p^{*'}_{1Io} + 2\frac{\bar{\alpha}^2}{\xi_o} I''_n(\bar{\alpha}\epsilon_i) \right\} \bar{C}_{1o} + \left\{ p^{*'}_{1Ko} + 2\frac{\bar{\alpha}^2}{\xi_o} K''_n(\bar{\alpha}\epsilon_i) \right\} \bar{C}_{2o} \\ & + \left\{ p^{*'}_{2Io} + \frac{2}{\xi_o} \left(-\frac{n}{\epsilon_i^2} I_n(\bar{\beta}_o\epsilon_i) + \frac{n}{\epsilon_i} \bar{\beta}_o I'_n(\bar{\beta}_o\epsilon_i) \right) \right\} \bar{C}_{3o} \\ & + \left\{ p^{*'}_{2Ko} + \frac{2}{\xi_o} \left(-\frac{n}{\epsilon_i^2} K_n(\bar{\beta}_o\epsilon_i) + \frac{n}{\epsilon_i} \bar{\beta}_o K'_n(\bar{\beta}_o\epsilon_i) \right) \right\} \bar{C}_{4o} \\ & + \left\{ p^{*'}_{3Io} + \frac{2}{\xi_o} (-i\bar{\alpha}) \bar{\beta}_o I'_{n+1}(\bar{\beta}_o\epsilon_i) \right\} \bar{C}_{5o} \\ & + \left\{ p^{*'}_{3Ko} + \frac{2}{\xi_o} (-i\bar{\alpha}) \bar{\beta}_o K'_{n+1}(\beta_o\epsilon_i) \right\} \bar{C}_{6o} \end{aligned} \right]$$

where $p^{*'}_{1Io}$, $p^{*'}_{1Ko}$, $p^{*'}_{2Io}$, $p^{*'}_{2Ko}$, $p^{*'}_{3Io}$, $p^{*'}_{3Ko}$ are given in Appendix D.

3.4 DETERMINATION OF THE UNSTEADY FLUID LOADING ON THE SHELL

The net fluid loads on the shell arising from the perturbation terms are given by:

$$q_x = \left(\tau'_{rxi} \Big|_{r=a_i-\delta} - \tau'_{rxo} \Big|_{r=a_i+\delta} \right), \tag{3.73}$$

$$q_\theta = \left(\tau'_{r\theta i} \Big|_{r=a_i-\delta} - \tau'_{r\theta o} \Big|_{r=a_i+\delta} \right), \tag{3.74}$$

$$q_r = \left(\tau'_{rri} \Big|_{r=a_i-\delta} - \tau'_{rro} \Big|_{r=a_i+\delta} \right). \tag{3.75}$$

Here q_x, q_θ, and q_r are the axial, circumferential and radial loads, respectively.

Equations (3.73)-(3.75) can be expressed in the following form:

$$q_x = \sum_{m=1}^{\infty} \bar{Q}_{xmn} \cos n\theta \, e^{i\omega t}, \tag{3.76}$$

$$q_\theta = \sum_{m=1}^{\infty} \bar{Q}_{\theta mn} \sin n\theta \, e^{i\omega t} , \tag{3.77}$$

$$q_r = \sum_{m=1}^{\infty} \bar{Q}_{rmn} \cos n\theta \, e^{i\omega t} , \tag{3.78}$$

where

$$\bar{Q}_{xmn} = \left(\bar{\tau}'_{rxi} \Big|_{r=a_i-\delta} - \bar{\tau}'_{rxo} \Big|_{r=a_i+\delta} \right) , \tag{3.79}$$

$$\bar{Q}_{\theta mn} = \left(\bar{\tau}'_{r\theta i} \Big|_{r=a_i-\delta} - \bar{\tau}'_{r\theta o} \Big|_{r=a_i+\delta} \right) , \tag{3.80}$$

$$\bar{Q}_{rmn} = \left(\bar{\tau}'_{rri} \Big|_{r=a_i-\delta} - \bar{\tau}'_{rro} \Big|_{r=a_i+\delta} \right) , \tag{3.81}$$

and the transformed functions Q^*_{xmn}, $Q^*_{\theta mn}$ and Q^*_{rmn} can be defined as

$$Q^*_{xmn}(\alpha) = \tau^{*'}_{rxi} \Big|_{r=a_i-\delta} - \tau^{*'}_{rxo} \Big|_{r=a_i+\delta} , \tag{3.82}$$

$$Q^*_{\theta mn}(\alpha) = \tau^{*'}_{rxi} \Big|_{r=a_i-\delta} - \tau^{*'}_{rxo} \Big|_{r=a_i+\delta} , \tag{3.83}$$

$$Q^*_{rmn}(\alpha) = \tau^{*'}_{rxi} \Big|_{r=a_i-\delta} - \tau^{*'}_{rxo} \Big|_{r=a_i+\delta} . \tag{3.84}$$

The transformed function $Q^*_{xmn}(\alpha)$, $Q^*_{\theta mn}(\alpha)$, $Q^*_{rmn}(\alpha)$ are defined as in equation (3.10).

In order to find the fluid loading, one has to find the constants $\bar{C}_{1i}$, $\bar{C}_{3i}$, $\bar{C}_{5i}$ and $\bar{C}_{1o}$ to $\bar{C}_{6o}$. This is done as follows.

First, the boundary conditions for the inner and annular flow (equations (3.37)-(3.39) and (3.56)-(3.62)) are put in matrix form:

$$\left[B\right] \left\{C\right\} = \left\{R^*\right\} , \tag{3.85}$$

where matrix [B] is (9 x 9), {C} is a (9 x 1) vector which contains the constants, and [R^*] is a (1 x 9) matrix. Similarly, the fluid forces given by equations (3.82)-(3.84) are put in matrix form:

$$\left[T\right] \left\{C\right\} = \left\{Q^*\right\} , \tag{3.86}$$

where matrix [T] is (3 x 9), and {Q^*} is a (3 x 1) matrix. From equation (3.85), one can solve for {C} ,

$$\left\{C\right\} = \left[B\right]^{-1} \left\{R^*\right\} . \tag{3.87}$$

Substituting for {C} into equation (3.86), one obtains

$$\left[T\right] \left[B\right]^{-1} \left\{R^*\right\} = \left\{Q^*\right\} . \tag{3.88}$$

The elements of matrices [T], [B], {R^*} and {Q^*} are all given in Appendix E.

Taking the inverse Fourier transform of (3.88) will lead to the unsteady viscous loads $\overline{Q}_{xmn}$, $\overline{Q}_{\theta mn}$, and $\overline{Q}_{rmn}$ given by equations (3.79), (3.80) and (3.81), respectively. The equations of motion are solved using Galerkin's method. In connection with this method, the fluid dynamic forces are written in suitable form, as the so-called generalized fluid forces. The amplitudes of the generalized forces are given by:

$$\overline{q}_{xkm} = \frac{1}{a_i^2} \frac{\gamma}{\rho_s h} \int_0^L a_i \Phi_k'(x) \overline{Q}_{xmn}(x) dx , \tag{3.89}$$

$$\bar{q}_{\theta km} = \frac{1}{L^2}\ \frac{\gamma}{\rho_s h} \int_0^L \Phi_k(x)\ \bar{Q}_{\theta mn}(x)\ dx \ , \tag{3.90}$$

$$\bar{q}_{rkm} = \frac{1}{L^2}\ \frac{\gamma}{\rho_s h} \int_0^L \Phi_k(x)\ \bar{Q}_{rmn}(x)\ dx \ , \tag{3.91}$$

taking the Fourier transform of (3.89)-(3.91) and making use of the non-dimensional terms, the generalized forces are

$$\bar{q}_{xkm} = \frac{\eta}{2\pi\rho_i U^2} \int_{-\infty}^{\infty} Q^*_{xmn}(\bar{\alpha})\ G_{km}(\bar{\alpha})\ d\bar{\alpha} \ , \tag{3.92}$$

$$\bar{q}_{\theta km} = \frac{\eta\epsilon_i}{2\pi\rho_i U^2} \int_{-\infty}^{\infty} Q^*_{\theta mn}(\bar{\alpha})\ H_{km}(\bar{\alpha})\ d\bar{\alpha} \ , \tag{3.93}$$

$$\bar{q}_{rkm} = \frac{\eta\epsilon_i}{2\pi\rho_i U^2} \int_{-\infty}^{\infty} Q^*_{rmn}(\bar{\alpha})\ H_{km}(\bar{\alpha})\ d\bar{\alpha} \ , \tag{3.94}$$

where $\eta = \dfrac{\rho_i a_i}{\rho_s h}$, $\zeta = \dfrac{x}{L}$ and (3.95)

$$G_{km}(\alpha) = \int_0^1 \Phi_k(\zeta)\ e^{-i\bar{\alpha}\zeta}\ d\zeta \times \int_0^1 \Phi_m(\zeta)\ e^{i\bar{\alpha}\zeta}\ d\zeta \ , \tag{3.96}$$

$$H_{km}(\alpha) = \int_0^1 \Phi'_k(\zeta)\ e^{-i\bar{\alpha}\zeta}\ d\zeta \times \int_0^1 \Phi_m(\zeta)\ e^{i\bar{\alpha}\zeta}\ d\zeta \ . \tag{3.97}$$

The integrations in equations (3.96) and (3.97) can be performed analytically and the resultant expressions in terms of $\bar{\alpha}$ are given in Appendix F. However, the integrals in the fluid force terms (3.92)-(3.94) are very complex and cannot be evaluated analytically. Therefore, the integrations are performed numerically using the two-point Gaussian quadrature technique. Finally, the generalized fluid forces are expressed in terms of the shell displacements as follows:

$$\bar{q}_{xkm} = \bar{q}^{(1)}_{xkm}\ \bar{A}_{mn} + \bar{q}^{(2)}_{xkm}\ \bar{B}_{mn} + \bar{q}^{(3)}_{xkm}\ \bar{C}_{mn}\ , \tag{3.98}$$

$$\bar{q}_{\theta km} = \bar{q}^{(1)}_{\theta km}\ \bar{A}_{mn} + \bar{q}^{(2)}_{\theta km}\ \bar{B}_{mn} + \bar{q}^{(3)}_{\theta km}\ \bar{C}_{mn}\ , \tag{3.99}$$

$$\bar{q}_{rkm} = \bar{q}^{(1)}_{rkm}\ \bar{A}_{mn} + \bar{q}^{(2)}_{rkm}\ \bar{B}_{mn} + \bar{q}^{(3)}_{rkm}\ \bar{C}_{mn}\ . \tag{3.100}$$

Expressions for $\bar{q}^{(1)}_{xkm}$, $\bar{q}^{(2)}_{xkm}$, $\bar{q}^{(3)}_{xkm}$, $\bar{q}^{(1)}_{\theta km}$, $\bar{q}^{(2)}_{\theta km}$, $\bar{q}^{(3)}_{\theta km}$, $\bar{q}^{(1)}_{rkm}$, $\bar{q}^{(2)}_{rkm}$, and $\bar{q}^{(3)}_{rkm}$ are given in Appendix E, equations (E.1.5).

3.5 SOLUTION TO THE EQUATIONS OF MOTION

The modified Flügge's shell equations (2.5)-(2.7) may be written in a general form:

$$\mathcal{L}_m(u,v,w) = 0 \qquad m = 1,2,\ldots \tag{3.101}$$

The solution for the displacements u, v, and w given by equations (3.1)-(3.3) are approximate solutions; hence, they would not necessarily satisfy the shell equations (2.5)-(2.7); then we would have, in general

$$\mathcal{L}_m(u,v,w) \neq 0 \qquad \text{for } m = 1,2,\ldots \tag{3.102}$$

Equation (3.102) is solved using Galerkin's method. In this method, we multiply equation (3.102) by a set of weighted functions, using the same comparison functions employed in the series solutions of the displacements, then integrate the new expression over the domain (0 to L, in this case). The resultant integral is then put identically equal to zero, i.e.,

$$\int_0^L f_k(x)\ \mathcal{L}_m(u,v,w)\ dx = 0\ , \qquad k = 1,2,\ldots \qquad m = 1,2,3 \tag{3.103}$$

where $f_k(x)$ are the weighting functions.

The shell equations (2.6) and (2.7) are weighted by the eigenfunction of a beam, $\Phi_k(x)$, while equation (2.5) is weighted by the eigenfunction derivatives $a_i\Phi_k'(x)$.

After integrating equation (3.103), we obtain the following set of linear homogeneous algebraic equations:

$$\sum_{k=1}^{\infty} \sum_{m=1}^{\infty} \left(A^{(1)}_{kmn} \bar{A}_{mn} + A^{(2)}_{kmn} \bar{B}_{mn} + A^{(3)}_{kmn} \bar{C}_{mn} \right) = 0,$$

$$\sum_{k=1}^{\infty} \sum_{m=1}^{\infty} \left(A^{(4)}_{kmn} \bar{A}_{mn} + A^{(5)}_{kmn} \bar{B}_{mn} + A^{(6)}_{kmn} \bar{C}_{mn} \right) = 0,$$

$$\sum_{k=1}^{\infty} \sum_{m=1}^{\infty} \left(A^{(7)}_{kmn} \bar{A}_{mn} + A^{(8)}_{kmn} \bar{B}_{mn} + A^{(9)}_{kmn} \bar{C}_{mn} \right) = 0, \tag{3.104}$$

where the coefficients $\left\{ A^{(1)}_{kmn} \ldots\ldots A^{(9)}_{kmn} \right\}$ are given in Appendix G.

A solution to the infinite sets of equations (3.102) is impossible to obtain; hence, the series solutions (3.1)-(3.3) may be truncated so as to have a set of finite number of terms, which of course must converge. It was shown in fact in Ref. [48], that the solution converges by considering only the first three terms. Consequently, only the first three terms in the Galerkin series are retained.

The set of equations (3.104) may be written in matrix form

$$\left[A \right] \left\{ X \right\} = \left\{ 0 \right\} , \tag{3.105}$$

where

$$\left\{ X \right\} = \left[\bar{A}_{1n}, \bar{A}_{2n}, \bar{A}_{3n} ; \bar{B}_{1n}, \bar{B}_{2n}, \bar{B}_{3n} ; \bar{C}_{1n}, \bar{C}_{2n}, \bar{C}_{3n} \right]^T \tag{3.106}$$

is a 9-element column vector, and [A] is a 9 x 9 matrix. The structure of matrix [A] is shown in Appendix G.

The frequencies of the system found by setting the determinant of matrix [A] in equation (3.105) equal to zero; that is

$$\det \left[A \left(\Omega, \bar{U}_i, \bar{U}_o, \text{fluid, material and geometrical properties} \right) \right] = 0 . \tag{3.107}$$

It should be noted that, the unsteady viscous forces are complicated functions of the frequency Ω. Therefore, an iteration procedure is needed to find the frequencies of the system for a given set of fluid and shell parameters.

The numerical integrations, and the iteration method render this method of solution computationally very costly for the annular flow case. For this reason, another method of solution is derived, as will be seen in the following chapter.

3.6 INVISCID THEORY

The inviscid theory may be deduced from the viscous theory by setting

$$\begin{aligned} \bar{\psi} &= 0 , \\ \mu &= 0 , \\ U(r) &= U. \end{aligned} \tag{3.108}$$

However, the unsteady inviscid forces are also derived using potential flow theory. The derivation of the fluid forces is given in Appendix H. The generalized fluid-dynamic forces are rearranged as quadratic functions of the frequency parameter Ω, where

$$\bar{q}_{xkm} = \bar{q}_{\theta km} = 0 \quad ,$$

$$\bar{q}^{(1)}_{rkm} = 0 \quad ,$$

$$\bar{q}^{(2)}_{rkm} = 0 \quad ,$$

$$\bar{q}^{(3)}_{rkm} = \left(\Omega^2 \bar{\bar{q}}^{(1)}_{rkm} + \Omega \bar{\bar{q}}^{(2)}_{rkm} + \Omega \bar{\bar{q}}^{(3)}_{rkm} \right) \quad . \tag{3.109}$$

The matrix equation (3.105) can, therefore, be written in the form

$$\Omega^2 \left[M \right] \left\{ X \right\} + \Omega \left[C \right] \left\{ X \right\} + \left[K \right] \left\{ X \right\} = \left\{ 0 \right\} \quad , \tag{3.110}$$

where $\{X\}$ is as defined in (3.106) and the matrices $[M]$, $[C]$ and $[K]$ are given in Appendix H.

Using the following equation

$$\{Y\} = \begin{bmatrix} \{X\} \\ \Omega\{X\} \end{bmatrix} , \tag{3.111}$$

we can reduce the second-order equation (3.110) to a first-order equation i.e.,

$$\left[\begin{bmatrix} [0] & [I] \\ [K] & [C] \end{bmatrix} + \Omega \begin{bmatrix} [-I] & [0] \\ [0] & [M] \end{bmatrix}\right]\{Y\} = \{0\} , \tag{3.112}$$

or

$$\Big[[P] + \Omega[Q]\Big]\{Y\} = \{0\} , \tag{3.113}$$

where [I] is the identity matrix.

Thus, the problem for incompressible inviscid flow is now reduced to one of solving for the eigenvalues of equation (3.113).

CHAPTER IV

METHOD OF SOLUTION II:

TRAVELLING WAVE-TYPE SOLUTION

In this Chapter the shell is assumed to be simply supported at both ends. The fluid forces are evaluated using a travelling wave-type solution.

Accordingly, the displacements u, v and w of the cylindrical shell are expressed in the following form

$$u(x,\theta,t) = i\, A_n \cos n\theta\, e^{i(\omega t-kx)} , \tag{4.1}$$

$$v(x,\theta,t) = B_n \sin n\theta\, e^{i(\omega t-kx)} , \tag{4.2}$$

$$w(x,\theta,t) = C_n \cos n\theta\, e^{i(\omega t-kx)} , \tag{4.3}$$

where A_n, B_n and C_n are constant coefficients and n is the circumferential wave number, k is the wave number of the axially travelling disturbances and ω the frequency of the disturbance. The perturbation velocities are assumed to have the following form:

$$\phi\ (x,\theta,r,t) = \bar{\phi}(r) \cos n\theta\, e^{i(\omega t-kx)} , \tag{4.4}$$

$$\psi_x\ (x,\theta,r,t) = \bar{\psi}_x\ (r) \sin n\theta\, e^{i(\omega t-kx)} , \tag{4.5}$$

$$\psi_r\ (x,\theta,r,t) = \bar{\psi}_r\ (r) \sin n\theta\, e^{i(\omega t-kx)} , \tag{4.6}$$

$$\psi_\theta\ (x,\theta,r,t) = \bar{\psi}_\theta\ (r) \cos n\theta\, e^{i(\omega t-kx)} , \tag{4.7}$$

where it is understood that the above relations are equally applicable for the internal and annular flow regions. In the forthcoming analysis, a subscript i is added to the pertinent equations to denote the inner flow, while the annular flow is denoted by a subscript o.

It is appropriate to mention that, the derivation of fluid forces here is very similar to what has been presented in Chapter III, but it is convenient to present this method in a separate chapter to avoid confusion between the two methods. The structure of this chapter parallels closely that of the previous one.

4.1 SOLUTION TO THE VELOCITY PERTURBATIONS

The velocity perturbations are governed by equations (2.28) and (2.37)-(2.39).

When the solution for ϕ given by equation (4.4) is substituted into equation (2.28), we obtain

$$\frac{\partial^2 \bar{\phi}}{\partial r^2} + \frac{1}{r}\frac{\partial \bar{\phi}}{\partial r} - \left(k^2 + \frac{n^2}{r^2} \right) \bar{\phi} = 0 . \tag{4.8}$$

Equation (4.8) is in the form of a modified Bessel equation of order n which has a complete solution

$$\bar{\phi}(r) = C_1 \, I_n(kr) + C_2 \, K_n(kr) , \tag{4.9}$$

where C_1 and C_2 are constants and $I_n(kr)$ and $K_n(kr)$ are the nth order Bessel functions of the first and second kind, respectively.

Upon substituting the solutions for ψ_r and ψ_θ given by (4.6) and (4.7) into equations (2.38) and (2.39), we obtain

$$i\omega \, \bar{\psi}_r = \nu \left[\frac{\partial^2 \bar{\psi}_r}{\partial r^2} + \frac{1}{r}\frac{\partial \bar{\psi}_r}{\partial r} - \left(\frac{n^2}{r^2} + k^2 + \frac{1}{r^2} \right) \bar{\psi}_r + \frac{2}{r^2} \, n \, \bar{\psi}_\theta \right] , \tag{4.9}$$

and

$$i\omega \, \bar{\psi}_\theta = \nu \left[\frac{\partial^2 \bar{\psi}_\theta}{\partial r^2} + \frac{1}{r}\frac{\partial \bar{\psi}_\theta}{\partial r} - \left(\frac{n^2}{r^2} + k^2 + \frac{1}{r^2} \right) \bar{\psi}_\theta + \frac{2}{r^2} \, n \, \bar{\psi}_r \right] . \tag{4.10}$$

Equations (4.9) and (4.10) are reduced to one single equation for $\bar{\psi}_r = - \bar{\psi}_\theta$; this equation is

$$\frac{\partial^2\bar{\psi}_r}{\partial r^2} + \frac{1}{r}\frac{\partial\bar{\psi}_r}{\partial r} - \left(\frac{i\omega}{\upsilon} + k^2 + \frac{(n+1)^2}{r^2} \right) \bar{\psi}_r = 0 \ . \tag{4.11}$$

Similarly, the solution for ψ_x given by (4.5) is substituted into equation (2.37), leading to

$$\frac{\partial^2\bar{\psi}_x}{\partial r^2} + \frac{1}{r}\frac{\partial\bar{\psi}_x}{\partial r} - \left(\frac{i\omega}{\upsilon} + k^2 + \frac{n^2}{r^2}\right) \bar{\psi}_x = 0 \ . \tag{4.12}$$

Equations (4.11) and (4.12) are modified Bessels function and admit the following solutions

$$\bar{\psi}_x(r) = C_3\ I_n(\beta r) + C_4\ K_n(\beta r) \quad , \tag{4.13}$$

and

$$\bar{\psi}_r(r) = -\ \bar{\psi}_\theta(r) = C_5\ I_{n+1}(\beta r) + C_6\ K_{n+1}(\beta r) \ , \tag{4.14}$$

where

$$\beta^2 = \left(\frac{i\omega}{\upsilon} + k^2 \right) \ .$$

4.2 DERIVATION OF THE UNSTEADY FLUID FORCES

The unsteady fluid stresses for the inner and annular regions are given in Chapter II by equations (2.24)-(2.26), repeated here for convenience:

$$\tau_{rx} = \mu \left[2\ \frac{\partial^2\phi}{\partial x\partial r} + \frac{1}{r}\ \frac{\partial^2\psi_x}{\partial x\partial\theta} - \frac{\partial^2\psi_\theta}{\partial x^2} - \frac{\psi_\theta}{r^2} + \frac{1}{r}\ \frac{\partial\psi_\theta}{\partial r} + \frac{\partial^2\psi_\theta}{\partial r^2} + \frac{1}{r^2}\ \frac{\partial\psi_r}{\partial\theta} - \frac{1}{r}\ \frac{\partial^2\psi_r}{\partial\theta\partial r} \right] , \tag{2.24}$$

$$\tau_{r\theta} = \mu \left[\frac{-2}{r^2}\ \frac{\partial\phi}{\partial\theta} + \frac{2}{r}\ \frac{\partial^2\phi}{\partial\theta\partial r} + \frac{1}{r}\ \frac{\partial\psi_x}{\partial r} - \frac{\partial^2\psi_x}{\partial r^2} + \frac{1}{r^2}\ \frac{\partial^2\psi_x}{\partial\theta^2} - \frac{1}{r}\ \frac{\partial^2\psi_\theta}{\partial\theta\partial x} + \frac{\partial^2\psi_r}{\partial x\partial r} - \frac{1}{r}\ \frac{\partial\psi_r}{\partial x} \right] , \tag{2.25}$$

$$\tau'_{rr} = - p' + 2\mu \left(\frac{\partial^2\phi}{\partial r^2} - \frac{1}{r^2}\frac{\partial\psi_x}{\partial\theta} + \frac{1}{r}\frac{\partial^2\psi_x}{\partial\theta\partial r} - \frac{\partial^2\psi_\theta}{\partial x\partial r} \right) , \tag{2.26}$$

where τ'_{rx}, $\tau'_{r\theta}$, τ'_{rr}, and p' may be expressed as

$$\tau'_{rx}(x,\theta,r,t) = \bar{\tau}'_{rx}(r) \cos n\theta \; e^{i(\omega t-kx)} , \tag{4.15}$$

$$\tau'_{r\theta}(x,\theta,r,t) = \bar{\tau}'_{r\theta}(r) \sin n\theta \; e^{i(\omega t-kx)} , \tag{4.16}$$

$$\tau'_{rr}(x,\theta,r,t) = \bar{\tau}'_{rr}(r) \cos n\theta \; e^{i(\omega t-kx)} , \tag{4.17}$$

$$p'(x,\theta,r,t) = \bar{p}'(r) \cos n\theta \; e^{i(\omega t-kx)} . \tag{4.18}$$

Upon substituting the assumed solution for ϕ, ψ_x, ψ_r, ψ_θ, τ'_{rx}, $\tau'_{r\theta}$, τ'_{rr} and p', equations (2.24)-(2.26) become

$$\bar{\tau}'_{rx}(r) = \mu \left(-2ik \frac{\partial\bar{\phi}}{\partial r} - \frac{ink}{r}\bar{\psi}_x + k^2 \bar{\psi}_\theta - \frac{\bar{\psi}_\theta}{r^2} + \frac{1}{r}\frac{\partial\bar{\psi}_\theta}{\partial r} + \frac{\partial^2\bar{\psi}_\theta}{\partial r^2} + \frac{n}{r^2}\bar{\psi}_r - \frac{n}{r}\frac{\partial\bar{\psi}_r}{\partial r} \right) , \tag{4.19}$$

$$\bar{\tau}'_{r\theta}(r) = \mu \left(\frac{2n}{r^2}\bar{\phi} - \frac{2n}{r}\frac{\partial\bar{\phi}}{\partial r} - \frac{n^2}{r^2}\bar{\psi}_x + \frac{1}{r}\frac{\partial\bar{\psi}_x}{\partial r} - \frac{\partial^2\bar{\psi}_x}{\partial r^2} - ikn\frac{\bar{\psi}_\theta}{r} + \frac{ik}{r}\bar{\psi}_r - ik\frac{\partial\bar{\psi}_r}{\partial r} \right) , \tag{4.20}$$

$$\bar{\tau}'_{rr}(r) = - p' + 2\mu \left(\frac{\partial^2\bar{\phi}}{\partial r^2} - \frac{n}{r^2}\bar{\psi}_x + \frac{n}{r}\frac{\partial\bar{\psi}_x}{\partial r} + ik\frac{\partial\bar{\psi}_\theta}{\partial r} \right) . \tag{4.21}$$

The solutions of these equations for internal and annular flow are given in Sections 4.3 and 4.4, respectively.

4.3 SOLUTION FOR THE INNER FLOW

In order to represent the inner flow, a subscript i is added to the foregoing, i.e.,

$$\bar{\phi}_i(r) = C_{1i}\, I_n(kr) + C_{2i}\, K_n(kr) , \tag{4.22}$$

$$\bar{\psi}_x(r) = C_{3i}\, I_n(\beta_i r) + C_{4i}\, K_n(\beta_i r), \tag{4.23}$$

$$\bar{\psi}_r(r) = C_{5i}\, I_{n+1}(\beta_i r) + C_{6i}\, K_{n+1}(\beta_i r), \tag{4.24}$$

Since $K_n(kr)$, $K_n(\beta r)$ and $K_{n+1}(\beta r)$ become infinitely large at $r \longrightarrow 0$, one must have

$$C_{2i} = C_{4i} = C_{6i} = 0.$$

Hence, the solutions simplify to

$$\bar{\phi}_i(r) = C_{1i}\, I_n(kr)\ , \tag{4.25}$$

$$\bar{\psi}_{xi}(r) = C_{3i}\, I_n(\beta_i r)\ , \tag{4.26}$$

$$\bar{\psi}_{ri}(r) = C_{5i}\, I_{n+1}(\beta_i r)\ , \tag{4.27}$$

where C_{1i}, C_{3i} and C_{5i} are constants to be determined.

4.3.1 Boundary Conditions

Upon substituting the solutions for ϕ_i, ψ_{xi}, $\psi_{\theta i}$, ψ_{ri}, u, v and w into the boundary conditions equations (2.56)-(2.58), we obtain

$$\left(-ik\, \bar{\phi}_i - \frac{n+1}{r}\, \bar{\psi}_{ri} - \frac{\partial \bar{\psi}_{ri}}{\partial r} \right)_{r=a_i-\delta} = \left(-\omega + k\, U_{\delta i} \right) A_n\ , \tag{4.28}$$

$$\left[-\frac{n}{r}\, \bar{\phi}_i + (-ik)\, \bar{\psi}_{ri} - \frac{\partial \bar{\psi}_{xi}}{\partial r} \right]_{r=a_i-\delta} = i\, \left(\omega - k\, U_{\delta i} \right) B_n\ , \tag{4.29}$$

$$\left[\frac{\partial \bar{\phi}_i}{\partial r} + \frac{n}{r}\, \bar{\psi}_{xi} - ik\, \bar{\psi}_{ri} \right]_{r=a_i-\delta} = i\, \left(\omega - k\, U_{\delta i} \right) C_n\ , \tag{4.30}$$

Substituting for $\bar{\phi}_i$, $\bar{\psi}_{xi}$, $\bar{\psi}_{ri}$, $\bar{\psi}_{\theta i}$ from equation (4.25)-(4.27) and using the following nondimensional terms

$$\bar{\alpha} = k a_i\ ,\quad \bar{\beta}_i = \beta_i a_i,\quad \bar{A}_n = \frac{A_n}{L}\ ,\quad \bar{B}_n = \frac{B_n}{L}\ ,\quad \bar{C}_n = \frac{C_n}{L}\ , \tag{4.31}$$

the boundary conditions may be written as

$$i\bar{\alpha}\, I_n(\bar{\alpha})\, \bar{C}_{1i} + \left\{ (n+1)\, I_{n+1}(\bar{\beta}_i) + \bar{\beta}_i\, I'_{n+1}(\bar{\beta}_i) \right\} \bar{C}_{5i} = \mathrm{U}\,(\Omega - \bar{\alpha}\, \bar{U}_{\delta i})\, \bar{A}_n \;, \quad (4.32)$$

$$-n\, I_n(\bar{\alpha})\, \bar{C}_{1i} - \bar{\beta}_i\, I'_n(\bar{\beta}_i)\, \bar{C}_{3i} - i\bar{\alpha}\, I_{n+1}(\bar{\beta}_i)\, \bar{C}_{5i} = i\mathrm{U}\,(\Omega - \bar{\alpha}\, \bar{U}_{\delta i})\, \bar{B}_n \;, \quad (4.33)$$

$$\bar{\alpha}\, I'_n(\bar{\alpha})\, \bar{C}_{1i} + n\, I_n(\bar{\beta}_i)\, \bar{C}_{3i} - i\bar{\alpha}\, I_{n+1}(\bar{\beta}_i)\, \bar{C}_{5i} = i\mathrm{U}\,(\Omega - \bar{\alpha}\, \bar{U}_{\delta i})\, \bar{C}_n \;, \quad (4.34)$$

where U, Ω, $\bar{U}_{\delta i}$, are the dimensionless terms given by equation (3.36), and $\bar{C}_{1i}$, $\bar{C}_{3i}$, $\bar{C}_{5i}$ are defined in equations (3.41).

4.3.2 Unsteady Fluid Forces For Inner Flow

The unsteady fluid stresses for the inner flow are given by equations (4.19)-(4.21) with a subscript i. Substituting for $\bar{\phi}_i$, $\bar{\psi}_{xi}$, $\bar{\psi}_{\theta i}$ and $\bar{\psi}_{ri}$ into the stress equations and using the dimensionless terms, the unsteady stresses are:

$$\bar{\tau}'_{rxi} = \frac{\rho_i \mathrm{U}}{\epsilon_i^2\, \xi_i} \Big[2\, i\bar{\alpha}^2\, I'_n(\bar{\alpha})\, \bar{C}_{1i} + (-in\, \bar{\alpha}\, I_n(\bar{\beta}_i))\, \bar{C}_{3i} + \big((1 - \bar{\alpha}^2 + n)\, I_{n+1}(\bar{\beta}_i) - \bar{\beta}_i (n+1)\, I'_{n+1}(\bar{\beta}_i) - \bar{\beta}_i^2\, I''_{n+1}(\bar{\beta}_i) \big)\, \bar{C}_{5i} \Big] , \quad (4.35)$$

$$\bar{\tau}'_{r\theta i} = \frac{\rho_i \mathrm{U}}{\epsilon_i^2\, \xi_i} \Big[\big[2n\, I_n(\bar{\alpha}) - 2n\, \bar{\alpha}\, I'_n(\bar{\alpha}) \big]\, \bar{C}_{1i} + \big[-n^2\, I_n(\bar{\beta}_i) + \bar{\beta}_i\, I'_n(\bar{\beta}_i) - \bar{\beta}_i^2\, I''_n(\bar{\beta}_i) \big]\, \bar{C}_{3i} + \big[i\, \bar{\alpha}\, (1+n)\, I_{n+1}(\bar{\beta}_i) - i\bar{\alpha}\, \bar{\beta}_i\, I'_{n+1}(\bar{\beta}_i) \big]\, \bar{C}_{5i} \Big] , \quad (4.36)$$

$$\bar{\tau}'_{rri} = \rho_i U \left[\begin{array}{l} \left[\bar{p}'_{1i} + 2\,\dfrac{\bar{\alpha}^2}{\xi_i}\,\dfrac{I''_n}{\epsilon_i^2}(\bar{\alpha}) \right] \bar{C}_{1i} \\ + \left[\bar{p}'_{2i} + \dfrac{2}{\xi_i \epsilon_i^2}\left((\bar{\beta}_i\, n\, I'_n(\bar{\beta}_i) - n\, I_n(\bar{\beta}_i)\right) \right] \bar{C}_{3i} \\ + \left[\bar{p}'_{3i} + \dfrac{2}{\xi_i \epsilon_i^2}\left(-i\,\bar{\alpha}\,\bar{\beta}_i \right) I'_{n+1}(\bar{\beta}_i) \right] \bar{C}_{5i} \end{array} \right] , \qquad (4.37)$$

where $\bar{p}'_{1i}$, $\bar{p}'_{2i}$ and $\bar{p}'_{3i}$ are given in Appendix D.

4.4 SOLUTION FOR THE ANNULAR FLOW

The solution for the annular flow is expressed by putting a subscript o to the velocity perturbation equations, which gives:

$$\bar{\phi}_o(r) = C_{1o}\, I_n(kr) + C_{2o}\, K_n(kr) \quad , \qquad (4.38)$$

$$\bar{\psi}_{xo}(r) = C_{3o}\, I_n(\beta_o r) + C_{4o}\, K_n(\beta_o r) \quad , \qquad (4.39)$$

$$\bar{\psi}_{ro}(r) = -\,\bar{\psi}_{\theta o}(r) = C_{5o}\, I_{n+1}(\beta_o r) + C_{6o}\, K_{n+1}(\beta_o r) \quad , \qquad (4.40)$$

where C_{1o}, C_{2o}, C_{3o}, C_{4o}, C_{5o} and C_{6o} are constants to be determined.

4.4.1 Boundary Conditions

Upon substituting the solutions ϕ_o, ψ_{xo} $\psi_{\theta o}$ and ψ_{ro} given by equations (4.4)-(4.7) into equations (2.61)-(2.66), we obtain at $r = a_i + \delta$

$$\left(-ik\,\bar{\phi}_o - \frac{(n+1)}{r}\,\bar{\psi}_{ro} - \frac{\partial \bar{\psi}_{ro}}{\partial r} \right)\Bigg|_{r=a_i+\delta} = \left(-\omega + U_{\delta o} k \right) A_n \; , \qquad (4.41)$$

$$\left(-\frac{n}{r}\,\bar{\phi}_o - \frac{\partial \bar{\psi}_{xo}}{\partial r} - ik\,\bar{\psi}_{ro} \right)\Bigg|_{r=a_i+\delta} = i\left(\omega - U_{\delta o}\, k \right) B_n \; , \qquad (4.42)$$

$$\left(\frac{\partial \bar{\phi}_o}{\partial r} + \frac{n}{r}\,\bar{\psi}_{xo} - ik\,\bar{\psi}_{ro} \right)\Bigg|_{r=a_i+\delta} = i\left(\omega - \bar{U}_{\delta o}\, k \right) C_n \; , \qquad (4.43)$$

and at a_o

$$\left(-ik\,\bar{\phi}_o - \frac{(n+1)}{r}\,\bar{\psi}_{ro} - \frac{\partial \bar{\psi}_{ro}}{\partial r} \right)_{r=a_o} = 0\,, \tag{4.44}$$

$$\left(-\frac{n}{r}\,\bar{\phi}_o - \frac{\partial \bar{\psi}_{xo}}{\partial r} - ik\,\bar{\psi}_{ro} \right)_{r=a_o} = 0\,, \tag{4.45}$$

$$\left(\frac{\partial \bar{\phi}_o}{\partial r} + \frac{n}{r}\,\bar{\psi}_{xo} - ik\,\bar{\psi}_{ro} \right)_{r=a_o} = 0\,. \tag{4.46}$$

Substituting equations (4.38)-(4.40) into equations (4.41)-(4.46) and using the nondimensional terms given by equation (3.55), we obtain

at $r = a_i + \delta$

$$i\,\bar{\alpha}\,I_n(\bar{\alpha})\,\bar{C}_{1o} + i\,\bar{\alpha}\,K_n(\bar{\alpha})\,\bar{C}_{2o} + \left\{ (n+1)\,I_{n+1}(\bar{\beta}_o) + \bar{\beta}_o\,I'_{n+1}(\bar{\beta}_o) \right\}\bar{C}_{5o}$$
$$+ \left\{ (n+1)\,K_{n+1}(\bar{\beta}_o) + \bar{\beta}_o\,K'_{n+1}(\bar{\beta}_o) \right\}\bar{C}_{6o} = \mu\,(\Omega - \bar{\alpha}\,\bar{U}_{\delta o})\,\bar{A}_n\,, \tag{4.47}$$

$$-n\,I_n(\bar{\alpha})\,\bar{C}_{1o} - n\,K_n(\bar{\alpha})\,\bar{C}_{2o} - \bar{\beta}_o\,I'_n(\bar{\beta}_o)\,\bar{C}_{3o} - \bar{\beta}_o\,K'_n(\bar{\beta}_o)\,\bar{C}_{4o}$$
$$- i\,\bar{\alpha}\,I_{n+1}(\bar{\beta}_o)\,\bar{C}_{5o} - i\,\bar{\alpha}\,K_{n+1}(\bar{\beta}_o)\,\bar{C}_{6o} = i\mu\,(\Omega - \bar{\alpha}\,\bar{U}_{\delta o})\bar{B}_n\,, \tag{4.48}$$

$$\bar{\alpha}\,I'_n(\bar{\alpha})\,\bar{C}_{1o} + \bar{\alpha}\,K'_n(\bar{\alpha})\,\bar{C}_{2o} + n\,I_n(\bar{\beta}_o)\,\bar{C}_{3o} + n\,K_n(\bar{\beta}_o)\,\bar{C}_{4o}$$
$$- i\,\bar{\alpha}\,I_{n+1}(\bar{\beta}_o)\,\bar{C}_{5o} - i\,\bar{\alpha}\,K_{n+1}(\bar{\beta}_o)\,\bar{C}_{6o} = i\mu\,(\Omega - \bar{\alpha}\,\bar{U}_{\delta o})\,\bar{C}_n\,, \tag{4.49}$$

and, at $r = a_o$

$$i\,\bar{\alpha}\,\epsilon_r\,I_n(\bar{\alpha}\epsilon_r)\,\bar{C}_{1o} + i\,\bar{\alpha}\,\epsilon_r\,K_n(\bar{\alpha}\epsilon_r)\,\bar{C}_{2o} +$$
$$\left\{ (n+1)\,I_{n+1}(\bar{\beta}_o\,\epsilon_r) + \bar{\beta}_o\,\epsilon_r\,I'_{n+1}(\bar{\beta}_o\,\epsilon_r) \right\}\bar{C}_{5o} +$$
$$\left\{ (n+1)\,K_{n+1}(\epsilon_r\,\bar{\beta}_o) + \bar{\beta}_o\,\epsilon_r\,K'_{n+1}(\bar{\beta}_o\,\epsilon_r) \right\}\bar{C}_{6o} = 0, \tag{4.50}$$

$$- n\, I_n(\bar{\alpha}\epsilon_r)\, \bar{C}_{1o} - n\, K_n(\bar{\alpha}\epsilon_r)\, \bar{C}_{2o} - \bar{\beta}_o\, \epsilon_r\, I_n'(\bar{\beta}_o\, \epsilon_r)\, \bar{C}_{3o} - \bar{\beta}_o\, \epsilon_r\, K_n'(\bar{\beta}_o\, \epsilon_r)\, \bar{C}_{4o}$$

$$- i\bar{\alpha}\, \epsilon_r\, I_{n+1}(\bar{\beta}_o\, \epsilon_r)\, \bar{C}_{5o} - i\bar{\alpha}\, \epsilon_r\, K_{n+1}(\bar{\beta}_o\, \epsilon_r)\, \bar{C}_{6o} = 0\,, \qquad (4.51)$$

$$\bar{\alpha}\, \epsilon_r\, I_n'(\bar{\alpha}\epsilon_r)\, \bar{C}_{1o} + \bar{\alpha}\, \epsilon_r\, K_n'(\bar{\alpha}\epsilon_r)\, \bar{C}_{2o} + n\, I_n(\bar{\beta}_o\, \epsilon_r)\, \bar{C}_{3o} + n\, K_n(\bar{\beta}_o\, \epsilon_r)\, \bar{C}_{4o}$$

$$- i\bar{\alpha}\, \epsilon_r\, I_{n+1}(\bar{\beta}_o\, \epsilon_r)\, \bar{C}_{5o} - i\bar{\alpha}\, \epsilon_r\, K_{n+1}(\bar{\beta}_o\, \epsilon_r)\, \bar{C}_{6o} = 0\,, \qquad (4.52)$$

where $\bar{\beta}_o = \beta_o a_i$, $\epsilon_r = \dfrac{a_o}{a_i}$ and $\bar{\alpha}$ is defined by equation (4.31).

4.4.2 Unsteady Fluid Forces for Annular Flow

The fluid forces in the annular flow are obtained by putting a subscript o in the stress equations (4.19)-(4.21). In a similar analysis as for the inner flow, the solutions for $\bar{\phi}_o$, $\bar{\psi}_{xo}$, $\bar{\psi}_{ro}$, $\bar{\psi}_{\theta o}$ from equation (4.38) -(4.40) are substituted into equations (4.19)-(4.21), and that leads to

$$\bar{\tau}'_{rxo} = \frac{\rho_i \rho_r U}{\epsilon_i^2 \xi_i \xi_r} \left[\begin{array}{l} - 2i\, \bar{\alpha}^2\, I_n'(\bar{\alpha})\, \bar{C}_{1o} - 2i\, \bar{\alpha}^2\, K_n'(\bar{\alpha})\, \bar{C}_{2o} \\ - in\bar{\alpha}\, I_n(\bar{\beta}_o)\, \bar{C}_{3o} - in\bar{\alpha}\, K_n(\bar{\beta}_o)\, \bar{C}_{4o} \\ + \left[\begin{array}{l} \left(1 - \bar{\alpha}^2 + n\right) I_{n+1}(\bar{\beta}_o) - \bar{\beta}_o(1+n)\, I_{n+1}'(\bar{\beta}_o) \\ - \bar{\beta}_o^2\, I_{n+1}''(\bar{\beta}_o) \end{array} \right] \bar{C}_{5o} \\ + \left[\begin{array}{l} \left(1 - \bar{\alpha}^2 + n\right) K_{n+1}(\bar{\beta}_o) - \bar{\beta}_o(1+n)\, K_{n+1}'(\bar{\beta}_o) \\ - \bar{\beta}_o^2\, K_{n+1}''(\bar{\beta}_o) \end{array} \right] \bar{C}_{6o} \end{array} \right]$$

(4.53)

$$\bar{\tau}'_{r\theta o} = \frac{\rho_r \rho_i \mu}{\epsilon_i^2 \xi_i \xi_r} \left[\begin{aligned} & \left\{ 2n\, I_n(\bar{\alpha}) - 2n\, \bar{\alpha}\, I'_n(\bar{\alpha}) \right\} \bar{C}_{1o} \\ + & \left\{ 2n\, K_n(\bar{\alpha}) - 2n\, \bar{\alpha}\, K'_n(\bar{\alpha}) \right\} \bar{C}_{2o} \\ + & \left\{ -n^2\, I_n(\bar{\beta}_o) + \bar{\beta}_o\, I'_n(\bar{\beta}_o) - \bar{\beta}_o^2\, I''_n(\bar{\beta}_o) \right\} \bar{C}_{3o} \\ + & \left\{ -n^2\, K_n(\bar{\beta}_o) + \bar{\beta}_o\, K'_n(\bar{\beta}_o) - \bar{\beta}_o^2\, K''_n(\bar{\beta}_o) \right\} \bar{C}_{4o} \\ + & \left\{ i\bar{\alpha}\,(n+1)\, I_{n+1}(\bar{\beta}_o) - i\bar{\alpha}\, \bar{\beta}_o\, I'_{n+1}(\bar{\beta}_o) \right\} \bar{C}_{5o} \\ + & \left\{ i\bar{\alpha}\,(n+1)\, K_{n+1}(\bar{\beta}_o) - i\bar{\alpha}\, \bar{\beta}_o\, K'_{n+1}(\bar{\beta}_o) \right\} \bar{C}_{6o} \end{aligned} \right], \tag{4.54}$$

and

$$\tau'_{rro} = \rho_r \rho_i \mu \left[\begin{aligned} & \left\{ \bar{p}'_{1Io} + 2\, \frac{\bar{\alpha}^2}{\xi_i \xi_r}\, \frac{I''_n(\bar{\alpha})}{\epsilon_i^2} \right\} \bar{C}_{1o} \\ + & \left\{ \bar{p}'_{1Ko} + 2\, \frac{\bar{\alpha}^2}{\xi_i \xi_r}\, \frac{K''_n(\bar{\alpha})}{\epsilon_i^2} \right\} \bar{C}_{2o} \\ + & \left\{ \bar{p}'_{2Io} + \frac{2}{\xi_i \xi_r \epsilon_i^2} \left[\bar{\beta}_o\, n\, I'_n(\bar{\beta}_o) - n\, I_n(\bar{\beta}_o) \right] \right\} \bar{C}_{3o} \\ + & \left\{ \bar{p}'_{2Ko} + \frac{2}{\xi_i \xi_r \epsilon_i^2} \left[\bar{\beta}_o\, n\, K'_n(\bar{\beta}_o) - n\, K_n(\bar{\beta}_o) \right] \right\} \bar{C}_{4o} \\ + & \left\{ \bar{p}'_{3Io} + \frac{2}{\xi_i \xi_r \epsilon_i^2} \left(-i\bar{\alpha}\, \bar{\beta}_o \right) I'_{n+1}(\bar{\beta}_o) \right\} \bar{C}_{5o} \\ + & \left\{ \bar{p}'_{3Ko} + \frac{2}{\xi_i \xi_r \epsilon_i^2} \left(-i\bar{\alpha}\, \bar{\beta}_o \right) K'_{n+1}(\bar{\beta}_o) \right\} \bar{C}_{6o} \end{aligned} \right] \tag{4.55}$$

where $\rho_r = \frac{\rho_o}{\rho_i}$, $\xi_r = \frac{\xi_o}{\xi_i}$, and $\bar{p}'_{1Io}$, $\bar{p}'_{1Ko}$, $\bar{p}'_{2Io}$, $\bar{p}'_{2Ko}$, $\bar{p}'_{3Io}$ and $\bar{p}'_{3Ko}$ represent the effect of the pressure perturbations in the annulus and expressions for these terms are given in Appendix D.

4.5 DETERMINATION OF THE UNSTEADY FLUID LOADING ON THE SHELL

The net fluid loads on the shell arising from the perturbation terms are

$$q_x = \left(\tau'_{rxi} \Big|_{r=a_i-\delta} - \tau'_{rxo} \Big|_{a_i+\delta} \right) , \tag{4.56}$$

$$q_\theta = \left(\tau'_{r\theta i} \Big|_{r=a_i-\delta} - \tau'_{r\theta o} \Big|_{r=a_i+\delta} \right) , \tag{4.57}$$

$$q_r = \left(\tau'_{rri} \Big|_{r=a_i-\delta} - \tau'_{rro} \Big|_{r=a_i+\delta} \right) , \tag{4.58}$$

where q_x, q_θ and q_r are the axial, circumferential and radial loads, respectively. Equations (4.56), (4.57) and (4.58) may be written in the following form:

$$q_x = \bar{q}_x(r) \cos n\theta \; e^{i(\omega t - kx)} , \tag{4.59}$$

$$q_\theta = \bar{q}_\theta(r) \sin n\theta \; e^{i(\omega t - kx)} , \tag{4.60}$$

$$q_r = \bar{q}_r(r) \cos n\theta \; e^{i(\omega t - kx)} , \tag{4.61}$$

where

$$\bar{q}_x(r) = \left(\bar{\tau}'_{rxi}(r) \Big|_{a_i-\delta} - \bar{\tau}'_{rxo}(r) \Big|_{a_i+\delta} \right) , \tag{4.62}$$

$$\bar{q}_\theta(r) = \left(\bar{\tau}'_{r\theta i}(r) \Big|_{a_i-\delta} - \bar{\tau}'_{r\theta o}(r) \Big|_{a_i+\delta} \right) , \tag{4.63}$$

$$\bar{q}_r(r) = \left(\bar{\tau}'_{rri}(r)\Big|_{a_i-\delta} - \bar{\tau}'_{rro}(r)\Big|_{a_i+\delta} \right) . \tag{4.64}$$

The fluid loading is found following the same analysis as in Chapter III. The boundary condition equations and the stress equations are put in matrix form as in equations (3.85) and (3.86). Finally, the fluid loading may be written as

$$\left[T\right] \left[B\right]^{-1} \left[R\right] = \left[\bar{q}\right] , \tag{4.65}$$

where $\{\bar{q}\}$ now represents $\{\bar{q}_x, \bar{q}_\theta, \bar{q}_r\}^T$.

The elements of matrices [T] and [B] are given in Appendix E.

The unsteady fluid stresses are evaluated as in equations (4.56)-(4.58). However, these stresses are expressed in a generalized force form in connection with the weighted residual method used in the solution of the equations of motion. The amplitudes of these generalized forces are defined here as

$$\bar{\bar{q}}_x = \frac{\gamma}{\rho_s h} \int_0^L \sin\frac{j\pi x}{L}\, \bar{q}_x\, e^{-ikx}\, dx , \tag{4.66}$$

$$\bar{\bar{q}}_\theta = \frac{\gamma}{\rho_s h} \int_0^L \sin\frac{j\pi x}{L}\, \bar{q}_\theta\, e^{-ikx}\, dx , \tag{4.67}$$

$$\bar{\bar{q}}_r = \frac{\gamma}{\rho_s h} \int_0^L \sin\frac{j\pi x}{L}\, \bar{q}_r\, e^{-ikx}\, dx , \tag{4.68}$$

Finally, the generalized fluid - forces are expressed in terms of the shell displacements, as follows:

$$\bar{q}_x = \bar{\bar{q}}_{x1}\,\bar{A}_n + \bar{\bar{q}}_{x2}\,\bar{B}_n + \bar{\bar{q}}_{x3}\,\bar{C}_n\ , \tag{4.69}$$

$$\bar{q}_\theta = \bar{\bar{q}}_{\theta 1}\,\bar{A}_n + \bar{\bar{q}}_{\theta 2}\,\bar{B}_n + \bar{\bar{q}}_{\theta 3}\,\bar{C}_n\ , \tag{4.70}$$

$$\bar{q}_r = \bar{\bar{q}}_{r1}\,\bar{A}_n + \bar{\bar{q}}_{r2}\,\bar{B}_n + \bar{\bar{q}}_{r3}\,\bar{C}_n\ , \tag{4.71}$$

where expressions for $\bar{\bar{q}}_{x1}$, $\bar{\bar{q}}_{x2}$, $\bar{\bar{q}}_{x3}$, $\bar{\bar{q}}_{\theta 1}$, $\bar{\bar{q}}_{\theta 2}$, $\bar{\bar{q}}_{\theta 3}$, $\bar{\bar{q}}_{r1}$, $\bar{\bar{q}}_{r2}$, and $\bar{\bar{q}}_{r3}$ are given in Appendix E, equations (E.2.6).

4.6 SOLUTION OF THE EQUATIONS OF MOTION

Similarly to Galerkin's method used in Chapter III, a weighted residual method is used here. The shell equation (2.5)-(2.7) are weighted by a sine function which satisfies the pinned-pinned condition at either end of the flexible shell. The weighting function is given by

$$f(x) = \sin\frac{j\pi x}{L}\ ; \tag{4.72}$$

the solution to the equations of motion may be written in operator form

$$\int_0^L f_j(x)\ \mathcal{L}(u,v,w)\ dx = 0\ . \tag{4.73}$$

After integrating equation (4.73), we obtain the following sets of linear homogeneous algebraic equations:

$$\begin{aligned} A_{jj}^{(1)}\,\bar{A}_n + A_{jj}^{(2)}\,\bar{B}_n + A_{jj}^{(3)}\,\bar{C}_n &= 0\ ,\\ A_{jj}^{(4)}\,\bar{A}_n + A_{jj}^{(5)}\,\bar{B}_n + A_{jj}^{(6)}\,\bar{C}_n &= 0\ ,\\ A_{jj}^{(7)}\,\bar{A}_n + A_{jj}^{(8)}\,\bar{B}_n + A_{jj}^{(9)}\,\bar{C}_n &= 0\ , \end{aligned} \tag{4.74}$$

where the coefficients $\left\{ A_{jj}^{(1)} \ldots\ldots A_{jj}^{(9)} \right\}$ are given in Appendix G.

The set of equations in (4.74) are put into matrix form

$$[A]\ \{X\} = \{0\}, \tag{4.75}$$

where

$$\{X\} = [\bar{A}_n,\ \bar{B}_n,\ \bar{C}_n]^T. \tag{4.76}$$

The frequencies of the system subjected to internal or annular flow can be found by setting the determinant of matrix [A] given by equation (4.75) to zero.

4.7 INVISCID THEORY

Following a similar analysis as in Section 3.5, the unsteady inviscid forces are given by

$$\bar{q}_x = \bar{q}_\theta = 0,$$

$$\bar{q}_{r1} = \bar{q}_{r2} = 0,$$

and

$$\bar{q}_{r3} = \left(\Omega^2\ \bar{q}_{r3}^{(1)} + \Omega\ \bar{q}_{r3}^{(2)} + \bar{q}_{r3}^{(3)} \right) \bar{C}_n\ , \tag{4.77}$$

where the expressions for $\bar{q}_{r3}^{(1)}$, $\bar{q}_{r3}^{(2)}$ and $\bar{q}_{r3}^{(3)}$ are derived in Appendix H. The elements of matrices [M], [K] and [C], in equation (3.112), are given in Appendix H.

CHAPTER V

THEORETICAL RESULTS

In this Chapter, the results of the investigation on the dynamical behaviour of the system, using the methods derived in Chapters III and IV, are presented. The systems considered differ from one another in many ways, according to

(a) whether the flow is internal or annular;

(b) whether the fluid is considered to be inviscid or viscous;

(c) whether the shell is assumed to be pinned or clamped at either end.

The systems considered also differ according to the values assigned to the various system parameters. These parameters are many, e.g. the shell thickness/radius ratio, length/radius ratio, the gap width, various physical properties of the fluid and of the shell materials, etc. It would be interesting to consider all possible combinations. However, that is not practical. The main goal of this study is to investigate the effects of unsteady viscous forces on the stability of a system subjected to internal and annular flow; hence, only the effects of gap width, which has the strongest influence on the unsteady viscous forces, are investigated. In order to assess the effects of unsteady viscous forces, we will be comparing results from the present theory with those from potential flow theory.

In Section 5.1, the stability of the system subjected to unsteady inviscid forces and steady viscous forces is presented using the Fourier Transform method. The same investigation is repeated in Section 5.2 using a travelling wave solution, where the results of the two methods of solution are compared.

The effects of unsteady viscous forces are then investigated in the presence or absence of steady viscous forces. Both methods of solution are considered. However, the effects of annular flow could not be investigated using the Fourier Transform method due to the high computational cost; hence, a detailed investigation on the effect of unsteady and steady viscous forces in internal or annular flow is presented in Section 5.3 using only the travelling wave solution. Finally, the stability of a system subjected to unsteady viscous forces in internal flow is presented in Section 5.4 using the Fourier Transform method.

Calculations are done for a steel shell subjected to water flow. Two gaps have been considered: the so called "1/10 gap-system"† in which the annular gap width is equal to one-tenth of the inner radius, and "1/100 gap-system", in which the gap is one-hundredth of the shell radius. The shell and fluid parameters for the two systems are given in Table 5.1.

---

† For comparison purposes, the parameters for the 1/10 gap-system given in Table 5.1 are the same as in Ref. [48].

Variable Parameters	Steel-water System	
	1/10 gap	1/100 gap
a_i (cm)	9.091	9.9
a_o (cm)	10	10
L (cm)	100	100
h (mm)	0.5	0.5
$\epsilon_i = (a_i/L)$	1/11	.099
$\epsilon_o = (a_o/L)$	1/10	1/10
$\epsilon_r = \frac{a_o}{a_i}$	1.10	1.01
$(h/a_i) \times 10^3$	5.5	5.05
$\eta = \left(\frac{\rho_i a_i}{\rho_s h}\right)$	23.30	25.36
$U = \left[\frac{E}{\rho_s(1-\nu_s^2)}\right]^{1/2}$ (m/s)	5308	5308
$E\ \left(N/m^2\right)$	1.99×10^{11}	1.99×10^{11}
ν_s	0.3	0.3
$\rho_r = \rho_o/\rho_i$	1	1
$\nu_i = \mu_i/\rho_i$ (m^2/s)	1.121×10^{-6}	1.121×10^{-6}

Table 5.1. Fluid used and shell parameters for the two systems in the calculations

It was shown in Ref. [48] that a 1/10 gap steel-water system loses stability first in its third circumferential mode ($n = 3$) for similar parameters as in Table 5.1. For this reason all calculations in this Thesis are done for the third circumferential mode.

Unless otherwise specified, when the system is subjected to internal flow, the annulus is filled with water $\left(\bar{U}_o = 0\right)$; on the other hand, if annular flow effects are investigated, the inner shell is filled with stagnant fluid $\left(\bar{U}_i = 0\right)$.

5.1 EFFECTS OF UNSTEADY INVISCID FORCES AND STEADY VISCOUS FORCES USING FOURIER TRANSFORM METHOD

5.1.1 Effects of the Unsteady Inviscid Forces

This section presents the results obtained for a system subjected to inviscid incompressible flow. The case of a clamped-clamped shell has been considered in detail in Ref. [48]; however, some cases will be presented here for comparison with the results obtained for a shell pinned at both ends.

It is seen in Section 3.5 that for inviscid theory, the governing matrix is reduced to an eigenvalue problem as in equation (3.112). The fluid forces given in Appendix E are evaluated numerically. A copy of the computer program used for this purpose is given in Appendix I. Equation (3.112) is solved using the IMSL subroutine EIGZC which provides the eigenvalues. A copy of the computer program is given in Appendix J. In this case, the steady viscous forces are not included.

5.1.1(a) Comparison with previous methods

The program is first compared with the results obtained earlier by Weaver and Unny [21]. In this case, the system consists of a simply supported steel shell conveying water. The flow is internal only, with no fluid in the annulus. The shell parameters are:

$$\epsilon_i = 1/2, \quad n = 5, \quad \eta = 12.73.$$

The dimensionless critical flow velocities for buckling and coupled-mode flutter obtained here and by Weaver and Unny are compared in Table 5.2. It is seen that the two sets of results are in reasonably good agreement.

	Nondimensional critical flow velocities	
	Buckling	Coupled-mode flutter
Weaver & Unny	5.10×10^{-2}	6.50×10^{-2}
Present work	5.00×10^{-2}	6.80×10^{-2}

Table 5.2. Comparison between present study and results by Weaver and Unny [21].

The difference in the critical flow velocities in the two theories could be attributed to the use of different equations to describe the shell motion (Kempner's equations in the previous work and Flügge's, shell equations in the present work).

5.1.1(b) Internal flow

The results presented here are for the 1/10 gap-system (see Table 5.1). In Fig. 2, the dimensionless frequencies, of the first two axial modes ($m = 1,2$) and the third circumferential mode ($n = 3$), are plotted against the dimensionless internal flow velocity, $\bar{U}_i$.

It is seen that the frequencies associated with the first and second axial modes decrease as the velocity $\bar{U}_i$ increases. The purely real frequency of the first axial mode vanishes at point B ($\bar{U}_i = 0.02$), indicating the loss of stability by buckling. Beyond this point the frequency becomes purely imaginary. However, at a higher flow velocity, point R where ($\bar{U}_i$ = 0.023), the frequency becomes real once more, indicating the restabilization of the system. Then, at point F ($\bar{U}_i$ = 0.024), the loci of the first and second axial modes coalesce. After coalescence, the frequencies become complex conjugate pairs which is the characteristic of coupled mode flutter.

The effect of end conditions is presented in Table 5.3. As expected, a shell with both ends pinned loses stability before a clamped-clamped one.

End conditions	Nondimensional critical flow velocities	
	Buckling	Coupled-mode flutter
Pinned-pinned	2.00×10^{-2}	2.40×10^{-2}
Clamped-clamped	2.50×10^{-2}	3.14×10^{-2}

Table 5.3. Critical flow velocities for buckling for a clamped-clamped and a pinned-pinned system with internal flow.

5.1.1(c) Annular flow

Typical results for a 1/10 gap-system subjected to annular flow are shown in Fig. 3. The dynamical behaviour of the system is similar to that system with internal flow: the system loses stability in its first axial mode (m = 1) at point B, it is restabilized at point R, and then the loci of the first and second mode coalesce at point F indicating the loss of stability by coupled-mode flutter.

The critical flow velocities for divergence and coupled-mode flutter are given in Table 5.4, where they are compared with the corresponding values when the flow is internal. It is found that, a shell subjected to a straight annular flow loses stability at much lower flow velocities than when it is subjected to internal flow, at least for a gap-radius ratio of 1/10.

	Nondimensional critical flow velocities	
	Divergence	Coupled-mode flutter
Internal flow ($\bar{U}_o = 0$)	2.00×10^{-2}	2.40×10^{-2}
Annular flow ($\bar{U}_i = 0$)	1.09×10^{-2}	1.40×10^{-2}

Table 5.4. Critical flow velocities for divergence and coupled-mode flutter of the 1/10-gap steel shell system subjected to an internal or annular flow of water.

5.1.1(d) Effect of gap-width

The effect of the gap width is illustrated in Table 5.5. It is seen that a 1/100 gap system is much less stable than the 1/10 gap system. This is so, because of the increase of the virtual mass associated with a smaller gap, which reduces the natural frequency at zero flow. (Recall that in these calculations the fluid flow is considered to be inviscid.)

Gap-to-radius ratio (g/a_i)	Nondimensional critical flow velocities	
	Buckling	Coupled-mode flutter
1/10	1.09×10^{-2}	1.40×10^{-2}
1/100	3.15×10^{-3}	4.0×10^{-3}

Table 5.5. The effect of annular gap width on the stability of the system (annular flow)

It is important to mention here that coupled mode flutter is only predicted by linear theory. For a similar problem, nonlinear theory [11], shows that coupled mode flutter should not materialize for a beam supported at both ends. In the present study, the system under investigation is not a beam but a shell; nevertheless, we expect it to have a similar behaviour to the system investigated in Ref. [11]. This argument is supported by the experimental results presented in Chapter VII. In the experiments, a silicone rubber shell is coaxially located in a rigid cylinder and clamped at both ends. The system is subjected to an annular flow, and the fluid flowing in the annulus is air. The experiment shows that the system loses stability by buckling as predicted by linear theory; however, coupled-mode flutter at higher flows was never observed.

Based on the above observations, the post-buckling instability, namely coupled-mode flutter will not be of further concern in this Thesis; thus, henceforth results for buckling alone will be discussed.

5.1.2 Effects of Steady Viscous Forces

In this section, the system is analyzed considering both the unsteady inviscid forces and the steady viscous forces — in contrast to the results up to this point, which were for inviscid flow.

5.1.2(a) Internal or annular flow

The effects of steady viscous forces for a 1/10 gap-system are illustrated in Table 5.6. The critical flow velocities for buckling, for internal and annular flow, are compared with the corresponding results from inviscid theory. It is seen that the steady viscous forces destabilize the system in the case of annular flow and stabilize it for the inner flow case. This could be explained by the effects of pressurization required to overcome frictional pressure drop. In the case of inner flow, the pressure on the interior side of the flexible shell is higher than on the annulus. The net pressure acting on the inner surface is in a radially outward direction. This pressure tends to increase the stiffness of the shell; hence, it delays the instability which is ultimately caused by the unsteady forces. In the case of annular flow, exactly the reverse applies. The pressure which is higher in the annulus than in the inner region tends to collapse the flexible shell, thus destabilizing the system.

	Nondimensional critical flow velocity for divergence	
	Inviscid forces	Inviscid and steady viscous forces
Internal ($\bar{U}_o = 0$)	2.00×10^{-2}	3.80×10^{-2}
Annular ($\bar{U}_i = 0$)	1.09×10^{-2}	2.4×10^{-3}

Table 5.6. Effect of steady viscous forces on the stability of a system subjected to internal or annular flow.

5.1.2(b) Effect of annular gap

The critical flow velocities at buckling for the two different gaps g/a_i = 1/10 and 1/100) taking into account the steady viscous forces are presented in Table 5.7, where they are compared with those from inviscid theory. In both theories, the system becomes less stable as the ratio of gap-size to radius decreases; however, the ratio between the critical flow velocities is 0.22 for the 1/10-gap system and 0.16 for the 1/100-gap system. This is an indication of the increased effect of the steady viscous forces for a smaller gap as a result of the increase in pressure required to drive the fluid in a smaller annulus.

Gap-size to radius ratio (g/a_i)	Nondimensional critical flow velocity for divergence		
	Inviscid only	Inviscid and steady viscous	Ratio
1/10	1.09×10^{-2}	2.40×10^{-3}	0.22
1/100	3.15×10^{-3}	4.95×10^{-4}	0.16

Table 5.7. Effect of steady viscous forces in annular flow for different gap-systems by the Fourier Transform method.

The investigation on the stability of a system subject to both unsteady and steady viscous forces in internal and annular flow has been completed using the Fourier Transform method. In the following section, a similar study is carried out using the travelling wave solution.

5.2 EFFECTS OF UNSTEADY INVISCID FORCES AND STEADY VISCOUS FORCES USING TRAVELLING WAVE SOLUTION

Before presenting the results, it is useful to discuss the nature of a travelling wave solution. As discussed in Ref. [31], the solution consists of two parts: the first part is associated with $e^{i(\omega t + kx)}$, and the second with $e^{i(\omega t - kx)}$, corresponding to a backward and a forward moving disturbance, respectively.

Examining the case of $e^{i(\omega t + kx)}$, the two roots of the frequency equation are represented by

$$\omega^+ = \omega_1^+ + i\,\omega_2^+ , \tag{5.2.1}$$

and

$$\omega^- = \omega_1^- - i\,\omega_2^- , \tag{5.2.2}$$

where ω^+ corresponds to the frequency of motion associated with a backward travelling wave, while ω^- corresponds to a forward travelling wave, and ω_1 and ω_2 are the real and imaginary parts of the frequency, respectively.

It is important to mention here that a travelling wave does not satisfy the boundary conditions for a shell pinned at both ends; however, as we will see later, if we use a wavelength equal to the length of the pinned-pinned shell in the analysis, we will be able to predict the buckling velocity for a pinned-pinned shell.

The unsteady inviscid forces for internal and annular flow have been derived in Appendix H. A copy of the program developed for studying the stability of the system subjected to these forces is given in Appendix K.

The wavelength used in the computation is equal to the length of a pinned-pinned shell.

5.2.1 Effect of the Unsteady Inviscid Forces

In this section, the steady viscous forces are not included in the calculations.

5.2.1(a) Effect of internal flow

A 1/10-gap system with stagnant fluid in the annulus is considered.

For the case of $e^{i(\omega t + kx)}$, the nondimensional frequencies Ω^+ and Ω^- (they correspond to the frequencies ω^+ and ω^-, respectively) are plotted against the dimensionless internal flow velocity $\bar{U}_i$ in Fig. 4. As expected, at zero flow, Ω^+ and Ω^- are equal in magnitude but of opposite signs. Physically, this represents the two waves of the same frequency which are travelling in opposite directions.

As we increase the flow velocity, both frequencies Ω^+ and Ω^- decrease in absolute value; however, Ω^+ decreases faster than Ω^-, until the former reaches zero at a velocity $\bar{U}_i = 0.0194$. Im (Ω^+) and Im(Ω^-) are zero throughout, indicating the absence of damping.

For a slightly higher value of $\bar{U}_i$, Ω^+ becomes negative, producing a new forward going wave; hence, no natural self-sustained backward travelling wave is possible in the system above a certain flow velocity. At a little higher flow velocity ($\bar{U}_i$ slightly less than 0.022), both frequencies meet at the Re(Ω)-axis where we have $\Omega^+ = \Omega^-$ and then become complex, indicating the threshold of flutter.

The results for $e^{i(\omega t - kx)}$ are given in Fig. 5. We see that this is simply a mirror image of Fig. 4. The instability threshold occurs at exactly the same critical flow velocity. Henceforth, only the backward travelling wave corresponding to $e^{i(\omega t + kx)}$ will be considered as the forward travelling wave gives identical results.

It is important to mention here that the velocity at which Ω^+ vanishes is of great interest to us. Although, the travelling wave solution does not satisfy the boundary conditions of a shell pinned at both ends, it nevertheless gives some insight into the velocity at which buckling occurs in a pinned-pinned shell.

In Fig. 6, the frequency Ω^+ is plotted against the dimensionless velocity and compared with the frequencies of a pinned-pinned shell obtained using the Fourier Transform method. It is seen that the frequencies of the two methods at zero flow ($\bar{U}_i = 0$) are the same. As we increase the flow velocity, the frequencies in both methods are reduced; however, they are appreciably different. Nevertheless, the real part becomes zero at approximately the same flow velocity for the two methods. In Table 5.8, we compare the flow velocity at divergence using the Fourier Transform method with the velocity at which Ω^+ vanishes in the travelling wave solution. It is apparent that the two values are almost the same, and this is an indication that the velocity at which Ω^+ vanishes may indeed correspond to the buckling velocity of a pinned-pinned shell.

Method of solution	Nondimensional critical flow for divergence
Fourier Transform method	2.00×10^{-2}
Travelling wave solution	1.94×10^{-2}

Table 5.8. Critical flow velocities at divergence for the Fourier transform and the travelling-wave methods of solution for internal flow

The difference in the results of the two methods could be attributed to the nature of the solutions. In the travelling wave solution, the unsteady forces are calculated by considering one axial mode only ($m = 1$); for the Fourier Transform method, on the other hand, these forces are determined using Galerkin's technique, which results in the coupling of three axial modes ($m = 1$, 2, and 3). In the latter method, the inertia and centrifugal forces for each mode could be decoupled (the derivatives involved in evaluating these terms are functions of time and the axial space coordinate, respectively); however, the Coriolis forces for the three modes are coupled because of their dependence on both time and axial space coordinate (x) [see equation (2.49)]. Hence, the Coriolis forces in the two methods of solution are different, and these are the forces which cause the difference in frequencies before buckling. At the point of divergence, the frequency is equal to zero; hence, the Coriolis forces are zero, and the centrifugal forces, which are responsible for divergence and are the same for the two methods, are the only forces acting on the system. Hence the results in Table 5.8 are not surprising.

Another important point which should be pointed out for causing the difference in the results is the difference in the boundary conditions considered beyond the shell ends. For the Fourier transform method the shell is assumed to be connected to a rigid cylinder at either end, whereas as for the travelling wave solution, the shell is considered to be infinitely long. Hence, the "actual" system is better represented by the Fourier transform method.

Based on the above discussion, the threshold for divergence in the travelling wave solution is taken to be the velocity at which Ω^+ vanishes.

5.2.1(b) Annular flow

In this case, the inner shell is filled with stagnant fluid, whilst the annular fluid is flowing with a velocity $\bar{U}_o$. The results for the 1/10-gap steel-water system are shown in Fig. 7 where the frequency Ω^+ is plotted against the dimensionless flow velocity in an Argand diagram. The dynamical behaviour of the system is similar to that of the internal flow case; the system loses stability first by divergence (Ω^+ is equal to zero), followed by flutter.

In Table 5.9, the critical flow velocities for buckling for internal and for annular flow are compared with the corresponding results from the Fourier Transform method. It is found that the two methods are in good agreement.

	Nondimensional critical flow velocities for divergence	
	Travelling wave solution	Fourier Transform method
Internal flow $(\bar{U}_i \neq 0); (\bar{U}_o = 0)$	1.94×10^{-2}	2.00×10^{-2}
Annular flow $(\bar{U}_o \neq 0); (\bar{U}_i = 0)$	1.03×10^{-2}	1.09×10^{-2}

Table 5.9. Comparison between results using travelling wave solution and Fourier Transform method for internal and annular flow for 1/10-gap system.

5.2.1(c) *Effect of gap size*

The effect of gap-width on the buckling velocity is illustrated in Table 5.10. The results agree with the corresponding ones from Fourier Transform method; the 1/100 gap-system is less stable than the 1/10 gap-system.

Gap-to-radius ratio	Nondimensional critical flow velocity for divergence	
	Travelling wave solution	Fourier Transform method
1/10	1.03×10^{-2}	1.09×10^{-2}
1/100	3.10×10^{-3}	3.15×10^{-3}

Table 5.10. Effect of annular gap width on the stability of the system subjected to annular flow for the two methods of solution.

5.2.2 Effect of the Steady Viscous Forces

The effect of annular flow with both unsteady invsicid forces and the steady viscous forces is investigated for both annular gaps used in the foregoing. The critical flow velocities for divergence are given in Table 5.11, where they are compared to those obtained using the inviscid theory. It is seen that the steady forces destabilize the system; the smaller the gap, the higher is the effect on the stability.

Gap-to-radius ratio (g/a_i)	Nondimensional critical flow velocity for divergence		Ratio
	Inviscid forces	Inviscid & steady viscous forces	
1/10	1.03×10^{-2}	2.35×10^{-3}	0.22
1/100	3.10×10^{-3}	4.95×10^{-4}	0.16

Table 5.11. Effect of steady viscous forces on the stability for the two gap-systems in annular flow predicted by the travelling wave method.

The results in Table 5.11 are in good agreement with those obtained from the Fourier Transform method in Table 5.7. This demonstrates the reliability of the travelling wave solution in predicting the buckling velocity of a pinned-pinned shell.

In this Section, we have used the travelling wave solution to study the stability of a system subjected to unsteady inviscid and steady viscous forces.

In the following Section, we will be dealing with the effects of both unsteady and steady viscous forces on the stability of the system. Thus, this is the full theory, where all effects considered in this Thesis are taken into account. The investigation is carried out using the travelling wave solution.

5.3 EFFECTS OF UNSTEADY AND STEADY VISCOUS FORCES USING THE TRAVELLING WAVE SOLUTION

In Section 4.6 the governing matrix [A] to be used in this case has been formulated. The elements of this matrix are given in Appendix G, and a copy of the computer program developed for studying the stability of the system is given in Appendix L. The effects of unsteady viscous forces are investigated first; then, the system is subjected to both unsteady and steady viscous forces.

In all cases considered, the results are compared with those from inviscid theory.

5.3.1 Effects of Unsteady Viscous Forces

As mentioned in Chapter II, there are two approximations for the boundary conditions:

(i) an averaged velocity, U_{av}, is presumed to be acting at the wall, which is determined via equations (2.50) and (2.51) for internal and annular flows, respectively;

(ii) the boundary conditions are applied at a distance δ from the wall, which is of the same order of magnitude as the shell deformation in the radial direction due to the turbulent flow excitation. The velocities associated with $\bar{\delta}$ † for internal and annular flows are given by equations (2.52) and (2.53), respectively.

It has been verified that any of the pressure perturbation equations (2.40)-(2.42) will lead to the same critical flow velocity at buckling when based on averaged velocity approximation at the boundary. However, equation (2.42) is the most appropriate one for carrying out a comparison between the effects of the two approximations with respect to the stability of the system. Hence equation (2.42) will be used in finding the pressure pertubation forces in the following analysis. The expressions for these forces are given in Appendix D.

5.3.1(a) Comparison between the two approximations for the velocities at the shell boundary

For the 1/10-gap system subjected to internal flow, the buckling velocities are plotted in Fig. 8 for a variable $\bar{\delta}$. It is found that, as $\bar{\delta}$ is increased, the buckling velocity converges toward the value obtained by the average velocity approximation.

In the experimental study presented in Chapter VII, we have measured the amplitude of vibration in the radial direction, w, for a silicone rubber shell coaxially located in a rigid cylinder and subjected to annular flow of air. We have found that the ratio $\frac{w}{(r_m - a_i)}$ varies between 0.01 and 0.02 for all the cases considered. This ratio is related to $\bar{\delta}$ in the theoretical study; hence, we can use this experimental range for $\bar{\delta}$ in the

† $\bar{\delta}$ is the nondimensional form for δ; it is equal to δ/a_i for the inner shell and to $\delta/(r_m - a_i)$ for the annulus.

theoretical approximation. In Table 5.12, the buckling velocities for $\bar{\delta}$ = 0.01 and 0.02 are compared with the value obtained from the averaged velocity approximation; the difference is found to be 18% and 13%, respectively. Thus, the averaged velocity approximation could be used for predicting approximately the buckling velocity of the system under investigation; moreover, this approximation is convenient when comparing the present theory with the inviscid theory in which the flow velocity is also constant across the cross-section.

	Nondimensional critical flow velocity for divergence
$\bar{\delta}$ = 0.01	2.3×10^{-2}
$\bar{\delta}$ = 0.02	2.2×10^{-2}
Average velocity approximation	1.95×10^{-2}

Table 5.12. Comparison between the buckling velocities for different $\bar{\delta}$ and the value obtained from the average velocity approximation

Based on the above discussion, the averaged velocity approximation will be used in the following analysis.

5.3.1(b) Calculation for internal flow

For a 1/10-gap system where the annular fluid is stagnant, the nondimensional frequency Ω^+ is plotted against the dimensionless internal flow velocity in Fig. 9, where it is compared with the corresponding curve from inviscid theory. It is found that the values of $\mathrm{Re}(\Omega^+)$ are almost the same in the two theories; while $\mathrm{Im}(\Omega^+)$ is now larger (of the order 10^{-4} as compared to zero). This represents the effects of fluid damping, an unsteady viscous effect. The critical flow velocities for divergence and flutter are compared in Table 5.13. It is shown that the velocities in the two theories are the same, which indicates how insignificant is the role of viscosity on the unsteady forces, at least for the internal flow and for the parameters considered. A similar conclusion has been reported in Ref. [52], where a theoretical study has been conducted for a silicone rubber shell clamped at both ends and conveying water.

	Nondimensional critical flow velocities	
	Buckling	Flutter
Unsteady inviscid forces	1.94×10^{-2}	2.20×10^{-2}
Unsteady viscous forces	1.95×10^{-2}	2.20×10^{-2}

Table 5.13. Comparison between critical flow velocities using unsteady forces from inviscid and viscous theories for internal flow ($g/a_i = 1/10$)

5.3.1(c) Calculation for annular flow

A 1/10-gap system is considered with stagnant fluid in the inner shell ($\bar{U}_i = 0$). In Fig. 10, the frequency-velocity curve is compared to the corresponding one from inviscid theory. The fluid viscosity slightly affects the frequency of the system before divergence; however, the critical flow velocities for divergence are essentially the same in the two theories, as shown in Table 5.14. These findings agree in principle with the theoretical study in Ref. [55] for a system consisting of a flexible beam clamped at both ends and coaxially located within a rigid cylinder, with water-flow in the annulus.

	Nondimensional critical flow velocity
Unsteady inviscid	1.03×10^{-2}
Unsteady viscous	1.03×10^{-2}

Table 5.14. Critical flow velocity for divergence for the two cases of unsteady inviscid and unsteady viscous forces for annular flow ($g/a_i = 1/10$).

The behaviour of the system with a smaller gap-size ($g/a_i = 1/100$) is quite different from the previous case, most notably the fluid viscosity has stronger effects on stiffness, hence on the frequency and the buckling velocity of the system. In Fig. 11, the frequency velocity curves for both viscous and inviscid theory subject to annular flow are compared. It is found that the fluid viscosity reduces the frequency of the system at zero flow velocity. As the flow velocity increases, the frequencies in the two theories are reduced; however, the frequency associated with the viscous theory decreases more slowly than the one from inviscid theory. In Table 5.15, we see that the velocity for divergence asociated with the viscous theory for annular flow is higher than the corresponding value from inviscid theory. This is because of the added stiffness in the system as a result of including the viscous perturbation forces. Hence, the unsteady viscous forces are more pronounced in a very narrow gap, rendering the system more stable.

	Nondimensional critical flow velocity for divergence
Unsteady inviscid	3.1×10^{-3}
Unsteady viscous	8.0×10^{-3} †

Table 5.15. Critical flow velocity for divergence for the two cases of unsteady inviscid and unsteady viscous theories in annular flow ($g/a_i = 1/100$).

5.3.2 Effect of Steady Viscous Forces in Annular Flow (Results with the Complete Theory)

Both systems (with different annular gaps) are considered here. In Table 5.16, we compare the velocities for divergence in this case with those from the unsteady viscous theory. It is found that the steady viscous forces have a destabilizing effect on the system; furthermore, these effects are more pronounced in 1/100-gap system.

Gap-to-radius ratio (g/a_i)	Nondimensional critical flow velocities for divergence	
	Unsteady viscous only	Unsteady viscous and steady viscous
1/10	1.03×10^{-2}	2.35×10^{-3}
1/100	8.0×10^{-3}	5.0×10^{-4}

Table 5.16. Effects of steady viscous forces for both gap-systems for annular flow.

† In connection with Fig. 11, perhaps nonuniformities in a real shell would precipitate buckling at 4.0×10^{-3} rather than 8.0×10^{-3}.

It seems that the critical flow velocities for divergence depend mainly on the steady viscous forces. This is verified by comparing the results for the two theories (steady viscous forces against unsteady and steady viscous forces together). In Table 5.17, we can see that for both gap systems, the flow velocities for buckling are the same. This shows again that the effects of unsteady viscous forces on divergence of the system are essentially insignificant.

Gap/radius ratio (g/a_1)	Nondimensional critical flow velocities for divergence	
	Steady viscous	Unsteady viscous and steady viscous
1/10	2.35×10^{-3}	2.35×10^{-3}
1/100	4.95×10^{-4}	5.0×10^{-4}

Table 5.17. Effects of steady viscous forces with and without unsteady viscous forces the two for gap systems subject to annular flow.

The frequency-velocity curve for a 1/100-gap system is plotted in Fig. 12, where it is compared with the corresponding one from inviscid theory including the steady viscous forces. It is shown that the frequencies of the system subjected to unsteady viscous forces are lower than for inviscid forces; nevertheless, the velocities for divergence are the same. Also to be seen in Fig. 12 is that the long "tail" in the locus of Fig. 11 is no longer present.

In this section we have found that, in the absence of steady viscous forces, the unsteady viscous effect is insignificant for a 1/10-gap system; however, this effect is more pronounced for a 1/100-gap system, rendering the system more stable. The situation is quite different when the steady viscous forces are included. For both gap systems, the stability of the system depends mainly on the steady viscous forces, and the unsteady viscous effects influence only the frequencies of the system prior to divergence.

Results in this Section were obtained using the travelling wave solution.

In the following Section, we will be dealing with the effect of unsteady viscous forces in internal flow using the Fourier Transform Method.

5.4 EFFECTS OF UNSTEADY VISCOUS FORCES (FOURIER TRANSFORM METHOD)

The elements of matrix [A] developed in Section 3.5 are given in Appendix G. This matrix involves both internal and annular flows. In this theory, the unsteady viscous forces are frequency-dependent; hence, an iteration method is needed to study the stability of the system. The computational costs associated with annular flow are very high; therefore, we will consider only the case of internal flow.

In this study the shell parameters are described as in the 1/10-gap system and omitting the annulus. Calculations are done for both clamped-clamped and pinned-pinned shells. A copy of the program is given in Appendix M.

The velocity applied at the boundary of the moving shell is based on the average velocity approximation.

5.4.1 Clamped-clamped Shell

The frequency-velocity curve is plotted in Argand diagram form in Fig. 13, where it is compared to the corresponding curve from inviscid theory. It is found that as the velocity increases, $Re(\Omega)$ in both theories is reduced by the same amount; $Im(\Omega)$ is of the order 10^{-5} for the viscous theory, as opposed to zero for inviscid theory. The buckling velocities in the two theories are the same ($\bar{U}_c = 0.026$); this indicates that the effects of viscosity are insignificant.

5.4.2 Pinned-pinned Shell

In Fig. 14, we compare again the frequency-velocity curves for viscous and inviscid theory, but with pinned-pinned end conditions. A similar conclusion is reached as in the clamped-clamped case: the fluid damping effects are essentially insignificant.

It is important to mention here that the results obtained in this Section using the Fourier Transform method are similar to the results obtained in Section 5.3 (Table 5.13) using the travelling wave solution; thus, we can have some confidence that both methods of solution are correct.

CHAPTER VI

EXPERIMENTAL APPARATUS

6.1 GENERAL DESCRIPTION OF APPARATUS

In parallel to the theoretical work, some experiments were conducted in order to check the theory. The experiments involve a cylindrical shell positioned in a rigid cylindrical pipe (Fig. 15). Two types of end conditions are considered:

(i) the shell is clamped at both ends;

(ii) the shell is clamped at one end and free at the other.

The shell is made of silicone rubber. The outer containment pipe is made of plexiglas, so that the shell within is clearly visible. The fluid flowing in the annulus and stationary inside the shell is air. The air is supplied from a metered supply, ultimately from an air compressor. A honeycomb, screens and a contracting section upstream of the annulus are employed to render the flow entering the annulus straight and quite uniform. The mean radius of the shell is 24.7 mm, wall-thickness/radius = 0.05. Experiments were conducted for various shell lengths, and different gap size between the inner shell and the cylindrical pipe. The length/radius ratio, L/a_i ranged between 5.5 and 7.0, and the gap/radius, g/a_i, was 0.1, 0.25 or 0.50.

In order to assess the presurization effect for the clamped-clamped shell, two cases are considered. In the first case, the air inside the shell is at a mean pressure equal to the atmospheric pressure as in the arrangement shown in Fig. 16(a). Subsequently, the test is repeated with the inner pressure equal to the static pressure of the annular flow at the downstream end of the shell, as in Fig. 16(b). For a clamped-free shell, of course, the pressurization effect could not be investigated since the downstream end of the shell is free as in Fig. 16(c).

6.2 SILICONE RUBBER SHELL

The shell is cast in a special mould, from a liquid silicone rubber which hardens with the aid of a catalyst. The mould consists of a rigid cylinder of aluminum coaxially located in a rigid cylindrical pipe made of plexiglas (Fig. 17). The diameter of the rigid cylinder is 48.26 mm and the inner diameter of the pipe is 50.80 mm. The difference in diameter represents twice the thickness of the rubber shell (so h = 1.27 mm).

The liquid rubber, free from air-bubbles, is injected from below in the mould. Care is taken in the moulding of the shell and in the machining and mounting of the various components of the apparatus to ensure uniformity of the shell to the extent possible.

Young's modulus of the shell is determined experimentally from the frequency of a cantilevered rod with various lengths. The average value for Young's modulus is E = 2.42 MPa. The density $\rho_s = 1.22 \times 10^3$ kg/m^3.

6.3 MEASUREMENT INSTRUMENTS

The flow velocity is measured either with a rotameter, upstream of the apparatus or with pitot tube utilized near the exit of the annulus. Small amplitude vibrations of the shell induced by flow turbulence are measured via one or two fibre-optic sensors ("Fotonic Sensors"), azimuthally separated by 140°. The signals from these sensors are processed by a dual channel Hewlett-Packard 5420A FFT Signal Analyzer. Power or Cross Spectral densities (PSDs or CSDs) yielded the dominant frequencies excited by the flow, which varied with increasing flow velocity. The instability (buckling) itself could be determined from the variation of frequency with flow velocity; however, the onset of instability could also be assessed visually.

6.4 TEST PROCEDURE

The following steps are involved in any given test:

(i) the fibre-optic probes are properly positioned and calibrated, so that for the vibration signal obtained, they would operate in a linear range;

(ii) the flow velocity is incremented in steps and at each step, a PSD or CSD was obtained (accordingly identifying different modes of vibration of the shell excited by the turbulent flow;

(iii) based on (ii), plots of frequency of the dominant modes of vibration versus flow velocity are obtained;

(iv) steps (ii) and (iii) are continued until the system lost stability.

Tests were conducted with nominally identical shells to verify the repeatability of the experiment.

Generally for a given shell, the first test was conducted with g/a_i = 0.25 and with the air in the inner shell at a mean pressure equal to the atmospheric pressure, as in Fig. 16(a). Subsequently the test was repeated with the inner pressure equal to that of the annular flow at the downstream end of the shell, as in Fig. 16(b).

The value of g/a_i was then changed from 0.25 to 0.50 or 0.10 by installing another plexiglas pipe with the appropriate inner diameter. Also the effect of L/a_i was investigated by changing the length-to-radius ratio from 7.0 to 5.5 in 0.5 steps.

CHAPTER VII

EXPERIMENTAL RESULTS

The behaviour of a clamped-clamped system is presented first, followed by the behaviour of a clamped-free system.

7.1 CLAMPED-CLAMPED SYSTEM

7.1.1 General Behaviour of Clamped-Clamped System

Generally, the second and third circumferential modes, $n = 2, 3$ (and, in both cases, the first axial one, $m = 1$) of the shell were most prominently excited by the turbulent flow. The amplitude of vibration was typically very small, ranging between 0 mm and 0.04 mm (measured at mid-span of the shell) for flow velocities in the annulus, U, in the range 0 to 50 m/s. This corresponds to a Reynolds number in the range of 0 to 5.1×10^4.

As the flow velocity was increased, the frequency of both modes, $n = 2$ and 3, was diminished, as shown in a typical case in Fig. 18. Physically, this reduction of the frequency with flow is associated with a "centrifugal" force proportional to $M_f U^2$, where M_f is the fluid added mass; this force is equivalent to a compressive load on the shell.

In this particular case, for $U = 45.5$ m/s, the shell buckled in the $n = 2$ mode. The amplitude of the buckling was very large, and the two sides of the shell, in its central portion, actually touched, as shown in Fig. 19(a). In some cases, as the flow velocity was increased further, the buckled shape was transformed quite abruptly from $n = 2$ to $n = 3$. In other cases, however, typically for the smaller values of L/a_i buckling occurred first in the $n = 3$ mode, as shown in Fig. 19(b).

No flutter of the shell was ever observed, in contrast to theoretical predictions, in Ref. [48] and here, that coupled-mode flutter succeeds divergence at higher flow velocities.

7.1.2 General Agreement between Theory and Experiment

It was seen in Chapter V that the dynamics and stability for a 1/10-gap system, which is subjected to unsteady and steady viscous forces corresponds closely to the behaviour of the same system when subjected to unsteady inviscid and steady viscous forces (as in Ref. [48]). For this reason, the experimental results are compared with their theoretical counter-parts obtained with the theory of Ref. [48].

The effect of L/a_i on the circumferential modes at buckling could give a good indication on the qualitative agreement between the theoretical and experimental results.

It is seen from Table 7.1 that theory and experiment agree with each other that the shorter the shell, the larger is the circumferential mode number associated with buckling.

Length-to-radius ratio (L/a_i)	Circumferential mode	
	Experimental	Theory
5.5	3	3
6	2	3
6.5	2	3
7	2	2

Table 7.1. Effect of the length-to-radius ratio L/a_i on the circumferential mode associated with buckling ($g/a_i = 0.25$, $P_A = P_B$).

For $L/a_i = 5.5$, in both theory and experiment the shell buckles in the same circumferential mode, $n = 3$; similarly for $L/a_i = 7$, instability associated with $n = 2$ is both predicted and observed. However, for $L/a_i = 6$ and 6.5, the theoretical circumferential mode number for buckling is different from the experimental one. This could be explained by the difference in axial tension to the shell. The state of zero tension on the shell assumed in the theory, is very difficult to achieve experimentally; a small difference in tension for a specific shell length could well cause the disagreement between theory and experiment. The effect of tension or compression on the circumferential mode at buckling is clearly discussed in Ref. [56].

Another reason for the difference between the theoretical and experimental results could be caused by a possible eccentricity in the moulding apparatus which would result in imperfections, favouring the lower circumferential mode ($n = 2$).

The difference in the theoretical critical flow velocities for buckling in $n = 2$ and $n = 3$ is generally small; that is why small differences in tension and imperfections are so important. For $L/a_i = 6$, $U_c = 58.0$ for $n = 2$; $U_c = 55.5$ for $n = 3$.

Furthermore, it should be noted that the qualitative disagreement for $L/a_i = 6$ and 6.5 is not a general one, but rather depends on the shell parameters as shown in Table 7.2. For a system with $L/a_i = 6$ and different gap sizes ($g/a_i = 0.1$, 0.5) theory and experiment are in good agreement regarding the circumferential mode at buckling.

g/a_i	Circumferential mode number n	
	Experiment	Theory
0.1	3	3
0.5	2	2

Table 7.2. Circumferential modes at buckling for $L/a_i = 6$ and $g/a_i = 0.1, 0.5$.

7.1.3 Quantitative Agreement with Theory

The so-called "standard" system will be discussed first. In this case, $L/a_i = 6.0$; $g/a_i = 0.25$ and the air within the shell is at the static pressure of the fluid flowing in the annulus at the downstream end of the shell [Fig. 16(b)]. Later, the effect of variations of these parameters on system behaviour will be discussed. In the experiments, the critical flow velocity is associated with the n = 2 mode, as shown in Fig. 20 (the same case as in Fig. 18), but then at higher flow there is a transition to the n = 3 mode. In this case, the theory predicts that the shell should buckle first in its third circumferential mode (Fig. 20). The results are summarized in Table 7.3.

Circumferential mode n	Critical flow velocity, U_c (m/s)	
	Experiment	Theory
2	45.3 ± 9%	58.0
3	48.6 ± 9%	55.5

Table 7.3. Critical flow velocities of the "basic" system. $L/a_i = 6$, $g/a_i = 0.25$ and $P_A = P_B$

The experimental results presented above are based on tests conducted with four nominally identical shells; the differences in the critical flow velocities (quoted in percent of the mean U_c) could be attributed to the imperfections and nonuniformity of the moulded shells and the associated apparatus.

It is important to reiterate that the coupled-mode flutter predicted by theory was not observed in any of the experiments. Thus the behaviour of the system beyond the first loss of stability by divergence - i.e. the post-buckling behaviour - cannot be successfully predicted by linear theory. This is usually the case. The same observations were made in the case of beam-like motions of a pipe supported at both ends and conveying fluid: linear theory predicts the occurrence of post-buckling coupled-mode flutter, which is not found experimentally. Nonlinear theory [11] shows that, in fact, coupled-mode flutter should not materialize, in agreement with experimental observations.

On the other hand, unlike the problem of the flow-conveying pipe, the system here under consideration is not entirely conservative, as it is subjected to unsteady viscous forces. In this respect, this problem is similar to that of a beam in axisymmetrically confined flow, already studied [31,57], which does develop post-buckling coupled-mode flutter [57], in the manner predicted by theory. The most likely reason for the difference between the beam system of Refs. [31,57] and the present one is that the maximum amplitude of the buckled system is small in the former case and extremely large in the present case. This obviously affects post-buckling behaviour in the experiments and reduces the chances of good agreement with linear theory, which, it is recalled, considers stability in terms of small perturbations about the original, undeformed equilibrium position [48].

The effect of the gap size, pressurization of the shell and changing the length-to-radius ratio are discussed next.

7.1.3(a) Effect of Gap Size

Three different gap-size/radius ratios were considered: $g/a_i = 0.1$, 0.25 and 0.5. Table 7.4 shows the effect of changing the gap size on the critical flow velocity for a system with $L/a_i = 6$ and $P_A = P_B$.

Gap-size/radius g/a_i	Critical flow velocity, U_c (m/s)	
	Experiment	Theory
0.10	29.7	32.0
0.25	45.3	58.0
0.50	59.2	79.3

Table 7.4. The effect of annular gap width on the stability of the system (n = 2).

There are two reasons for which the critical flow velocity is decreased as g/a_i is reduced:

(i) a higher virtual mass is associated with a smaller gap, which means a proportionally larger "compressive"-type fluid force acts on the shell reducing the natural frequency at zero flow;

(ii) a higher pressure is required to drive the flow in the narrow gap; this makes the inward-directed differential pressure across the shell larger, which tends to destabilize the system.

7.1.3(b) Effect of Pressurization

In order to examine the effect of pressurization on the stability of the system, two cases were considered: (i) the inner shell open to the atmosphere, as in Fig. 16(a); (ii) the stagnant inner fluid within the shell connected to the fluid in the annulus at $x = L$, as in Fig. 16(b). It is seen in Table 7.5 that, in the latter case, where the inner shell is pressurized to the same extent as the downstream end of the annular region, the system loses stability at a higher flow velocity than when the downstream end is open to the atmosphere. These results show that internal pressurization tends to stabilize the system.

Pressure (Pa)		Critical flow velocity, U_c (m/s)	
Inner shell	Annular	Experiment	Theory
$P_A = 0$	$P_B = 164.3$	29.6	41.4
$P_A = 391.4$	$P_B = 391.4$	45.3	58.0

Table 7.5. The effect of pressurization on stability for the system with $g/a_i = 0.25$, $L/a_i = 6$, $(n = 2)$

Theory and experiment are in good qualitative agreement; from Table 7.5, the ratio between the critical flow velocities in the two cases, is 1.41 for the theory and 1.53 for the experiment.

7.1.3(c) Effect of Changing Length-to-Radius Ratio, L/a_i

The critical flow velocity and corresponding circumferential modes for various length-to-radius ratios are shown in Fig. 21. The critical flow velocity decreases as the shell length increases: the shorter the shell, the larger is the circumferential mode number associated with buckling.

The disagreement between the theoretical and experimental results for $L/a_i = 6$ and 6.5 has been discussed earlier and may be attributed to the tension inadvertently applied on the shell in the experiments.

It has already been mentioned in the discussion of the dynamical behaviour of the "standard" system, that in some cases the shell loses stability in the $n = 2$ mode, but, if the flow is further increased, there is a transition to the $n = 3$ mode. In these experiments, this was only observed for shells with $L/a_i \geq 6$.

In all experiments presented in this paper, L/a_i was sufficiently small for the system to lose stability in one of its shell modes ($n \geq 2$). For sufficiently large L/a_i, however, the system would lose stability in the $n = 1$ mode, deforming laterally as a beam, similarly to the case of internal flow in the shell [20]. It has been shown that, for large enough L/a_i and for $n = 1$, the dynamics of the shell subjected to internal flow may be analyzed adequately by beam rather than shell theory [9]; the same should apply to shells in annular flow. Furthermore, the dynamics of cylindrical beams subjected to annular flow have already been studied, see for example Refs. [31,57]. Hence the general character of stability of the system in the $n = 1$ modes is well known and will not be elaborated upon here.

7.2 CLAMPED-FREE SYSTEM

Experiments on annular flow for a clamped-free shell have never been done heretofore. However, it is of interest that a case of flutter of a coaxial conical shell subjected to both internal and annular flow has been reported and has been attributed to the annular flow, and model experiments were conducted confirming that this was the case [58].

Despite the fact that all of the theoretical development in the annular flow case has been for cylindrical shells clamped at both ends [48], it was nevertheless considered desirable to undertake some experiments for the dynamics of clamped-free shells in annular flow.

7.2.1 General Behaviour of the System

In contrast to the clamped-clamped case, the system (being non-conservative) loses stability by flutter. The circumferential mode associated with the instability depends on the length/radius ratio and on the gap size.

The reduction in frequency, up to a point, and its subsequent increase as the flow velocity is raised is associated with the effective compressive load due to the flowing fluid, $M_f U^2(\partial^2 w/\partial x^2)$, which does work since the system is nonconversative. The loss of stability by flutter involves interaction of this force with the Coriolis force $M_f U(\partial^2 w/\partial x \partial t)$, as discussed in Ref. [2]; the system loses stability at point F of Fig. 22, by negative-damping, single-degree-of-freedom flutter. The amplitude of vibration before flutter ranged between 0 and 0.08 mm for flow velocities in the annulus in the range 0 to 51.1 m/s . The flutter instability was associated with very large vibrations, so the inner sides of the shell were actually touching, and the outer sides of the shell touched the inner cylinder wall.

Thus, in its essentials, the behaviour of clamped-free shell subjected to annular flow is similar to the internal flow case [2,20].

7.2.2 Effect of Gap Size

Three different gap-size/radius ratios were considered: $g/a_i = 0.1$, 0.25 and 0.5. Table 7.6 shows the effect of gap-size on the critical flow velocity and the circumferential mode associated with it.

Gap Size	Critical flow velocity, U_c(m/s)	Circumferential mode
0.1	37.1	4
0.25	46.8	4
0.5	55.3	3

Table 7.6. Effect of gap-size on the critical flow velocity the circumferential mode associated with it $L/a_i = 6$

A higher circumferential mode number is associated with smaller gap. Moreover, the critical flow velocity decreases as the gap size decreases. This behaviour is similar to that of the clamped-clamped case.

7.2.3 Effect of L/a_i

The effect of L/a_i the critical flow velocity and the circumferential mode associated with it are presented in Table 7.7.

L/a_i	Critical flow velocity, U_c(m/s)	Circumferential mode
6	37.1	4
6.5	35.5	4
7	31.1	3

Table 7.7. Effect of length-to-radius ratio L/a_i on stability and the circumferential mode associated with buckling ($g/a_i = 0.1$).

The critical flow velocity decreases as the shell length increases; However the shorter the shell, the larger is the circumferential mode number associated with flutter, again similarly to the case of internal flow [20].

CHAPTER VIII

CONCLUSION

This Thesis presents a theoretical and experimental investigation on the dynamical behaviour and the stability of cylindrical shell coaxially located in a cylindrical pipe and subjected to axial flow. In the theoretical analysis, the flow could be internal or annular, while for the experimental study only annular flow has been considered.

8.1 THEORETICAL STUDY

The aim of the theoretical study is to investigate the effects of unsteady viscous forces on the stability of the system as compared to the effects of inviscid forces. However, the effects of steady viscous forces derived in Ref. [48] are also studied. The derivation of inviscid fluid-dynamic forces is based on potential flow theory, while the unsteady viscous forces are derived using Navier-Stokes equations (see Chapter II).

Two methods of solution have been used in formulating the problem:

(i) the Fourier Transform method given in Chapter III;

(ii) the travelling wave solution given in Chapter IV.

In the first method, the shell could be clamped or pinned at both ends; while in the second method only a pinned-pinned shell could be considered.

The unsteady viscous forces are frequency-dependent; hence, an iteration method is needed to evaluate the frequencies of the system. For the Fourier Transform method, the stability of the system subjected to internal flow is investigated within acceptable computational costs; however, for the annular flow case, these costs are extremely high, rendering this method inconvenient to be used. For this reason, travelling wave solution has been developed, with the aid of which all calculations for annular flow can be done within reasonable costs.

8.1.1 Effects of Unsteady Inviscid Forces and Steady Viscous Forces

8.1.1(a) Fourier Transform method

When the system is subjected to inviscid forces only, it is seen that a shell pinned at both ends and subjected to internal or annular flow loses stability first by buckling, followed by coupled-mode flutter. The critical flow velocities associated with annular flow are much lower than those for internal flow.

It is important to mention here that the post-buckling instabilities predicted by linear theory was never observed experimentally; hence, we can rely on linear theory only for predicting the first type of instability i.e., buckling.

The effects of steady viscous forces are to stabilize the system for the internal flow case and destabilize it for the annular flow case. This could be explained by the effects of pressurization of the system. In the annular flow case, the pressure required to drive the fluid in the annulus is higher than the pressure in the inner shell. The net pressure difference acts radially inward, tending to collapse the system. The case of internal flow is exactly the opposite. The net pressure difference is now acting radially outward, which results in increasing the stiffness of the shell; hence delaying the buckling instability.

8.1.1(b) Travelling wave solution

The travelling wave solution has been developed mainly to investigate the effect of unsteady viscous forces in annular flow; nevertheless, the case of internal flow is also considered.

In this method, the motion is composed of one forward-travelling wave of frequency ω^+ and a backward-travelling wave with frequency ω^-. The wave-length used in the calculation is assumed to be the same as that of a pinned-pinned beam. For the case of internal flow with unsteady inviscid forces, the frequencies of both waves decrease as the flow velocity increases; however, at sufficiently high flow velocity ω^+ vanishes. When the flow velocity increases further, ω^+ becomes negative, indicating the presence of a new forward-travelling wave. At a slightly higher flow velocity, real parts of both frequencies ω^+ and ω^- become equal indicating the threshold of a flutter-type instability. It was found that the flow velocity at which $Re(\omega^+)$ vanishes corresponds closely to the buckling velocity for the pinned-pinned shell in the analysis using the Fourier Transform method. This finding is not regarded as a coincidence; it is rather based on physical grounds as the centrifugal forces are the same in both methods of solution, those being the forces which cause buckling in such gyroscopic conservative systems. Hence, in all analysis using the travelling wave solution, the velocity at buckling is taken to be the velocity at which $Re(\omega^+)$ vanishes.

In all cases considered, the qualitative agreement between the two methods of solution is excellent; however, the critical flow velocities for buckling using the travelling wave solution are slightly lower than those from the Fourier Transform method.

8.1.2 Effects of Unsteady Viscous Forces and Steady Viscous Forces

In the unsteady viscous theory, two approximations have been used to represent the effects of steady flow $U(r)$ on the moving boundary: (i) an averaged velocity is presumed to be acting at the wall; (ii) the boundary condition is applied at a distance δ from the wall.

These approximations have been introduced as a result of the unsatisfactory application of the no-slip condition at the moving wall. For the no-slip condition, the mean flow velocity at the wall is zero. Mathematically, this causes a problem in obtaining the centrifugal forces which are flow-velocity-square dependent. In the absence of these forces, the problem is not well defined physically, since the centrifugal forces are those which cause buckling.

8.1.2(a) Travelling wave solution

For the internal flow case, the buckling velocities using the two approximations have been compared. It was found that the buckling velocity associated with the second approximation using a nondimensional distance ($\bar{\delta}$ = 0.02) is 13% higher than that from the average velocity approximation. This value of $\bar{\delta}$ corresponds closely to the value measured experimentally for the non-dimensional shell deformation in the radial direction ($\frac{w}{r_m - a_i}$); hence, the prediction of the buckling velocity by the averaged velocity approximation is satisfactory and has been used in the viscous theory analysis.

The effects of unsteady viscous forces are investigated for internal and annular flow. The results are compared to the corresponding ones from inviscid theory. It is found that for internal flow and annular flow with 1/10-gap system, the effects of viscosity on the stability of the system are insignificant; however, for a smaller gap (g/a_i = 1/100), these effects are more pronounced, rendering the system more stable.

When both steady and unsteady viscous forces are applied, the results are quite different from the previous case. For the annular flow case, the loss of stability depends only on the steady viscous forces. The unsteady forces affect the frequency of the system before it becomes unstable.

8.1.2(b) Fourier Transform method

Only the case of internal flow is considered. For a shell clamped or pinned at both ends and subjected to unsteady viscous forces, the frequencies and the buckling velocities of the system are the same as in the case of inviscid theory. These results support what has been presented using the travelling wave solution.

8.2 EXPERIMENTAL STUDY

In the experiments, the shell could be clamped at both ends or clamped at one end and free at the other. The effect of length to radius (L/a_i) and gap-size to radius ratio (g/a_i) have been investigated. In the clamped-clamped case, the effect of pressurizing the inner shell has been studied.

8.2.1 Clamped-Clamped shell

In all cases considered, the shell loses stability by buckling in its second or third circumferential mode. This is the only type of instability observed in the experiment. (Post-buckling flutter instability predicted by linear theory was never observed experimentally.) This observation is significant as it demonstrates the invalidity of linear theory in predicting the post-buckling instabilities.

The system becomes less stable as L/a_i increases; however, the circumferential mode associated with buckling increases as L/a_i decreases.

The critical flow velocity for buckling decreases as the gap-size (g/a_i) is reduced, this is so because of the increase in the virtual mass which is associated with a smaller gap. The effect of pressurization of the inner shell is to stabilize the system.

The experimental results are compared with the theoretical ones in Ref. [48]. It is found that they are in a good qualitative agreement.

Quantitatively, the percentage difference varies for each gap-system. For $g/a_i = 0.1$, the difference is 10%; however, for the largest gap-system $g/a_i = 0.5$, the difference may reach 30%.

8.2.2 Clamped-Free Shell

For a clamped-free shell, the system loses stability by flutter (being a non-conservative system).

The effect of L/a_i and g/a_i are similar to the clamped-clamped case. The system becomes less stable as L/a_i is increased or g/a_i decreased; however, the circumferential mode associated with flutter increases as L/a_i or g/a_i is decreased.

The case of clamped-free system subjected to annular flow has never been studied theoretically; hence, the experimental results cannot be compared with their theoretical counterparts.

8.3 SUGGESTIONS FOR FUTURE WORK

In the theoretical analysis, we have faced a major problem in handling the boundary conditions for viscous theory. By applying the no-slip condition directly, we have failed to obtain the centrifugal forces. Therefore, we have introduced two approximations at the boundary to incorporate the effects of centrifugal forces. This problem of boundary condition in structures subjected to viscous flow is an important one in the flow-induced vibrations field and needs to be investigated further.

It would be interesting to simplify the annular flow case while using the Fourier Transform method, so as to be able to perform the calculations within reasonable computational costs.

As for the experimental work, we have only studied the annular flow case. One may suggest investigating the combined effects of internal and annular flow.

Finally, the case of clamped-free shell subjected to annular flow has been investigated experimentally; however, this case was never studied theoretically. It is important then to modify the present theory (for clamped-clamped or pinned-pinned shells) so as to be able to consider the case of a clamped-free shell.

REFERENCES

1. H. Ashley and G. Haviland, "Bending Vibrations of Pipe-line Containing Flowing Fluid", Journal of Applied Mechanics, Vol. 17, 1950, pp. 229-232.

2. Paidoussis, M.P., "Flow-Induced Vibrations in Nuclear Reactors and Heat Exchangers: Practical Experiences and State of Knowledge", in Practical Experineces with Flow Induced Vibrations, E. Naudascher and D. Rockwell, Eds, Springer-Verlag, Berlin, 1980, pp. 1-81.

3. Chen, S.S., "Parallel Flow-Induced Vibrations and Instabilities of Cylindrical Structures", Shock and Vibration Digest, Vol. 6, No. 10, 1974, pp. 1-10.

4. Paidoussis, M.P., "Instabilities in Cylindrical Structures", Applied Mechanics Reviews, Vol. 40, 1987, pp. 163-175.

5. Feodos'ev, V.P., "Vibrations and Stability of Pipe when Liquid Flows through it", Inzhenernyi Sbornik, Vol. 10, 1951, pp. 169-170.

6. Housner, G.W., "Bending Vibrations of a Pipe Line Containing Flowing Fluid", Journal of Applied Mechanics, Vol. 19, 1952, pp. 205-208.

7. Niordson, F.I., "Vibration of a Cylindrical Tube Containing Flowing Fluid", Kungliga Tekniska Hogskoluns Handlingar (Stockholm), No. 73, 1953.

8. Paidoussis, M.P. and Issid, N.T., "Dynamic Stability of Pipes Conveying Fluid", Journal of Sound and Vibrations, Vol. 33, 1974, pp. 267-294.

9. Paidoussis, M.P., "Flutter of Conservative Systems of Pipes Conveying Incompressible Fluid", Journal of Mechanical Engineering Science, Vol. 17, 1975, pp. 19-25.

10. Husseyin, K. and Plaut, R.H., "Transverse Vibrations and Stability of Systems with Gyroscopic Forces", Journal of Structural Mechanics, Vol. 3, 1974-5, pp. 163-177.

11. Holmes, P.J., Pipes Supported at Both Ends Cannot Flutter", Journal of Applied Mechanics, Vol. 45, pp. 619-622.

12. Naguleswaran, S. and Williams, C.J.H., "Lateral Vibrations of a Pipe Conveying Fluid", Journal of Mechanical Engineering Science, Vol. 10, 1968, pp. 228-238.

13. Liu, H-S. and Mote, C.D., Jr., "Dynamic Response of Pipes Transporting Fluids", ASME Journal of Engineering for Industry, Vol. 96, 1974, pp. 591-596.

14. Jendrzejczyk, J.A. and Chen, S.S., "Experiments on Tubes Conveying Fluid", Thin-Walled Structures, Vol. 3, 1985, pp. 109-134.

15. Benjamin, T.B., "Dynamics of a System of Articulated Pipes Conveying Fluid. I. Theory", Proceedings of the Royal Society (London), Vol. 261(A), 1961, pp. 457-486.

16. Benjamin, T.B., "Dynamics of a System of Articulated Pipes Conveying Fluid. II. Experiments", Proceedings of the Royal Society (London), Vol. 261(A), 1961, pp. 487-499.

17. Gregory, R.W. and Paidoussis, M.P., "Unstable Oscillation of Tubular Cantilevers Conveying Fluid. I. Theory", Proceedings of the Royal Society (London), Vol. 293(A), 1966, pp. 512-527.

18. Gregory, R.W. and Paidoussis, M.P., "Unstable Osicllation of Tubular Cantilevers Conveying Fluid. II. Experiments", Proceedings of the Royal Society (London), Vol. 293(A), 1966, pp. 528-542.

19. Paidoussis, M.P. and Denise, J-P., "Flutter of Thin Cylindrical Shells Conveying Fluid", Journal of Sound and Vibration, Vol. 16, 1971, pp. 459-461.

20. Paidoussis, M.P. and Denise, J-P., "Flutter of Thin Cylindrical Shells Conveying Fluid", Journal of Sound and Vibration, Vol. 20, 1972, pp. 9-26.

21. Weaver, D.S. and Unny, T.E., "On the Dynamic Stability of Fluid-Conveying Pipes", Journal of Applied Mechanics, Vol. 40, 1973, pp. 48-52.

22. Shayo, L.K. and Ellen, C.H., "The Stability of Finite Length Circular Cross-Section Pipes Conveying Inviscid Fluid", Journal of Sound and Vibration", Vol. 37, 1974, pp. 535-545.

23. Weaver, D.S. and Myklatun, B., "On the Stability of Thin Pipes with an Internal Flow", Journal of Sound and Vibrations, Vol. 31, 1973, pp. 399-410.

24. Pham, T.T. and Misra, A.K., "Dynamic Stability of Cylindrical Shells Subjected to Axial Flow and a Linearly Varying Axial Load", Proceedings 8th Canadian Congress of Applied Mechanics, Moncton, N.B., 1981, pp. 143-144.

25. Weaver, D.S. and Paidoussis, M.P., "On Collapse and Flutter Phenomena of Thin Tubes Conveying Fluid", Journal of Sound and Vibration, Vol. 50, 1977, pp. 117-132.

26. Grotberg, J.B. and David, S.H., "Fluid-Dynamic Flapping of a Collapsible Channel: Sound Generation and Flow Limitation", Journal of Biomechanics, Vol. 13, 1980, pp. 219-230.

27. Webster, P.M., Sawatzky, P.P., Hoffstein, V., Leblanc, R., Hinchey, M.J. and Sullivan, P.A., "Wall Motion in Expiratory Flow Limitations: Choke and Flutter", Journal of Applied Physiology, Vol. 59, 1985, pp. 1304-1312.

28. Paidoussis, M.P., "Dynamics of Flexible Slender Cylinders in Axial Flow. Part 1. Theory", Journal of Fluid Mechanics, Vol. 26, 1966, pp. 717-736.

29. Paidoussis, M.P., "Dynamics of Flexible Slender Cylinders in Axial Flow. Part 2. Experiments", Journal of Fluid Mechanics, Vol. 26, 1966, pp. 737-751.

30. Paidoussis, M.P., "Dynamics of Cylindrical Structures Subjected to Axial Flow", Journal of Sound and Vibrations, Vol. 29, 1973, pp. 365-385.

31. Paidoussis, M.P. and Ostoja-Starzewski, M., "Dynamics of Flexible Cylinders in Subsonic Axial Flow", AIAA Journal, Vol. 19, 1981, pp. 1467-1475.

32. Chen, S.S., "Vibration of Nuclear Fuel Bundles", Nuclear Engineering and Design, Vol. 35, 1975, pp. 399-422.

33. Paidoussis, M.P., "The Dynamics of Clusters of Flexible Cylinders in Axial Flow: Theory and Experiments", Journal of Sound and Vibration, Vol. 65, 1979, pp. 391-417.

34. Dowell, E.H., Aeroelasticity of Plates and Shells. Noordhoff International, Leyden, 1975.

35. Dowell, E.H. and Widnall, S.E., "Generalized Aerodynamic Forces on an Oscillating Cylindrical Shell", Quarterly of Applied Mathematics, XXIV, 1966, pp. 1-17.

36. Hobson, D.E., "Fluid-Elastic Instabilities Caused by Flow in an Annulus", in Proceedings of 3rd Int. Conference on Vibration of Nuclear Plant, Keswick, U.K., 1982, pp. 440-463.

37. Mateescu, D. and Paidoussis, M.P., "The Unsteady Potential Flow in an Axially Variable Annulus and its Effects on the Dynamics of the Oscillating Rigid Center-body", Journal of Fluids Engineering, Vol. 107, 1985, pp. 421-427.

38. Mateescu, D. and Paidoussis, M.P., "Unsteady Viscous Effects on the Annular-Flow-Induced Instabilities of a Rigid Cylindrical Body in a Narrow Duct", Journal of Fluids and Structures, Vol. 1, 1987, pp. 197-215.

39. Krajcinovic, D., "Vibrations of Two Coaxial Cylindrical Shells Containing Fluid", Nuclear Engineering and Design, Vol. 30, 1974, pp. 242-248.

40. Au-Yang, M.K., "Free Vibration of Fluid-Coupled Coaxial Cylindrical Shells of Different Lengths", Journal of Applied Mechanics, Vol. 98, 1976, pp. 480-484.

41. Brown, S.J. and Lieb, B.W., "A Comparison of Experimental and Theoretical Vibration Results to Narrow-Gap, Fluid-Coupled, Coaxial Flexible Cylinders", Paper No. 80-C2/PVP-104, American Society of Mechanical Engineers, New York, 1978.

42. Chen, S.S., Wambsganss, M.W. and Jendrzejczyk, J.A., "Added Mass and Damping of a Vibrating Rod in Confined Viscous Fluids", Journal of Applied Mechanics, Vol. 98, 1976, pp. 325-329.

43. Yeh, T.T. and Chen, S.S., "Dynamics of a Cylindrical Shell System Coupled by Viscous Fluid", Journal of Acoustical Society of America, Vol. 62, 1977, pp. 262-270.

44. Dowell, E.H., Flutter of Plates and Shells in Practice, in "Practical Experiences with Flow-Induced Vibrations", E. Naudascher and D. Rockwell Eds., Springer-Verlag, Berlin, 1980, pp. 160-174.

45. Chen, S.S., "Dynamics of a Rod-Shell System Conveying Fluid", Nuclear Engineering and Design, Vol. 30, 1974, pp. 223-233.

46. Weppelink, H., "Free Vibrations of Finite Circular Cylindrical Shells and Tubes With and Without a Surrounding Fluid", Ph.D. Thesis, Technische Hogeschool Twente, Enschede, The Netherlands, 1979.

47. Paidoussis, M.P., Chan, S.P. and Misra, A.K., "Dynamics and Stability of Coaxial Cylindrical Shells Containing Flowing Fluid", Journal of Sound and Vibration, Vol. 97, 1985, pp. 201-235.

48. Paidoussis, M.P., Misra, A.K. and Chan, S.P., "Dynamics and Stability of Coaxial Cylindrical Shells Conveying Viscous Fluid", Journal of Applied Mechanics, Vol. 52, 1985, pp. 389-396.

49. Laufer, J., "The Structure of Turbulence in Fully-Developed Pipe Flow", NACA Technology Note 2954, 1953.

50. Brighton, J.A. and Jones, J.B., "Fully developed Turbulent Flow in Annuli", Journal of Basic Engineering, Vol. 1964, pp. 835-844.

51. Lawn, C.J. and Elliot, C.J., "Fully developed Turbulent Flow through Concentric Annuli", Journal of Mechanical Engineering Science, Vol. 114, N3, 1972, pp. 193-204.

52. Murdock, J.W., "Fluid Mechanics and its Applications", Houghton Mifflin Company, Boston, 1976.

53. Mateescu, A.D., "Fluid-Elastic Vibrations and Stability of Cylindrical Shells Conveying Axial Flow", M.Eng. Thesis, McGill University, Canada, 1984.

54. Ventres, C.S., "Shear Flow Aerodynamics: Lifting Surface Theory", AIAA Journal, Vol. 13, No. 9, 1975, pp. 1183-1187.

55. Sim, W.-G., "Stability of a Flexible Cylinder in Axisymmetrically Confined Flow", M.Eng. Thesis, McGill University, July, 1987.

56. Flügge, W., "Stresses in Shells", Springer-Verlag, New York Inc. 1967.

57. Paidoussis, M.P. and Pettigrew, M.J., "Dynamics of Flexible Cylinders in Axisymmetrically Confined Flow", Journal of Applied Mechanics, Vol. 46, 1979, pp. 37-44.

58. Ziada, S., Bühlmann, E.T. and Bolleter, V., "Model Tests on Shell Flutter Due to Flow at Both Sides", To be published in Journal of Fluids and Structures, 2, No. 2, March 1988.

59. Schlicting, D., "Boundary-Layer Theory", McGraw Hill Book Company, Seventh Edition, 1979.

60. Bélanger, F., "Experiments on the Unsteady Pressure Generated by Oscillation of a Cylinder in a Duct with Annular Flow", M.Eng. Thesis, McGill University, 1987.

61. McLachlan, N.W., "Bessel Functions for Engineers", Oxford University Press, London, 1941.

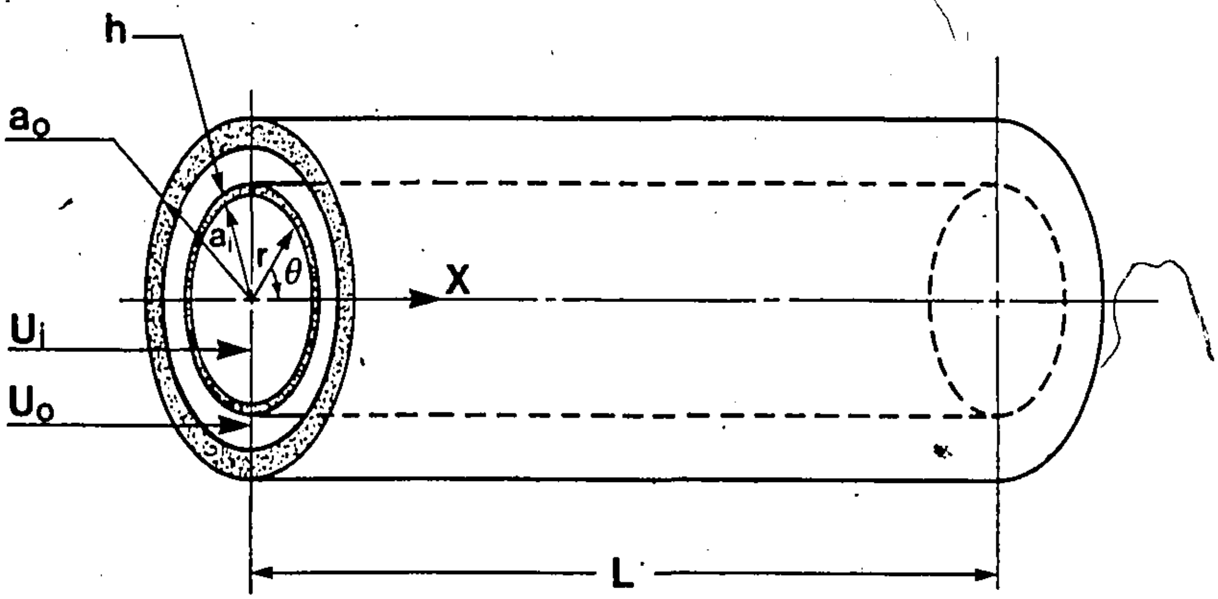

Figure 1. Diagram of the system.

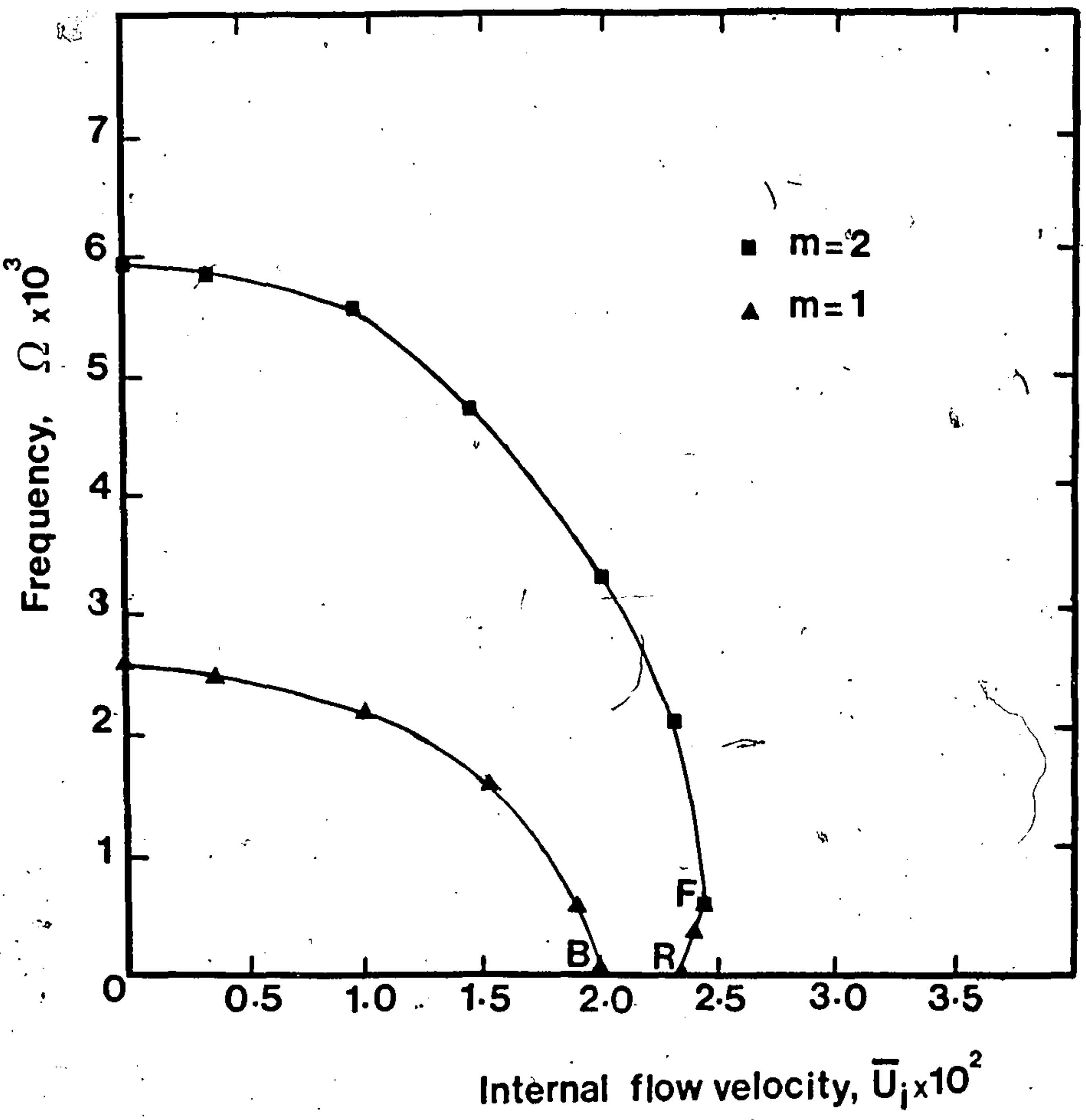

Figure 2. Frequency-velocity curves for a system subjected to internal flow obtained using Fourier transform method, $g/a_i = 1/10$; $\bar{U}_o = 0$.

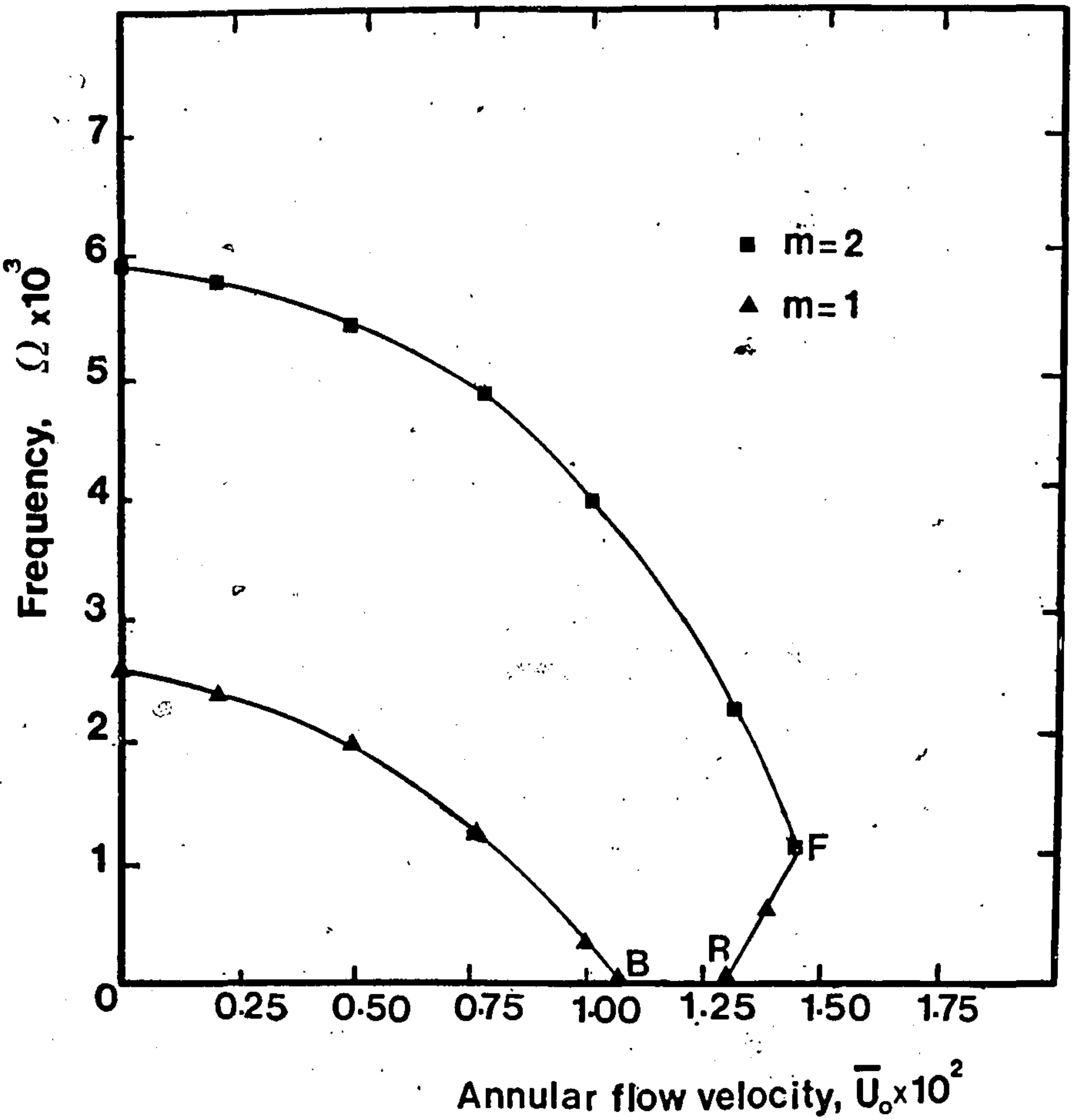

Figure 3. Frequency-velocity curves for a 1/10 gap-system subjected to annular flow obtained using Fourier transform method, $\bar{U}_i = 0$.

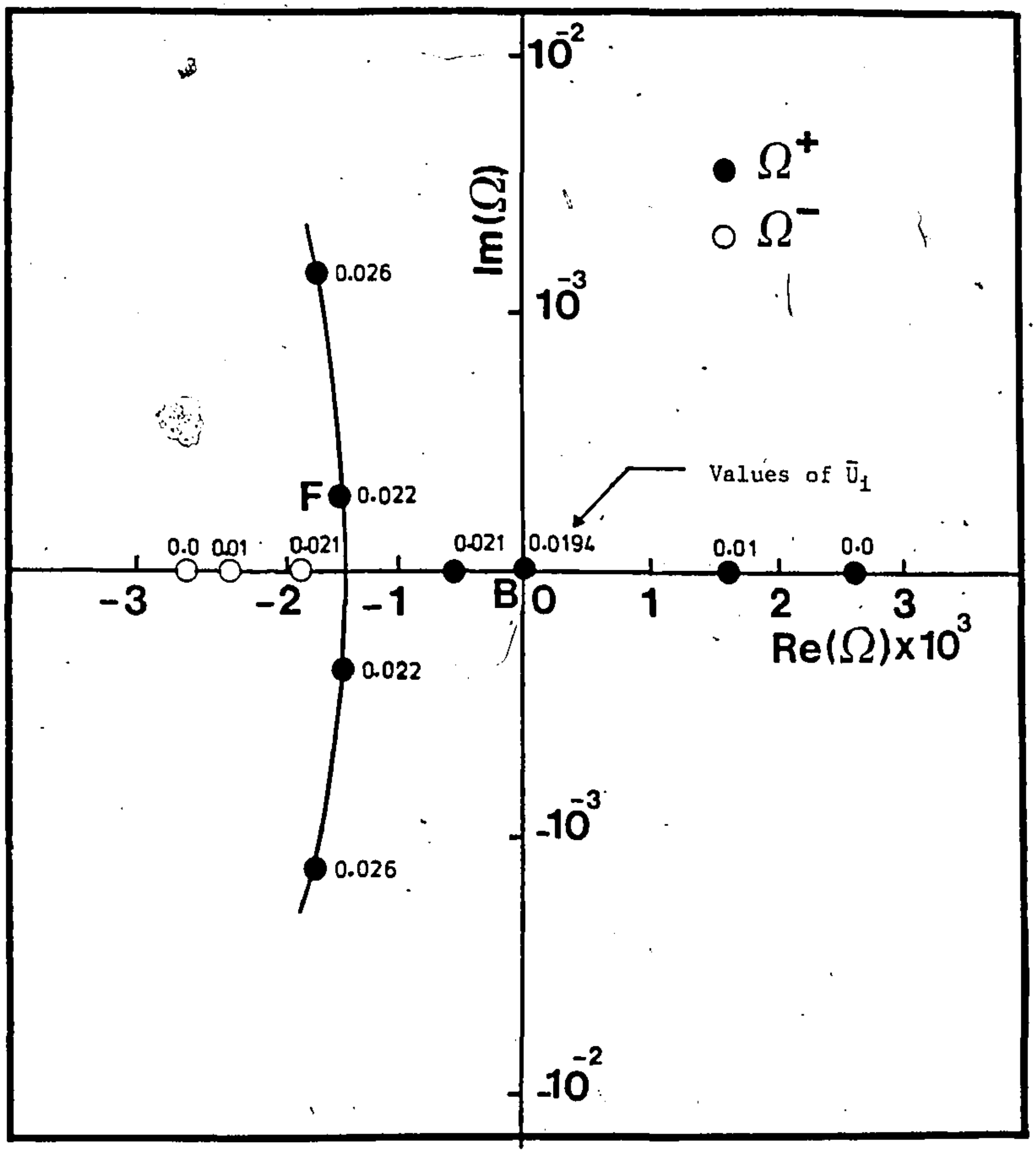

Figure 4. Argand diagram for the dimensionless frequency Ω as a function of the dimensionless internal flow velocity $\bar{U}_i$, where $\bar{U}_o = 0$; solution with $e^{i(\omega t + kx)}$.

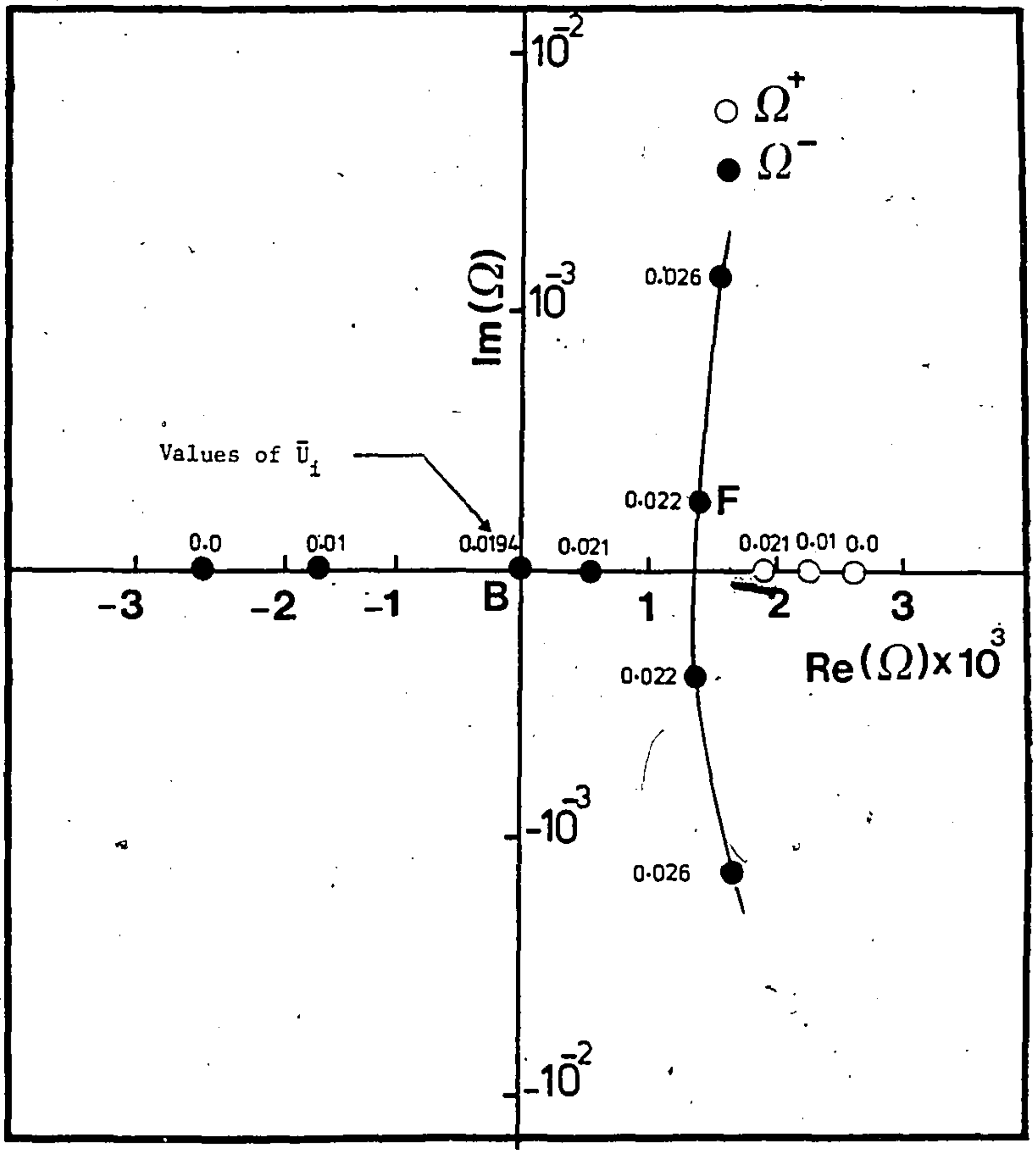

Figure 5. Argand diagram for the dimensionless frequency Ω as a function of the dimensionless internal flow velocity $\bar{U}_i$, where $\bar{U}_o = 0$; solution with $e^{i(\omega t - kx)}$.

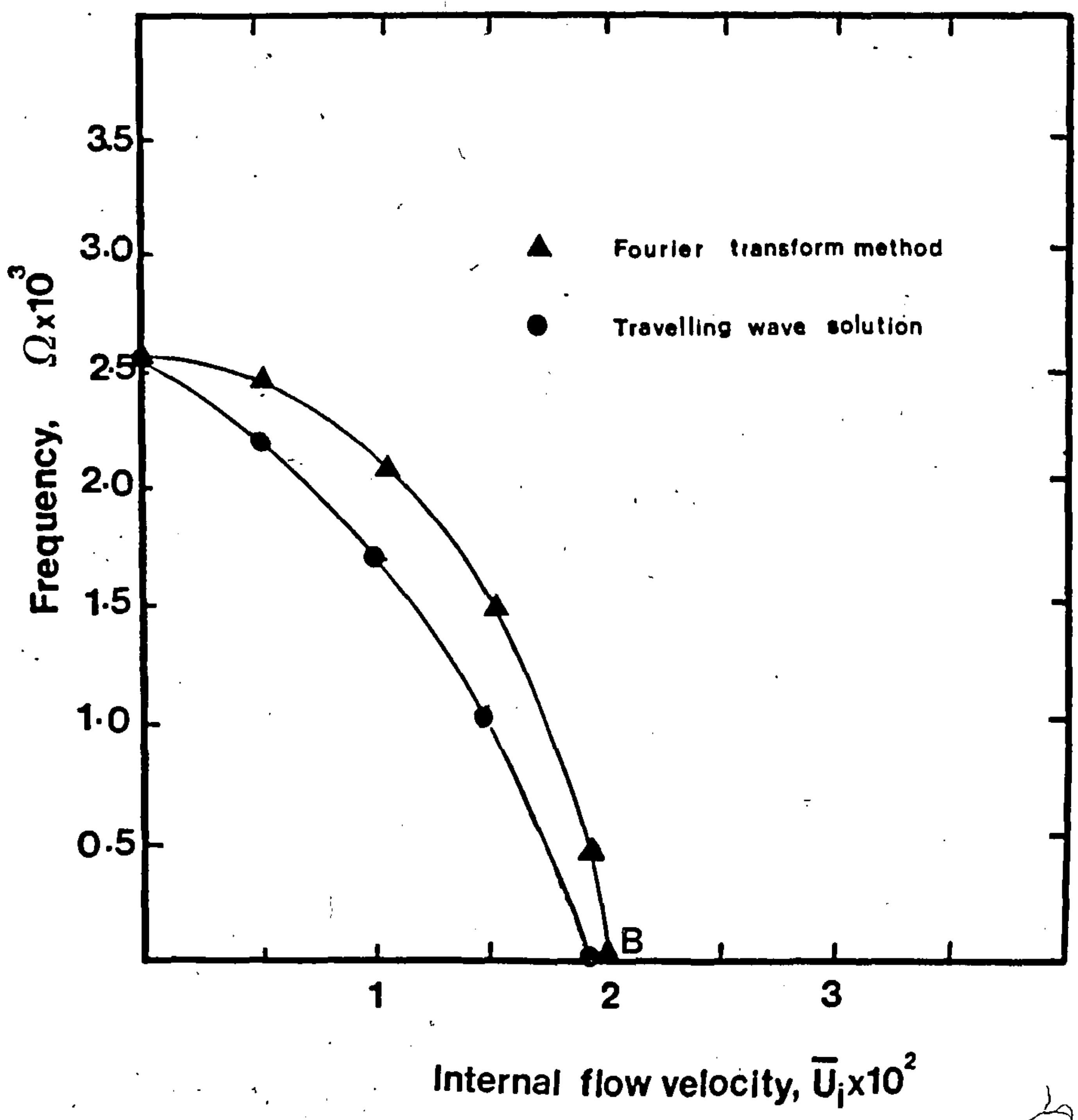

Figure 6. Comparison between the frequency-velocity curves in internal flow, obtained by the Fourier transform method and the travelling wave solution with $e^{i(\omega t + kx)}$; only Ω^+ is plotted.

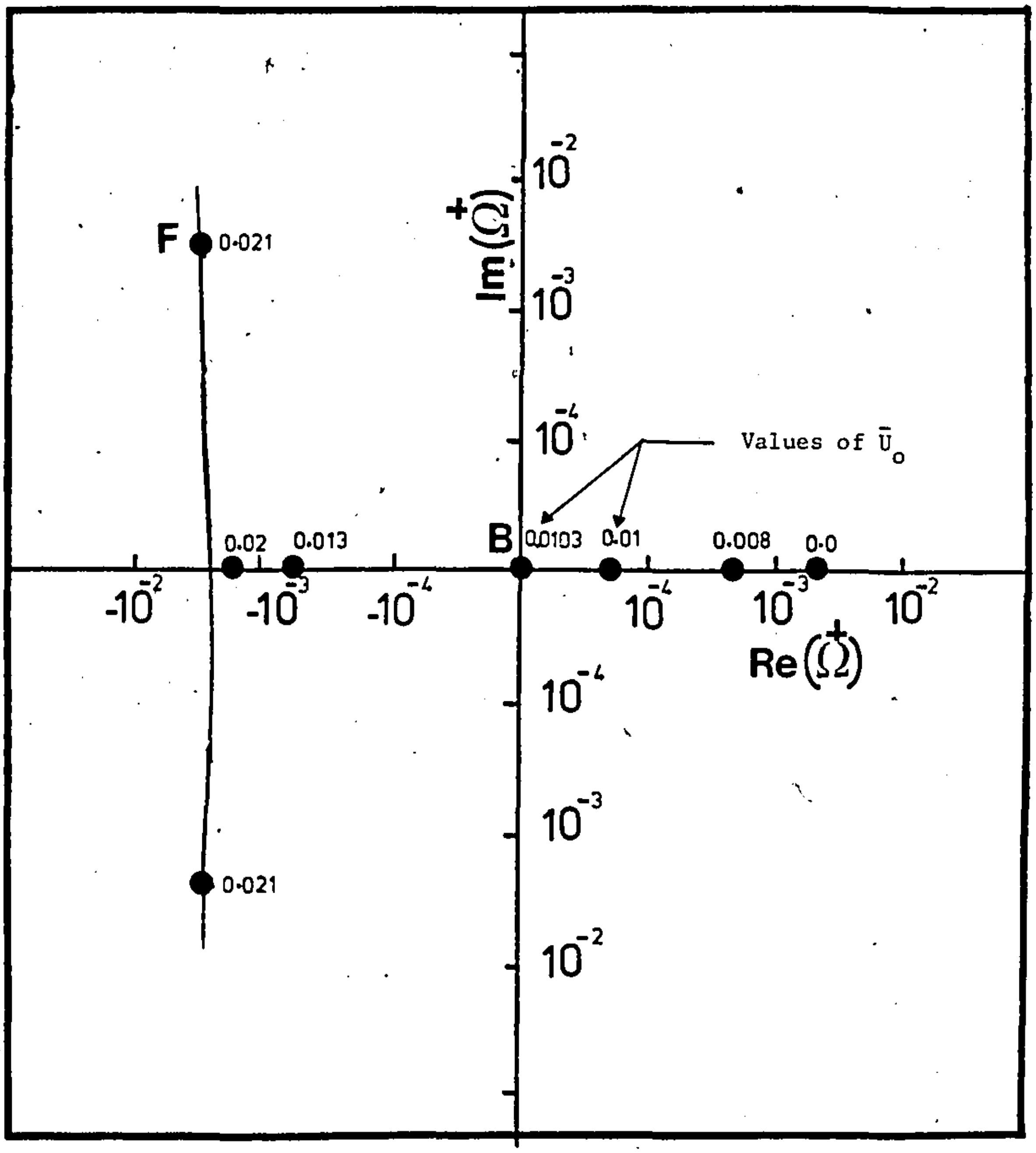

Figure 7. Argand diagram for the dimensionless frequency Ω^+ as a function of the dimensionless annular flow velocity $\bar{U}_o$, for a 1/10 gap-system; solution with $e^{i(\omega t + kx)}$.

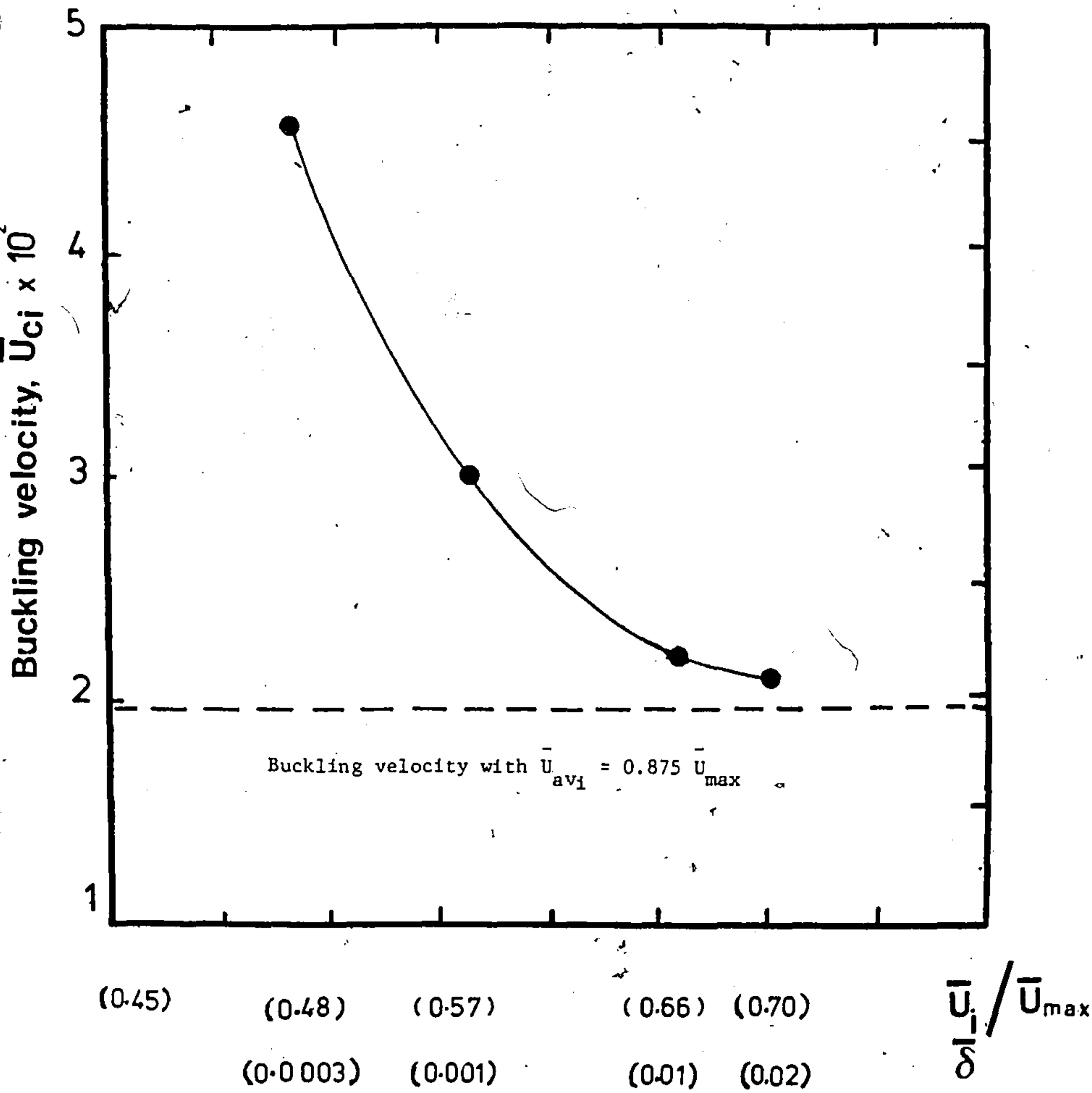

Figure 8. Buckling flow velocities obtained by the variable δ approximation as compared to the average velocity approximation.

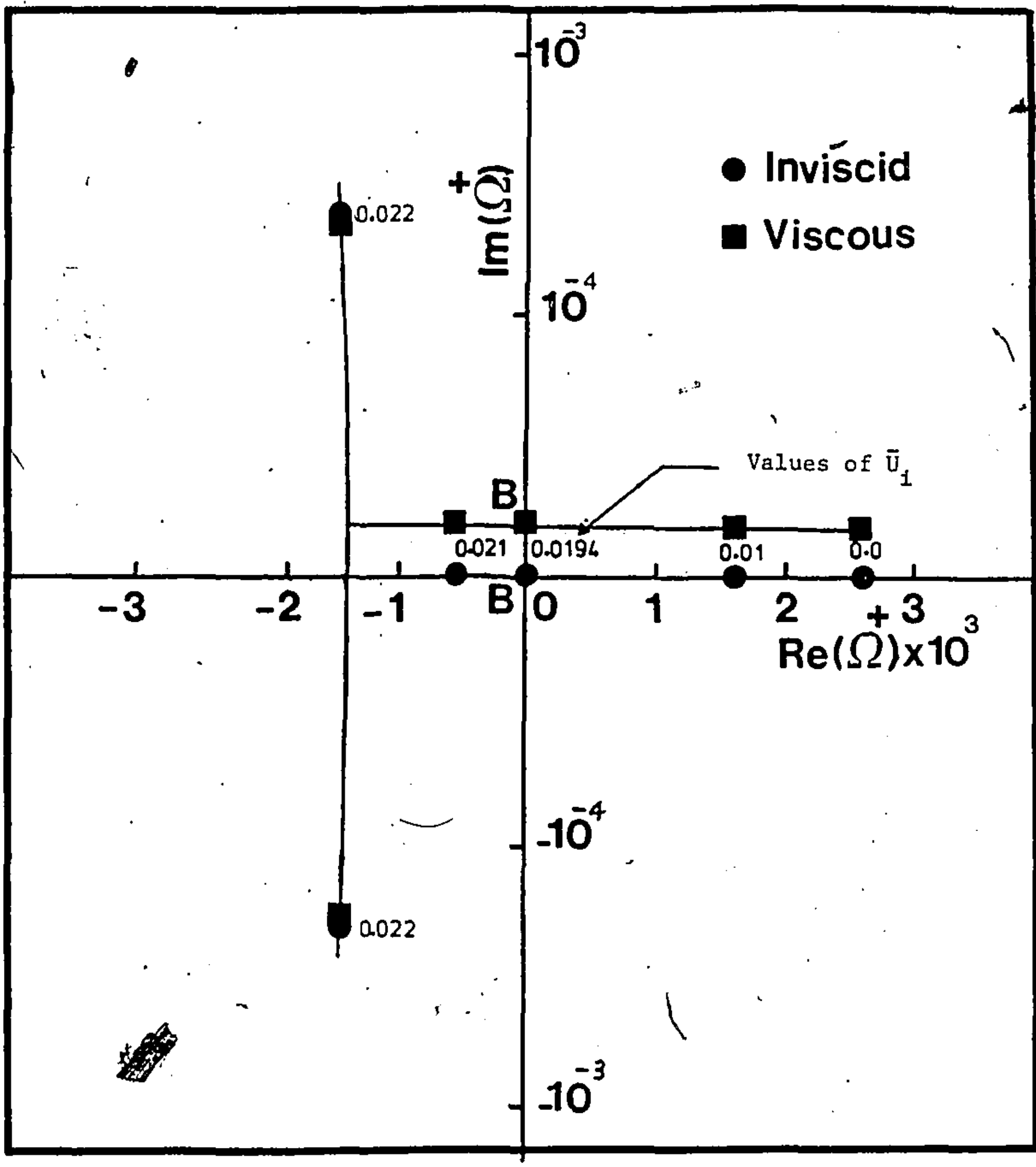

Figure 9. Argand diagram for the dimensionless frequency Ω^+ as a function of the dimensionless internal flow velocity $\bar{U}_i$ with or without the unsteady viscous forces; solution with $e^{i(\omega t + kx)}$.

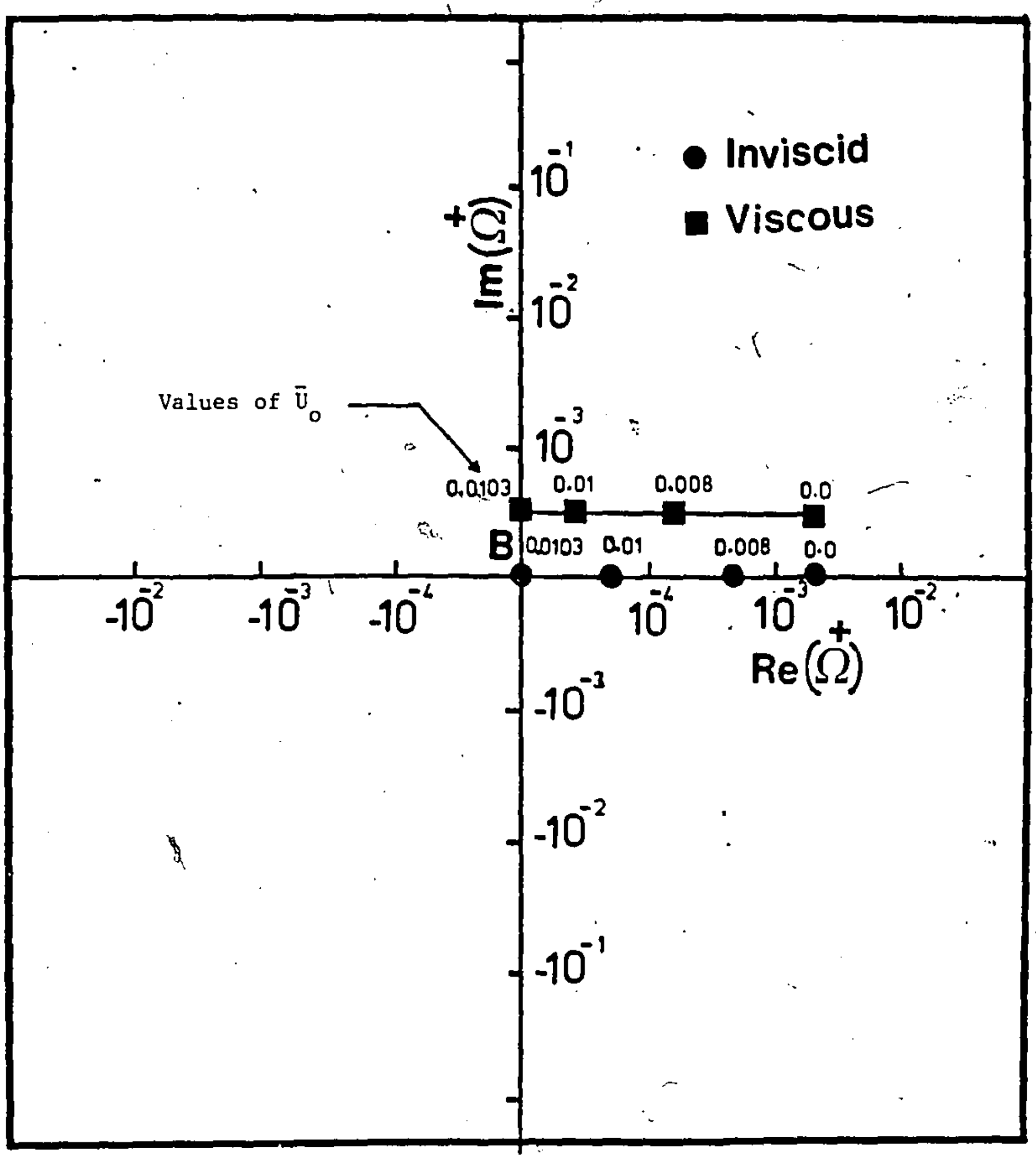

Figure 10. Argand diagram for the dimensionless frequency Ω^+ as a function of the dimensionless annular flow velocity $\bar{U}_o$ with or without the unsteady viscous forces; solution with $e^{i(\omega t + kx)}$.

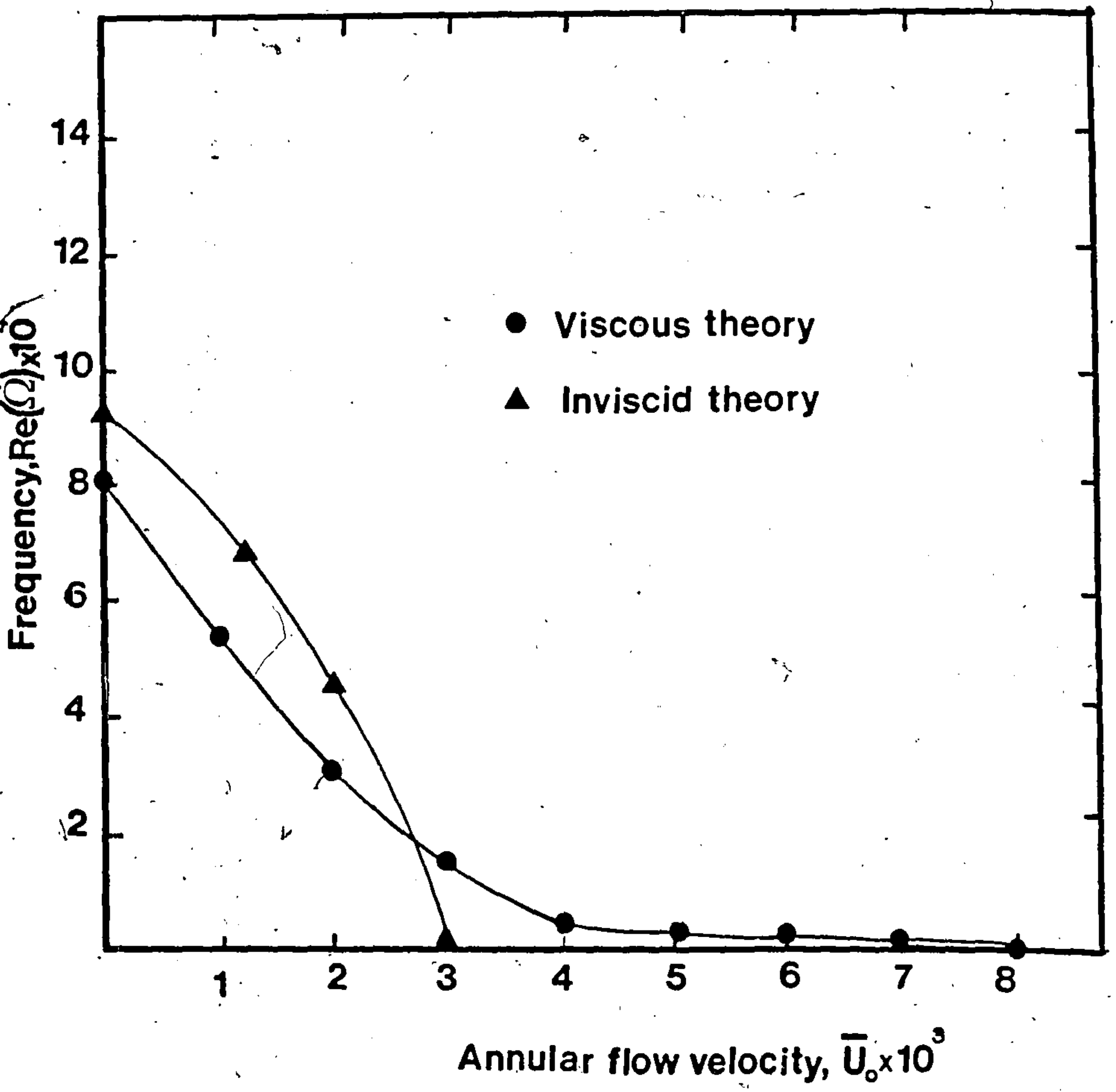

Figure 11. Frequency-velocity curves for a 1/100-gap system in annular flow, subjected to either purely inviscid forces or with unsteady viscous forces.

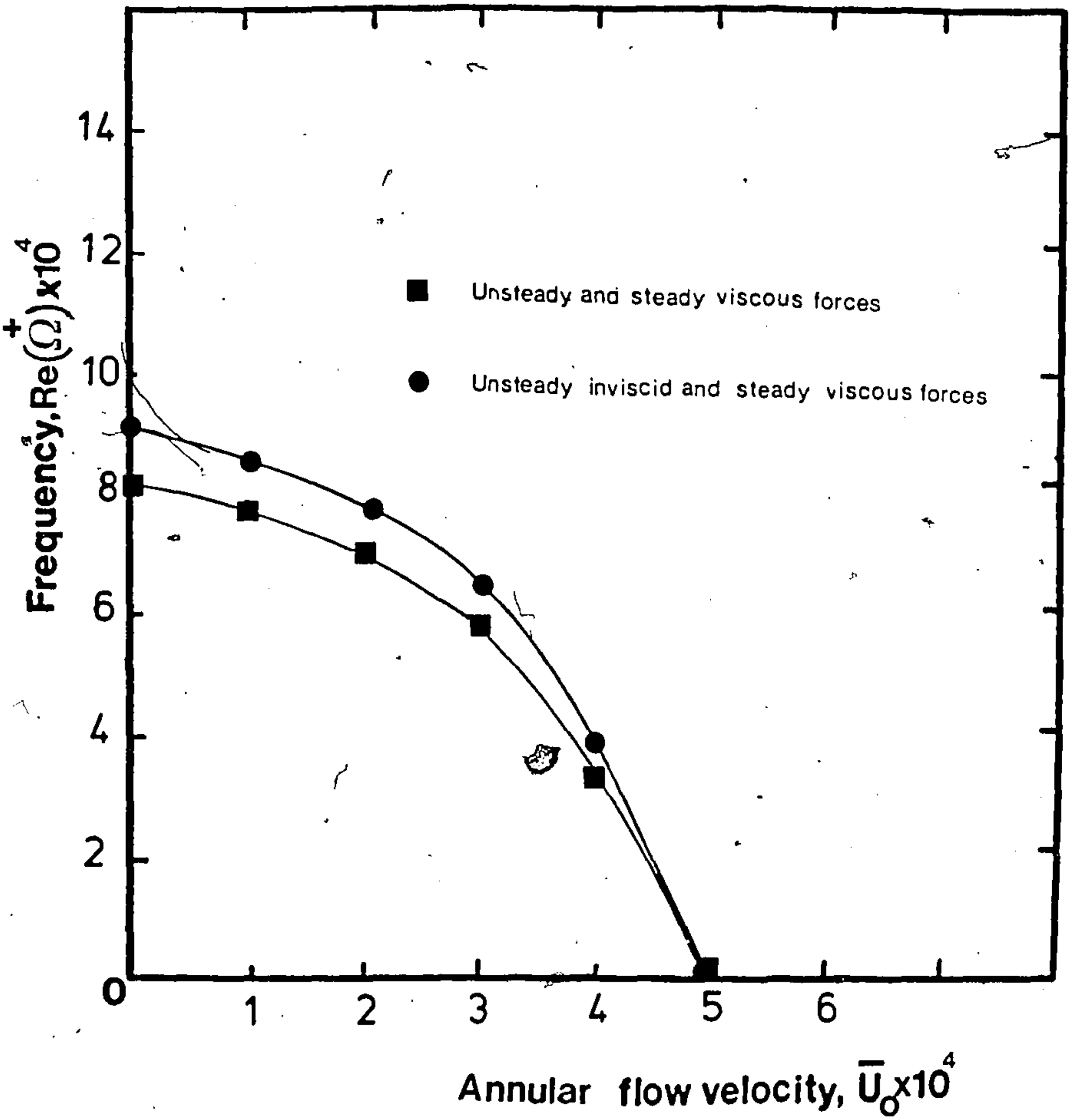

Figure 12. Frequency-velocity curves for annular flow for unsteady inviscid and steady viscous forces or unsteady viscous and steady viscous forces, $g/a_i = 1/100$.

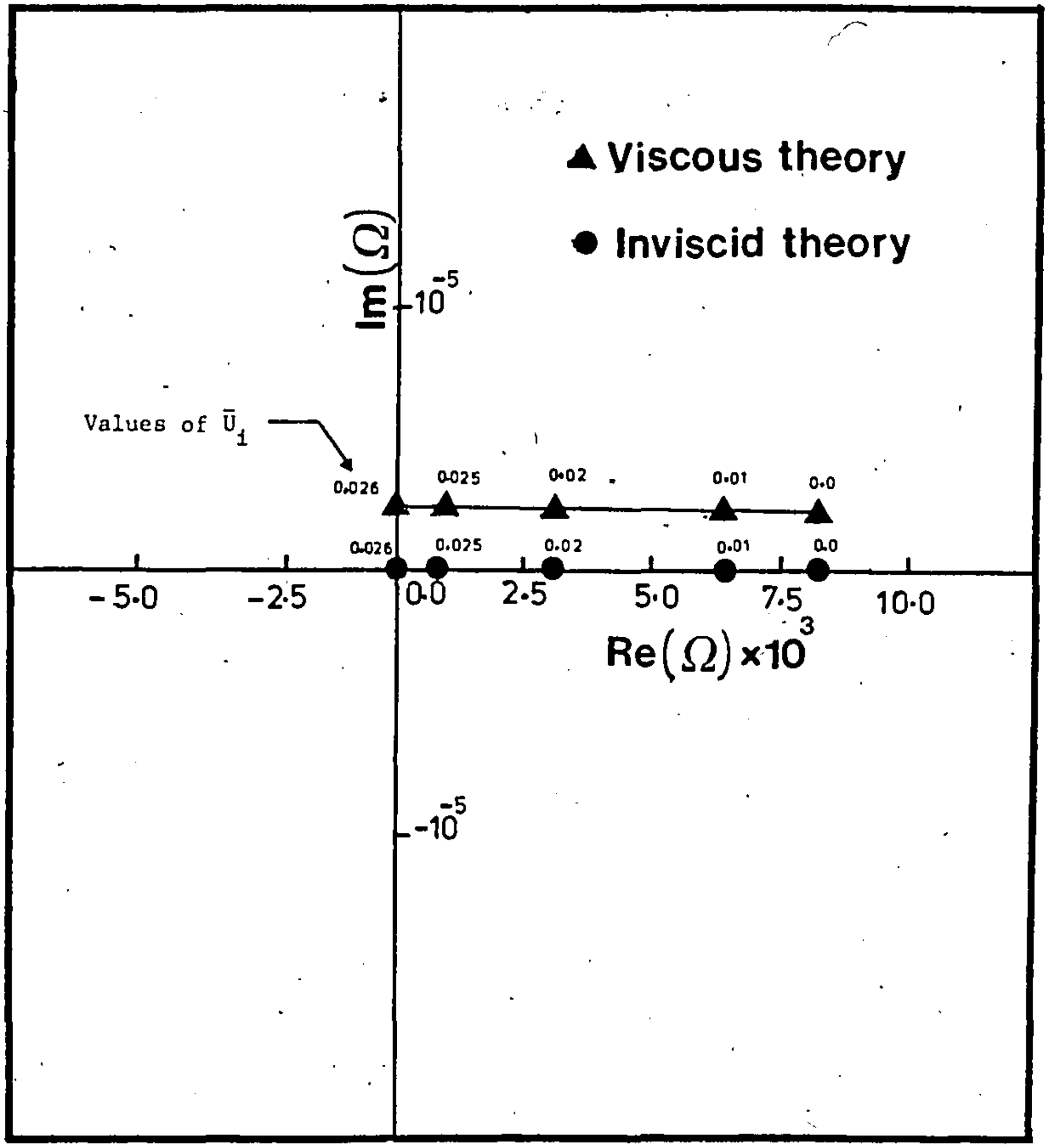

Figure 13. Argand diagram for the dimensionless frequency Ω as a function of the dimensionless internal flow velocity $\bar{U}_i$, using Fourier transform method (clamped-clamped shell).

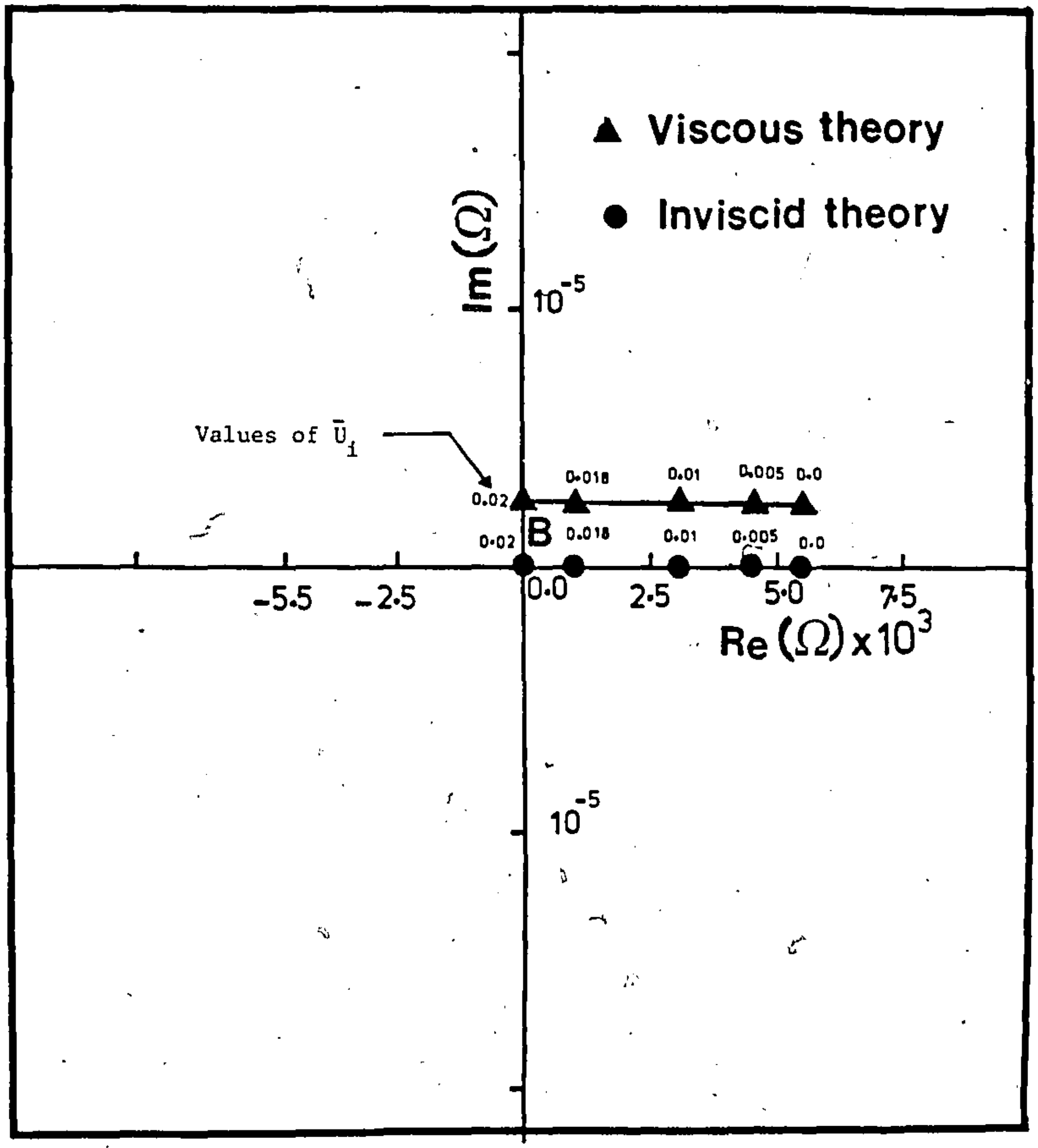

Figure 14. Argand diagram for the dimensionless frequency Ω as a function of the dimensionless internal flow velocity $\bar{U}_i$, using Fourier transform method (pinned-pinned shell).

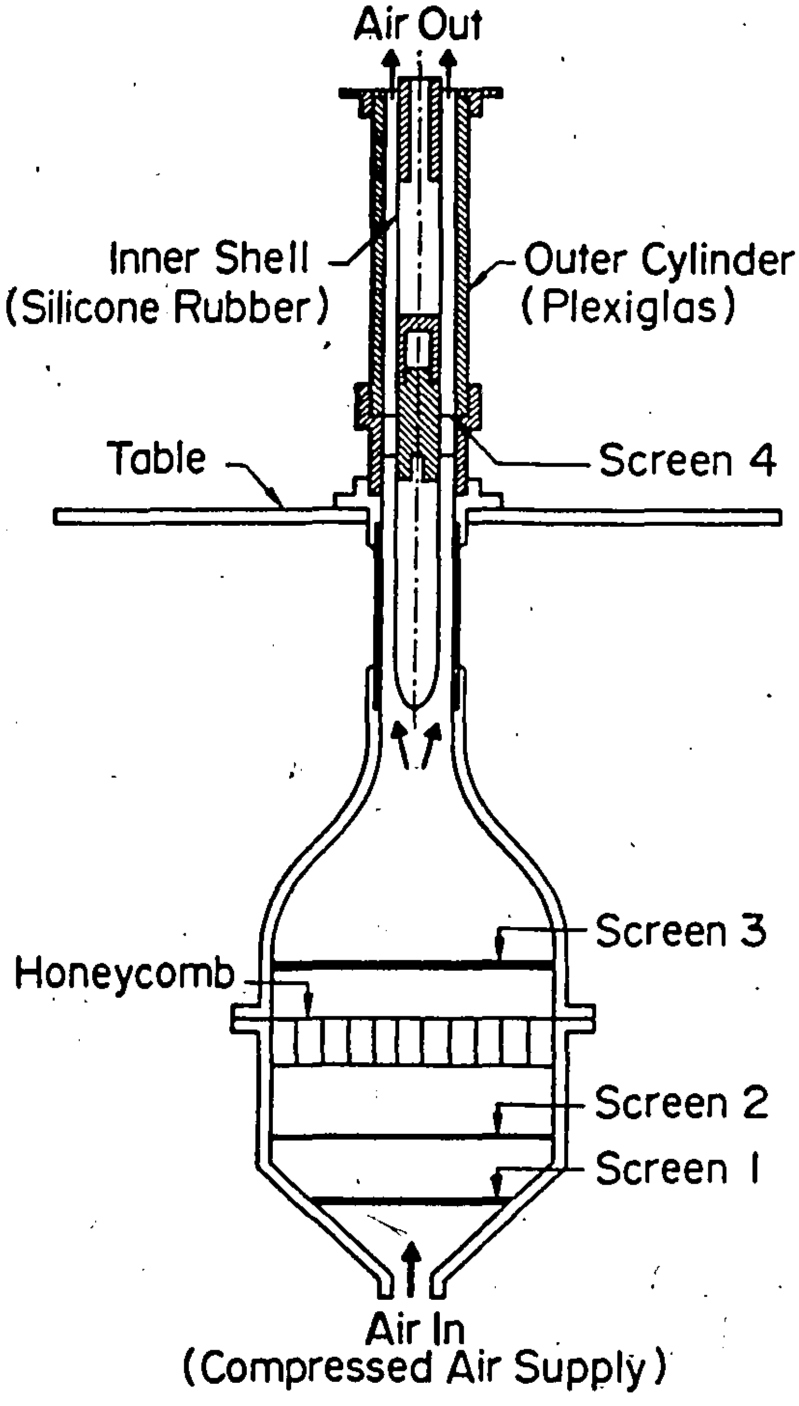

Figure 15. Schematic diagram for the experimental apparatus and the flow inlet section.

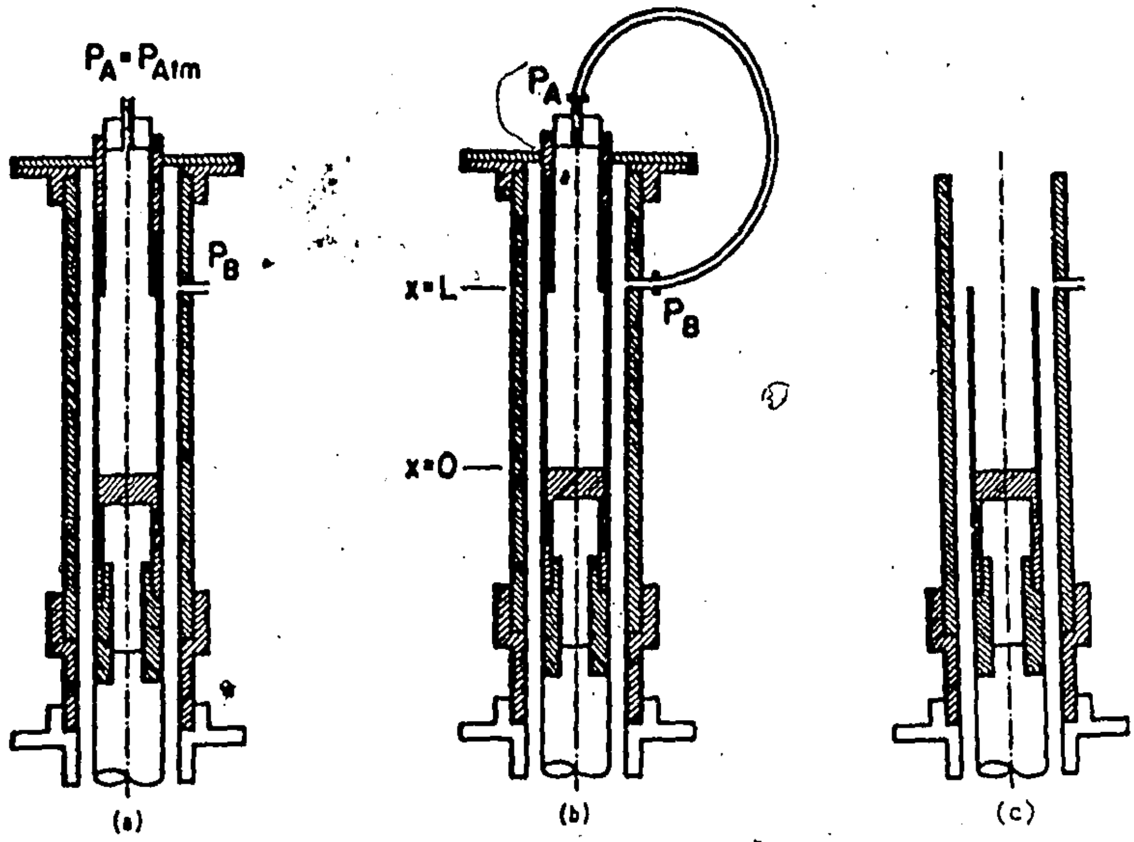

Figure 16. The two different arrangements for the internal pressure in the clamped-clamped shell : (a) with the mean pressure in the shell, P_A, equal to the atmospheric pressure; (b) with P_A equal to the static pressure in the annular flow at $x = L^A$; (c) the arrangement for the clamped-free shell.

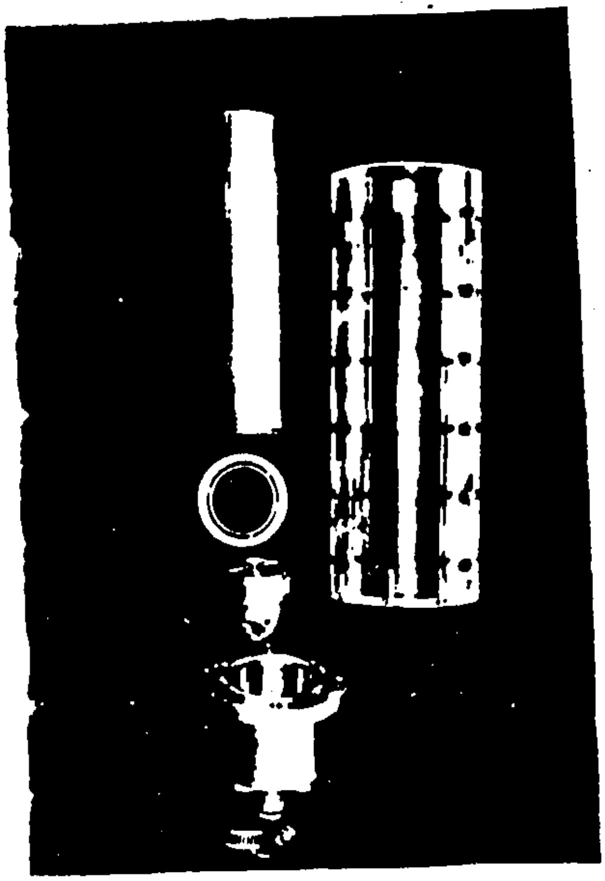

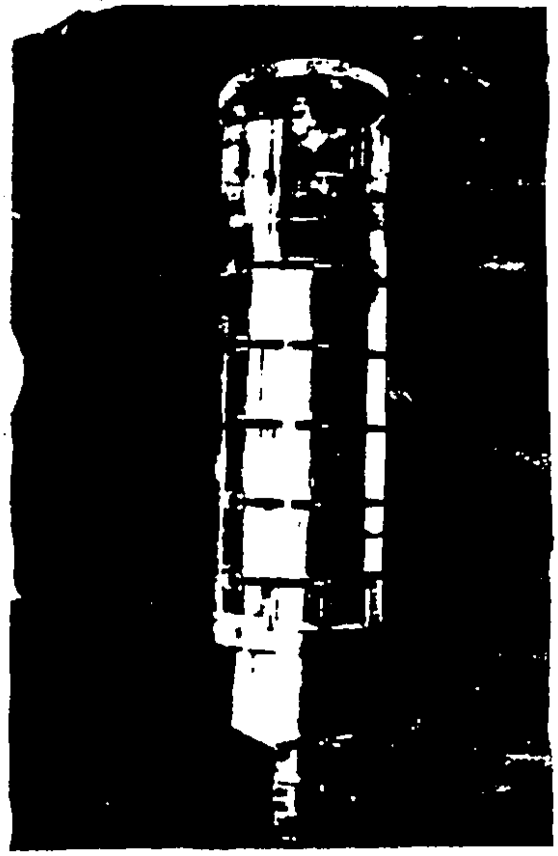

Figure 17. Moulding apparatus of the silicone rubber shell.

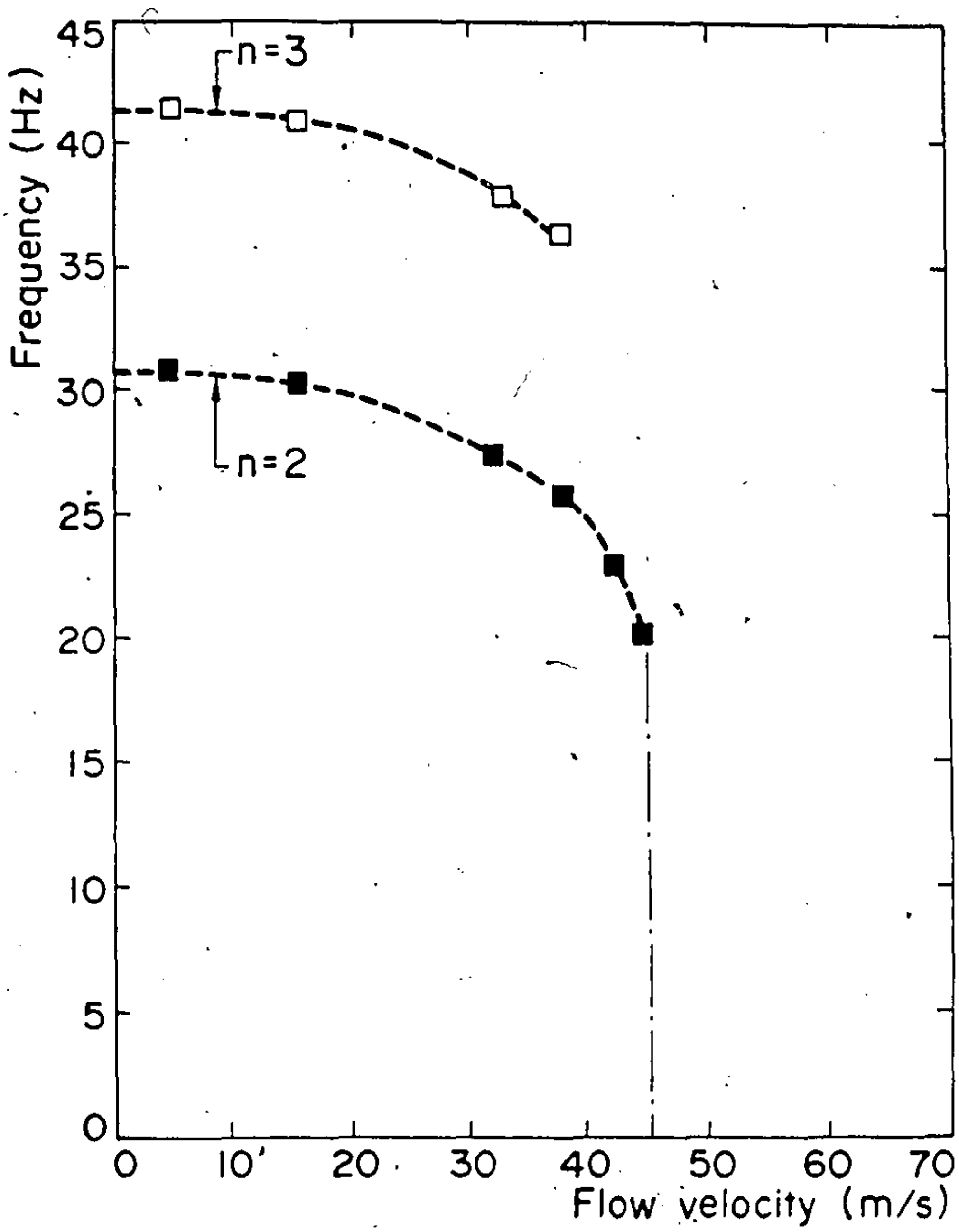

Figure 18. Experimental frequency-velocity curves for a clamped-clamped shell (L/a_i = 6, g/a_i = 0.25 and n = 2,3).

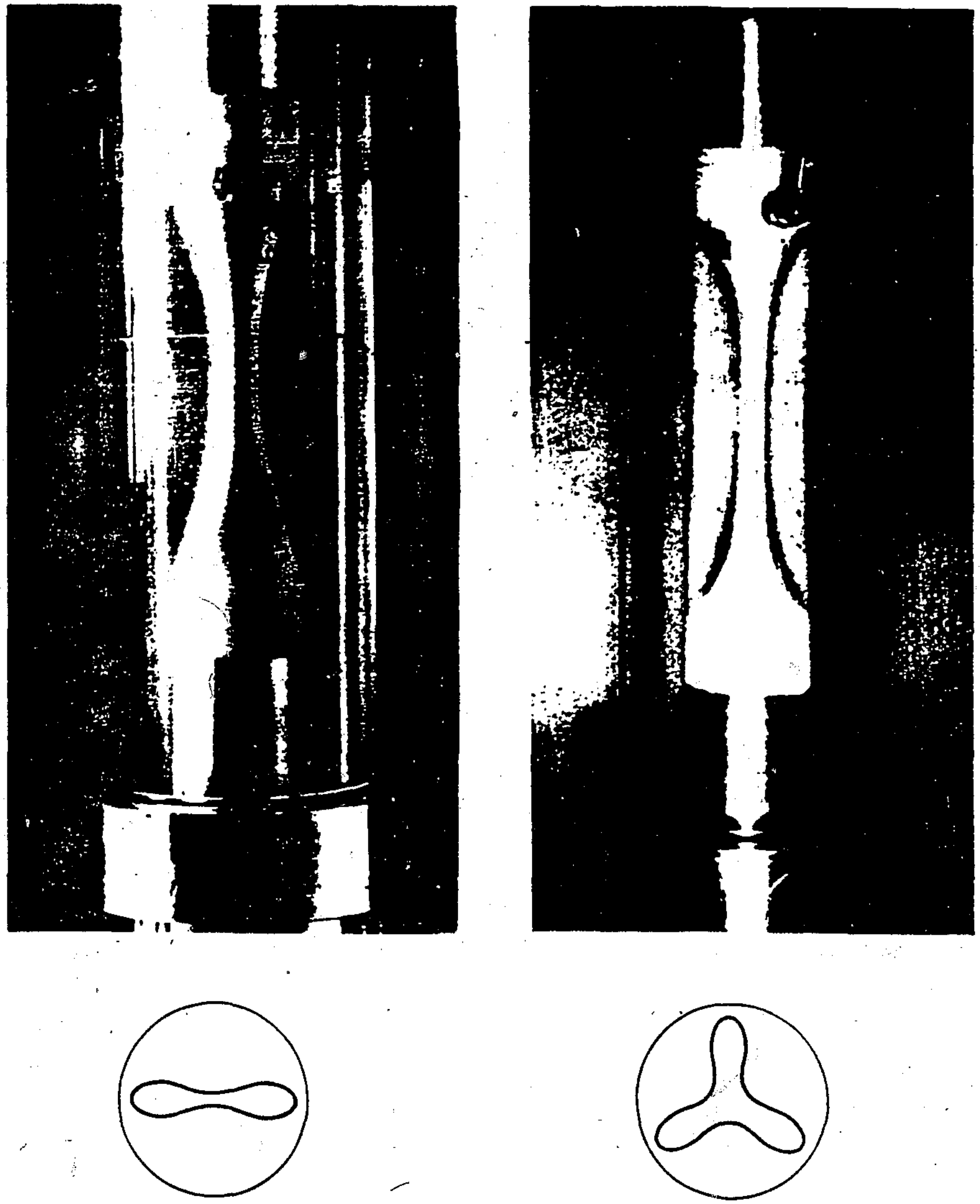

(a) (b)

Figure 19. Buckled shell in (a) n = 2 mode,
(b) n = 3 mode.

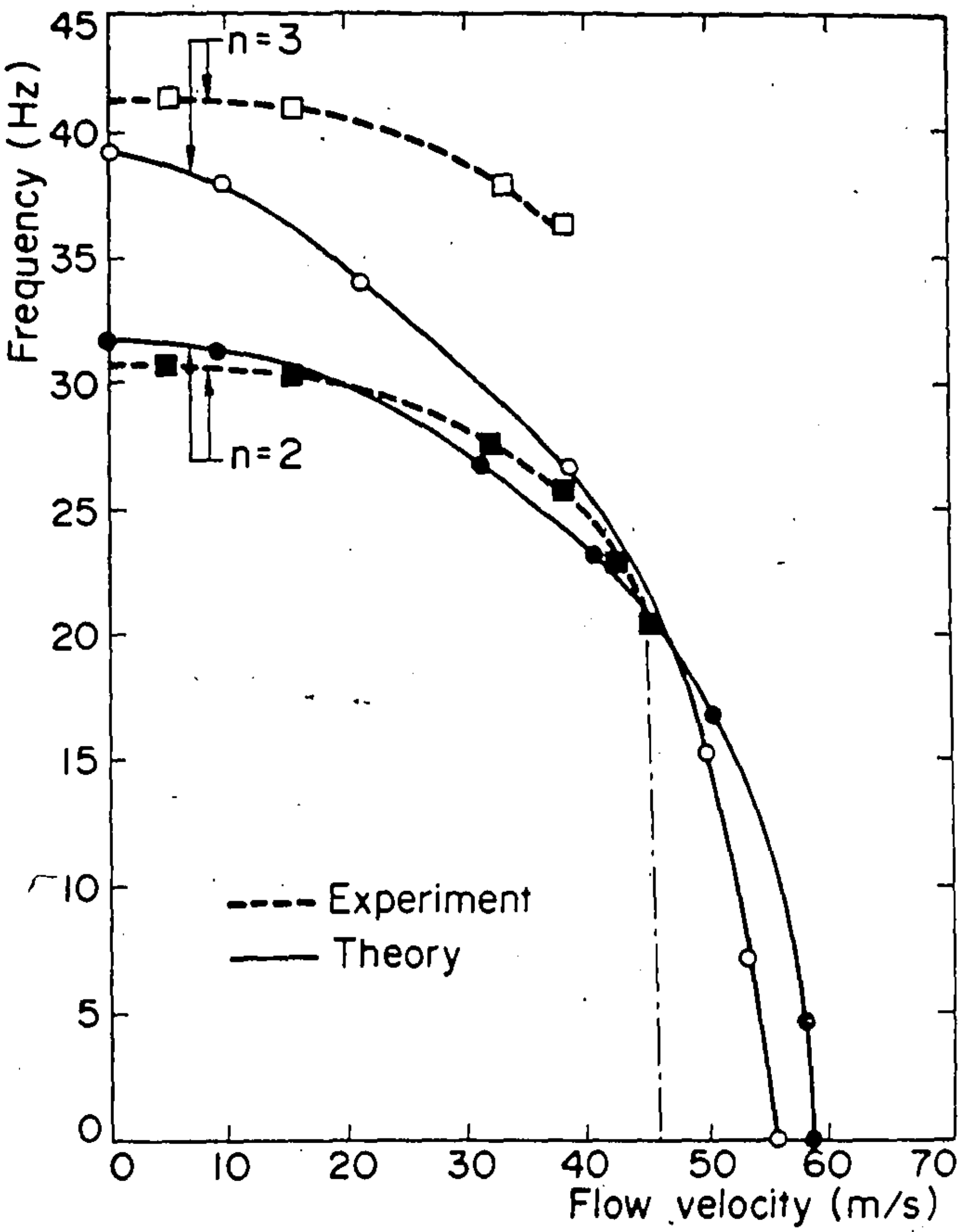

Figure 20. Variation of frequency with flow velocity for the two principal circumferential modes excited by the flow ($L/a_i = 6$, $g/a_i = 0.25$, $P_A = P_B$).

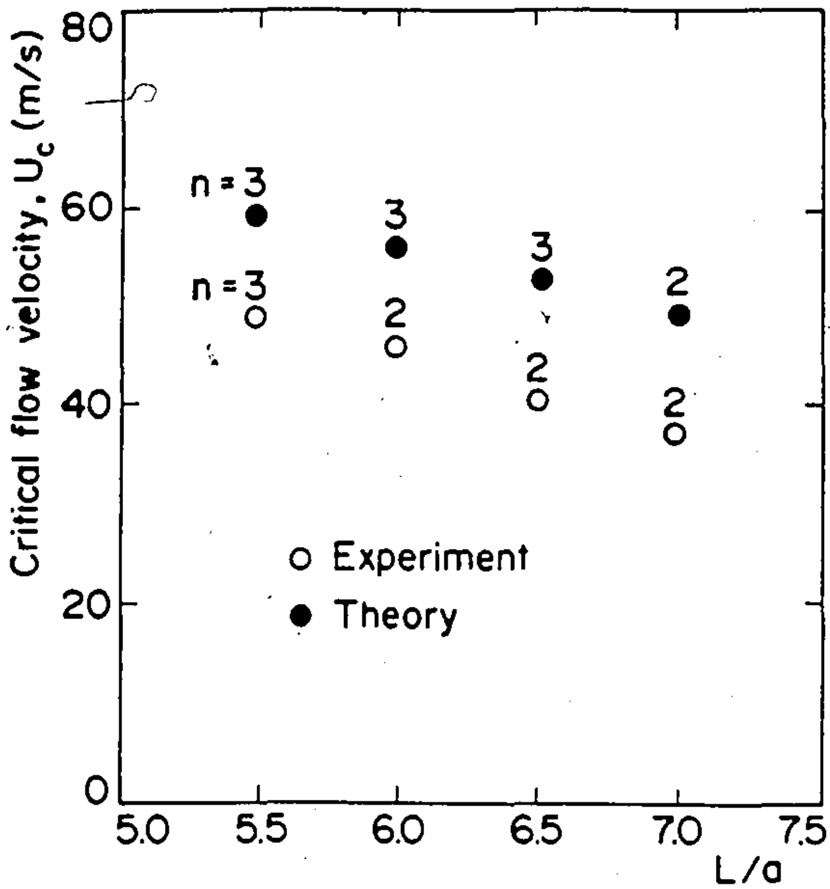

Figure 21. Effect of length-to-radius ratio L/a_i on the buckling velocity and the circumferential mode associated with it (g/a_i = 0.25, $P_A = P_B$).

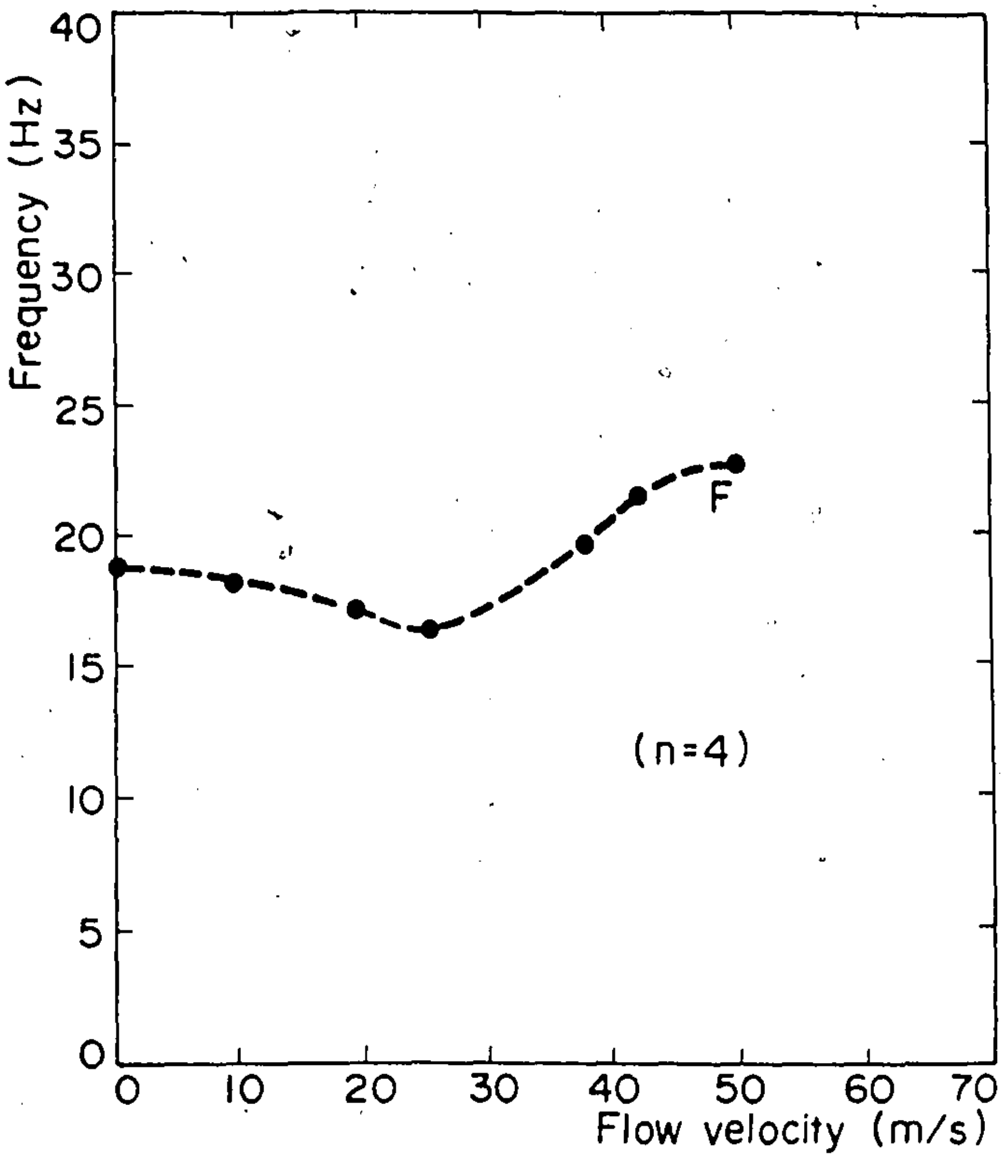

Figure 22. Frequency-velocity curve for a clamped-free shell (L/a_i = 6, g/a_i = 0.25).

APPENDIX A

DERIVATION OF THE STEADY FORCES

In the derivation of the equations of motion, the shell is assumed to be pre-stressed by the following loads:

(i) a constant axial force per unit area

$$\bar{P}_x = B_f \; , \tag{A.1}$$

(ii) an axially symmetric normal pressure

$$\bar{P}_r = - \left(C_f x + D_f \right) \; . \tag{A.2}$$

The associated axial and hoop stress resultants are

$$\bar{N}_x = B_f(\tfrac{1}{2} L - x) - \upsilon_s \, a_i \, (\tfrac{1}{2} L C_f + D_f) \; , \tag{A.3}$$

$$N_\theta = - a_i \left(C_f x + D_f \right) \; . \tag{A.4}$$

The effect of the above forces and stresses appear in the equations of motion as q_1, q_2 and q_3, where

$$q_1 = \left[(1 - \upsilon_s^2) \, / \, Eh \right] \bar{N}_x \; , \tag{A.5}$$

$$q_2 = \left[a_i(1 - \upsilon_s^2) \, / \, Eh \right] \bar{P}_x \; , \tag{A.6}$$

$$q_3 = \left[a_i(1 - \upsilon_s^2) \, / \, Eh \right] \bar{P}_r \; . \tag{A.7}$$

The derivation of these loads was done in Ref. [48]. In this Appendix, the expressions for q_1, q_2 and q_3 are simply given without going through the complete derivation. However, a description of how one can arrive at the final expressions is attempted.

A.1 STATIC FLUID PRESSURE AND THE SURFACE FRICTIONAL FORCES

The flow is assumed to be fully developed turbulent, incompressible and viscous. The fluid pressure and the surface frictional forces, inside a circular cylinder and in the annulus between two coaxial cylinders, are derived by assuming the cylinders to be rigid.

The schematic of the system is shown in Fig. 1. The flow velocity components in the cylindrical coordinates x, θ, r are $U + u_x$, u_θ, and u_r respectively†; U is the mean velocity in the axial direction while u_x, u_θ, u_r are the fluctuating velocity components of the turbulent flow. For a flow velocity U and static pressure P, the time-mean Navier-Stokes equations are [52]

$$\frac{1}{\rho}\frac{\partial P}{\partial x} = -\frac{1}{r}\frac{d}{dr}\left(r\,\overline{u_x u_r}\right) + \frac{\nu}{r}\frac{d}{dr}\left(r\frac{dU}{dr}\right), \tag{A.8}$$

$$\frac{1}{\rho}\frac{\partial P}{\partial r} = -\frac{1}{r}\frac{d}{dr}\left(r\,\overline{u_r^2}\right) + \frac{1}{r}\left(\overline{u_\theta^2}\right), \tag{A.9}$$

$$0 = \frac{d}{dr}\left(\overline{u_r u_\theta}\right) + \frac{2}{r}\left(\overline{u_r u_\theta}\right). \tag{A.10}$$

After going through some mathematical manipulations, the following relationships were obtained, for internal and for annular flow.

(i) Internal Flow

$$P_i(x,r) = -2\frac{\rho_i}{a_i}U_{\tau i}^2 x - \rho_i\,\overline{u}_{ri}^2 + \rho_i\int_{a_i}^{r}\frac{\overline{u}_{\theta i}^2 - \overline{u}_{ri}^2}{r}\,dr + P_i(0,a_i) \tag{A.11}$$

where $U_{\tau i}$, the so-called stress velocity, is given by

$$U_{\tau i} = \left[-\nu_i\left.\frac{dU_i}{dr}\right|_{r=a}\right]^{1/2}, \tag{A.12a}$$

---

† The analysis applies to both internal and annular regions.

$$= \left(\frac{\tau_{wi}}{\rho_i} \right)^{1/2} , \tag{A.12b}$$

$$= \left(\frac{1}{8} f_i U_i^2 \right)^{1/2} ; \tag{A.12c}$$

where

a_i is the radius of the inner cylinder

U_i is the mean axial velocity of the internal flow

τ_{wi} is the fluid frictional force per unit area of the interior surface of the shell

f_i friction factor

$P_i(x,r)$ is the internal time-mean pressure

$P_i(0,a_i)$ is the internal fluid pressure at the position $x = 0$, $r = a_i$

ρ_i and υ_i are the fluid density and kinematic viscosity, respectively;

$\overline{(\ )}$ represents the time-mean of ( )

i is a subscript to denote the internal flow

(ii) Annular Flow

$$P_o(x,r) = -\left(\frac{2a_o}{(a_o^2 - r_m^2)} \right) \rho_o U_{\tau oo}^2 \, x - \rho_o \overline{u_{ro}^2} + \rho_o \int_{a_i}^{r} \frac{\overline{u_{\theta o}^2} - \overline{u_{ro}^2}}{r} \, dr + P_o(0,a_i) , \tag{A.13}$$

where

$$U_{\tau oo} = \left(-\upsilon_o \frac{dU_o}{dr} \bigg|_{r=a_o} \right)^{1/2} , \tag{A.14a}$$

$$= \left(\frac{\tau_{woo}}{\rho_o} \right)^{1/2} , \tag{A.14b}$$

$$= \left[\frac{1}{8} \left(\frac{a_o^2 - r_m^2}{a_o(a_o - a_i)} \right) f_o \, U_o^2 \right]^{1/2} , \tag{A.14c}$$

$$U_{\tau oi} = \left(-\upsilon_o \frac{dU_o}{dr} \bigg|_{r=a_i} \right)^{1/2} , \tag{A.15a}$$

$$= \left(\frac{\tau_{woi}}{\rho_o} \right)^{1/2} \tag{A.15b}$$

$$= \left[\frac{a_o}{a_i} \left(\frac{r_m^2 - a_i^2}{a_o^2 - r_m^2} \right) U_{\tau oo}^2 \right]^{1/2} \tag{A.15c}$$

where

U_o is the mean axial velocity in the annulus

$P_o(x,r)$ is the annular time-mean pressure

$P_o(0,a_i)$ is the annular fluid pressure at the position $x = 0$, $r = a_i$

$U_{\tau oo}$ is the stress velocity at the inner surface of the outer cylinder

$U_{\tau oi}$ is the stress velocity at the outer surface of the inner cylinder

f_o is the friction factor in the annulus

τ_{woi} is the fluid frictional force per unit area of the outer surface of the inner cylinder

τ_{woo} is the fluid frictional force per unit area of the inner surface of the outer cylinder

ρ_o and υ_o are the fluid density and kinematic viscosity, respectively

r_m is the radius at which the mean velocity U_o is maximum

a_o is the inner radius of the outer cylinder

o is a subscript to denote the annular fluid

In order to find $U_{\tau i}$, $U_{\tau oi}$ and $U_{\tau oo}$, one must evaluate f_i, f_o and r_m. First, r_m cannot be determined analytically. Based on some experimental data [50,51], it is found that for the cases considered, r_m could be approximated by its counterpart in the case of laminar flow.

$$r_m = \left\{ \frac{a_o^2 - a_i^2}{2 \ln (a_o/a_i)} \right\}^{1/2} \tag{A.16}$$

The friction factor f is a function of the Reynolds number Re, and the relative roughness of the pipe k/d, where k is the average height of the surface protrusions and d is the pipe diameter. The friction factor may be found graphically from a Moody diagram which is a plot of f versus Re for different k/d. Alternatively, it may be determined with a number of empirical formulas. A common practice is to use the Colebrook equation [52], which is

$$\frac{1}{(f)^{1/2}} = -2 \log_{10} \left[\frac{k/d}{3.7} + \frac{2.51}{Re(f)^{1/2}} \right] . \tag{A.17}$$

To avoid solving the implicit Colebrook equation, it may be modified as follows [52]

$$\frac{1}{(f)^{1/2}} = -2 \log_{10} \left[\frac{k/d}{3.7} + \frac{2.51}{Re(f_a)^{1/2}} \right] , \tag{A.18}$$

where f_a is given by the following equation derived by Moody and matches equation (A.17) within ± 5%:

$$f_a = 0.0055 \left\{ 1 + \left[20,000 \left(\frac{k}{d} \right) + \frac{10^6}{Re} \right]^{1/3} \right\} . \tag{A.19}$$

Equations (A.18) and (A.19) are applicable for both internal and annular flow. For internal flow, the friction factor f_i is found by setting d equal to the diameter of the inner cylinder d_i and Re to Re_i, where

$$Re_i = \frac{U_i d_i}{\upsilon_i} ; \tag{A.20}$$

for the annular flow, in place of the diameter of the pipe, the hydraulic diameter, D_h, is used along with the Reynolds number Re_o, which is defined as

$$Re_o = \frac{U_o D_h}{\nu_o} , \tag{A.21}$$

where

$$D_h = 2(a_o - a_i) . \tag{A.22}$$

A.2 BASIC LOADS

The radial basic load on the shell is

$$\overline{P}_r = P_i(x,a_i) - P_o(x,a_i) . \tag{A.23}$$

Taking equations (A.11) and (A.13) evaluated at $r = a_i$, $\overline{P}_r$ may be expressed as

$$\overline{P}_r = \left\{ - \frac{2\rho_i U_{\tau i}^2}{a_i} + \left(\frac{2a_o}{a_o^2 - r_m^2} \right) \rho_o U_{\tau oo}^2 \right\} x + P_i(0,a_i) - P_o(0,a_i) , \tag{A.24}$$

where the fact that $\overline{u_{ro}^2}$ must vanish at the wall has been utilized.

The axial basic load is

$$\overline{P}_x = \tau_{wi} + \tau_{woi} . \tag{A.25}$$

hence

$$\overline{P}_x = \rho_i U_{\tau i}^2 + \rho_o U_{\tau oi}^2 . \tag{A.26}$$

Comparing (A.1) and (A.2) with (A.24) and (A.26) one may find that

$$B_f = \rho_i U_{\tau i}^2 + \rho_o U_{\tau wi}^2 , \tag{A.27}$$

$$C_f = \frac{2\rho_i}{a_i} U_{\tau i}^2 - \frac{2a_o}{a_o^2 - r_m^2} \rho_o U_{\tau oo}^2 , \tag{A.28}$$

$$D_f = P_o(0,a) - P_i(0,a) , \tag{A.29}$$

where

$$P_o(0,a) = \frac{2a_o}{a_o^2 - r_m^2} \rho_o U_{\tau oo}^2 L + P_{atm} \tag{A.30}$$

$$P_i(0,a) = \frac{2\rho_i}{a_i} U_{\tau i}^2 L + P_{atm} \tag{A.31}$$

Having defined the constants B_f, C_f and D_f, the basic forces q_1, q_2 and q_3 are then evaluated.

APPENDIX B

MATHEMATICAL MANIPULATION OF EQUATION (2.33)

In this Appendix the proof is given of the mathematical manipulation of equation (2.33) to give equation (2.35). It is recalled that the former is

$$\rho \frac{\partial}{\partial t} \left(\bar{\nabla} \times \bar{\psi} \right) = \mu \nabla^2 \left(\bar{\nabla} \times \bar{\psi} \right) . \tag{B.1}$$

Now, $\frac{\partial}{\partial t} \left(\bar{\nabla} \times \bar{\psi} \right)$ could be written as

$$\bar{\nabla} \times \frac{\partial \bar{\psi}}{\partial t} , \tag{B.2}$$

and using $\nabla^2 \bar{A} = \bar{\nabla} \left(\bar{\nabla} \cdot \bar{A} \right) - \bar{\nabla} \times \left(\bar{\nabla} \times \bar{A} \right)$ one may write

$$\nabla^2 \left(\bar{\nabla} \times \bar{\psi} \right) = \bar{\nabla} \left[\bar{\nabla} \cdot \left(\bar{\nabla} \times \bar{\psi} \right) \right] - \bar{\nabla} \times \left(\bar{\nabla} \times \left(\bar{\nabla} \times \bar{\psi} \right) \right) . \tag{B.3}$$

Using the fact that, the divergence of a curl of a vector is equal to zero, equation (B.3) reduces to

$$\nabla^2 \left(\bar{\nabla} \times \bar{\psi} \right) = - \bar{\nabla} \times \left(\bar{\nabla} \times \left(\bar{\nabla} \times \bar{\psi} \right) \right) ; \tag{B.4}$$

similarly,

$$\bar{\nabla} \times \left(\bar{\nabla} \times \bar{\psi} \right) = \bar{\nabla} \left(\bar{\nabla} \cdot \bar{\psi} \right) - \nabla^2 \bar{\psi} \tag{B.5}$$

and hence

$$\bar{\nabla} \times \left(\bar{\nabla} \times \left(\bar{\nabla} \times \bar{\psi} \right) \right) = \bar{\nabla} \times \left[\bar{\nabla} \left(\bar{\nabla} \cdot \bar{\psi} \right) \right] - \bar{\nabla} \times \left(\nabla^2 \bar{\psi} \right) . \tag{B.6}$$

The Curl of gradient of $\bar{\nabla} \cdot \bar{\psi}$ vanishes; then, equation (B.6) reduces to

$$\bar{\nabla} \times \left(\bar{\nabla} \times \left(\bar{\nabla} \times \bar{\psi} \right) \right) = - \bar{\nabla} \times \left(\nabla^2 \bar{\psi} \right) . \tag{B.7}$$

Substituting for $\bar{\nabla} \times \left(\bar{\nabla} \times \bar{\nabla} \times \bar{\psi} \right)$ into equation (B.4), leads to

$$\nabla^2 \left(\bar{\nabla} \times \bar{\psi} \right) = \bar{\nabla} \times \left(\nabla^2 \bar{\psi} \right) . \tag{B.8}$$

Using equations (B.2) and (B.8), one can rewrite equation (B.1) in the form of equation (2.35).

$$\bar{\nabla} \times \left[\rho \frac{\partial \bar{\psi}}{\partial t} - \mu \nabla^2 \bar{\psi} \right] = 0. \tag{B.9}$$

APPENDIX C

INTEGRALS INVOLVING CHARACTERISTIC BEAM FUNCTION

The constants a_{km}, b_{km}, d_{km}, e_{km}, f_{km}, g_{km}, h_{km} and j_{km} required in the analysis in Chapter III can be written in nondimensional form using the variable $\zeta = \frac{x}{L}$, as follows:

$$\begin{aligned}
\bar{\delta}_{km} &= \int_0^1 \Phi_k(\zeta)\ \Phi_m(\zeta)\ d\zeta \\
a_{km} &= \int_0^1 \frac{d\Phi_k}{d\zeta}\frac{d\Phi_m}{d\zeta}\ d\zeta \\
b_{km} &= \int_0^1 \frac{d\Phi_k}{d\zeta}\ \frac{d^3\Phi_m}{d\zeta^3}\ d\zeta \\
d_{km} &= \int_0^1 \Phi_k\ \frac{d^2\Phi_m}{d\zeta^2}\ d\zeta \\
e_{km} &= \int_0^1 \zeta\ \frac{d\Phi_k}{d\zeta}\ \frac{d^3\Phi_m}{d\zeta^3}\ d\zeta \\
f_{km} &= \int_0^1 \frac{d\Phi_k}{d\zeta}\ \Phi_m\ d\zeta \\
g_{km} &= \int_0^1 \zeta\ \frac{d\Phi_k}{d\zeta}\ \frac{d\Phi_m}{d\zeta}\ d\zeta \\
h_{km} &= \int_0^1 \zeta\ \Phi_k\ \frac{d^2\Phi_m}{d\zeta^2}\ d\zeta \\
j_{km} &= \int_0^1 \zeta\ \Phi_k\ \Phi_m\ d\zeta
\end{aligned} \qquad (C.1)$$

where Φ_k and Φ_m are characteristic eigenfunctions of a beam.

C.1 CLAMPED-CLAMPED BEAM

In this case, the mth eigenfunction is defined as

$$\Phi_m(\zeta) = \cosh(\lambda_m \zeta) - \cos(\lambda_m \zeta) - \sigma_m \left[\sinh(\lambda_m \zeta) - \sin(\lambda_m \zeta) \right], \tag{C.2}$$

where λ_m and σ_m are the eigenvalue and the characteristic constant, respectively. $\Phi_k(\zeta)$ is represented by equation (C.2) with a subscript k instead of m.

The values for the integrals for a clamped-clamped beam as given in Ref. [48] are listed below:

$$\bar{\delta}_{km} = \delta_{km} = 1 \quad \text{for} \quad m = k,$$
$$= 0 \quad \text{for} \quad m \neq k,$$

$$a_{km} = \frac{4\lambda_k^2 \lambda_m^2}{\lambda_k^4 - \lambda_m^4} \left[(-1)^{k+m} + 1 \right] \left(\lambda_m \sigma_m - \lambda_k \sigma_k \right) \text{ for } k \neq m,$$

$$a_{kk} = -\lambda_k \sigma_k \left(2 - \lambda_k \sigma_k \right), \tag{C.3}$$

$$b_{km} = 0 \qquad \text{for } k \neq m,$$

$$b_{kk} = -\lambda_k^4, \tag{C.4}$$

$$d_{km} = -a_{km}, \tag{C.5}$$

$$e_{km} = \frac{-4(3\lambda_m^4 + \lambda_k^4)\lambda_k^3 \lambda_m^3 \sigma_k \sigma_m}{(\lambda_m^4 - \lambda_k^4)^2} \left[(-1)^{k+m} - 1 \right] \text{ for } k \neq m,$$

$$e_{kk} = \frac{-\lambda_k^4}{2}, \tag{C:6}$$

$$f_{km} = \frac{4\,\lambda_k^2\,\lambda_m^2}{\lambda_k^4 - \lambda_m^4}\left[(-1)^{k+m} - 1\right] \quad \text{for } k \neq m\,,$$

$$f_{kk} = 0\,, \tag{C.7}$$

$$g_{km} = \frac{(-1)^{k+m}\,4\,\lambda_k^2\,\lambda_m^2}{(\lambda_m^4 - \lambda_k^4)}\left(\lambda_k\sigma_k - \lambda_m\sigma_m\right) - \frac{2(\lambda_m^4 + \lambda_k^4)}{\lambda_m^4 - \lambda_k^4}\,f_{km} \quad \text{for } k \neq m\,,$$

$$g_{kk} = \frac{\lambda_k\sigma_k}{2}\left(\lambda_k\sigma_k - 2\right)\,, \tag{C.8}$$

$$h_{km} = \frac{(-1)^{k+m}\,4\,\lambda_k^2\,\lambda_m^2\,(\lambda_m\sigma_m - \lambda_k\sigma_k)}{\lambda_m^4} + \frac{(3\,\lambda_m^4 + \lambda_k^4)}{\lambda_m^4 - \lambda_k^4}\,f_{km} \quad \text{for } k \neq m\,,$$

$$h_{kk} = \frac{\lambda_k\sigma_k}{2}\left(2 - \lambda_k\sigma_k\right)\,, \tag{C.9}$$

$$j_{km} = 16\,\lambda_k^3\,\lambda_m^3\,\sigma_k\,\sigma_m\left[(-1)^{k+m} - 1\right] \quad \text{for } k \neq m\,,$$

$$j_{kk} = \frac{1}{2}\,; \tag{C.10}$$

for a clamped-clamped beam, σ_m is defined as

$$\sigma_m = \frac{\cosh\lambda_m - \cos\lambda_m}{\sinh\lambda_m - \sin\lambda_m} = \frac{\sinh\lambda_m + \sin\lambda_m}{\cosh\lambda_m - \cos\lambda_m}\,,$$

and the eigenvalues λ_m are the roots of the transcendental equation,

$$\cosh\lambda_m\,\cos\lambda_m - 1 = 0$$

C.2 PINNED-PINNED BEAM

The mth eigenfunction for a pinned-pinned beam is given by

$$\Phi_m(\zeta) = \sin m\pi\zeta \ . \tag{C.11}$$

The values for the integrals are listed below

$$\bar{\delta}_{km} = 0 \quad \text{for } k \neq m \ ,$$

$$\bar{\delta}_{kk} = \frac{1}{2} \ , \tag{C.12}$$

$$a_{km} = 0 \quad \text{for } k \neq m \ ,$$

$$a_{kk} = \frac{k^2\pi^2}{2} \ , \tag{C.13}$$

$$b_{km} = 0 \quad \text{for } k \neq m \ ,$$

$$b_{kk} = -\frac{k^4\pi^4}{2} \ , \tag{C.14}$$

$$d_{mk} = 0 \quad \text{for } k \neq m \ ,$$

$$d_{kk} = -a_{kk} \ , \tag{C.15}$$

$$e_{km} = -\frac{k\,m^3\pi^3\,(k^2+m^2)}{(k^2-m^2)^2}\left[\,(-1)^{k+m} - 1\,\right] \quad \text{for } k \neq m \ ,$$

$$e_{kk} = -\frac{\pi^4 k^4}{4} \ , \tag{C.16}$$

$$f_{km} = \frac{km}{(k^2 - m^2)} \left[(-1)^{k+m} - 1 \right] \qquad \text{for } k \neq m \text{ ,}$$

$$f_{kk} = 0 \text{ ,} \tag{C.17}$$

$$g_{km} = mk \left(\frac{(k^2 + m^2)}{(k^2 - m^2)^2} \right) \left[(-1)^{k+m} - 1 \right] \quad \text{for } k \neq m \text{ ,}$$

$$g_{kk} = \frac{k^2 \pi^2}{2} \text{ ,} \tag{C.18}$$

$$h_{km} = \frac{-2\ km^3}{(k^2 - m^2)^2} \left[(-1)^{k+m} - 1 \right] \quad \text{for } k \neq m \text{ ,}$$

$$h_{kk} = -\frac{k^2 \pi^2}{2} \text{ ,} \tag{C.19}$$

$$j_{km} = \frac{2\ km}{(k^2 - m^2)\pi^2} \left[(-1)^{k+m} - 1 \right] \quad \text{for } k \neq m \text{ ,}$$

$$j_{kk} = \frac{1}{4} \text{ .} \tag{C.20}$$

APPENDIX D

DETERMINATION OF THE PRESSURE PERTURBATIONS

The pressure perturbation equations are given in Chapter II by equations (2.40)-(2.42); upon integrating equation (2.42) with respect to r, we obtain

$$\rho \left[\frac{\partial \phi}{\partial t} \Big|_{r_1}^{r_2} + \int_{r_1}^{r_2} U \frac{\partial^2 \phi}{\partial x \partial r}\, dr \Big|_{r_1}^{r_2} + \int_{r_1}^{r_2} U \frac{\partial}{\partial x} \left(\frac{1}{r} \frac{\partial \psi_x}{\partial \theta} - \frac{\partial \psi_\theta}{\partial x} \right) dr \right] = - p' \Big|_{r_1}^{r_2} \tag{D.1}$$

D.1 FOURIER TRANSFORM SOLUTION

The expressions for ψ_r, ψ_θ, ψ_x, ϕ, p' are given in equations (3.5)-(3.8) and (3.48), respectively. Upon substituting for ψ_r, ψ_θ, ψ_x, ϕ, p' into equations (2.40),(2.41) and (D.1), we obtain

$$\rho \left[i\omega \left(\frac{\partial \bar{\phi}}{\partial x} \right) + U \frac{\partial^2 \phi}{\partial x^2} + U \frac{\partial}{\partial x} \left(\frac{\bar{\psi}_\theta}{r} + \frac{\partial \bar{\psi}_\theta}{\partial r} - \frac{n}{r} \bar{\psi}_r \right) + \left(\frac{\partial \bar{\phi}}{\partial r} + \frac{n}{r} \bar{\psi}_x - \frac{\partial \bar{\psi}_\theta}{\partial x} \right) \frac{dU}{dr} \right] = - \frac{\partial \bar{p}'}{\partial x} , \tag{D.2}$$

$$\rho \left[i\omega \bar{\phi} + U \frac{\partial \bar{\phi}}{\partial x} - \frac{r}{n} U \frac{\partial}{\partial x} \left(\frac{\partial \bar{\psi}_r}{\partial x} - \frac{\partial \bar{\psi}_x}{\partial r} \right) \right] = - \bar{p}' , \tag{D.3}$$

$$\rho \left[i\omega \bar{\phi} \Big|_{r_1}^{r_2} + \int_{r_1}^{r_2} U \frac{\partial^2 \phi}{\partial x \partial r}\, dr + \int_{r_1}^{r_2} U \frac{\partial}{\partial x} \left(\frac{1}{r} \bar{\psi}_x - \frac{\partial \bar{\psi}_\theta}{\partial x} \right) \right] = - \bar{p}' \Big|_{r_1}^{r_2} ; \tag{D.4}$$

substituting for $\bar{\psi}_r$, $\bar{\psi}_\theta$, $\bar{\psi}_x$, $\bar{\phi}$ and $\bar{p}'$ as defined by (3.9) into equations (D.2)-(D.4) and taking the Fourier transform of the resulting equations we get

$$\rho \left[i\omega\, \phi^* - i\alpha U \phi^* + U \left\{ -\frac{(n+1)}{r} \psi_r^* - \frac{\partial \psi_r^*}{\partial r} \right\} + \frac{i}{\alpha} \left\{ \frac{\partial \phi^*}{\partial r} + \frac{n}{r} \psi_x^* - i\alpha\, \psi_r^* \right\} \frac{dU}{dr} \right] = p^{*'} , \qquad (D.5)$$

$$\rho \left[i\omega\, \phi^* - i\alpha U \phi^* - \frac{r}{n}\, U(-i\alpha) \left\{ -i\alpha\, \psi_r^* - \frac{\partial \psi_x^*}{\partial r} \right\} \right] = -\, p^{*'} , \qquad (D.6)$$

$$\rho \left[i\omega\, \phi^* \Big|_{r_1}^{r_2} - i\alpha \int_{r_1}^{r_2} U \frac{\partial \phi^*}{\partial r} dr + (-i\alpha) \int_{r_1}^{r_2} U \left(\frac{n}{r} \psi_x^* - i\alpha\, \psi_r^* \right) \right] dr = -\, p^{*'} \Big|_{r_1}^{r_2} \qquad (D.7)$$

D.1.1 Inner flow

The solution for the inner flow is expressed by putting a subscript i to equations (D.3)-(D-7).

The flow velocity $U_i(r)$ is given by the power law [59]

$$U_i(r) = U_{max} \left(1 - \frac{r}{a_i} \right)^{1/s_i} , \qquad (D.8)$$

where s_i is a constant which depends on the Reynolds number Re_i, where

$$Re_i = \frac{U_{mi}\, d_i}{\nu_i} , \qquad (D.9)$$

a_i and d_i are the radius and the diameter of the shell, respectively. Different values for s are given in Ref. [59] for variable Re.

U_{mi} is the average velocity which is defined by

$$U_{mi} = 2 \int_0^{a_i} \frac{U_i(r) r dr}{a_i^2} . \qquad (D.10)$$

The solutions for ϕ_i^*, ψ_{ri}^* and ψ_{xi}^* are given in Chapter III by equations (3.28)-(3.30).

Using the following non-dimensional terms

Using the following non-dimensional terms

$$\bar{r} = \frac{r}{a_i}, \quad \Omega = \frac{\omega a_i}{u}, \quad \bar{\alpha} = \alpha L, \quad \bar{U}_i = \frac{U_i}{u},$$

where u is given by equation (3.36), and substituting ϕ_i^*, ψ_{ri}^* and ψ_{xi}^* into equations (D.5)-(D.7), we obtain

$$\rho_i u \left[\left\{ \frac{i\,\Omega\, I_n(\bar{\alpha}\varepsilon_i)}{\varepsilon_i} - i\,\bar{\alpha}\,\bar{U}_i\, I_n(\bar{\alpha}\varepsilon_i) + \frac{i\, I_n'(\alpha\varepsilon_i)}{\varepsilon_i}\frac{d\bar{U}_i}{d\bar{r}} \right\} \bar{C}_{1i} + \left\{ \left(\frac{in}{\bar{\alpha}\varepsilon_i}\right) I_n(\bar{\beta}_i\varepsilon_i)\frac{d\bar{U}_i}{d\bar{r}} \right\} \bar{C}_{3i} + \left[\frac{I_{n+1}}{\varepsilon_i}(\bar{\beta}_i\varepsilon_i)\frac{d\bar{U}_i}{d\bar{r}} - \frac{(n+1)}{\varepsilon_i} I_{n+1}(\bar{\beta}_i\varepsilon_i)\,\bar{U}_i - \bar{\beta}_i\, I_{n+1}'(\bar{\beta}_i\varepsilon_i)\,\bar{U}_i \right] \bar{C}_{5i} \right] = -\,p_i^{*\prime}, \tag{D.11}$$

$$\rho_i u \left[\left\{ \frac{i\,\Omega\, I_n(\bar{\alpha}\varepsilon_i)}{\varepsilon_i} - i\,\bar{\alpha}\,\bar{U}_i\, I_n(\bar{\alpha}\varepsilon_i) \right\} \bar{C}_{1i} + \frac{i\varepsilon_i}{n}\bar{\alpha}\,\bar{U}_i \left\{ -\bar{\beta}_i\, I_n'(\bar{\beta}_i\varepsilon_i) \right\} \bar{C}_{3i} + \frac{i\varepsilon_i}{n}\bar{\alpha}\,\bar{U}_i \left\{ -i\bar{\alpha}\, I_{n+1}(\bar{\beta}_i\varepsilon_i) \right\} \bar{C}_{5i} \right] = -\,p_i^{*\prime} \tag{D.12}$$

$$\rho_i u \left[\left\{ \frac{i\,\Omega\, I_n(\alpha r)}{\varepsilon_i} \Big|_0^{a_i-\delta} - i\bar{\alpha} \int_0^{a_i-\delta} \bar{U}_i\, \alpha\, I_n'(\alpha r)\, dr \right\} \bar{C}_{1i} + \left\{ (-i\bar{\alpha}) \int_0^{a_i-\delta} \bar{U}_i \frac{n}{r} I_n(\beta_i r)dr \right\} \bar{C}_{3i} + \left\{ \frac{(-i\bar{\alpha})^2}{L} \int_0^{a_i-\delta} \bar{U}_i\, I_{n+1}(\bar{\beta}_i r)dr \right\} \bar{C}_{5i} \right] = -\,p_i^{*\prime} \Big|_0^{a_i-\delta} \tag{D.13}$$

Any one of equations (D.11), (D.12) or (D.13) may be used in evaluating the pressure perturbations $p_i^{*'}$.

$p_{1i}^{*'}$, $p_{2i}^{*'}$ and $p_{3i}^{*'}$ defined in equation (3.51) may now be evaluated. At $r=a_i-\delta$, we obtain

(i) from (D.11) ,

$$p_{1i}^{*'} = \left[\frac{i\ \Omega\ I_n}{\epsilon_i} (\bar{\alpha}\epsilon_i) - i\ \bar{\alpha}\ \bar{U}_{\delta i}\ I_n(\bar{\alpha}\epsilon_i) + \frac{i}{\epsilon_i}\ I_n'(\bar{\alpha}\epsilon_i)\ \frac{d\bar{U}_{\delta i}}{d\bar{r}} \right], \tag{D.14a}$$

$$p_{2i}^{*'} = \left[\frac{in}{\bar{\alpha}\epsilon_i}\ I_n(\bar{\beta}_i\epsilon_i)\ \frac{d\bar{U}_{\delta i}}{d\bar{r}} \right], \tag{D.14b}$$

$$p_{3i}^{*'} = \frac{I_{n+1}}{\epsilon_i}\ (\bar{\beta}_i\epsilon_i)\frac{d\bar{U}_{\delta i}}{d\bar{r}} - \left[\frac{(n+1)}{\epsilon_i}\ I_{n+1}(\bar{\beta}_i\epsilon_i) + \bar{\beta}_i\ I_{n+1}'(\bar{\beta}_i\epsilon_i) \right] \bar{U}_{\delta i}, \tag{D.14c}$$

where $\bar{U}_{\delta i}$ is the velocity $\bar{U}_i$ evaluated at $r=a_i-\delta$;

(ii) from (D.12) ,

$$p_{1i}^{*'} = \left[\frac{i\ \Omega\ I_n}{\epsilon_i} (\bar{\alpha}\epsilon_i) - i\bar{\alpha}\ \bar{U}_{\delta i}\ I_n(\bar{\alpha}\epsilon_i) \right], \tag{D.15a}$$

$$p_{2i}^{*'} = \left[i\ \frac{\epsilon_i\bar{\alpha}}{n}\ \bar{U}_{\delta i} \left\{ -\ \bar{\beta}_i\ I_n'(\bar{\beta}_i\epsilon_i) \right\} \right], \tag{D.15b}$$

$$p_{3i}^{*'} = \left[i\ \frac{\epsilon_i\bar{\alpha}}{n} \left\{ -\ i\bar{\alpha}\ I_{n+1}(\bar{\beta}_i\epsilon_i) \right\} \bar{U}_{\delta i} \right]; \tag{D.15c}$$

(iii) the pressure $p^{*'}$ at $r=0$ in equation (D.13) being zero because $I_n(0)=0$, hence, $p_{1i}^{*'}$, $p_{2i}^{*'}$ and $p_{3i}^{*'}$ at $r=a_i-\delta$ are given by

$$p_{1i}^{*'} = \frac{i\ \Omega}{\epsilon_i}\ I_n(\bar{\alpha}\epsilon_i) - i\ \bar{\alpha} \left\{ \int \bar{\alpha}\ \bar{U}_i\ I_n'(\alpha r)] dr \right\}_{r=a_i-\delta}, \tag{D.16a}$$

$$p_{2i}^{*'} = \left\{ (-i\bar{\alpha}) \int \bar{U}_i\ \frac{n}{r}\ I_n(\bar{\beta}_i r) dr \right\}_{r=a_i-\delta}, \tag{D.16b}$$

$$p_{3i}^{*'} = \left\{ (-i\bar{\alpha})^2 \int \bar{U}_i \, I_{n+1}(\beta_i r) \, dr \right\}_{r=a_i-\delta} \qquad \text{(D.16c)}$$

the integrations in (D.16 a, b and c) will be evaluated at the end of this Appendix.

D.1.2 Annular flow

The solution for the annular flow is expressed by putting a subscript o to equations (2.40)-(2.42). The flow velocity $U_o(r)$ may be expressed by the law of the wall [51,52].

$$\frac{U_o}{U_{\tau 01}} = 2.44 \ln \left(\frac{y_1 U_{\tau 01}}{\nu_o} \right) + 4.9 \,, \qquad \text{(D.17)}$$

where $U_{\tau 01}$ is the stress velocity and is defined by (A.14a,b,c), ν_o is the kinematic viscosity of the fluid in the annulus, and

$$y_1 = r - a_i \,.$$

Equation (D.17) is applicable only between $r = a_i$ and $r = r_m$, where r_m is the radius at which the mean velocity U_o is maximum. r_m is given by equation (A.16).

In this Thesis, we have assumed a simple form for $U_o(r)$ as compared to equation (D.17), which is represented by

$$U_o(r) = U_{maxo} \left(\frac{r - a_i}{r_m - a_i} \right)^{1/s_o} . \qquad \text{(D.18)}$$

The solutions for ϕ_o^*, ψ_{ro}^*, and ψ_{xo}^* are given in Chapter III by equations (3.52)-(3.54). Substituting for ϕ_o^*, ψ_{ro}^*, and ψ_{xo}^* into equations (D.5)-(D.7), the nondimensionalized equations become

$$\rho_r \rho_i U \left[\begin{array}{l} \left\{ \frac{i\ \Omega\ I_n\ (\bar{\alpha}\varepsilon_i)}{\varepsilon_i} - i\ \bar{\alpha}\ \bar{U}_o\ I_n(\bar{\alpha}\varepsilon_i) + \frac{i}{\varepsilon_i}\ I_n'(\bar{\alpha}\varepsilon_i)\ \frac{d\bar{U}_o}{d\bar{r}} \right\} \bar{C}_{1o} \\ + \left\{ \frac{i\ \Omega\ K_n\ (\bar{\alpha}\varepsilon_i)}{\varepsilon_i} - i\ \bar{\alpha}\ \bar{U}_o\ K_n(\bar{\alpha}\varepsilon_i) + \frac{i}{\varepsilon_i}\ K_n'(\bar{\alpha}\varepsilon_i)\ \frac{d\bar{U}_o}{d\bar{r}} \right\} \bar{C}_{2o} \\ + \left\{ \left(\frac{in}{\bar{\alpha}\varepsilon_i} \right) I_n(\bar{\beta}_o\varepsilon_i)\ \frac{d\bar{U}_o}{dr} \right\} \bar{C}_{3o} + \left\{ \left(\frac{in}{\bar{\alpha}\varepsilon_i} \right) K_n\ (\bar{\beta}_o\varepsilon_i)\ \frac{d\bar{U}_o}{dr} \right\} \bar{C}_{4o} \\ + \left\{ \frac{I_{n+1}(\bar{\beta}_o\varepsilon_i)}{\varepsilon_i}\ \frac{d\bar{U}_o}{dr} - \bar{U}_o \left\{ \frac{(n+1)}{\varepsilon_i}\ I_{n+1}(\bar{\beta}_o\varepsilon_i) + \bar{\beta}_o\ I_{n+1}'(\bar{\beta}_o\varepsilon_i) \right\} \right\} \bar{C}_{5o} \\ + \left\{ \frac{K_{n+1}(\bar{\beta}_o\varepsilon_i)}{\varepsilon_i}\ \frac{d\bar{U}_o}{dr} - \bar{U}_o \left\{ \frac{(n+1)}{\varepsilon_i}\ K_{n+1}(\bar{\beta}_o\varepsilon_i) + \bar{\beta}_o\ K_{n+1}'(\bar{\beta}_o\varepsilon_i) \right\} \right\} \bar{C}_{6o} \end{array} \right] = -\ p_o^{*'}$$

(D.19)

$$\rho_r \rho_i U \left[\begin{array}{l} \left\{ \frac{i\ \Omega\ I_n(\bar{\alpha}\varepsilon_i)}{\varepsilon_i} - i\bar{\alpha}\ \bar{U}_o I_n(\bar{\alpha}\varepsilon_i) \right\} \bar{C}_{1o} + \left\{ \frac{i\ \Omega\ K_n(\bar{\alpha}\varepsilon_i)}{\varepsilon_i} - i\bar{\alpha}\ \bar{U}_o K_n(\bar{\alpha}\varepsilon_i) \right\} \bar{C}_{2o} \\ + \frac{i\varepsilon_i}{n}\ \bar{\alpha}\ \bar{U}_o\ \left\{ -\ \bar{\beta}_o\ I_n'(\bar{\beta}_o\varepsilon_i) \right\} \bar{C}_{3o} + \frac{i\varepsilon_i}{n}\ \bar{\alpha}\ \bar{U}_o\ \left\{ -\ \bar{\beta}_o\ K_n'(\bar{\beta}_o\varepsilon_i) \right\} \bar{C}_{4o} \\ + \frac{i\varepsilon_i}{n}\ \bar{\alpha}\ \bar{U}_o\ \left\{ -\ i\bar{\alpha}\ I_{n+1}(\bar{\beta}_o\varepsilon_i) \right\} \bar{C}_{5o} + \frac{i\varepsilon_i}{n}\ \bar{\alpha}\ \bar{U}_o \left\{ -\ i\bar{\alpha}\ K_{n+1}(\bar{\beta}_o\varepsilon_i) \right\} \bar{C}_{6o} \end{array} \right] = -\ p_o^{*'}$$

(D.20)

$$\rho_r \rho_i U \left[\begin{array}{l} \left\{ \frac{i\Omega}{\epsilon_i} I_n(\alpha r) \Big|_{a_i+\delta}^{r_m} - i\,\bar{\alpha} \int_{a_i+\delta}^{r_m} \bar{U}_o\, I_n(\alpha r)\, dr \right\} \bar{C}_{1o} \\ \left\{ \frac{i\Omega}{\epsilon_i} K_n(\alpha r) \Big|_{a_i+\delta}^{r_m} - i\,\bar{\alpha} \int_{a_i+\delta}^{r_m} \bar{U}_o\, K_n(\alpha r)\, dr \right\} \bar{C}_{2o} \\ + \left\{ (-i\bar{\alpha}) \int_{a_i+\delta}^{r_m} \bar{U}_o \frac{n}{r} I_n(\beta_i r) dr \right\} \bar{C}_{3o} \\ + \left\{ (-i\bar{\alpha}) \int_{a_i+\delta}^{r_m} \bar{U}_o \frac{n}{r} K_n(\beta_i r) dr \right\} \bar{C}_{4o} \\ + \left\{ \frac{(-i\alpha)^2}{L} \int_{a_i+\delta}^{r_m} \bar{U}_o\, I_{n+1}(\beta_i r) dr \right\} \bar{C}_{5o} \\ + \left\{ \frac{(-i\alpha)^2}{L} \int_{a_i+\delta}^{r_m} \bar{U}_o\, K_{n+1}(\beta_i r) dr \right\} \bar{C}_{6o} \end{array} \right] = - p_o^{*'} \Big|_{a_i+\delta}^{r_m} \tag{D.21}$$

Now one can find $p^{*'}_{1Io}$, $p^{*'}_{1Ko}$, $p^{*'}_{2Io}$, $p^{*'}_{2Ko}$, $p^{*'}_{3Io}$ and $p^{*'}_{3Ko}$. At $r=a_i+\delta$, we obtain the following.

(i) From Equation (D.19):

$$p^{*'}_{1Io} = \left\{ \frac{i\,\Omega\, I_n(\bar{\alpha}\epsilon_i)}{\epsilon_i} - i\,\bar{\alpha}\,\bar{U}_{\delta o}\, I_n(\bar{\alpha}\epsilon_i) + \frac{i}{\epsilon_i} I_n'(\bar{\alpha}\epsilon_i) \frac{d\bar{U}_{\delta o}}{dr} \right\}, \tag{D.22a}$$

$$p^{*'}_{1Ko} = \left\{ \frac{i\,\Omega\, K_n(\bar{\alpha}\epsilon_i)}{\epsilon_i} - i\,\bar{\alpha}\,\bar{U}_{\delta o}\, K_n(\bar{\alpha}\epsilon_i) + \frac{i}{\epsilon_i} K_n'(\bar{\alpha}\epsilon_i) \frac{d\bar{U}_{\delta o}}{dr} \right\}, \tag{D.22b}$$

$$p^{*'}_{2Io} = \left\{ \frac{in}{\bar{\alpha}\epsilon_i} I_n (\bar{\beta}_o \epsilon_i) \frac{d\bar{U}_{\delta o}}{d\bar{r}} \right\} , \quad (D.22c)$$

$$p^{*'}_{2Ko} = \left\{ \frac{in}{\bar{\alpha}\epsilon_i} K_n (\bar{\beta}_o \epsilon_i) \frac{d\bar{U}_{\delta o}}{d\bar{r}} \right\} , \quad (D.22d)$$

$$p^{*'}_{3Io} = \left\{ \frac{I_{n+1}}{\epsilon_i} (\bar{\beta}_o \epsilon_i) \frac{d\bar{U}_{\delta o}}{dr} - \left\{ \frac{(n+1)}{\epsilon_i} I_{n+1}(\bar{\beta}_o \epsilon_i) + \bar{U}_{\delta o}\bar{\beta}_o I'_{n+1}(\bar{\beta}_o \epsilon_i) \right\} \bar{U}_{\delta o} \right\} , \quad (D.22e)$$

$$p^{*'}_{3Ko} = \left\{ \frac{K_{n+1}}{\epsilon_i} (\bar{\beta}_o \epsilon_i) \frac{d\bar{U}_{\delta o}}{dr} - \left\{ \frac{(n+1)}{\epsilon_i} K_{n+1}(\bar{\beta}_o \epsilon_i) + \bar{U}_{\delta o}\bar{\beta}_o K'_{n+1}(\bar{\beta}_o \epsilon_i) \right\} \bar{U}_{\delta o} \right\} , \quad (D.22f)$$

where $\bar{U}_{\delta o}$ is the velocity $\bar{U}_o$ evaluated at $r=a_i+\delta$.

(ii) From equation (D.20):

$$p^{*'}_{1Io} = \left\{ \frac{i\ \Omega\ I_n}{\epsilon_i} (\bar{\alpha}\epsilon_i) - i\bar{\alpha}\ \bar{U}_{\delta o}\ I_n(\bar{\alpha}\epsilon_i) \right\} , \quad (D.23a)$$

$$p^{*'}_{1Ko} = \left\{ \frac{i\ \Omega\ K_n}{\epsilon_i} (\bar{\alpha}\epsilon_i) - i\bar{\alpha}\ \bar{U}_{\delta o}\ K_n(\bar{\alpha}\epsilon_i) \right\} \quad (D.23b)$$

$$p^{*'}_{2Io} = \frac{i\epsilon_i}{n} \bar{\alpha}\ \bar{U}_{\delta o} \left\{ -\bar{\beta}_o\ I'_n(\bar{\beta}_o \epsilon_i) \right\} , \quad (D.23c)$$

$$p^{*'}_{2Ko} = \frac{i\epsilon_i}{n} \bar{\alpha}\ \bar{U}_{\delta o} \left\{ -\bar{\beta}_o\ K'_n(\bar{\beta}_o \epsilon_i) \right\} , \quad (D.23d)$$

$$p^{*'}_{3Io} = \frac{i\epsilon_i}{n} \bar{\alpha}\ \bar{U}_{\delta o} \left\{ -i\bar{\alpha}\ I_{n+1}(\bar{\beta}_o \epsilon_i) \right\} , \quad (D.23e)$$

$$p^{*'}_{3Ko} = \frac{i\epsilon_i}{n} \bar{\alpha}\ \bar{U}_{\delta o} \left\{ -i\bar{\alpha}\ K_{n+1}(\bar{\beta}_o \epsilon_i) \right\} . \quad (D.23f)$$

(iii) Equation (D.21) gives the pressure difference between r_m and a_i. It has been reported [60] that, for narrow annuli, the pressure difference is almost zero. Hence the pressure perturbation is the same at any point in the annulus. Therefore, the pressure perturbation $p_o^{*'}$ at $r=a_i+\delta$ is evaluated from equation (D.21) as follows: the integration is performed first, then the pressure perturbation $p_o^{*'}$ is only evaluated at $r=a_i+\delta$, so that

$$p_{1Io}^{*'} = \left\{ \frac{i\,\Omega}{\epsilon_i} I_n(\bar{\alpha}\epsilon_i) - \left\{ i\bar{\alpha} \int \alpha\, \bar{U}_o\, I_n'(\alpha r) dr \right\}_{r=a_i+\delta} \right\} \tag{D.24a}$$

$$p_{1Ko}^{*'} = \left\{ \frac{i\,\Omega}{\epsilon_i} K_n(\bar{\alpha}\epsilon_i) - \left\{ i\bar{\alpha} \int \alpha\, \bar{U}_o\, K_n'(\alpha r) dr \right\}_{r=a_i+\delta} \right\} \tag{D.24b}$$

$$p_{2Io}^{*'} = \left\{ (-i\bar{\alpha}) \int \bar{U}_o \frac{n}{r} I_n(\beta_i r)\, dr \right\}_{r=a_i+\delta} \tag{D.24c}$$

$$p_{2Ko}^{*'} = \left\{ (-i\bar{\alpha}) \int \bar{U}_o \frac{n}{r} K_n(\beta_i r)\, dr \right\}_{r=a_i+\delta} \tag{D.24d}$$

$$p_{3Io}^{*'} = \left\{ (-i\bar{\alpha})^2 \int \bar{U}_o\, I_{n+1}(\beta_i r)\, dr \right\}_{r=a_i+\delta} \tag{D.24e}$$

$$p_{3Ko}^{*'} = \left\{ (-i\bar{\alpha})^2 \int \bar{U}_o\, K_{n+1}(\beta_i r)\, dr \right\}_{r=a_i+\delta} \tag{D.24f}$$

D.2 TRAVELLING WAVE SOLUTION

The expressions for ϕ, ψ_x, ψ_θ, ψ_r, p' are given by (4.4)-(4.7) and (4.18), respectively.

Upon substituting ~~for ϕ~~, ψ_x, ψ_θ, ψ_r, p' into equations (2.40)-(2.42), we obtain

$$\rho\left[\, i\omega\,\bar{\phi} - ik\,U\,\bar{\phi} + U\left\{ -\frac{(n+1)}{r}\,\bar{\psi}_r - \frac{\partial\bar{\psi}_r}{\partial r} \right\} + \frac{i}{k}\left\{ \frac{\partial\bar{\phi}}{\partial r} + \frac{n}{r}\,\bar{\psi}_x - ik\,\bar{\psi}_r \right\}\frac{dU}{dr}\right] = -\,\bar{p}' \,, \tag{D.25}$$

$$\rho\left[\, i\omega\,\bar{\phi} - ik\,U\,\bar{\phi} - \frac{r}{n}\,U\,(-ik)\left\{ -ik\,\bar{\psi}_r - \frac{\partial\bar{\psi}_x}{\partial r} \right\}\right] = -\,\bar{p}' \,, \tag{D.26}$$

$$\rho\left[\, i\omega\,\bar{\phi}\,\Big|_{r_1}^{r_2} - i\bar{k}\int_{r_1}^{r_2} U\,\frac{\partial\bar{\phi}}{\partial r}\,dr + (-ik)\int_{r_1}^{r_2} U\left(\frac{n}{r}\,\bar{\psi}_x - ik\,\bar{\psi}_r\right)dr\right] = -\,\bar{p}'\,\Big|_{r_1}^{r_2} \,. \tag{D.27}$$

following the same analysis as in the Fourier Transform method, we can arrive at the expressions for the pressure perturbation terms.

D.2.1 Internal flow

The pressure perturbations $\bar{p}'_{1i}$, $\bar{p}'_{2i}$ and $\bar{p}'_{3i}$ defined in equation (4.37) may now be evaluated as follows:

(i) from (D.25)

$$\bar{p}'_{1i} = \frac{1}{\varepsilon_i}\left\{ (i\Omega I_n(\bar{\alpha}) - i\,\bar{\alpha}\,\bar{U}_i\, I_n(\bar{\alpha}) + I'_n(\bar{\alpha})\frac{d\bar{U}_{\delta i}}{dr} \right\} \tag{D.28a}$$

$$\bar{p}'_{2i} = \frac{in}{\bar{\alpha}\varepsilon_i}\, I_n(\bar{\beta}_i)\,\frac{d\bar{U}_{\delta i}}{d\bar{r}}, \tag{D.28b}$$

$$\bar{p}'_{3i} = \frac{I_{n+1}}{\varepsilon_i}(\bar{\beta}_i)\,\frac{d\bar{U}_{\delta i}}{dr} - \frac{(n+1)}{\varepsilon_i}\, I_{n+1}(\bar{\beta}_i)\bar{U}_{\delta i} - \frac{\bar{\beta}_i}{\varepsilon_i}\, I'_{n+1}(\bar{\beta}_i)\bar{U}_{\delta i} \;; \tag{D.28c}$$

(ii) from (D.26)

$$\bar{p}'_{1i} = \frac{1}{\varepsilon_i}\left\{ i\Omega I_n(\bar{\alpha}) - i\bar{\alpha}\,\bar{U}_{\delta i}\, I_n(\bar{\alpha})\right\} , \tag{D.29a}$$

$$\bar{p}'_{2i} = \frac{i}{n\varepsilon_i}\left[-\bar{\alpha}\,\bar{\beta}_i I'_n(\bar{\beta}_i)\,\bar{U}_{\delta i}\right] , \tag{D.29b}$$

$$\bar{p}'_{3i} = \frac{i\bar{\alpha}}{n\epsilon_i}\left(-i\bar{\alpha}\, I_{n+1}(\bar{\beta}_i)\right)\bar{U}_{\delta i}\ ; \tag{D.29c}$$

(iii) from (D.27)

$$\bar{p}'_{1i} = \frac{i\Omega}{\epsilon_i} I_n(\bar{\alpha}) - \frac{i\bar{\alpha}}{\epsilon_i}\left[\int \bar{U}_i k\, I'_n(kr)\right)dr\Big]_{r=a_i-\delta}\ , \tag{D.30a}$$

$$\bar{p}'_{2i} = \left(\left(-\frac{i\bar{\alpha}}{\epsilon_i}\right)\int \bar{U}_i \frac{n}{r} I_n(\beta_i r)dr\right]_{r=a_i-\delta}\ , \tag{D.30b}$$

$$\bar{p}'_{3i} = \left(\left(\frac{(i\bar{\alpha})^2}{\epsilon_i L}\int \bar{U}_i\, I_{n+1}(\beta_i r)dr\right]_{r=a_i-\delta}\ . \tag{D.30c}$$

The integrations for (D.30a,b and c) are given at the end of this Appendix.

D.2.2 Annular flow

(i) from the axial direction equation (D.26), we get

$$\bar{p}'_{1Io} = \left(\frac{i\,\Omega\, I_n(\bar{\alpha})}{\epsilon_i} - \frac{i\bar{\alpha}}{\epsilon_i}\bar{U}_{\delta o}\, I_n(\bar{\alpha}) + \frac{I'_n(\bar{\alpha})}{\epsilon_i}\frac{d\bar{U}_{\delta o}}{d\bar{r}}\right)\ , \tag{D.31a}$$

$$\bar{p}'_{1Ko} = \left(\frac{i\,\Omega\, K_n(\bar{\alpha})}{\epsilon_i} - \frac{i\bar{\alpha}}{\epsilon_i}\bar{U}_{\delta o}\, K_n(\bar{\alpha}) + \frac{K'_n(\bar{\alpha})}{\epsilon_i}\frac{d\bar{U}_{\delta o}}{d\bar{r}}\right)\ , \tag{D.31b}$$

$$\bar{p}'_{2Io} = \left(\frac{in}{\bar{\alpha}\epsilon_i} I_n(\bar{\beta}_o)\frac{d\bar{U}_{\delta o}}{d\bar{r}}\right)\ , \tag{D.31c}$$

$$\bar{p}'_{2Ko} = \left(\frac{in}{\bar{\alpha}\epsilon_i} K_n(\bar{\beta}_o)\frac{d\bar{U}_{\delta o}}{d\bar{r}}\right)\ , \tag{D.31d}$$

$$\bar{p}'_{3Io} = \left(\frac{I_{n+1}}{\epsilon_i}(\bar{\beta}_o)\frac{d\bar{U}_{\delta o}}{d\bar{r}} - \frac{n+1}{\epsilon_i} I_{n+1}(\bar{\beta}_o)\bar{U}_{\delta o} - \frac{\bar{\beta}_o}{\epsilon_i} I'_{n+1}(\bar{\beta}_o)\bar{U}_{\delta o}\right] \tag{D.31e}$$

$$p'_{3Ko} = \left(\frac{K_{n+1}}{\epsilon_i}(\bar{\beta}_o)\frac{d\bar{U}_{\delta o}}{d\bar{r}} - \frac{n+1}{\epsilon_i} K_{n+1}(\bar{\beta}_o)\bar{U}_{\delta o} - \frac{\bar{\beta}_o}{\epsilon_i} K'_{n+1}(\bar{\beta}_o)\bar{U}_{\delta o}\right] \tag{D.31f}$$

(ii) from the circumferential direction equation (D.26), we obtain

$$\bar{p}'_{1Io} = \frac{1}{\epsilon_i}\left[\, i\,\Omega\, I_n(\bar{\alpha}) - i\,\bar{\alpha}\,\bar{U}_{\delta o}\, I_n(\bar{\alpha})\right], \tag{D.32a}$$

$$\bar{p}'_{1Ko} = \frac{1}{\epsilon_i}\left[\, i\,\Omega\, K_n(\bar{\alpha}) - i\,\bar{\alpha}\,\bar{U}_{\delta o}\, K_n(\bar{\alpha})\right], \tag{D.32b}$$

$$\bar{p}'_{2Io} = \frac{i}{n}\left(-\bar{\alpha}\,\frac{\bar{\beta}_o}{\epsilon_i}\, I'_n(\bar{\beta}_o)\,\bar{U}_{\delta o}\right], \tag{D.32c}$$

$$\bar{p}'_{2Ko} = \frac{i}{n}\left(-\bar{\alpha}\,\frac{\bar{\beta}_o}{\epsilon_i}\, K'_n(\bar{\beta}_o)\,\bar{U}_{\delta o}\right] \tag{D.32d}$$

$$\bar{p}'_{3Io} = \frac{i\bar{\alpha}}{n\,\epsilon_i}\left(-i\,\bar{\alpha}\, I_{n+1}(\bar{\beta}_o)\,\bar{U}_{\delta o}\right], \tag{D.32e}$$

$$\bar{p}'_{3Ko} = \frac{i\bar{\alpha}}{n\,\epsilon_i}\left(-i\,\bar{\alpha}\, K_{n+1}(\bar{\beta}_o)\,\bar{U}_{\delta o}\right]; \tag{D.32f}$$

(iii) finally from the radial direction equation (D.27), we obtain

$$\bar{p}'_{1Io} = \frac{1}{\epsilon_i}\left[\, i\,\Omega\, I_n(\bar{\alpha})\right] - \left[\, i\,\bar{\alpha}\int \bar{U}_o k\, I'_n(kr)\, dr\right]_{r=a_i+\delta}, \tag{D.33a}$$

$$\bar{p}'_{1Ko} = \frac{1}{\epsilon_i}\left[\, i\,\Omega\, K_n(\bar{\alpha})\right] - \left[\, i\,\bar{\alpha}\int \bar{U}_o k\, K'_n(kr)\, dr\right]_{r=a_i+\delta}, \tag{D.33b}$$

$$\bar{p}'_{2Io} = \left[\left(-\frac{i\bar{\alpha}}{\epsilon_i}\right)\int \bar{U}_o\,\frac{n}{r}\, I_n(\bar{\beta}_o r)\, dr\right]_{r=a_i+\delta}, \tag{D.33c}$$

$$\bar{p}'_{2Ko} = \left[\left(-\frac{i\bar{\alpha}}{\epsilon_i}\right)\int \bar{U}_o\,\frac{n}{r}\, K_n(\bar{\beta}_o r)\, dr\right]_{r=a_i+\delta}, \tag{D.33d}$$

$$\bar{p}'_{3Io} = \frac{1}{L}\left[\left(-\frac{i\bar{\alpha}}{\epsilon_i}\right)^2\int \bar{U}_o\, I_{n+1}(\beta_o r)\, dr\right]_{r=a_i+\delta}, \tag{D.33e}$$

$$\bar{p}'_{3Ko} = \frac{1}{L}\left[\left(-\frac{i\bar{\alpha}}{\epsilon_i}\right)^2\int \bar{U}_o\, K_{n+1}(\beta_o r)\, dr\right]_{r=a_i+\delta}. \tag{D.33f}$$

D.3 INTEGRATION

The integrations in (D.16), (D.24), (D.30) and (D.33) may be performed analytically as described below.

The flow velocity U_i and U_o are given by equations (D.8) and (D.18), respectively, as follows:

$$\bar{U}_i = \bar{U}_{maxi} \left(1 - \frac{r}{a_i} \right)^{1/s_i}$$

and

$$\bar{U}_o = \bar{U}_{maxo} \left(\frac{r - a_i}{r_m - a_i} \right)^{1/s_o} .$$

The integrations may be performed analytically by rewriting the flow velocity as a second order polynomial of r, as follows:

$$\bar{U}_i = \bar{U}_{maxi} \left(A_o + A_1 \frac{r}{a_i} + A_2 \frac{r^2}{a_i^2} \right) , \tag{D.34}$$

and

$$\bar{U}_o = \bar{U}_{maxo} \left(A_o + A_1 \frac{r_m - r}{r_m - a_i} + A_2 \left(\frac{r_m - r}{r_m - a_i} \right)^2 \right) , \tag{D.35}$$

where $\bar{U}_{maxi}$ is the velocity at $r = 0$ and $\bar{U}_{maxo}$ is the velocity at $r = r_m$. The following integrations are needed for evaluating the pressure perturbations;

$$\int \frac{\bar{U}_i(r)}{r} I_n(\beta_i r) \, dr , \tag{D.36}$$

$$\int \bar{U}_i k \, I_n'(kr) \, dr ,$$

$$\int \bar{U}_i(r) \, I_{n+1}(\beta_i r) \, dr , \tag{D.37}$$

$$\int \frac{\bar{U}_o(r)}{r} I_n(\beta_o r) \, dr , \tag{D.38}$$

$$\int \bar{U}_o k\, I_n'(kr)\, dr \,, \tag{D.39}$$

$$\int \bar{U}_o k\, K_n'(kr)\, dr \,, \tag{D.40}$$

$$\int \frac{\bar{U}_o(r)}{r}\, K_n(\beta_o r)\, dr \,, \tag{D.41}$$

$$\int \bar{U}_o(r)\, I_{n+1}(\beta_o r)\, dr \,, \tag{D.42}$$

$$\int \bar{U}_o(r)\, K_{n+1}(\beta_o r)\, dr \,, \tag{D.43}$$

The above integrations may now be easily evaluated as in Ref. [61].

APPENDIX E

DETERMINATION OF THE GENERALIZED FLUID FORCES

In this Appendix the unsteady fluid forces are expressed in terms of the shell displacements. For the time being, the analysis is equally applicable for the two methods of solution given in Chapters III and IV: the Fourier Transform and travelling wave solutions.

In Chapter II, the boundary condition equations are expressed in matrix form as follows:

$$\left[B \right] \left\{ C \right\} = \left\{ R \right\} , \tag{E.1}$$

where

$\left[B \right]$ is a (9 x 9) matrix,

$\left\{ C \right\}$ is a (9 x 1) vector which represent the constants,

$\left\{ \bar{C}_{1i}, \bar{C}_{3i}, \bar{C}_{5i}, \bar{C}_{1o}, \bar{C}_{2o}, \bar{C}_{3o}, \bar{C}_{4o}, \bar{C}_{5o}, \bar{C}_{6o} \right\}^T$,

$\left\{ R \right\}$ is a (9 x 1) vector which represent the shell displacements where the asterisk, used in the main text in equation (3.85), has been omitted here for the time being.

The unsteady fluid loading is given by:

$$\left[T \right] \left\{ C \right\} = \left\{ Q \right\} , \tag{E.2}$$

where

$\left[T \right]$ is a (3 x 9) matrix, and $\left\{ Q \right\}$ is a (3 x 1) vector which represents the unsteady fluid stresses $\left\{ Q_x, Q_\theta, Q_r \right\}^T$.

Solving for $\left\{ C \right\}$ from (E.1), we obtain

$$\left\{ C \right\} = \left[B \right]^{-1} \left\{ R \right\} . \tag{E.3}$$

Substituting for $\left\{ C \right\}$ from (E.3) into (E.2), we get

$$[T]\,[B]^{-1}\{R\} = \{Q\}. \tag{E.4}$$

The unsteady fluid stress vector $\{Q\}$ is now related to the shell displacement vector $\{R\}$ by equation (E.4).

Inversion of matrix [B]

Equation (E.1) may be written as

$$[B]_i\,\{C\}_i = \{R\}_i, \tag{E.5}$$

and

$$[B]_o\,\{C\}_o = \{R\}_o, \tag{E.6}$$

where (E.5) represents the boundary conditions for the inner flow which is given by

$$\begin{bmatrix} b_{11} & b_{12} & b_{13} \\ b_{21} & b_{22} & b_{23} \\ b_{31} & b_{32} & b_{33} \end{bmatrix} \begin{Bmatrix} C_{1i} \\ C_{3i} \\ C_{5i} \end{Bmatrix} = \begin{Bmatrix} R_1 \\ R_2 \\ R_3 \end{Bmatrix} \tag{E.7}$$

and (E.6) represents the corresponding boundary conditions for the annular flow case,

$$\begin{bmatrix} b_{44} & b_{45} & b_{46} & b_{47} & b_{48} & b_{49} \\ b_{54} & b_{55} & b_{56} & b_{57} & b_{58} & b_{59} \\ b_{64} & b_{65} & b_{66} & b_{67} & b_{68} & b_{69} \\ b_{74} & b_{75} & b_{76} & b_{77} & b_{78} & b_{79} \\ b_{84} & b_{85} & b_{86} & b_{87} & b_{88} & b_{89} \\ b_{94} & b_{95} & b_{96} & b_{97} & b_{98} & b_{99} \end{bmatrix} \begin{Bmatrix} C_{1o} \\ C_{2o} \\ C_{3o} \\ C_{4o} \\ C_{5o} \\ C_{6o} \end{Bmatrix} = \begin{Bmatrix} R_4 \\ R_5 \\ R_6 \\ R_7 \\ R_8 \\ R_9 \end{Bmatrix} \tag{E.8}$$

The two matrices $[B_i]$ and $[B_o]$ are inverted separately by an IMSL subroutine. The inverse matrices for $[B_i]$ and $[B_o]$ are denoted by $[D_i]$ and $[D_o]$, respectively. The total matrix $[D]$ is given by

$$\left[D\right] = \begin{bmatrix} \left[D_i\right] & \left[0\right] \\ \left[0\right] & \left[D_o\right] \end{bmatrix} = \left[B\right]^{-1} \tag{E.9}$$

Finally the vector $\{C\}$ is given by

$$\left[D\right] \left\{R\right\} = \left\{C\right\} \tag{E.10}$$

and in a detailed form by

$$\begin{bmatrix} d_{11} & d_{12} & d_{13} & 0 & 0 & 0 & 0 & 0 & 0 \\ d_{21} & d_{22} & d_{23} & 0 & 0 & 0 & 0 & 0 & 0 \\ d_{31} & d_{32} & d_{33} & 0 & 0 & 0 & 0 & 0 & 0 \\ 0 & 0 & 0 & d_{44} & d_{45} & d_{46} & d_{47} & d_{48} & d_{49} \\ 0 & 0 & 0 & d_{54} & d_{55} & d_{56} & d_{57} & d_{58} & d_{59} \\ 0 & 0 & 0 & d_{64} & d_{65} & d_{66} & d_{67} & d_{68} & d_{69} \\ 0 & 0 & 0 & d_{74} & d_{75} & d_{76} & d_{77} & d_{78} & d_{79} \\ 0 & 0 & 0 & d_{84} & d_{85} & d_{86} & d_{87} & d_{88} & d_{89} \\ 0 & 0 & 0 & d_{94} & d_{95} & d_{96} & d_{97} & d_{98} & d_{99} \end{bmatrix} \begin{Bmatrix} R_1 \\ R_2 \\ R_3 \\ R_4 \\ R_5 \\ R_6 \\ R_7 \\ R_8 \\ R_9 \end{Bmatrix} = \begin{Bmatrix} C_{1i} \\ C_{3i} \\ C_{5i} \\ C_{1o} \\ C_{2o} \\ C_{3o} \\ C_{4o} \\ C_{5o} \\ C_{6o} \end{Bmatrix} \tag{E.11}$$

One can find now the unsteady fluid forces $\{Q\}$ in terms of the shell displacements as given by (E.4),

$$\left\{Q\right\} = \left[S\right] \left\{R\right\} , \tag{E.12}$$

where

$$\left[S\right] = \left[T\right] \left[D\right] . \tag{E.13}$$

Finally, the unsteady stresses are given by

$$Q_x^{(1)} = S_{11} R_1 + S_{14} R_4 ,$$

$$Q_x^{(2)} = S_{12} R_2 + S_{15} R_5 ,$$

$$Q_x^{(3)} = S_{13} R_3 + S_{16} R_6 , \qquad \text{(E.14)}$$

$$Q_\theta^{(1)} = S_{21} R_1 + S_{24} R_4 ,$$

$$Q_\theta^{(2)} = S_{22} R_2 + S_{25} R_5 ,$$

$$Q_\theta^{(3)} = S_{23} R_3 + S_{26} R_6 , \qquad \text{(E.15)}$$

and

$$Q_r^{(1)} = S_{31} R_1 + S_{32} R_4 ,$$

$$Q_r^{(2)} = S_{32} R_2 + S_{35} R_5 ,$$

$$Q_r^{(3)} = S_{33} R_3 + S_{36} R_6 . \qquad \text{(E.16)}$$

$Q_x^{(1)}$, $Q_x^{(2)}$, $Q_x^{(3)}$ are the coefficients of $\bar{A}_n$, $\bar{B}_n$, $\bar{C}_n$ in Flugge's equation for axial direction.

Similar definitions pertain to $Q_\theta^{(1)}$, $Q_\theta^{(2)}$, $Q_\theta^{(3)}$ and $Q_r^{(1)}$, $Q_r^{(2)}$, $Q_r^{(3)}$.

E.1 FOURIER TRANSFORM SOLUTION

For the Fourier Transform method, the vector {R} is denoted by {R*} as in (3.85) and {Q} by {Q*} as in (3.86). The elements of matrix [B] are taken from the boundary condition equations (3.37)-(3.40) and (3.56)-(3.62); they are:

$$b_{11} = - i\bar{\alpha}\epsilon_i \; I_n(\bar{\alpha}\epsilon_i), \; b_{12} = 0, \; b_{13} = - \left((n+1) I_{n+1}(\bar{\beta}_i \epsilon_i) + (\epsilon_i \bar{\beta}_i) \; I'_{n+1}(\bar{\beta}_i \epsilon_i) \right) ,$$

$$b_{21} = - n \; I_n(\bar{\alpha}\epsilon_i), \; b_{22} = -(\bar{\beta}_i \; \epsilon_i) \; I'_n(\bar{\beta}\epsilon_i), \; b_{23} = - i \bar{\alpha} \epsilon_i \; I_{n+1}(\bar{\beta}_i \epsilon_i),$$

$$b_{31} = \epsilon_i \bar{\alpha} \; I'_n(\bar{\alpha}\epsilon_i), \; b_{32} = n I_n(\bar{\beta}_i \epsilon_i), \; b_{33} = - i \bar{\alpha} \epsilon_i \; I_{n+1}(\bar{\beta}_i \epsilon_i).$$

$b_{44} = -i\bar{\alpha}\varepsilon_i\, I_n(\bar{\alpha}\varepsilon_i)$, $b_{45} = -i\bar{\alpha}\varepsilon_i\, K_n(\bar{\alpha}\varepsilon_i)$, $b_{46} = 0$, $b_{47} = 0$,

$b_{48} = -\left[\,(n+1) I_{n+1}(\bar{\beta}_o\varepsilon_i) + (\varepsilon_i\bar{\beta}_o)\, I'_{n+1}(\bar{\beta}_o\varepsilon_i)\right]$,

$b_{49} = -\left[\,(n+1) K_{n+1}(\bar{\beta}_o\varepsilon_i) + (\varepsilon_i\bar{\beta}_o)\, K'_{n+1}(\bar{\beta}_o\varepsilon_i)\right]$,

$b_{54} = -\, n\, I_n(\bar{\alpha}\varepsilon_i)$, $b_{55} = -\, n\, K_n(\bar{\alpha}\varepsilon_i)$, $b_{56} = -\,(\bar{\beta}_o\varepsilon_i)\, I'_n(\bar{\beta}_o\varepsilon_i)$,

$b_{57} = -\,(\bar{\beta}_o\varepsilon_i)\, K'_n(\bar{\beta}_o\varepsilon_i)$, $b_{58} = -\, i\bar{\alpha}\varepsilon_i\, I_{n+1}(\bar{\beta}_o\varepsilon_i)$, $b_{59} = -\, i\bar{\alpha}\varepsilon_i\, K_{n+1}(\bar{\beta}_o\varepsilon_i)$,

$b_{64} = \varepsilon_i\bar{\alpha}\, I'_n(\bar{\alpha}\varepsilon_i)$, $b_{65} = \varepsilon_i\bar{\alpha}\, K'_n(\bar{\alpha}\varepsilon_i)$, $b_{66} = n\, I_n(\bar{\beta}_o\varepsilon_i)$,

$b_{67} = n\, K_n(\bar{\beta}_o\varepsilon_i)$, $b_{68} = -\, i\bar{\alpha}\varepsilon_i\, I_{n+1}(\bar{\beta}_o\varepsilon_i)$, $b_{69} = -\, i\bar{\alpha}\varepsilon_i\, K_{n+1}(\bar{\beta}_o\varepsilon_i)$,

$b_{74} = -\, i\bar{\alpha}\varepsilon_o\, I_n(\bar{\alpha}\varepsilon_o)$, $b_{75} = -\, i\bar{\alpha}\varepsilon_o\, K_n(\bar{\alpha}\varepsilon_o)$,

$b_{76} = 0$, $b_{77} = 0$,

$b_{78} = -\left[\,(n+1)\, I_{n+1}(\bar{\beta}_o\varepsilon_o) + \varepsilon_o\bar{\beta}_o\, I'_{n+1}(\bar{\beta}_o\varepsilon_o)\right]$,

$b_{79} = -\left[\,(n+1)\, K_{n+1}(\bar{\beta}_o\varepsilon_o) + \varepsilon_o\bar{\beta}_o\, K'_{n+1}(\bar{\beta}_o\varepsilon_o)\right]$,

$b_{84} = -\, n\, I_n(\bar{\alpha}\varepsilon_o)$, $b_{85} = -\, n\, K_n(\bar{\alpha}\varepsilon_o)$, $b_{86} = -\,(\bar{\beta}_o\varepsilon_o)\, I'_n(\bar{\beta}_o\varepsilon_o)$,

$b_{87} = -\,(\bar{\beta}_o\varepsilon_o)\, K'_n(\bar{\beta}_o\varepsilon_o)$, $b_{88} = -\, i\bar{\alpha}\varepsilon_o\, I_{n+1}(\bar{\beta}_o\varepsilon_o)$, $b_{89} = -\, i\bar{\alpha}\varepsilon_o\, K_{n+1}(\bar{\beta}_o\varepsilon_o)$,

$$b_{94} = \varepsilon_o \bar{\alpha}\ I_n'(\bar{\alpha}\varepsilon_o),\ b_{95} = \varepsilon_o \bar{\alpha}\ K_n'(\bar{\alpha}\varepsilon_o),\ b_{96} = n\ I_n(\bar{\beta}_o\varepsilon_o),$$

$$b_{97} = n\ K_n(\bar{\beta}_o\varepsilon_o),\ b_{98} = -\ i\bar{\alpha}\,\varepsilon_o\ I_{n+1}(\bar{\beta}_o\varepsilon_o),\ b_{99} - i\bar{\alpha}\,\varepsilon_o\ K_{n+1}(\bar{\beta}_o\varepsilon_o). \tag{E.1.1}$$

The elements of vector $\{R^*\}$ is given by:

$$R_1^* = \mathrm{U}\ (\varepsilon_i\bar{\alpha}\ \Omega - \varepsilon_i^2\bar{\alpha}^2\bar{U}_{\delta i})\ \Phi_m^*\ \bar{A}_{mn}$$

$$R_2^* = i\,\mathrm{U}\,(\Omega - \varepsilon_i\bar{\alpha}\ \bar{U}_{\delta i})\ \Phi_m^*\ \bar{B}_{mn}$$

$$R_3^* = i\ \mathrm{U}(\Omega - \varepsilon_i\bar{\alpha}\ \bar{U}_{\delta o})\ \Phi_m^*\ \bar{C}_{mn}$$

$$R_4^* = \mathrm{U}\ (\varepsilon_i\bar{\alpha}\ \Omega - \varepsilon_i^2\bar{\alpha}^2\bar{U}_{\delta i})\ \Phi_m^*\ \bar{A}_{mn}$$

$$R_5^* = i\ \mathrm{U}(\Omega - \bar{\alpha}\,\varepsilon_i\ \bar{U}_{\delta o})\ \Phi_m^*\ \bar{B}_{mn}$$

$$R_6^* = i\ \mathrm{U}(\Omega - \bar{\alpha}\,\varepsilon_i\ \bar{U}_{\delta o})\ \Phi_m^*\ \bar{C}_{mn}$$

$$R_7^* = R_8^* = R_9^* = 0. \tag{E.1.2}$$

In a more convenient way we can rewrite (E.1.2) as

$$R_1^* = \bar{R}_1\ \Phi_m^*\ \bar{A}_{mn}\ ,\quad R_2^* = \bar{R}_2\ \Phi_m^*\ \bar{B}_{mn},\quad R_3^* = \bar{R}_3\ \Phi_m^*\ \bar{C}_{mn}$$

$$R_4^* = \bar{R}_4\ \Phi_m^*\ \bar{A}_{mn},\quad R_5^* = \bar{R}_5\ \Phi_m^*\ \bar{A}_{mn},\quad R_6^* = \bar{R}_6\ \Phi_m^*\ \bar{A}_{mn} \tag{E.1.3}$$

where

$$\bar{R}_1 = \mathrm{U}(\varepsilon_i\bar{\alpha}\ \Omega - \varepsilon_i^2\bar{\alpha}^2\bar{U}_{\delta i}),\ \bar{R}_2 = i\mathrm{U}(\Omega - \varepsilon_i\bar{\alpha}\ \bar{U}_{\delta i}),\ \bar{R}_3 = \bar{R}_2\ ,$$

$$\bar{R}_4 = \mathrm{U}(\varepsilon_i\bar{\alpha}\ \Omega - \varepsilon_i^2\bar{\alpha}^2\bar{U}_{\delta o}),\ \bar{R}_5 = i\mathrm{U}(\Omega - \varepsilon_i\bar{\alpha}\ \bar{U}_{\delta o}),\ \bar{R}_6 = \bar{R}_5\ ,$$

The elements of [T] of equation (E.2) are given by:

$$T_{11} = \frac{\rho_i \mathrm{U}}{\xi_i}\ \left\{ -2\ i\bar{\alpha}^2\ I_n'(\bar{\alpha}\varepsilon_i)\right\}\ ,\ T_{12} = \frac{\rho_i \mathrm{U}}{\zeta_i}\ \left\{ \frac{i\bar{\alpha}n}{\varepsilon_i}\ I_n(\bar{\beta}_i\varepsilon_i)\right\}\ ,$$

$$T_{13} = \frac{\rho_i u}{\xi_i} \left\{ \frac{1}{\epsilon_i^2} + \frac{n}{\epsilon_i^2} - \bar{\alpha}^2 \right\} I_{n+1}(\bar{\beta}_i \epsilon_i) - \frac{\bar{\beta}_i}{\epsilon_i} (1+n) \; I'_{n+1}(\bar{\beta}_i \epsilon_i)$$

$$- \bar{\beta}_i^2 \; I''_{n+1}(\bar{\beta}_i \epsilon_i) \; ,$$

$$T_{14} = -\frac{\rho_r \rho_i u}{\xi_o} \left\{ -2 \; i\bar{\alpha}^2 I'_n(\bar{\alpha}\epsilon_i) \right\} , \quad T_{15} = -\frac{\rho_r \rho_i u}{\xi_o} \left\{ -2 \; i\bar{\alpha}^2 K'_n(\bar{\alpha}\epsilon_i) \right\} ,$$

$$T_{16} = -\frac{\rho_r \rho_i u}{\xi_o} \left\{ -\frac{i\bar{\alpha}n}{\epsilon_i} I'_n(\bar{\beta}_i \epsilon_i) \right\} , \quad T_{17} = -\frac{\rho_r \rho_i u}{\xi_o} \left\{ -\frac{i\bar{\alpha}n}{\epsilon_i} K'_n(\bar{\beta}_i \epsilon_i) \right\} ,$$

$$T_{18} = -\frac{\rho_r \rho_i u}{\xi_o} \left[\left\{ \frac{1}{\epsilon_i^2} + \frac{n}{\epsilon_i^2} - \bar{\alpha}^2 \right\} I_{n+1}(\bar{\beta}_o \epsilon_i) - \frac{\bar{\beta}_o}{\epsilon_i} (1+n) \; I'_{n+1}(\bar{\beta}_o \epsilon_i) \right.$$
$$\left. - \bar{\beta}_o^2 \; I''_{n+1}(\bar{\beta}_o \epsilon_i) \right] ,$$

$$T_{19} = -\frac{\rho_r \rho_i u}{\xi_o} \left[\left\{ \frac{1}{\epsilon_i^2} + \frac{n}{\epsilon_i^2} - \bar{\alpha}^2 \right\} K_{n+1}(\bar{\beta}_o \epsilon_i) - \frac{\bar{\beta}_o}{\epsilon_i} (1+n) \; K'_{n+1}(\bar{\beta}_o \epsilon_i) \right.$$
$$\left. - \bar{\beta}_o^2 K''_{n+1}(\bar{\beta}_o \epsilon_i) \right] ,$$

$$T_{21} = \frac{\rho_i u}{\xi_i} \left(\frac{2n}{\epsilon_i^2} I_n(\bar{\alpha}\epsilon_i) - \frac{2n}{\epsilon_i} \bar{\alpha} \; I'_n(\bar{\alpha}\epsilon_i) \right) ,$$

$$T_{22} = \frac{\rho_i u}{\xi_i} \left(-\frac{n^2}{\epsilon_i^2} I_n(\bar{\beta}_i \epsilon_i) - \bar{\beta}_i^2 \; I''_n(\bar{\beta}_i \epsilon_i) + \frac{\bar{\beta}_i}{\epsilon_i} \; I'_n(\bar{\beta}_i \epsilon_i) \right) ;$$

$$T_{23} = \frac{\rho_i u}{\xi_i} \left(\frac{i\bar{\alpha}}{\epsilon_i} (1+n) \; I_{n+1}(\bar{\beta}_i \epsilon_i) - i\bar{\alpha} \; \bar{\beta}_i \; I'_{n+1}(\bar{\beta}_i \epsilon_i) \right) ,$$

$$T_{24} = -\frac{\rho_r \rho_i u}{\xi_o} \left(\frac{2n}{\epsilon_i^2} I_n(\bar{\alpha}\epsilon_i) - \frac{2n}{\epsilon_i} \bar{\alpha} \; I'_n(\bar{\alpha}\epsilon_i) \right) ,$$

$$T_{25} = -\frac{\rho_r \rho_i u}{\xi_o} \left(\frac{2n}{\epsilon_i^2} K_n(\bar{\alpha}\epsilon_i) - \frac{2n}{\epsilon_i} \bar{\alpha} \; K'_n(\bar{\alpha}\epsilon_i) \right) ,$$

$$T_{26} = -\frac{\rho_r \rho_i \mu}{\xi_o} \left[-\frac{n^2}{\epsilon_i^2} I_n(\bar{\beta}_o \epsilon_i) - \bar{\beta}_o^2 I_n''(\bar{\beta}_o \epsilon_i) + \frac{\bar{\beta}_o}{\epsilon_i} I_n'(\bar{\beta}_o \epsilon_i) \right]$$

$$T_{27} = -\frac{\rho_r \rho_i \mu}{\xi_o} \left[-\frac{n^2}{\epsilon_i^2} K_n(\bar{\beta}_o \epsilon_i) - \bar{\beta}_o^2 K_n''(\bar{\beta}_o \epsilon_i) + \frac{\bar{\beta}_o}{\epsilon_i} K_n'(\bar{\beta}_o \epsilon_i) \right]$$

$$T_{28} = -\frac{\rho_r \rho_i \mu}{\xi_o} \left[\frac{i\bar{\alpha}}{\epsilon_i} (n+1) I_{n+1}(\bar{\beta}_o \epsilon_i) - i\bar{\alpha}\, \bar{\beta}_o\, I_{n+1}'(\bar{\beta}_o \epsilon_i) \right]$$

$$T_{29} = -\frac{\rho_r \rho_i \mu}{\xi_o} \left[\frac{i\bar{\alpha}}{\epsilon_i} (n+1) K_{n+1}(\bar{\beta}_o \epsilon_i) - i\bar{\alpha}\, \bar{\beta}_o\, K_{n+1}'(\bar{\beta}_o \epsilon_i) \right]$$

$$T_{31} = \rho_i \mu \left\{ p_{1i}^{*'} + \frac{2}{\xi_i} \bar{\alpha}^2 I_n''(\bar{\alpha}\epsilon_i) \right\} ,$$

$$T_{32} = \rho_i \mu \left\{ p_{1i}^{*'} + \frac{2}{\xi_i} \left[-\frac{n}{\epsilon_i^2} I_n(\bar{\beta}_i \epsilon_i) + \frac{n}{\epsilon_i} \bar{\beta}_i\, I_n'(\bar{\beta}_i \epsilon_i) \right] \right\} ,$$

$$T_{33} = \rho_i \mu \left\{ p_{1i}^{*'} + \frac{2}{\xi_i} \left[-i\bar{\alpha}\, \bar{\beta}_i\, I_{n+1}'(\bar{\beta}_i \epsilon_i) \right] \right\} ,$$

$$T_{34} = -\rho_r \rho_i \mu \left\{ p_{1Io}^{*'} + \frac{2\bar{\alpha}^2}{\xi_o} I_n''(\bar{\alpha}\epsilon_i) \right\} ,$$

$$T_{35} = -\rho_r \rho_i \mu \left\{ p_{1Ko}^{*'} + \frac{2\bar{\alpha}^2}{\xi_o} K_n''(\bar{\alpha}\epsilon_i) \right\} ,$$

$$T_{36} = -\rho_r \rho_i \mu \left\{ p_{2Io}^{*'} + \frac{2}{\xi_o} \left[-\frac{n}{\epsilon_i^2} I_n(\bar{\beta}_o \epsilon_i) + \frac{n}{\epsilon_i} \bar{\beta}_o\, I_n'(\bar{\beta}_o \epsilon_i) \right] \right\} ,$$

$$T_{37} = -\rho_r \rho_i \mu \left\{ p_{2Ko}^{*'} + \frac{2}{\xi_o} \left[-\frac{n}{\epsilon_i^2} K_n(\bar{\beta}_o \epsilon_i) + \frac{n}{\epsilon_i} \bar{\beta}_o\, K_n'(\bar{\beta}_o \epsilon_i) \right] \right\} ,$$

$$T_{38} = -\rho_r \rho_i \mu \left\{ p_{3Io}^{*'} + \frac{2}{\xi_o} (-i\bar{\alpha})\, \bar{\beta}_o\, I_{n+1}'(\bar{\beta}_o \epsilon_i) \right\} ,$$

$$T_{39} = -\rho_r \rho_i \mu \left\{ p_{3Ko}^{*'} + \frac{2}{\xi_o} (-i\bar{\alpha})\, \bar{\beta}_o\, K_{n+1}'(\bar{\beta}_o \epsilon_i) \right\} .$$

Finally, using equations (3.92)-(3.94) and (E.1.4)-(E.1.6) we can write the generalized forces as:

$$\bar{q}^{(1)}_{xkm} = \frac{\eta}{2\pi\rho_i u^2} \int_{-\infty}^{\infty} \left(S_{11}\, \overline{R_1} + S_{14}\, \overline{R_4} \right) G_{km}(\bar{\alpha})\, d\bar{\alpha} \ ,$$

$$\bar{q}^{(2)}_{xkm} = \frac{\eta}{2\pi\rho_i u^2} \int_{-\infty}^{\infty} \left(S_{12}\, \overline{R_2} + S_{15}\, \overline{R_5} \right) G_{km}(\bar{\alpha})\, d\bar{\alpha} \ ,$$

$$\bar{q}^{(3)}_{xkm} = \frac{\eta}{2\pi\rho_i u^2} \int_{-\infty}^{\infty} \left(S_{13}\, \overline{R_3} + S_{16}\, \overline{R_6} \right) G_{km}(\bar{\alpha})\, d\bar{\alpha} \ ,$$

$$\bar{q}^{(1)}_{\theta km} = \frac{\eta\, \varepsilon_i}{2\pi\rho_i u^2} \int_{-\infty}^{\infty} \left(S_{21}\, \overline{R_1} + S_{24}\, \overline{R_4} \right) H_{km}(\bar{\alpha})\, d\bar{\alpha} \ ,$$

$$\bar{q}^{(2)}_{\theta km} = \frac{\eta\, \varepsilon_i}{2\pi\rho_i u^2} \int_{-\infty}^{\infty} \left(S_{22}\, \overline{R_2} + S_{25}\, \overline{R_5} \right) H_{km}(\bar{\alpha})\, d\bar{\alpha} \ ,$$

$$\bar{q}^{(3)}_{\theta km} = \frac{\eta\, \varepsilon_i}{2\pi\rho_i u^2} \int_{-\infty}^{\infty} \left(S_{23}\, \overline{R_3} + S_{26}\, \overline{R_6} \right) H_{km}(\bar{\alpha})\, d\bar{\alpha} \ ,$$

$$\bar{q}^{(1)}_{rkm} = \frac{\eta\, \varepsilon_i}{2\pi\rho_i u^2} \int_{-\infty}^{\infty} \left(S_{31}\, \overline{R_1} + S_{34}\, \overline{R_4} \right) H_{km}(\bar{\alpha})\, d\bar{\alpha} \ ,$$

$$\bar{q}^{(2)}_{rkm} = \frac{\eta\, \varepsilon_i}{2\pi\rho_i u^2} \int_{-\infty}^{\infty} \left(S_{32}\, \overline{R_2} + S_{35}\, \overline{R_5} \right) H_{km}(\bar{\alpha})\, d\bar{\alpha} \ ,$$

$$\bar{q}^{(3)}_{rkm} = \frac{\eta\, \varepsilon_i}{2\pi\rho_i u^2} \int_{-\infty}^{\infty} \left(S_{33}\, \overline{R_3} + S_{36}\, \overline{R_6} \right) H_{km}(\bar{\alpha})\, d\bar{\alpha} \ , \tag{E.1.5}$$

where $G_{km}(\bar{\alpha})$ and $H_{km}(\bar{\alpha})$ are given in Appendix F and R_1, R_2, R_3, R_4, R_5 and R_6 are given in equation (E.1.3).

E.2 TRAVELLING-WAVE SOLUTION

The vector {Q} given by (E.4) is denoted by $\{\bar{q}\}$ in equation (4.77). The coefficients for matrix [B] given by (4.32)-(4.34) and (4.47)-(4.52) are

$$b_{11} = i\bar{\alpha}\; I_n(\bar{\alpha}) \;,\quad b_{12} = 0 \;,\quad b_{13} = (n+1) I_{n+1}(\bar{\beta}_i) + \bar{\beta}_i\; I'_{n+1}(\bar{\beta}_i) \;,$$

$$b_{21} = -\, n\, I_n(\bar{\alpha}) \;,\quad b_{22} = -\bar{\beta}_i\; I'_n(\bar{\beta}_i) \;,\quad b_{23} = -\, i\bar{\alpha}\; I_{n+1}(\bar{\beta}_i) \;,$$

$$b_{31} = \bar{\alpha}\, I'_n(\bar{\alpha}) \;,\quad b_{32} = n\, I_n(\bar{\beta}_i) \;,\quad b_{33} = -\, i\bar{\alpha}\; I_{n+1}(\bar{\beta}_i) \;,$$

$$b_{44} = i\bar{\alpha}\; I_n(\bar{\alpha}) \;,\quad b_{45} = i\bar{\alpha}\; K_n(\bar{\alpha}) \;,\quad b_{46} = 0 \;,\quad b_{47} = 0 \;,$$

$$b_{48} = (n+1) I_{n+1}(\bar{\beta}_o) + \bar{\beta}_o\; I'_{n+1}(\bar{\beta}_o) \;,$$

$$b_{49} = (n+1) K_{n+1}(\bar{\beta}_o) + \bar{\beta}_o\; K'_{n+1}(\bar{\beta}_o) \;,$$

$$b_{54} = -\, n\; I_n(\bar{\alpha}) \;,\quad b_{55} = -\, n\; K_n(\bar{\alpha}) \;,\quad b_{56} = -\,\bar{\beta}_o\; I'_n(\bar{\beta}_o) \;,$$

$$b_{57} = -\,\bar{\beta}_o K'_n(\bar{\beta}_o) ,\quad b_{58} = -\, i\bar{\alpha}\; I_{n+1}(\bar{\beta}_o) \;,\quad b_{59} = -\, i\bar{\alpha}\; K_{n+1}(\bar{\beta}_o) \;,$$

$$b_{64} = \bar{\alpha}\; I'_n(\bar{\alpha}) \;,\quad b_{65} = \bar{\alpha}\; K'_n(\bar{\alpha}) \;,\quad b_{66} = n\; I_n(\bar{\beta}_o) \;,$$

$$b_{67} = n\; K_n(\bar{\beta}_o) \;,\quad b_{68} = -\, i\bar{\alpha}\; I_{n+1}(\bar{\beta}_o) \;,\quad b_{69} = -\, i\bar{\alpha}\; K_{n+1}(\bar{\beta}_o) \;,$$

$$b_{74} = i\bar{\alpha}\,\varepsilon_r\; I_n(\bar{\alpha}\varepsilon_r) \;,\quad b_{75} = i\bar{\alpha}\,\varepsilon_r\; K_n(\bar{\alpha}\varepsilon_r) ,$$

$$b_{76} = 0 ,\quad b_{77} = 0 ,$$

$$b_{78} = (n+1)\; I_{n+1}(\bar{\beta}_o\varepsilon_r) + (\bar{\beta}_o\varepsilon_r)\; I'_{n+1}(\bar{\beta}_o\varepsilon_r) \;,$$

$$b_{79} = (n+1)\, K_{n+1}(\bar{\beta}_o \varepsilon_r) + (\bar{\beta}_o \varepsilon_r)\, K'_{n+1}(\bar{\beta}_o \varepsilon_r)\ ,$$

$$b_{84} = -\, n\, I_n(\bar{\alpha}\varepsilon_r)\ , \quad b_{85} = -\, n\, K_n(\bar{\alpha}\varepsilon_r)\ , \quad b_{86} = -\,(\bar{\beta}_o \varepsilon_r)\, I'_n(\bar{\beta}_o \varepsilon_r)\ ,$$

$$b_{87} = -(\bar{\beta}_o \varepsilon_r)\, K'_n(\bar{\beta}_o \varepsilon_r)\ , \quad b_{88} = -\, i\bar{\alpha}\varepsilon_r\, I_{n+1}(\bar{\beta}_o \varepsilon_r)\ , \quad b_{89} = -\, i\bar{\alpha}\varepsilon_r\, K_{n+1}(\bar{\beta}_o \varepsilon_r)\ ,$$

$$b_{94} = \bar{\alpha}\ \varepsilon_r\ I'_n\ (\bar{\alpha}\varepsilon_r)\ , \quad b_{95} = \bar{\alpha}\ \varepsilon_r\ K'_n(\bar{\alpha}\varepsilon_r)\ , \quad b_{96} = n\ I_n(\bar{\beta}_o \varepsilon_r)\ ,$$

$$b_{97} = n\ K_n(\bar{\beta}_o \varepsilon_r)\ , \quad b_{98} = i\,\bar{\alpha}\,\varepsilon_r\ I_{n+1}(\bar{\beta}_o \varepsilon_r)\ , \quad b_{99} = i\,\bar{\alpha}\,\varepsilon_r\ K_{n+1}(\bar{\beta}_o \varepsilon_r)\ . \qquad (E.2.1)$$

The element of matrix [T] are given by

$$T_{11} = \frac{\rho_i U}{\varepsilon_i^2\, \xi_i} \left(-2\ i\bar{\alpha}^2\, I'_n(\bar{\alpha}) \right)\ , \quad T_{12} = \frac{\rho_i U}{\varepsilon_i^2\, \xi_i} \left(-\, in\bar{\alpha}\ I_n(\bar{\beta}_i) \right)\ ,$$

$$T_{13} = \frac{\rho_i U}{\varepsilon_i^2\, \xi_i} \left((1 - \bar{\alpha}^2 + n)\ I_{n+1}(\bar{\beta}_i) - \bar{\beta}_i\ (n+1)\ I'_{n+1}(\bar{\beta}_i) - \bar{\beta}_i^2\, I''_{n+1}(\bar{\beta}_i) \right)\ ,$$

$$T_{14} = \frac{\rho_r \rho_i U}{\varepsilon_i^2\, \xi_i \xi_r} \left(\left\{ 2\ i\bar{\alpha}^2\, I'_n(\bar{\alpha}) \right\} \right)\ , \quad T_{15} = \frac{\rho_r \rho_i U}{\varepsilon_i^2\, \xi_i \xi_r} \left(\left\{ 2\ i\bar{\alpha}^2\, K'_n(\bar{\alpha}) \right\} \right)\ ,$$

$$T_{16} = \frac{\rho_r \rho_i U}{\varepsilon_i^2\, \xi_i \xi_r} \left(-\left\{ -in\bar{\alpha}\ I_n(\bar{\beta}_o) \right\} \right)\ , \quad T_{17} = \frac{\rho_r \rho_i U}{\varepsilon_i^2\, \xi_i \xi_r} \left(-\left\{ -in\bar{\alpha}\ K_n(\bar{\beta}_o) \right\} \right)\ ,$$

$$T_{18} = \frac{\rho_r \rho_i U}{\varepsilon_i^2\, \xi_i \xi_r} \left(-\left\{ (1 - \bar{\alpha}^2 + n) I_{n+1}(\bar{\beta}_o) - \bar{\beta}_o (n+1) I'_{n+1}(\bar{\beta}_o) - \bar{\beta}_o^2\, I''_{n+1}(\bar{\beta}_o) \right\} \right)\ ,$$

$$T_{19} = \frac{\rho_r \rho_i U}{\varepsilon_i^2\, \xi_i \xi_r} \left(-\left\{ (1 - \bar{\alpha}^2 + n) K_{n+1}(\bar{\beta}_o) - \bar{\beta}_o (n+1) K'_{n+1}(\bar{\beta}_o) - \bar{\beta}_o^2\, K''_{n+1}(\bar{\beta}_o) \right\} \right)\ ,$$

$$T_{21} = \frac{\rho_i u}{\varepsilon_i^2 \xi_i} \left[2n \ I_n(\bar{\alpha}) - 2n \ \bar{\alpha} \ I_n'(\bar{\alpha}) \right] ,$$

$$T_{22} = \frac{\rho_i u}{\varepsilon_i^2 \xi_i} \left[- n^2 \ I_n(\bar{\beta}_i) + \ \bar{\beta}_i \ I_n'(\beta_i) - \bar{\beta}_i^2 \ I_n''(\bar{\beta}_i) \right] ,$$

$$T_{23} = \frac{\rho_i u}{\varepsilon_i^2 \xi_i} \left[i\bar{\alpha} \ (1+n) \ I_{n+1}(\bar{\beta}_i) - \cancel{i\bar{\alpha} \ \bar{\beta}_i} \ I_{n+1}'(\bar{\beta}_i) \right] ,$$

$$T_{24} = \frac{\rho_r \rho_i u}{\varepsilon_i^2 \xi_i \xi_r} \left[- \left(2n \ I_n(\bar{\alpha}) - 2n \ \bar{\alpha} \ I_n'(\bar{\alpha}) \right) \right] ,$$

$$T_{25} = \frac{\rho_r \rho_i u}{\varepsilon_i^2 \xi_i \xi_r} \left[- \left(2n \ K_n(\bar{\alpha}) - 2n \ \bar{\alpha} \ K_n'(\bar{\alpha}) \right) \right] ,$$

$$T_{26} = \frac{- \rho_r \rho_i u}{\varepsilon_i^2 \xi_i \xi_r} \left[- \ n^2 \ I_n(\bar{\beta}_o) + \bar{\beta}_o \ I_n'(\beta_o) - \bar{\beta}_o^2 \ I_n''(\bar{\beta}_o) \right] ,$$

$$T_{27} = \frac{- \rho_r \rho_i u}{\varepsilon_i^2 \xi_i \xi_r} \left[- \ n^2 \ K_n(\bar{\beta}_o) + \bar{\beta}_o \ K_n'(\beta_o) - \bar{\beta}_o^2 \ K_n''(\bar{\beta}_o) \right] ,$$

$$T_{28} = \frac{\rho_r \rho_i u}{\varepsilon_i^2 \xi_i \xi_r} \left[- \left(i\bar{\alpha} \ (n+1) \ I_{n+1}(\bar{\beta}_o) \ - \ i\bar{\alpha} \ \bar{\beta}_o \ I_{n+1}'(\bar{\beta}_o) \right) \right] ,$$

$$T_{29} = \frac{\rho_r \rho_i u}{\varepsilon_i^2 \xi_i \xi_r} \left[- \left(i\bar{\alpha} \ (n+1) \ K_{n+1}(\bar{\beta}_o) \ - \ i\bar{\alpha} \ \bar{\beta}_o \ K_{n+1}'(\bar{\beta}_o) \right) \right] ,$$

$$T_{31} = \rho_i u \left(\bar{p}_{1i}' + \frac{2\bar{\alpha}^2}{\xi_i \varepsilon_i^2} \ I_n''(\bar{\alpha}) \right) ,$$

$$T_{32} = \rho_i u \left(\bar{p}_{2i}' + \frac{2}{\xi_i \varepsilon_i^2} \left[\bar{\beta}_i n \ I_n'(\bar{\beta}_i) - n \ I_n(\bar{\beta}_i) \right] \right) ,$$

$$T_{33} = \rho_i \mu \left[\bar{P}'_{3i} + \frac{2}{\xi_i \epsilon_i^2} \left(-i\bar{\alpha}\, \bar{\beta}_i\, I'_{n+1}(\beta_i) \right) \right],$$

$$T_{34} = -\rho_r \rho_i \mu \left[\bar{P}'_{1Io} + \frac{2\bar{\alpha}^2}{\xi_i \xi_r} \frac{I''_n(\bar{\alpha})}{\epsilon_i^2} \right],$$

$$T_{35} = -\rho_r \rho_i \mu \left[\bar{P}'_{1Ko} + \frac{2\bar{\alpha}^2}{\xi_i \xi_r} \frac{K''_n(\bar{\alpha})}{\epsilon_i^2} \right],$$

$$T_{36} = -\rho_r \rho_i \mu \left[\bar{P}'_{2Io} + \frac{2}{\xi_i \xi_r \epsilon_i^2} \left(\bar{\beta}_o n\, I'_n(\bar{\beta}_o) - n\, I_n(\bar{\beta}_o) \right) \right],$$

$$T_{37} = -\rho_r \rho_i \mu \left[\bar{P}'_{2Ko} + \frac{2}{\xi_i \xi_r \epsilon_i^2} \left(\bar{\beta}_o n\, K'_n(\bar{\beta}_o) - n\, K_n(\bar{\beta}_o) \right) \right],$$

$$T_{38} = -\rho_r \rho_i \mu \left[\bar{P}'_{3Io} + \frac{2}{\xi_i \xi_r \epsilon_i^2} \left((-i\bar{\alpha}\, \bar{\beta}_o)\, I'_n(\bar{\beta}_o) \right) \right],$$

$$T_{39} = -\rho_r \rho_i \mu \left[\bar{P}'_{3Ko} + \frac{2}{\xi_i \xi_r \epsilon_i^2} \left((-i\bar{\alpha}\, \bar{\beta}_o)\, K'_n(\bar{\beta}_o) \right) \right], \tag{E.2.2}$$

and the vector $\{R\}$ is given by

$$R_1 = \mu\, (\Omega_i - \bar{\alpha}\, \bar{U}_{\delta i})\, \bar{A}_n,$$

$$R_2 = i\mu\, (\Omega - \bar{\alpha}\, \bar{U}_{\delta i})\, \bar{B}_n,$$

$$R_3 = i\mu\, (\Omega - \bar{\alpha}\, \bar{U}_{\delta i})\, \bar{C}_n,$$

$$R_4 = \mu\, (\Omega - \bar{\alpha}\, \bar{U}_{\delta o})\, \bar{A}_n,$$

$$R_5 = iU\,(\Omega - \bar{\alpha}\;\bar{U}_{\delta o})\;\bar{B}_n\ ,$$

$$R_6 = iU\,(\Omega - \bar{\alpha}\;\bar{U}_{\delta o})\;\bar{C}_n\ ,$$

$$R_7 = R_8 = R_9 = 0. \tag{E.2.3}$$

We can rewrite (E.2.3) in the following form

$$R_1 = \bar{R}_1\,\bar{A}_n\ ,\quad R_2 = \bar{R}_2\,\bar{B}_n$$

$$R_3 = \bar{R}_3\,\bar{C}_n\ ,\quad R_4 = \bar{R}_4\,\bar{A}_n$$

$$R_5 = \bar{R}_5\,\bar{B}_n\ ,\quad R_6 = \bar{R}_6\,\bar{C}_n \tag{E.2.4}$$

where

$$\bar{R}_1 = U\,(\Omega - \bar{\alpha}\,\bar{U}_{\delta i})\ ,\quad \bar{R}_2 = iU(\Omega - \bar{\alpha}\,\bar{U}_{\delta i})\ ,\quad \bar{R}_3 = \bar{R}_2$$

$$\bar{R}_4 = U\,(\Omega - \bar{\alpha}\,\bar{U}_{\delta o})\ ,\quad \bar{R}_5 = iU\,(\Omega - \bar{\alpha}\;\bar{U}_{\delta o})\ ,\ \bar{R}_6 = \bar{R}_5\ . \tag{E.2.5}$$

Finally, using equations (4.66-4.68) and (E.2.4), the generalized forces are written as:

$$\bar{q}_{x1} = \frac{\epsilon_i \eta}{\rho_i U^2}\,(S_{11}\,\bar{R}_1 + S_{14}\,\bar{R}_4)\;\bar{\delta}_{jj}\ ,$$

$$\bar{q}_{x2} = \frac{\epsilon_i \eta}{\rho_i U^2}\,(S_{12}\,\bar{R}_2 + S_{15}\,\bar{R}_5)\;\bar{\delta}_{jj}\ ,$$

$$\bar{q}_{x3} = \frac{\epsilon_i \eta}{\rho_i U^2}\,(S_{13}\,\bar{R}_3 + S_{16}\,\bar{R}_6)\;\bar{\delta}_{jj}\ , \tag{E.2.6}$$

$$\bar{q}_{\theta 1} = \frac{\epsilon_i \eta}{\rho_i U^2}\,(S_{21}\,\bar{R}_1 + S_{24}\,\bar{R}_4)\;\bar{\delta}_{jj}\ ,$$

$$\bar{q}_{\theta 2} = \frac{\epsilon_i \eta}{\rho_i u^2} (S_{22} \bar{R}_2 + S_{25} \bar{R}_5) \bar{\delta}_{jj} ,$$

$$\bar{q}_{\theta 3} = \frac{\epsilon_i \eta}{\rho_i u^2} (S_{23} \bar{R}_3 + S_{26} \bar{R}_6) \bar{\delta}_{jj} ,$$

$$\bar{q}_{r1} = \frac{\epsilon_i \eta}{\rho_i u^2} (S_{31} \bar{R}_1 + S_{34} \bar{R}_4) \bar{\delta}_{jj} ,$$

$$\bar{q}_{r1} = \frac{\epsilon_i \eta}{\rho_i u^2} (S_{32} \bar{R}_2 + S_{35} \bar{R}_5) \bar{\delta}_{jj} ,$$

$$\bar{q}_{r1} = \frac{\epsilon_i \eta}{\rho_i u^2} (S_{33} \bar{R}_3 + S_{36} \bar{R}_6) \bar{\delta}_{jj} ,$$

where $\bar{\delta}_{jj} = \frac{1}{2}$, for $j = 1$.

APPENDIX F

THE EXPRESSIONS FOR $H_{km}(\bar{\alpha})$ AND $G_{km}(\bar{\alpha})$

$H_{km}(\bar{\alpha})$ is defined in equation (3.97) as follows:

$$H_{km}(\bar{\alpha}) = \int_0^1 \Phi_k(\zeta)\ e^{-i\bar{\alpha}\zeta}\ d\zeta \times \int_0^1 \Phi_m(\zeta)\ e^{i\bar{\alpha}\zeta}\ d\zeta\ ,$$

and $G_{km}(\bar{\alpha})$ is given by equation (3.96) as

$$G_{km}(\bar{\alpha}) = \int_0^1 \Phi_k'(\zeta)\ e^{-i\bar{\alpha}\zeta}\ d\zeta \times \int_0^1 \Phi_m(\zeta)\ e^{i\alpha\zeta}\ d\zeta\ ,$$

where $\Phi_m(\zeta)$ (or $\Phi_k(\zeta)$) is the beam eigenfunction function.

F.1 CLAMPED-CLAMPED BEAM

For a clamped-clamped beam, the characteristic beam function has the form

$$\Phi_m(\zeta) = \cosh\lambda_m\zeta - \cos\lambda_m\zeta - \sigma_m(\sinh\ \lambda_m\zeta - \sin\lambda_m\zeta), \qquad \text{(F.1)}$$

which satisfies

$$\Phi_m^{iv}(\zeta) = \lambda_m^4\,\Phi_m(\zeta). \qquad \text{(F.2)}$$

The eigenvalues λ_m and the constants σ_m for the clamped-clamped beam are defined in Appendix C.

F.1.1 Expression for $H_{km}(\bar{\alpha})$

The expression for $H_{km}(\bar{\alpha})$ has been evaluated in Ref. [48], and is given here as follows:

$$H_{km}(\bar{\alpha}) = \frac{1}{(\bar{\alpha})^4 - \lambda_m^4} \left\{ A_m\left[(-1)^{m+1}\, e^{i\bar{\alpha}} + 1\right] - B_m \bar{\alpha} \left[(-1)^{m+1}\, e^{i\bar{\alpha}} + 1\right]\right\}$$

$$\times \frac{1}{(\bar{\alpha})^4 - \lambda_k^4} \left\{ A_k\left[(-1)^{k+1}\, e^{i\bar{\alpha}} + 1\right] - B_k \bar{\alpha} \left[(-1)^{k+1}\, e^{i\bar{\alpha}} + 1\right]\right\},$$

where

$$A_m = 2\lambda_m^3 \sigma_m \,, \quad B_m = 2\, i\, \lambda_m^2 \,,$$

$$A_k = 2\lambda_k^3 \sigma_k \,, \quad B_k = 2\, i\, \lambda_k^2 \,. \tag{F.3}$$

Equation (F.3) holds for all values of $\bar{\alpha}$ except when $\bar{\alpha}^4 = \lambda_m^4$ or λ_k^4, i.e. when

$$\bar{\alpha} = \pm\, \lambda_m \,,\ \pm\, i\, \lambda_m \,,\ \pm\, \lambda_k \text{ or } i\, \lambda_k \,. \tag{F.4}$$

For $\bar{\alpha} = \pm\, i\, \lambda_m$, $\pm\, \lambda_m$, the integration $\int_0^1 \Phi_m(\zeta)\, e^{i\bar{\alpha}\zeta}\, d\zeta$ in equation (3.97) is given by:

$$\int_0^1 \Phi_m(\zeta)\, e^{i\lambda_m\zeta}\, d\zeta = \frac{1}{(-2\lambda_m)} \left[(-1)^{m+1}\, e^{i\lambda_m} \left(i\, \lambda_m\, \sigma_m + \lambda_m - i\right) + i\right], \tag{F.5}$$

$$\int_0^1 \Phi_m(\zeta)\, e^{-i\lambda_m\zeta}\, d\zeta = \frac{1}{(-2\lambda_m)} \left[(-1)^{m+1}\, e^{-i\lambda_m} \left(i\, \lambda_m\, \sigma_m - \lambda_m - i\right) + i\right], \tag{F.6}$$

$$\int_0^1 \Phi_m(\zeta)\, e^{-\lambda_m\zeta}\, d\zeta = \frac{1}{(-2\lambda_m)} \left[(-1)^{m+1}\, e^{-\lambda_m} \left(\lambda_m\, \sigma_m - \lambda_m - 1\right) + 1\right], \tag{F.7}$$

$$\int_0^1 \Phi_m(\zeta)\, e^{\lambda_m\zeta}\, d\zeta = \frac{1}{(-2\lambda_m)} \left[(-1)^{m+1}\, e^{\lambda_m} \left(\lambda_m\, \sigma_m - \lambda_m - 1\right) + 1\right], \tag{F.8}$$

and for the integral $\int_0^1 \Phi_k(\zeta) e^{-i\bar{\alpha}\zeta}\, d\zeta$, when $\bar{\alpha} = \pm\, \lambda_m$, $\pm\, i\, \lambda_k$, the correct expressions can be obtained by replacing the subscript m by k in equations (F.5)-(F.8).

F.1.2 Derivation of $G_{km}(\bar{\alpha})$

Let us consider the integral

$$\int_0^1 \Phi_k'(\zeta)\, e^{-i\bar{\alpha}\zeta}\, d\zeta \,. \tag{F.9}$$

Integrating (F.9) by parts, we obtain

$$\Phi_k(\zeta)\, e^{-i\bar{\alpha}\zeta} \Big|_0^1 + i\,\bar{\alpha} \int_0^1 \Phi_k(\zeta)\, e^{-i\bar{\alpha}\zeta}\, d\zeta \,. \tag{F.10}$$

Using the fact that

$$\Phi_k(0) = \Phi_k(1) = 0 \,,$$

equation (F.10) reduces to

$$i\,\bar{\alpha} \int_0^1 \Phi_k(\zeta)\, e^{-i\bar{\alpha}\zeta}\, d\zeta \,, \tag{F.11}$$

and finally $G_{km}(\bar{\alpha})$ may be written as

$$\begin{aligned} G_{km}(\bar{\alpha}) &= i\,\bar{\alpha} \int_0^1 \Phi_k(\zeta)\, e^{-i\bar{\alpha}\zeta}\, d\zeta \times \int_0^1 \Phi_m(\zeta)\, e^{-i\bar{\alpha}\zeta}\, d\zeta \\ &= i\,\bar{\alpha}\, H_{km}(\bar{\alpha}) \,. \end{aligned} \tag{F.12}$$

$G_{km}(\bar{\alpha})$ may now be evaluated.

F.2 PINNED-PINNED BEAM

For a pinned-pinned beam, the characteristic beam function has the form:

$$\Phi_m(\zeta) = \sin m\pi\zeta \,. \tag{F.13}$$

F.2.1 Expression for $H_{km}(\bar{\alpha})$

Let us consider the integral

$$\int_0^1 \Phi_m(\zeta)\, e^{i\bar{\alpha}\zeta}\, d\zeta \; . \tag{F.14}$$

Upon substituting (F.13) into (F.14) and integrating by parts, we obtain

$$\int_0^1 \sin m\pi\zeta \; e^{i\bar{\alpha}\zeta}\, d\zeta = \frac{\left[-e^{i\bar{\alpha}}(-1)^{m+1}+1\right] m\pi}{-\bar{\alpha}^2 + m^2\pi^2} \; . \tag{F.15}$$

then we consider the integral

$$\int_0^1 \Phi_k(\zeta)\, e^{-i\bar{\alpha}\zeta}\, d\zeta \; ; \tag{F.16}$$

substituting for $\Phi_k(\zeta)$ into (F.16) and integrating by parts, we get

$$\int_0^1 \sin k\pi\zeta \; e^{-i\bar{\alpha}\zeta}\, d\zeta = \frac{\left[-e^{-i\bar{\alpha}}(-1)^{k+1}+1\right] k\pi}{-\bar{\alpha}^2 + k^2\pi^2} \; . \tag{F.17}$$

Finally $H_{km}(\bar{\alpha})$ may be written as:

$$H_{km}(\bar{\alpha}) = \frac{\left[-e^{-i\bar{\alpha}}(-1)^{k+1}+1\right]\left[-e^{i\bar{\alpha}}(-1)^{m+1}+1\right] m k \pi^2}{\left(-\bar{\alpha}^2+k^2\pi^2\right)\left(-\bar{\alpha}^2+m^2\pi^2\right)} \; . \tag{F.18}$$

F.2.2 Expression for $G_{km}(\bar{\alpha})$

$G_{km}(\bar{\alpha})$ is evaluated using equation (F.12), where $H_{km}(\bar{\alpha})$ is now given by equation (F.18).

APPENDIX G

STRUCTURE OF MATRIX [A]

G.1 FOURIER TRANSFORM METHOD

In this Appendix, the structure of matrix [A] is described in detail. The matrix is given for the case of k, m = 1, 2, 3.

The structure of matrix A is shown below

$$
\begin{array}{c}
\\ k = 1 \\ \\ \\ k = 2 \\ \\ \\ k = 3 \\ \\
\end{array}
\left[\begin{array}{ccccccccc}
A^{(1)}_{11n} & A^{(1)}_{12n} & A^{(1)}_{13n} & A^{(2)}_{11n} & A^{(2)}_{12n} & A^{(2)}_{13n} & A^{(3)}_{11n} & A^{(3)}_{12n} & A^{(3)}_{13n} \\
A^{(4)}_{11n} & A^{(4)}_{12n} & A^{(4)}_{13n} & A^{(5)}_{11n} & A^{(5)}_{12n} & A^{(5)}_{13n} & A^{(6)}_{11n} & A^{(6)}_{12n} & A^{(6)}_{13n} \\
A^{(7)}_{11n} & A^{(7)}_{12n} & A^{(7)}_{13n} & A^{(8)}_{11n} & A^{(8)}_{12n} & A^{(8)}_{13n} & A^{(9)}_{11n} & A^{(9)}_{12n} & A^{(9)}_{13n} \\
A^{(1)}_{21n} & A^{(1)}_{22n} & A^{(1)}_{23n} & A^{(2)}_{21n} & A^{(2)}_{22n} & A^{(2)}_{23n} & A^{(3)}_{21n} & A^{(3)}_{22n} & A^{(3)}_{23n} \\
A^{(4)}_{21n} & A^{(4)}_{22n} & A^{(4)}_{23n} & A^{(5)}_{21n} & A^{(5)}_{22n} & A^{(5)}_{23n} & A^{(6)}_{21n} & A^{(6)}_{22n} & A^{(6)}_{23n} \\
A^{(7)}_{21n} & A^{(7)}_{22n} & A^{(7)}_{23n} & A^{(8)}_{21n} & A^{(8)}_{22n} & A^{(8)}_{23n} & A^{(9)}_{21n} & A^{(9)}_{22n} & A^{(9)}_{23n} \\
A^{(1)}_{31n} & A^{(1)}_{32n} & A^{(1)}_{33n} & A^{(2)}_{31n} & A^{(2)}_{32n} & A^{(2)}_{23n} & A^{(3)}_{31n} & A^{(3)}_{32n} & A^{(3)}_{33n} \\
A^{(4)}_{31n} & A^{(4)}_{32n} & A^{(4)}_{23n} & A^{(5)}_{31n} & A^{(5)}_{32n} & A^{(5)}_{23n} & A^{(6)}_{31n} & A^{(6)}_{32n} & A^{(6)}_{33n} \\
A^{(7)}_{31n} & A^{(7)}_{32n} & A^{(7)}_{23n} & A^{(8)}_{31n} & A^{(8)}_{32n} & A^{(8)}_{23n} & A^{(9)}_{31n} & A^{(9)}_{32n} & A^{(9)}_{33n}
\end{array}\right]
$$

where $A^{(\ell)}_{kmn}$ (k,m = 1, 2, 3; ℓ = 1, 2, ... 9, n = 2, 3) are given as follows:

$$A^{(\ell)}_{kmn} = E^{(\ell)}_{kmn} + F^{(\ell)}_{kmn} + Q^{(\ell)}_{kmn}$$

there $E^{(\ell)}_{kmn}$ represents the elements for free vibration of the shell, $F^{(\ell)}_{kmn}$ represents the steady fluid forces and $Q^{(\ell)}_{kmn}$ represents the unsteady fluid forces. The coefficients of matrix [A] are given below:

$$A_{kmn}^{(1)} = E_{kmn}^{(1)} + F_{kmn}^{(1)} + Q_{kmn}^{(1)} ,$$

where

$$E_{kmn}^{(1)} = \varepsilon_i^2 \; b_{km} + (\nu_s - 1)(k_s + 1)n^2 \; \frac{a_{km}}{2} + \Omega^2 \; a_{km} ,$$

$$F_{kmn}^{(1)} = \Gamma_{i1} \; \varepsilon_i^2 e_{km} + \Gamma_{i2} \; \varepsilon_i^2 b_{km} - \Gamma_{i4} \; n^2 g_{km} - \Gamma_{i5} \; n^2 a_{km} ,$$

$$Q_{kmn}^{(1)} = \bar{q}_{xkm}^{(1)} ;$$

$$A_{kmn}^{(2)} = E_{kmn}^{(2)} + F_{kmn}^{(2)} + Q_{kmn}^{(2)} ,$$

$$E_{kmn}^{(2)} = (1 + \nu_s)n \; a_{km}/2 ,$$

$$F_{kmn}^{(2)} = \Gamma_{i3} \; \frac{n}{\varepsilon_i} \; f_{km} ,$$

$$Q_{kmn}^{(2)} = \bar{q}_{xkm}^{(2)} ;$$

$$A_{kmn}^{(3)} = E_{kmn}^{(3)} + F_{kmn}^{(3)} + Q_{kmn}^{(3)} ,$$

$$E_{kmn}^{(3)} = (\nu_s + (\nu_s - 1)k_s \; \frac{n^2}{2} \; a_{km} - k_s \; \varepsilon_i^2 b_{km} ,$$

$$F_{kmn}^{(3)} = \frac{\Gamma_{i3}}{\varepsilon_i} \; f_{km} - \Gamma_{i4} \; g_{km} - \Gamma_{i5} \; a_{km} ,$$

$$Q_{kmn}^{(3)} = \bar{q}_{xkm}^{(3)} ;$$

$$A_{kmn}^{(4)} = E_{kmn}^{(4)} + F_{kmn}^{(4)} + Q_{kmn}^{(4)} ,$$

$$E_{kmn}^{(4)} = -(1 + \nu_s)n \; \varepsilon_i^2 \; \frac{d_{km}}{2} ,$$

$$F_{kmn}^{(4)} = 0 ,$$

$$Q_{kmn}^{(4)} = \bar{q}_{\theta km}^{(1)} ;$$

$$A^{(5)}_{kmn} = E^{(5)}_{kmn} + F^{(5)}_{kmn} + Q^{(5)}_{kmn} ,$$

$$E^{(5)}_{kmn} = -n^2\,\bar{\delta}_{km} + (1+3k_s)(1-\nu_s)\;\varepsilon_i^2\;\frac{d_{km}}{2} + \Omega^2\,\bar{\delta}_{km} ,$$

$$F^{(5)}_{kmn} = \Gamma_{i1}\;\varepsilon_i^2\,b_{km} + \Gamma_{i2}\;\varepsilon_i^2\,d_{km} - \Gamma_{i4}\;n^2\;j_{km} - \Gamma_{i5}\;n^2\;\bar{\delta}_{km} ,$$

$$Q^{(5)}_{kmn} = \bar{q}^{(2)}_{\theta km} ;$$

$$A^{(6)}_{kmn} = E^{(6)}_{kmn} + F^{(6)}_{kmn} + Q^{(6)}_{kmn} ,$$

$$E^{(6)}_{kmn} = -\,n\;\bar{\delta}_{km} + (3-\nu_s)\;k_s\;n\;\varepsilon_i^2\;\frac{d_{km}}{2} ,$$

$$F^{(6)}_{kmn} = -\,\Gamma_{i4}\;n\;j_{km} - \Gamma_{i5}\;n\;\bar{\delta}_{im} ,$$

$$Q^{(6)}_{kmn} = \bar{q}^{(2)}_{\theta km} ;$$

$$A^{(7)}_{kmn} = E^{(7)}_{kmn} + F^{(7)}_{kmn} + Q^{(7)}_{kmn} ,$$

$$E^{(7)}_{kmn} = \lambda_m^4\;\varepsilon_i^4\;k_s\;\bar{\delta}_{km} - (2\nu_s - k_s(1-\nu_s)n^2)\;\varepsilon_i^2\;\frac{d_{km}}{2} ,$$

$$F^{(7)}_{kmn} = \Gamma_{i4}\;\varepsilon_i^2\;h_{km} + \Gamma_{i5}\;\varepsilon_i^2\;d_{km} ,$$

$$Q^{(7)}_{kmn} = \bar{q}^{(1)}_{rkm} ;$$

$$A^{(8)}_{kmn} = E^{(8)}_{kmn} + F^{(8)}_{kmn} + Q^{(8)}_{kmn} ,$$

$$E^{(8)}_{kmn} = k_s(3-\nu_s)n\;\varepsilon_i^2\;\frac{d_{km}}{2} - n\;\bar{\delta}_{km} ,$$

$$F^{(8)}_{kmn} = -\,\Gamma_{i4}\;n\;j_{km} - \Gamma_{i5}\;n\;\bar{\delta}_{km} ,$$

$$Q^{(8)}_{kmn} = \bar{q}^{(2)}_{rkm} ;$$

$$A_{kmn}^{(9)} = E_{kmn}^{(9)} + F_{kmn}^{(9)} + Q_{kmn}^{(9)} ,$$

$$E_{kmn}^{(9)} = - k_s \left\{ (\lambda_m^4 \epsilon_i^4 + (n^2 - 1)^2) \bar{\delta}_{km} - 2 n^2 \epsilon_i^2 d_{km} \right\} - \bar{\delta}_{km} + \Omega_q^2 \bar{\delta}_{km} ,$$

$$F_{kmn}^{(9)} = \Gamma_{i1} \epsilon_i^2 b_{km} + \Gamma_{i2} \epsilon_i^2 d_{km} - \Gamma_{i4} n^2 j_{km} - \Gamma_{i5} n^2 \bar{\delta}_{km} ,$$

$$Q_{kmn}^{(9)} = \bar{q}_{rkm}^{(3)} ;$$

where $\bar{q}_{xkm}^{(1)}$, $\bar{q}_{xkm}^{(2)}$, $\bar{q}_{xkm}^{(3)}$, $\bar{q}_{\theta km}^{(1)}$, $\bar{q}_{\theta km}^{(2)}$, $\bar{q}_{\theta km}^{(3)}$, $\bar{q}_{rkm}^{(1)}$, $\bar{q}_{rkm}^{(2)}$, and $\bar{q}_{rkm}^{(3)}$ are given in Appendix F and Γ_{i1}, Γ_{i2}, Γ_{i3}, Γ_{i4} and Γ_{i5} are as follows:

$$\Gamma_{i1} = - \frac{LB_f}{\Lambda} , \Gamma_{i3} = - \epsilon_i \Gamma_{i1} , \Gamma_{i4} = - \frac{a_i LC_f}{\Lambda}, \Gamma_{i5} = - \frac{a_i D_f}{\Lambda} ,$$

$$\Gamma_{i2} = \frac{\nu_s}{2} \Gamma_{i4} - \frac{\Gamma_{i1}}{2} + \nu_s \Gamma_{i5} ,$$

where $\Lambda = \dfrac{Eh}{1-\nu^2}$.

B_f, C_f, D_f are defined in Appendix A by equations (A.27)-(A.29).

G.2 TRAVELLING WAVE SOLUTION

Matrix [A] is given by equation (4.74) as follows:

$$\begin{bmatrix} A_{jj}^{(1)} & A_{jj}^{(2)} & A_{jj}^{(3)} \\ A_{jj}^{(4)} & A_{jj}^{(5)} & A_{jj}^{(6)} \\ A_{jj}^{(7)} & A_{jj}^{(8)} & A_{jj}^{(9)} \end{bmatrix} ,$$

where $A_{jj}^{(\ell)}$ ($j = 1$, $\ell = 1,2, \ldots 9$) are given as follows:

$$A_{jj}^{(\ell)} = E_{jj}^{(\ell)} + F_{jj}^{(\ell)} + Q_{jj}^{(\ell)}$$

where $E_{jj}^{(\ell)}$, $F_{jj}^{(\ell)}$, $Q_{jj}^{(\ell)}$ are the elements for free vibration of the shell, steady fluid forces, and the unsteady fluid forces, respectively.

The coefficients of matrix [A] are given below:

$$A_{jj}^{(1)} = E_{jj}^{(1)} + F_{jj}^{(1)} + Q_{jj}^{(1)} ,$$

where

$$E_{jj}^{(1)} = \left[-\bar{\alpha}^2 + (1+\nu_s)(-n^2) + k_s \left(\frac{1-\nu_i}{2}\right)(-n^2) + \Omega^2 \right] \bar{\delta}_{jj} ,$$

$$F_{jj}^{(1)} = -\bar{\alpha}^2 \Gamma_{i1} \bar{b}_{jj} + \Gamma_{i2} (-\bar{\alpha}^2) \bar{\delta}_{jj} - \Gamma_{i4} n^2 \bar{b}_{jj} - \Gamma_{i5} n^2 \bar{\delta}_{jj} ,$$

$$Q_{jj}^{(1)} = \frac{\bar{q}_{x1}}{i} ;$$

$$A_{jj}^{(2)} = E_{jj}^{(2)} + F_{jj}^{(2)} + Q_{jj}^{(2)} ,$$

$$E_{jj}^{(2)} = \left(\frac{1+\nu_s}{2}\right)(-\bar{\alpha}) n \, \bar{\delta}_{jj} ,$$

$$F_{jj}^{(2)} = \frac{\Gamma_{i3}}{i} (n) \, \bar{\delta}_{jj} ,$$

$$Q_{jj}^{(2)} = \frac{\bar{q}_{x2}}{i} ;$$

$$A_{jj}^{(3)} = E_{jj}^{(3)} + F_{jj}^{(3)} + Q_{jj}^{(3)} ,$$

$$E_{jj}^{(3)} = \left\{ -\bar{\alpha}\,\nu_s + k_s \left[\left(\frac{1-\nu_s}{2}\right)(-n^2)(-\bar{\alpha}) - \bar{\alpha}^3 \right] \right\} \bar{\delta}_{jj} ,$$

$$F_{jj}^{(3)} = \frac{\Gamma_{i3}}{i} \bar{\delta}_{jj} - \bar{\alpha}\,\Gamma_{i4} \bar{b}_{jj} - \bar{\alpha}\,\Gamma_{i5} \bar{\delta}_{jj} ,$$

$$Q_{jj}^{(3)} = \frac{\bar{q}_{x3}}{i} ;$$

$$A_{jj}^{(4)} = E_{jj}^{(4)} + F_{jj}^{(4)} + Q_{jj}^{(4)} ,$$

$$E_{jj}^{(4)} = \frac{1+\nu_s}{2} (-n)\bar{\alpha} \, \bar{\delta}_{jj} ,$$

$$F_{jj}^{(4)} = 0 ,$$

$$Q_{jj}^{(4)} = \bar{q}_{\theta 1} ;$$

$$A_{jj}^{(5)} = E_{jj}^{(5)} + F_{jj}^{(5)} + Q_{jj}^{(5)} ,$$

$$E_{jj}^{(5)} = \left[-n^2 + (\frac{1-\nu_s}{2})(-\bar{\alpha}^2) \right] + k_s \left[\frac{3}{2} (1-\nu_s)(-\bar{\alpha}^2) + \Omega^2 \right] \bar{\delta}_{jj} ,$$

$$F_{jj}^{(2)} = -\bar{\alpha}^2 \Gamma_{i1} \bar{b}_{jj} + \Gamma_{i2}(-\bar{\alpha}^2) \bar{\delta}_{jj} - \Gamma_{i4} n^2 \bar{b}_{jj} - \Gamma_{i5} n^2 \bar{\delta}_{jj} ,$$

$$Q_{jj}^{(5)} = \bar{q}_{\theta 2} ;$$

$$A_{jj}^{(6)} = E_{jj}^{(6)} + F_{jj}^{(6)} + Q_{jj}^{(6)} ,$$

$$E_{jj}^{(6)} = k_s \left(-(\frac{3-\nu_s}{2})(-\bar{\alpha}^2) - n \right) \bar{\delta}_{jj} - n \bar{\delta}_{jj} ,$$

$$F_{jj}^{(6)} = - \Gamma_{i4} n \bar{b}_{jj} - \Gamma_{i5} n \bar{\delta}_{jj} ,$$

$$Q_{jj}^{(6)} = \bar{q}_{\theta 3} ;$$

$$A_{jj}^{(7)} = E_{jj}^{(7)} + F_{jj}^{(7)} + Q_{jj}^{(7)} ,$$

$$E_{jj}^{(7)} = \left\{ -\bar{\alpha} \nu_s + k_s \left[(\frac{1-\nu_s}{2}) \bar{\alpha} n^2 - \bar{\alpha}^3 \right] \right\} \bar{\delta}_{jj} ,$$

$$F_{jj}^{(7)} = - \Gamma_{i4} \bar{\alpha} \bar{b}_{jj} - \Gamma_{i5} \bar{\alpha} \bar{\delta}_{jj} ,$$

$$Q_{jj}^{(7)} = \bar{q}_{r1} ;$$

$$A_{jj}^{(8)} = E_{jj}^{(8)} + F_{jj}^{(8)} + Q_{jj}^{(8)} ,$$

$$E_{jj}^{(8)} = k_s (\frac{3-\nu_s}{2})(-\bar{\alpha}) n \bar{\delta}_{jj} - n \bar{\delta}_{jj} ,$$

$$F_{jj}^{(8)} = - \Gamma_{i4} n \bar{b}_{jj} - \Gamma_{i5} n \bar{\delta}_{jj} ,$$

$$Q_{jj}^{(8)} = \bar{q}_{r2} ;$$

$$A_{jj}^{(9)} = E_{jj}^{(9)} + F_{jj}^{(9)} + Q_{jj}^{(9)} ,$$

$$E_{jj}^{(9)} = \left[-1 + k_s (- \bar{\alpha}^4 - 2\bar{\alpha}^2 n^2 - (n^2 - 1)^2 + \Omega^2 \right] \bar{\delta}_{jj} ,$$

$$F_{jj}^{(9)} = - \bar{\alpha}^2 \Gamma_{i1} \bar{b}_{jj} + \Gamma_{i2} (-\bar{\alpha}^2) \bar{\delta}_{jj} - \Gamma_{i4} n^2 \bar{b}_{jj} - \Gamma_{i5} n^2 \bar{\delta}_{jj} ,$$

$$Q_{jj}^{(9)} = \bar{q}_{r3} ;$$

since we have only considered the first mode $j = 1$ then

$$\bar{\delta}_{jj} = \int_0^1 \sin^2 \bar{\alpha} \xi \, d\xi ,$$

and $$\bar{b}_{jj} = \int_0^1 \xi \sin^2 \bar{\alpha} \xi \, d\xi .$$

APPENDIX H

INVISCID FLOW THEORY

In this Appendix, the unsteady viscid forces are derived using two different methods.

H.1 FROM VISCOUS THEORY

It has been described in Chapters III and IV that the unsteady viscous forces reduce to inviscid forces by setting

$$\bar{\psi} = 0 \ , \quad \mu = 0 \ , \quad U(r) = U_c \tag{H.1}$$

where U_c is a constant velocity.

In this method, the frequency equation of the system is obtained by setting the determinant of the coefficient matrix [A] in equation (3.105) and (4.75) equal to zero; that is

$$\det\left[\,A\,\right] = 0 \ ,$$

where the elements of matrix [A] are given in Appendix G. This method requires an iteration technique to find the frequencies of the system.

H.2 POTENTIAL FLOW THEORY

In the inviscid theory, the pressure perturbation is the only unsteady force that can be derived using potential flow theory as in Ref. [48].

H.2.1 Derivation of the Pressure Perturbation

The flow velocity is expressed as follows:

$$V = \bar{U} + \bar{\nabla}\phi \ , \tag{H.2.1}$$

where $\bar{U}$ is the mean flow velocity and $\bar{\nabla}\phi$ is the velocity potential which describes the velocity perturbations.

Applying the continuity equation, we get

$$\nabla^2 \phi = 0 \ . \tag{H.2.2}$$

The pressure perturbation is derived using the unsteady Bernoulli equation and is given by

$$p'(x,\theta,r,t) = -\rho \left[\frac{\partial \phi}{\partial t} + U \frac{\partial \phi}{\partial x} \right] . \tag{H.2.3}$$

The above analysis is equally applicable for inner and annular flow.

H.2.2 Inner flow

The inner flow is denoted by putting a subscript i to equations (H.2.2) and (H.2.3), hence

$$\nabla^2 \phi_i = 0 \ , \tag{H.2.4}$$

$$p_i' = -\rho_i \left(\frac{\partial \phi_i}{\partial t} + U_i \frac{\partial \phi_i}{\partial x} \right) , \tag{H.2.5}$$

and the boundary condition is given by

$$\left. \frac{\partial \phi_i}{\partial r} \right|_{r=a_i} = \frac{\partial w}{\partial t} + U_i \frac{\partial w}{\partial x} \ . \tag{H.2.6}$$

H.2.3 Annular flow

The annular flow is denoted by a subscript o

$$\nabla^2 \phi_o = 0 \ , \tag{H.2.7}$$

$$p_o' = -\rho \left(\frac{\partial \phi_o}{\partial t} + U_o \frac{\partial \phi_o}{\partial x} \right) , \tag{H.2.8}$$

and the boundary condition is given by

$$\left. \frac{\partial \phi_o}{\partial r} \right|_{r=a_i} = \frac{\partial w}{\partial t} + U_o \frac{\partial w}{\partial x} \ , \tag{H.2.9}$$

$$\left. \frac{\partial \phi_o}{\partial r} \right|_{r=a_o} = 0 \ . \tag{H.2.10}$$

The two methods of solution described in Chapters III and IV are applied here next.

H.3 FOURIER TRANSFORM METHOD

The following analysis is applicable for a shell clamped or pinned at both ends.

ϕ_i, ϕ_o, p_i, ρ_o and w have been defined by equation (3.8) and (3.48), respectively. Following the same procedure as in Chapter III, we arrive at a final expression for the generalized forces in the radial direction

$$\bar{q}^{(3)}_{rkm} = \left(\Omega^2 \, \bar{q}^{(1)}_{rkm} + \Omega \, \bar{q}^{(2)}_{rkm} + \bar{q}^{(3)}_{rkm} \right) , \tag{H.3.1}$$

where $\bar{q}^{(1)}_{rkm}$, $\bar{q}^{(2)}_{rkm}$ and $\bar{q}^{(3)}_{rkm}$ are given in Ref. [48]. They are:

$$\bar{q}^{(1)}_{rkm} = \frac{\eta_i}{2\pi\varepsilon_i} \left[\int_{-\infty}^{\infty} E_n(\bar{\alpha}) \, H_{km}(\bar{\alpha}) \, d\bar{\alpha} - \rho_r \int_{-\infty}^{\infty} F_n(\bar{\alpha}) \, H_{km}(\bar{\alpha}) \, d\bar{\alpha} \right] , \tag{H.3.2}$$

$$\bar{q}^{(2)}_{rkm} = \frac{\eta}{\pi} \bar{U}_i \int_{-\infty}^{\infty} E_n(\bar{\alpha}) \, H_{km}(\bar{\alpha}) \, d\bar{\alpha} \tag{H.3.3}$$

$$- \frac{\eta}{\pi} \bar{U}_o \, \rho_r \int_{-\infty}^{\infty} E_n(\bar{\alpha}) \, H_{km}(\bar{\alpha}) \, d\bar{\alpha} ,$$

$$\bar{q}^{(3)}_{rkm} = \frac{\eta \, \varepsilon_i \bar{U}_i^2}{\pi} \int_{-\infty}^{\infty} \bar{\alpha} \, E_n(\bar{\alpha}) \, H_{km}(\bar{\alpha}) \, d\bar{\alpha} \tag{H.3.4}$$

$$- \frac{\eta \, \varepsilon_i \bar{U}_o^2}{\pi} \rho_r \int_{-\infty}^{\infty} \bar{\alpha} \, F_n(\bar{\alpha}) \, H_{km}(\bar{\alpha}) \, d\bar{\alpha} ,$$

where $$E_n(\bar{\alpha}) = \frac{I_n(\bar{\alpha}\varepsilon_i)}{I_n'(\bar{\alpha}\varepsilon_i)}$$

and $$F_n(\bar{\alpha}) = \frac{I_n'(\bar{\alpha}\varepsilon_o) \, K_n(\bar{\alpha}\varepsilon_i) - I_n(\bar{\alpha}\varepsilon_i) \, K_n'(\bar{\alpha}\varepsilon_o)}{I_n'(\bar{\alpha}\varepsilon_o) \, K_n'(\bar{\alpha}\varepsilon_i) - I_n'(\bar{\alpha}\varepsilon_i) \, K_n'(\bar{\alpha}\varepsilon_o)}$$

Having defined the unsteady forces, we can write the elements of matrices [K], [M] and [C] as in equation (3.110).

H.3.1 Matrix [K]

Elements of [K] are equal to corresponding elements of [A] with $F_{kmn}^{(\ell)} = Q_{kmn}^{(\ell)} = 0$, except for those specified below

$$K_{kmn}^{(1)} = E_{kmn}^{(1)} - \Omega^2 a_{km} ,$$

$$K_{kmn}^{(5)} = E_{kmn}^{(5)} - \Omega^2 \bar{\delta}_{km} ,$$

$$K_{kmn}^{(9)} = E_{kmn}^{(9)} - (\Omega^2 \bar{\delta}_{km} + \bar{q}_{rkm}^{(3)} ,$$

where $\bar{q}_{rkm}^{(3)}$ is given by equation (H.3.4) and a_{km}, $\bar{\delta}_{km}$ are given in Appendix C.

H.3.2 Matrix [M]

This is a (9×9) matrix. Its elements are equal to zero except for the following

$$M_{kmn}^{(1)} = a_{km} ,$$

$$M_{kmn}^{(5)} = \bar{\delta}_{km} ,$$

$$M_{kmn}^{(9)} = \bar{\delta}_{km} + \bar{q}_{rkm}^{(1)}$$

where $\bar{q}_{rkm}^{(1)}$ is given by equation (H.3.2).

H.3.3 Matrix [C]

This is again a (9×9) matrix with all elements equal to zero except for $C_{kmn}^{(9)}$ which is equal to $\bar{q}_{rkm}^{(2)}$, where $\bar{q}_{rkm}^{(2)}$ is given by equation (H.3.3).

H.4 TRAVELLING WAVE SOLUTION

To the author's knowledge, this is the first time a travelling wave solution is used in deriving the inviscid fluid forces in the annular flow case.

Following the same analysis as in Chapter IV, ϕ_i, ϕ_o, p_i', p_o' and w are defined as follows:

$$\phi_i(x,\theta,r,t) = \bar{\phi}_i(x,r) \cos n\theta \, e^{i(\omega t-kx)} \tag{H.4.1}$$

$$\phi_o(x,\theta,r,t) = \bar{\phi}_o(x,r) \cos n\theta \, e^{i(\omega t-kx)} \tag{H.4.2}$$

$$p_i'(x,\theta,r,t) = \bar{p}_i'(x,r) \cos n\theta \, e^{i(\omega t-kx)} \tag{H.4.3}$$

$$p_o'(x,\theta,r,t) = \bar{p}_o'(x,r) \cos n\theta \, e^{i(\omega t-kx)} \tag{H.4.4}$$

$$w(x,\theta,r,t) = C_n \cos n\theta \, e^{i(\omega t-kx)} \tag{H.4.5}$$

The solution for $\bar{\phi}_i$ and $\bar{\phi}_o$ have been expressed in terms of modified Bessel functions by equation (4.28) and (4.45), that is

$$\bar{\phi}_i(r) = I_n(kr) \, C_{1i} \, , \tag{H.4.6}$$

$$\bar{\phi}_o(r) = I_n(kr) \, C_{1o} + K_n(kr) \, C_{2o} \, . \tag{H.4.7}$$

H.4.1 Solution for the inner flow

Upon substituting for ϕ_i and p_i' from (H.4.1) and (H.4.3) into (H.2.5), we obtain

$$\bar{p}_i' = - \rho_i \left(i\omega \, \bar{\phi}_i - U_i(-ik)\bar{\phi}_i \right) . \tag{H.4.8}$$

Using the same non-dimensional terms as in Chapter IV

$$\omega = \frac{\Omega U}{a_i} \, , \quad k = \frac{\bar{\alpha}}{a_i} , \quad \bar{U}_i = \frac{U_i}{U} \, , \quad \bar{C}_{1i} = \frac{C_{1i}}{L} \, ,$$

equation (H.4.8) may be rewritten as:

$$\bar{p}_i' = -\frac{\rho_i U}{\varepsilon_i}\left(i\,(\Omega - \bar{\alpha}\,\bar{U}_i)\right) I_n(kr)\bar{C}_{1i} \; . \tag{H.4.9}$$

Substituting ϕ_i and w from equation (H.4.1) and (H.4.5) into equation (H.2.6), we get

$$\left.\frac{\partial\bar{\phi}_i}{\partial r}\right|_{r=a_i} = i(\omega - k\,U_i)C_n \; ; \tag{H.4.10}$$

substituting for $\bar{\phi}_i$ from (H.4.6) into (H.4.10), we can rewrite the latter in non-dimensional form as follows

$$\bar{\alpha}\, I_n'(kr)\, \bar{C}_{1i} = iU(\Omega - \bar{\alpha}\,\bar{U}_i)\bar{C}_n \; , \tag{H.4.10}$$

where

$$\bar{C}_n = \frac{C_n}{L} \; . \tag{H.4.11}$$

Finally, solving for $\bar{C}_{1i}$ from equation (H.4.10) and substituting the solution into (H.4.9), we get at $r=a_i$

$$\bar{p}_i' = \rho_i\frac{U^2}{\varepsilon_i}(\Omega^2 - 2\bar{\alpha}\,\bar{U}_i\,\Omega + \bar{\alpha}^2 U^2)\,\bar{E}_n(\bar{\alpha}) \; , \tag{H.4.12}$$

where $\quad \bar{E}_n(\bar{\alpha}) = \dfrac{I_n(\bar{\alpha})}{\bar{\alpha} I_n'(\bar{\alpha})} \; .$

<u>H.4.2 Solution for the annular flow</u>

Upon substituting for ϕ_o and p_o', from equations (H.4.2) and (H.4.4), into (H.2.8), (H.2.9), (H.2.10), we obtain

$$\bar{p}_o' = -\rho_o\,(i\omega - i\,k\,U_o)\bar{\phi}_o \; , \tag{H.4.13}$$

$$\left.\frac{\partial\phi_o}{\partial r}\right|_{r=a_i} = (i\omega - i\,k\,U_o)C_n \; , \tag{H.4.14}$$

$$\left.\frac{\partial \phi_o}{\partial r}\right|_{r=a_o} = 0 \quad . \tag{H.4.15}$$

Substituting for $\bar{\phi}_o$ from (H.4.7) into the above equations, and using the following non-dimensional terms:

$$\bar{U}_o = \frac{U_o}{u} \quad , \quad \rho_o = \rho_r \rho_i \ ,$$

equations (H.4.13), (H.4.14) and (H.4.15) may be written as

$$\bar{p}_o' = -\frac{\rho_r \rho_i u}{\epsilon_i} \left(i\Omega - i\bar{\alpha}\,\bar{U}_o \right) \left\{ I_n(kr)\bar{C}_{1o} + K_n(kr)\bar{C}_{2o} \right\} , \tag{H.4.16}$$

$$\bar{\alpha} \left[I_n'(\bar{\alpha})\bar{C}_{1o} + K_n'(\bar{\alpha})\bar{C}_{2o} \right] = u \left(i\Omega - i\bar{\alpha}\,\bar{U}_o \right) \bar{C}_n , \tag{H.4.17}$$

$$\bar{\alpha} \left[I_n'(\bar{\alpha}\epsilon_r)\bar{C}_{1o} + K_n'(\bar{\alpha}\epsilon_r)\bar{C}_{2o} \right] = 0 \ . \tag{H.4.18}$$

Solving for $\bar{C}_{1o}$ and $\bar{C}_{2o}$ from (H.4.17) and (H.4.18), we obtain

$$\bar{C}_{1o} = \frac{-i\ (\Omega - \bar{\alpha}\,\bar{U}_o)\bar{C}_n\ K_n'(\epsilon_r\bar{\alpha})}{\bar{\alpha}\,[K_n'(\bar{\alpha})\ I_n'(\bar{\alpha}\epsilon_r) - K_n'(\bar{\alpha}\epsilon_r)\ I_n'(\bar{\alpha})]} \ , \tag{H.4.19}$$

$$\bar{C}_{2o} = \frac{i\ (\Omega - \bar{\alpha}\,\bar{U}_o)\bar{C}_n\ I_n'(\epsilon_r\bar{\alpha})}{\bar{\alpha}\,[K_n'(\bar{\alpha})\ I_n'(\bar{\alpha}\epsilon_r) - K_n'(\bar{\alpha}\epsilon_r)\ I_n'(\bar{\alpha})]} \ . \tag{H.4.20}$$

Substituting for $\bar{C}_{1o}$ and $\bar{C}_{2o}$ into (H.4.12), the pressure perturbation $\bar{p}_o'$ evaluated at $r=a_i$

$$\left.\bar{p}_o'\right|_{r=a_i} = \frac{\rho_r \rho_i u^2}{\epsilon_i} \left(\Omega^2 - 2\bar{\alpha}\,\bar{U}_o\,\Omega + \bar{\alpha}^2\,\bar{U}_o^2 \right) \bar{F}_n(\bar{\alpha})\bar{C}_n \ , \tag{H.4.21}$$

where
$$\bar{F}_n(\bar{\alpha}) = \frac{K_n(\bar{\alpha})\ I_n'(\bar{\alpha}\varepsilon_r) - K_n'(\bar{\alpha}\varepsilon_r)\ I_n(\bar{\alpha})}{K_n'(\bar{\alpha})\ F_n'(\bar{\alpha}\varepsilon_r) - K_n'(\bar{\alpha}\varepsilon_r)\ I_n'(\bar{\alpha})} \tag{H.4.22}$$

H.4.3 Pressure Loading

The pressure load on the shell is defined by

$$q_{r3}\Big|_{r=a_i} = p_i'\Big|_{r=a_i} - p_o'\Big|_{r=a_i}, \tag{H.4.23}$$

where

$$q_{r3} = \bar{q}_{r3} \cos n\theta\ e^{i(\omega t - kx)}. \tag{H.4.24}$$

Hence,

$$\bar{q}_{r3} = \bar{p}_i'\Big|_{r=a_i} - \bar{p}_o'\Big|_{r=a_i}, \tag{H.4.24}$$

or

$$\bar{q}_{r3} = \rho_i U^2 \left[\Omega^2\ \bar{q}_{r3}^{(1)} + \Omega\ \bar{q}_{r3}^{(2)} + \bar{q}_{r3}^{(3)} \right], \tag{H.4.25}$$

$$\bar{q}_{r3}^{(1)} = \frac{1}{\varepsilon_i} \left[\frac{\bar{E}_n(\bar{\alpha})}{\bar{\alpha}} - \rho_r \frac{\bar{F}_n(\bar{\alpha})}{\bar{\alpha}} \right], \tag{H.4.26}$$

$$\bar{q}_{r3}^{(2)} = \frac{1}{\varepsilon_i} \left[2\ \bar{U}_o\ \rho_r\ \bar{F}_n(\bar{\alpha}) - 2\ \bar{U}_i\ \bar{E}_n(\bar{\alpha}) \right], \tag{H.4.27}$$

$$\bar{q}_{r3}^{(3)} = \frac{1}{\varepsilon_i} \left[\bar{\alpha}\ \bar{U}_i^2\ \bar{E}_n(\bar{\alpha}) - \bar{\alpha}\ \bar{U}_o\ \rho_r\ \bar{F}_n(\bar{\alpha}) \right]. \tag{H.4.28}$$

The amplitude of the generalized force as defined in equation (4.68) is given by

$$\bar{\bar{q}}_{r3} = \frac{\gamma}{\rho_s h} \int_o^L \sin \frac{j\pi x}{L}\ \bar{q}_{r3}\ e^{-ikx} dx \tag{H.4.29}$$

Non-dimensionally

$$\bar{q}_{r3} = \left[\Omega^2 \, \bar{q}_{r3}^{(1)} + \Omega \, \bar{q}_r^{(2)} + \bar{q}_r^{(3)} \right] , \tag{H.4.30}$$

where

$$\bar{q}_{r3}^{(1)} = \varepsilon_i \eta \, \bar{q}_{r3}^{(1)} \, \bar{\delta}_{jj} \tag{H.4.31}$$

$$\bar{q}_{r3}^{(2)} = \varepsilon_i \eta \, \bar{q}_{r3}^{(2)} \, \bar{\delta}_{jj} \tag{H.4.32}$$

$$\bar{q}_{r3}^{(3)} = \varepsilon_i \eta \, \bar{q}_{r3}^{(3)} \, \bar{\delta}_{jj} \tag{H.4.33}$$

where

$$\bar{\delta}_{jj} = \bar{\delta}_{11} = \int_0^L \sin^2 \frac{\pi x}{L} \, dx \quad \text{for } j = 1 . \tag{H.4.34}$$

We can now write the elements of matrix [K], [M] and [C].

H.4.4.7 Matrix [K]

Elements of [K] are equal to corresponding elements of [A] with $F_{jj}^{(\ell)} = Q_{jj}^{(\ell)} = 0$, except for those specified in the following matrix

$$\left[K \right] = \begin{bmatrix} K_{jj}^{(1)} & & \\ & K_{jj}^{(5)} & \\ & & K_{jj}^{(9)} \end{bmatrix}$$

which are given by

$$K_{jj}^{(1)} = E_{jj}^{(1)} - \Omega^2 \, \bar{\delta}_{jj} ,$$

$$K_{jj}^{(5)} = E_{jj}^{(5)} - \Omega^2 \, \bar{\delta}_{jj} ,$$

$$K_{jj}^{(9)} = E_{jj}^{(9)} - \Omega^2 \, \bar{\delta}_{jj} + \bar{q}_{r3}^{(3)} ,$$

where $\bar{q}_{r3}^{(3)}$ is given by (H.4.33) and $\bar{\delta}_{jj}$ is given by (H.4.34)

H.4.5 Matrix [M]

The structure of matrix [M] is given below

$$\begin{bmatrix} M_{jj}^{(1)} & 0 & 0 \\ 0 & M_{jj}^{(5)} & 0 \\ 0 & 0 & M_{jj}^{(9)} \end{bmatrix}$$

where

$$M_{jj}^{(1)} = \bar{\delta}_{jj} \ ,$$

$$M_{jj}^{(5)} = \bar{\delta}_{jj} \ ,$$

$$M_{jj}^{(9)} = \bar{\delta}_{jj} + \bar{q}_{r3}^{(1)} \ ,$$

where $\bar{q}_{r3}^{(1)}$ is given by (H.4.31).

I.4.6 Matrix [C]

The structure of matrix [C] is given as

$$\begin{bmatrix} 0 & 0 & 0 \\ 0 & 0 & 0 \\ 0 & 0 & C_{jj}^{(9)} \end{bmatrix}$$

where $C_{11}^{(9)} = \bar{q}_{r3}^{(2)}$.

APPENDIX I

COMPUTER PROGRAM FOR CALCULATING THE INTEGRALS IN THE UNSTEADY INVISCID FORCES

This program evaluates the integrals with unsteady inviscid forces. The program is originally developed in Ref. [48] for the clamped-clamped case. In this Appendix, the program for pinned-pinned shell is presented here.

Program Structure

MAIN PROGRAM

COMPLEX FUNCTION IN

COMPLEX FUNCTION KN

DOUBLE PRECISION FUNCTION R

DOUBLE PRECISION FUNCTION F

DOUBLE PRECISION FUNCTION FA

```
C***********************************************************************
C     COMPUTER PROGRAM FOR CALCULATING THE INTEGRALS IN THE GENERALIZED*
C     FLUID  FORCES
C     PINNED PINNED SHELL
C***********************************************************************
C
C***********************************************************************
C     MAIN PROGRAM                                                     *
C***********************************************************************
      IMPLICIT COMPLEX*16(A-Z)
      REAL*8 C(3),P(3),PI,GAMA,EI,EO,X1,X2,D
      INTEGER N,K,M,I
      COMMON PI,GAMA
      COMMON/DATA1/C,P
      INP(Y)=N*IN(Y,N)/Y+IN(Y,N+1)
      KNP(Y)=N*KN(Y,N)/Y-KN(Y,N+1)
      PI=3.14159265358979D0
      GAMA=0.5772156649011618D0
      P(1)=3.1416D0
      P(2)=6.2832D0
      P(3)=9.42D0
      EI=.099D0
      EO=1.D0/10.D0
      N=3
      D=2.D0
      DO 2 K=1,3
      DO 2 M=1,3
      X1=-50.D0+D/2*(1-DSQRT(1/3.D0))
      X2=-50.D0+D/2*(1+DSQRT(1/3.D0))
      Q1=(0.D0,0.D0)
      Q2=Q1
      Q3=Q2
      Q4=Q3
      Q5=Q4
      Q6=Q5
      DO 1 I=1,98
      EIX=X1*EI
      EOX=X1*EO
      INIX=IN(EIX,N)
      INOX=IN(EOX,N)
      KNIX=KN(EIX,N)
      KNOX=KN(EOX,N)
      INPIX=INP(EIX)
      INPOX=INP(EOX)
      KNPIX=KNP(EIX)
      KNPOX=KNP(EOX)
      DEM=INPOX*KNPIX-INPIX*KNPOX
      EN=INIX/INPIX
      FN=(INPOX*KNIX-INIX*KNPOX)/DEM
C
       II=(0.D0,1.0D0)
         F1=CDEXP(-II*X1)
         F2=CDEXP(II*X1)
          HKM=(F1*(-1)**(K)-1)*(F2*(-1)**(M)-1)*M*K*PI**2/(-X1**2+
     &M**2*PI**2)/(-X1**2+K**2*PI**2)
      QG1=EN*HKM
      QG2=FN*HKM
      Q1=Q1+QG1/X1
```

```
      Q2=Q2+QG2/X1
      Q3=Q3+QG1*X1
      Q4=Q4+QG2*X1
      Q5=Q5+QG1
      Q6=Q6+QG2
      X1=X1+D
      IF(I.EQ.49) X1=X2
    1 CONTINUE
      PRINT10,N,K,M
   10 FORMAT('-','N=',I1,' K=',I1,' M=',I1)
      PRINT11,Q1
      PRINT12,Q2
      PRINT13,Q3
      PRINT14,Q4
      PRINT15,Q5
      PRINT16,Q6
    2 CONTINUE
      PRINT40
   11 FORMAT('0','Q1=(',2D24.16,1X,')')
   12 FORMAT('0','Q2=(',2D24.16,1X,')')
   13 FORMAT('0','Q3=(',2D24.16,1X,')')
   14 FORMAT('0','Q4=(',2D24.16,1X,')')
   15 FORMAT('0','Q5=(',2D24.16,1X,')')
   16 FORMAT('0','Q6=(',2D24.16,1X,')')
   40 FORMAT('1')
      STOP
      END
C
C***********************************************************************
C     COMPLEX FUNCTION H                                              *
C***********************************************************************
      COMPLEX FUNCTION H*16(AB,K,M)
      IMPLICIT COMPLEX*16(A-Z)
      REAL*8 AB,C(3),P(3),AB1
      INTEGER K,M,J,M1
      COMMON/DATA1/C,P
      H=(1.D0,0.D0)
      I=(0.D0,1.D0)
      AB1=AB
      M1=M
      DO 1 J=1,2
      IF(DABS(AB).EQ.M1) GO TO 10
      A=2*C(M1)*P(M1)**3
      B=I*2*P(M1)**2
      E1=(-1)**(M1+1)*CDEXP(I*AB1)+1
      E2=E1-2
      IM=(A*E1-B*AB1*E2)/(AB1**4-P(M1)**4)
      GO TO 11
   10 IF(J.EQ.2) GO TO 20
      IM=((I*C(M1)*P(M1)**3-I*P(M1)**2+AB*P(M1)**2)*(-1)**(M1+1)*
     #CDEXP(I*AB)+I*P(M1)**2)/(-2*AB**3)
      GO TO 11
   20 IM=((-I*C(M1)*P(M1)**3+I*P(M1)**2+AB*P(M1)**2)*(-1)**(M1+1)*
     #CDEXP(-I*AB)-I*2*P(M1)**2)/(-2*AB**3)
   11 H=H*IM
      M1=K
      AB1=-AB
    1 CONTINUE
```

```
      RETURN
      END
C
C*************************************************************************
C     SUBPROGRAMS FOR CALCULATING THE BESSEL FUNCTIONS                  *
C*************************************************************************
      COMPLEX FUNCTION IN*16(X,N)
      IMPLICIT REAL*8(A-Z)
      COMPLEX*16 W,X,Y,Z,T,T1,T2,T3,T4,I,DCMPLX,DCONJG
      INTEGER K,N
      COMMON PI,GAMA
      I=(0.D0,1.D0)
      IF(CDABS(X).GE.20.D0) GO TO 10
      IN=(0.D0,0.D0)
      K=0
   11 T=(X/2)**(2*K)/FA(K)/FA(N+K)
      IF(CDABS(T).LT.1.D-12) GO TO 12
      IN=IN+T
      K=K+1
      GO TO 11
   12 IN=(X/2)**N*IN
      RETURN
   10 T1=(4*N**2-1)/8/X
      T2=T1*(4*N**2-9)/16/X
      T3=CDEXP(X)/CDSQRT(2*PI*X)
      T4=CDEXP(-X)/CDSQRT(2*PI*X)
      Y=X-DCONJG(X)
      Z=DCMPLX(0.D0,CDABS(Y))
      W=Y+Z
      IF(CDABS(Y).EQ.0.D0) GO TO 14
      IF(CDABS(W).EQ.0.D0) GO TO 13
   14 IN=T3*(1-T1+T2)+(-1)**N*I*T4*(1+T1+T2)
      RETURN
   13 IN=T3*(1-T1+T2)+(-1)**(N+1)*I*T4*(1+T1+T2)
      RETURN
      END
C
      COMPLEX FUNCTION KN*16(X,N)
      IMPLICIT REAL*8(A-Z)
      COMPLEX*16 X,KN1,T,T1,T2,T3
      INTEGER N,M,K,I
      COMMON PI,GAMA
      IF(CDABS(X).GE.15.D0) GO TO 40
      IF(N.EQ.0) GO TO 46
      KN=FA(N-1)*(2/X)**N
      IF(N.EQ.1) GO TO 45
      M=N-1
      DO 41 I=1,M
   41 KN=KN+(-1)**I*FA(N-I-1)/FA(I)*(2/X)**(N-2*I)
   45 KN=KN/2
      GO TO 47
   46 KN=(0.D0,0.D0)
   47 KN1=(0.D0,0.D0)
      K=0
   43 T=(X/2)**(N+2*K)/FA(K)/FA(N+K)*(CDLOG(X/2)-(F(K+1)+F(N+K+1))/2)
      IF(CDABS(T).LT.1.D-12) GO TO 42
      KN1=KN1+T
      K=K+1
```

```
      GO TO 43
42    KN=KN+KN1*(-1)**(N+1)
      RETURN
40    T1=(4*N**2-1)/8/X
      T2=T1*(4*N**2-9)/16/X
      T3=CDEXP(-X)*CDSQRT(PI/2/X)
      KN=T3*(1+T1+T2)
      RETURN
      END
C
      DOUBLE PRECISION FUNCTION R(K)
      IMPLICIT REAL*8(A-Z)
      INTEGER K,I
      R=0.D0
      DO 40 I=1,K
40    R=R+1.D0/I
      RETURN
      END
C
      DOUBLE PRECISION FUNCTION F(K)
      IMPLICIT REAL*8(A-Z)
      INTEGER K
      COMMON PI,GAMA
      IF(K.EQ.1) GO TO 50
      F=R(K-1)-GAMA
      RETURN
50    F=-GAMA
      RETURN
      END
C
      DOUBLE PRECISION FUNCTION FA(K)
      IMPLICIT REAL*8(A-Z)
      INTEGER K,L
      FA=1.D0
      L=1
21    FA=FA*L
      IF(L.GE.K) GO TO 22
      L=L+1
      GO TO 21
22    CONTINUE
      RETURN
      END
```

APPENDIX J

COMPUTER PROGRAM FOR INVISCID THEORY USING FOURIER TRANSFORM METHOD

The program calculates the dimensionless frequency Ω for each flow velocity, the flow could be internal or annular. The program is originally developed in Ref. [48] for the clamped-clamped case and modified here for the pinned-pinned case.

Program Structure

MAIN PROGRAM

SUBROUTINE MKMAT

SUBROUTINE CMAT

SUBROUTINE REDUCE

SUBROUTINE EIGZC

```
C**********************************************************************
C     COMPUTER PROGRAM FOR THE CASE OF STEADY VISCOUS FORCES AND
C     UNSTEADY INVISCID FORCES                                         *
C                           PIN-PIN                                    *
C**********************************************************************
C
C**********************************************************************
C     MAIN PROGRAM                                                     *
C**********************************************************************
      IMPLICIT REAL*8(A-H,O-Z)
      COMPLEX*16 MM(9,9),KK(9,9),CC(9,9),AA(18,18)/324*(0.D0,0.D0)/,
     #BB(18,18)/324*(0.D0,0.D0)/,EIGA(18),EIGB(18),Z(18,18),WK(18,36),
     #OMEGA,Q1(3,3),Q2(3,3),Q3(3,3),Q4(3,3),Q5(3,3),Q6(3,3)
      REAL*8 NU
      COMMON/DATA1/NU,SK,EI,EO,ER,C(3),P(3),N
      COMMON/DATA2/ZI,DR,PI
      COMMON/DATA3/Q1,Q2
      COMMON/DATA4/Q3,Q4
      COMMON/DATA5/Q5,Q6
      COMMON/DATA6/PPI,PPO,PO,PL,RMS,DEN,DDI,VIS
      DATA IA/18/,IB/18/,NN/18/,IJOB/2/,IZ/18/
      PI=DARCOS(-1.D0)
      P(1)=3.1416D0
      P(2)=6.2632D0
      P(3)=9.42D0
      EI=1/11.D0
      EO=0.1D0
      ER=10/11.D0
      RMS=(1-ER**2)/2/DLOG(1/ER)
      NU=0.30D0
      SK=(5.50D-3)**2/12
      ZI=2.330D1
      DR=1.D0
      N=3
      DEN=998.6D0
      DDI=8.261D-7
      VIS=1.1216D-6
      DO 3 K=1,3
      DO 3 M=1,3
      READ(5,*) Q1(K,M),Q2(K,M),Q3(K,M),Q4(K,M),Q5(K,M),Q6(K,M)
    3 CONTINUE
      CALL CONT(C,P)
      CALL PREMAT(MM,KK)
      UO=(0.0D0,0.D0)
      UI=0.0395D0
      CALL MKMAT(UI,UO,MM,KK)
      CALL CMAT(UI,UO,CC)
      CALL REDUCE(MM,KK,CC,AA,BB)
      CALL EIGZC(AA,IA,BB,IB,NN,IJOB,EIGA,EIGB,Z,IZ,WK,INFER,IER)
      PRINT10,UI,UO
   10 FORMAT('1','FLOW VELOCITY INSIDE THE INNER CYLINDER=',F8.5/'0','FL
     #OW VELOCITY IN THE ANNULAR REGION=',F8.5)
      PRINT13,PPO
   13 FORMAT('-','GAUGE PRESSURE AT THE UPSTREAM END OF THE CYLINDERS IN
     # THE ANNULAR FLUID REGION=',D24.16,' N/M**2')
      PRINT14,PPI
   14 FORMAT('0',52X,'IN THE INNER FLUID REGION=',D24.16,' N/M**2')
      PRINT15,PO,PL
```

```
  15  FORMAT('-','AXIAL COMPRESSIVE LOAD ACTING ON THE X=0 END OF THE IN
     #NER CYLINDER=',D24.16,' N/M'/'0',37X,'X=L END',22X,'=',D24.16,' N/
     #M')
      PRINT11
  11  FORMAT('-','THE FREQUENCIES ARE:')
      DO 20 I=1,18
      OMEGA=-EIGA(I)/EIGB(I)
  20  PRINT12,OMEGA
  12  FORMAT('0','(',2D24.16,1X,')')
  1   CONTINUE
      PRINT100
  100 FORMAT('1')
      STOP
      END
C
C***********************************************************************
C     SUBROUTINE CONT                                                  *
C***********************************************************************
      SUBROUTINE CONT(C,P)
      IMPLICIT REAL*8(A-H,O-Z)
      DIMENSION A(3,3),B(3,3),C(3),D(3,3),SE(3,3),SF(3,3),G(3,3),H(3,3),
     #SJ(3,3),SL(3,3),DEL(3,3),P(3)
      INTEGER KL,K,M
      COMMON/CON1/A,B,D,DEL
      COMMON/CON2/SE,SF,G,H,SJ,SL
       PI=3.1416D0
      DO 3 K=1,3
      DO 3 M=1,3
      IF(K.EQ.M) GO TO 1
C     PC=P(M)*C(M)-P(K)*C(K)
      KL=K+M
       IF(MOD(KL,2).EQ.0) GO TO 40
      A(K,M)=0.D0
      B(K,M)=0.D0
      D(K,M)=-A(K,M)
      SE(K,M)=K*M**3*PI**2*2*(K**2+M**2)/(K**2-M**2)**2
      SF(K,M)=-2*K*M/(K**2-M**2)
      G(K,M)=-K*M*2*(K**2+M**2)/(K**2-M**2)**2
      H(K,M)=4*K*M**3/(K**2-M**2)**2
      SJ(K,M)=-4*K*M/(K**2-M**2)**2/PI**2
      DEL(K,M)=0.D0
      GO TO 3
 40       A(K,M)=0.D0
          B(K,M)=0.D0
          D(K,M)=0.D0
          SE(K,M)=0.D0
          SF(K,M)=0.D0
          G(K,M)=0.D0
          H(K,M)=0.D0
          SJ(K,M)=0.D0
          DEL(K,M)=0.D0
          GO TO 3
  1   A(K,K)=P(K)**2/2
      B(K,K)=-P(K)**4/2
      D(K,K)=-A(K,K)
      SE(K,K)=B(K,K)/2
      SF(K,K)=0.D0
      G(K,K)=A(K,K)/2
```

```
      H(K,K)=-G(K,K)
      SJ(K,K)=0.25D0
      DEL(K,K)=.5D0
    3 CONTINUE
        DO 60 K=1,3
        DO 60 M=1,3
          WRITE(6,61) SE(K,M)
   61       FORMAT('0',F10.4)
   60     CONTINUE
      RETURN
      END
C
C*****************************************************************************
C     SUBROUTINE PREMAT                                                       *
C*****************************************************************************
      SUBROUTINE PREMAT(MM,KK)
      IMPLICIT REAL*8(A-H,O-Z)
      DIMENSION A(3,3),B(3,3),D(3,3),DEL(3,3),COEM(3,3,3),COE(9,3,3)
      COMPLEX*16 MM(9,9),KK(9,9),Q1(3,3),Q2(3,3)
      REAL*8 NU
      INTEGER H
      COMMON/DATA1/NU,SK,EI,EO,ER,C(3),P(3),N
      COMMON/DATA2/ZI,DR,PI
      COMMON/DATA3/Q1,Q2
      COMMON/CON1/A,B,D,DEL
      COMMON/COEF/COE
      DO 9 I=1,9
      DO 9 J=1,9
      MM(I,J)=(0.D0,0.D0)
    9 KK(I,J)=(0.D0,0.D0)
      C1=ZI/2/PI/EI
      C2=C1*DR
      DO 3 K=1,3
      DO 3 M=1,3
      COEM(1,K,M)=A(K,M)
      COEM(2,K,M)=DEL(K,M)
    3 COEM(3,K,M)=DEL(K,M)+C1*Q1(K,M)-C2*Q2(K,M)
      DO 4 K=1,3
      DO 4 M=1,3
      COE(1,K,M)=(EI**2*B(K,M)+(NU-1)*(SK+1)*N**2*A(K,M)/2)
      COE(2,K,M)=-(1+NU)*N*EI**2*D(K,M)/2
      COE(3,K,M)=(P(M)*EI)**4*SK*DEL(K,M)-(2*NU-SK*(1-NU)*N**2)
     C*EI**2*D(K,M)/2
      COE(4,K,M)=((1+NU)*N*A(K,M)/2)
      COE(5,K,M)=-N**2*DEL(K,M)+(1+3*SK)*(1-NU)*EI**2*D(K,M)/2
      COE(6,K,M)=SK*(3-NU)*N*EI**2*D(K,M)/2-N*DEL(K,M)
      COE(7,K,M)=((NU+(NU-1)*SK*N**2/2)*A(K,M)-SK*EI**2*B(K,M))
      COE(8,K,M)=-N*DEL(K,M)+(3-NU)*SK*N*EI**2*D(K,M)/2
    4 COE(9,K,M)=-SK*(((P(M)*EI)**4+(N**2-1)**2)*DEL(K,M)-2*(N*EI)
     #**2*D(K,M))-DEL(K,M)
      K=0
      DO 5 I=1,7,3
      K=K+1
      DO 5 M=1,3
      DO 5 L=1,3
      H=L-1
      MM(I+H,M+3*H)=COEM(L,K,M)
    5 CONTINUE
```

```
      RETURN
      END
C
C ***********************************************************************
C     SUBROUTINE MKMAT                                                  *
C***********************************************************************
      SUBROUTINE MKMAT(UI,UO,MM,KK)
      IMPLICIT REAL*8(A-H,O-Z)
      COMPLEX*16 MM(9,9),KK(9,9),Q3(3,3),Q4(3,3),CCOE(9,3,3)
      INTEGER W,V,HH
      REAL*8 NU
      DIMENSION A(3,3),B(3,3),D(3,3),SE(3,3),SF(3,3),G(3,3),H(3,3),
     #SJ(3,3),SL(3,3),COE(9,3,3),DEL(3,3)
      COMMON/DATA1/NU,SK,EI,EO,ER,C(3),P(3),N
      COMMON/DATA2/ZI,DR,PI
      COMMON/DATA4/Q3,Q4
      COMMON/DATA6/PPI,PPO,PO,PL,RMS,DEN,DDI,VIS
      COMMON/CON1/A,B,D,DEL
      COMMON/CON2/SE,SF,G,H,SJ,SL
      COMMON/COEF/COE
      FA(RR,RE)=DSQRT(0.0055*(1+(20000*RR+1.D6/RE)**(1./3.)))
      F(RR,RE)=1/(-4*DLOG10(RR/3.7+2.51/RE/FA(RR,RE)))**2
      SU=5.3082D3
      UOM=UO*SU
      UIM=UI*SU
      RR=0.D0
      RO=UOM*2*(EO-EI)/VIS
      RI=UIM*2*EI/VIS
      IF(RI.EQ.0.D0) GO TO 10
      FI=F(RR,RI)
      GO TO 11
   10 FI=0.D0
   11 IF(RO.EQ.0.D0) GO TO 12
      FO=F(RR,RO)
      GO TO 13
   12 FO=0.D0
   13 PPI=DEN*FI*UIM**2/EI
      PPO=DEN*FO*UOM**2/(EO-EI)
      UTBS=(1-RMS)/2/(1-ER)*FO*UOM**2
      UTAS=(RMS-ER**2)/2/ER/(1-ER)*FO*UOM**2
      UTS=FI*UIM**2/2
      BB=UTS+UTAS
      CC=2*UTS/EI-2*UTBS/EO/(1-RMS)
      DD=(PPO-PPI)/DEN
      GM1=-BB*DDI/EI
      GM2=-(NU*CC*DDI+GM1)/2-NU*DD*DDI
      GM3=BB*DDI
      GM4=-CC*DDI
      GM5=-DD*DDI
      C3=UI**2*ZI*EI/2/PI
      C4=UO**2*ZI*EI*DR/2/PI
      PO=((NU*EI*CC-BB)/2+NU*EI*DD)*DEN
      PL=((NU*EI*CC+BB)/2+NU*EI*DD)*DEN
      DO 4 K=1,3
      DO 4 M=1,3
      CCOE(1,K,M)=COE(1,K,M)+GM1*EI**2*SE(K,M)+GM2*EI**2*B(K,M)-GM4*N**
     #2*G(K,M)-GM5*N**2*A(K,M)
      CCOE(2,K,M)=COE(2,K,M)
```

```
      CCOE(3,K,M)=COE(3,K,M)+GM4*EI**2*H(K,M)+GM5*EI**2*D(K,M)
      CCOE(4,K,M)=COE(4,K,M)+GM3*N/EI*SF(K,M)
      CCOE(5,K,M)=COE(5,K,M)+GM1*EI**2*H(K,M)+GM2*EI**2*D(K,M)-GM4*N**
     #2*SJ(K,M)-GM5*N**2*DEL(K,M)
      CCOE(6,K,M)=COE(6,K,M)-GM4*N*SJ(K,M)-GM5*N*DEL(K,M)
      CCOE(7,K,M)=COE(7,K,M)+GM3/EI*SF(K,M)-GM4*G(K,M)-GM5*A(K,M)
      CCOE(8,K,M)=COE(8,K,M)-GM4*N*SJ(K,M)-GM5*N*DEL(K,M)
    4 CCOE(9,K,M)=COE(9,K,M)+GM1*EI**2*H(K,M)+GM2*EI**2*D(K,M)-GM4*N**2*
     #SJ(K,M)-GM5*N**2*DEL(K,M)+C3*Q3(K,M)-C4*Q4(K,M)
      K=0
      DO 5 I=1,7,3
      K=K+1
      DO 5 M=1,3
      W=-1
      DO 5 V=1,7,3
      W=W+1
      DO 5 L=1,3
      HH=L-1
      KK(I+HH,M+V-1)=CCOE(L+3*W,K,M)
    5 CONTINUE
      CCL=GM1*EI**2*H(1,1)+GM2*EI**2*D(1,1)-GM4*N**2*
     #SJ(1,1)-GM5*N**2*DEL(1,1)
        WRITE(6,55) CCL
   55   FORMAT('0',D11.4)
      RETURN
      END
C
C***********************************************************************
C     SUBROUTINE CMAT                                                  *
C***********************************************************************
      SUBROUTINE CMAT(UI,UO,CC)
      IMPLICIT REAL*8 (A-H,O-Z)
      COMPLEX*16 CC(9,9),Q5,Q6
      COMMON/DATA2/ZI,DR,PI
      COMMON/DATA5/Q5(3,3),Q6(3,3)
      DO 2 I=1,9
      DO 2 J=1,9
    2 CC(I,J)=(0.D0,0.D0)
      C5=UI*ZI/PI
      C6=UO*ZI*DR/PI
      DO 1 K=1,3
      DO 1 M=1,3
      CC(3*K,6+M)=-C5*Q5(K,M)+C6*Q6(K,M)
    1 CONTINUE
      RETURN
      END
C
C***********************************************************************
C     SUBROUTINE REDUCE                                                *
C***********************************************************************
      SUBROUTINE REDUCE(MM,KK,CC,AA,BB)
      COMPLEX*16 AA(18,18),BB(18,18),MM(9,9),KK(9,9),CC(9,9)
      DO 1 I=1,9
      AA(I,I+9)=(1.D0,0.D0)
      BB(I,I)=(-1.D0,0.D0)
    1 CONTINUE
      DO 2 I=1,9
      DO 2 J=1,9
```

```
      AA(9+I,J)=KK(I,J)
      AA(9+I,9+J)=CC(I,J)
      BB(9+I,9+J)=MM(I,J)
    2 CONTINUE
      RETURN
      END
//GO.SYSIN DD *
(0.9488942682409000D-01,0.0000000000000000D+00)
(-0.3388882646536831D+00,0.2530009449472896D-14)
(0.8963660194668257D+00,0.0000000000000000D+00)
(-0.3125736140399624D+01,0.3654727955866147D-11)
(-0.7510231870242804D-05,0.0000000000000000D+00)
(0.1405221268812409D-04,-0.9186404257521180D-13)
(-0.1562600697365384D-18,-0.2042373375506055D-06)
(-0.8547107142611914D-15,0.3839032126031192D-06)
(-0.2026874670384583D-17,-0.4874609543353414D-03)
(-0.1677557461862756D-11,0.9161303960358518D-03)
(0.2980415091981127D-18,-0.2517401932134774D+00)
(0.2998648803911531D-13,0.8905105289948569D+00)
(0.3380570860220098D-04,0.0000000000000000D+00)
(-0.5671535404586738D-03,0.6789390407096391D-14)
(-0.1174624146655580D+00,0.0000000000000000D+00)
(0.6064926740006390D+00,0.1149235066738984D-10)
(-0.2329329050940974D-04,0.0000000000000000D+00)
(0.4358372896014636D-04,-0.2831139353028704D-12)
(-0.1562600697365384D-18,0.2042373375515842D-06)
(0.8558348092392442D-15,-0.3839032126048518D-06)
(-0.2026874670384583D-17,0.4874609543353422D-03)
(0.1677560751174119D-11,-0.9161303960358665D-03)
(0.2980415091981125D-18,0.2517401932134774D+00)
(-0.2998862526071301D-13,-0.8905105289948569D+00)
(0.9397415820746215D-01,0.0000000000000000D+00)
(-0.3299706561406452D+00,-0.3428192176519597D-14)
(0.3551985421936918D+01,0.0000000000000000D+00)
(-0.1217679965761827D+02,-0.8219501584326605D-11)
(-0.1932193425764670D-04,0.0000000000000000D+00)
(0.3643946515632464D-04,0.1811084324637418D-12)
(0.1645526999083061D-18,0.6337767299870169D-06)
(0.5055735053178416D-15,-0.1191311275914592D-05)
(0.1316268166584047D-16,0.1512631768261931D-02)
(0.5052250294961182D-11,-0.2842844208701724D-02)
(0.1872529253174458D-17,-0.4471872546438655D+00)
(-0.7893170320271388D-13,0.1545004117643541D+01)
(0.3380570860220076D-04,0.0000000000000000D+00)
(-0.5671535404586774D-03,0.6789390407096391D-14)
(-0.1174624146655580D+00,0.0000000000000000D+00)
(0.6064926740006390D+00,0.1149235066738984D-10)
(-0.2329329050941151D-04,0.0000000000000000D+00)
(0.4358372896014987D-04,-0.2831139353028704D-12)
(0.1645526999083062D-18,-0.6337767299880196D-06)
(-0.5066702456320618D-15,0.1191311275920182D-05)
(0.1316268166584047D-16,-0.1512631768261992D-02)
(-0.5052371129682607D-11,0.2842844208701988D-02)
(0.1872529253174458D-17,0.4471872546438655D+00)
(0.7891892788411455D-13,-0.1545004117643541D+01)
(0.9249605669901730D-01,0.0000000000000000D+00)
(-0.3161251213563608D+00,0.2208347268234370D-13)
(0.7862707203612402D+01,0.0000000000000000D+00)
```

```
(-0.2624399823606381D+02,0.3623762246243465D-10)
(-0.7224513115367823D-04,0.0000000000000000D+00)
(0.1351774657193256D-03,-0.8943857238535201D-12)
//
```

APPENDIX K

COMPUTER PROGRAM FOR INVISCID THEORY USING TRAVELLING-WAVE SOLUTION

This program calculates the dimensionless frequency Ω for each flow velocity. The flow could be internal or annular. Steady viscous and unsteady inviscid forces are considered.

Program Structure

MAIN PROGRAM

SUBROUTINE PREMAT

SUBROUTINE UNSFO

SUBROUTINE STFOR

SUBROUTINE MATRIX

COMPLEX FUNCTION IN

COMPLEX FUNCTION HN

DOUBLE PRECISION F

DOUBLE PRECISION FA

DOUBLE PRECISION R

```
C*********************************************************************
C     COMPUTER PROGRAM FOR THE CASE OF STEADY VISCOUS FORCES AND     *
C     UNSTEADY INVISCID FORCES USING TRAVELLING-WAVES SOLUTION       *
C
C*********************************************************************
C
C*********************************************************************
C     MAIN PROGRAM                                                   *
C*********************************************************************
      IMPLICIT REAL*8(A-H,O-Z)
       COMPLEX*16 MM(3,3),
     &KK(3,3),CC(3,3),AA(6,6),BB(6,6),EIGA(6),EIGB(6),Z(6,6),WK(6,12),
     &OMEGA
     #,FS,UO,MIL,COE(2,9),CCO2(2,9)
      INTEGER INFER(3),MS,N
        EXTERNAL FS
      REAL*8 NI,NO,UI
      COMMON/DATA1/NI,NO,SKI,SKO,CIG(3),P(3),N
      COMMON/DATA2/EI,EO,ER,HR,URR
      COMMON/DATA3/ZI,ZO,USR,DSR
      COMMON/DATA7/UI,UO
      COMMON/AREA1/AAA
      COMMON/DATA5/PPI,PPO,PO(2),PL(2),RMS,DEN,DDI,DDO,VIS,CA,CB
      DATA EPS/1.D-10/,NSIG/5/,NGUESS/1/,ITMAX/10/,II/1/
      DATA IA/6/,IB/6/,NN/6/,IJOB/0/,IZ/6/
      COMMON/COCE/COE
      COMMON/CCCE/CCOE
      COMMON/CLLE/QTRI,QTRI2,QTRI3
C ---------------------------------
C      DATAS REQUIRED FOR SHELL
C ---------------------------------
      PI=3.141617D0
      CIG(1)=0.98250221457623D0
      CIG(2)=1.00077731190727D0
      CIG(3)=0.99996645012540D0
      P(1)=4.7300407448627D0
      P(2)=7.85320462409584D0
      P(3)=10.99560783800167D0
C ------------------------------------
C          SMALL GAP,STEEL-WATER SYSTEM
C ------------------------------------
         EI=1/11.D0
       EO=1/10.D0
       ER=EI/EO
      ZI=23.3D0
      SU=5308.D0
      NI=.3D0
      LEN=1.0D0
      SKI=(5.5D-3)**2/12
      N=3
C ---------------------------------
       CALL PREMAT
     UI=.0395D0
       UO=(0.0D0,0.D0)
      MS=1
      NK=MS-1
         CALL UNSFO(UI,UO)
           CALL STFOR(UI,UO,GM1)
```

```
      CALL MATRA(MM,KK,CC,AA,BB)
            DO 14 K=1,6
           WRITE(6,419) (AA(K,J),J=1,6)
 419        FORMAT('0',6(D11.4,1X))
 14       CONTINUE
            DO 114 K=1,6
           WRITE(6,319) (BB(K,J),J=1,6)
 319        FORMAT('0',6(D11.4,1X))
 114      CONTINUE
      CALL EIGZC(AA,IA,BB,IB,NN,IJOB,EIGA,EIGB,Z,IZ,WK,INFER,IER)
       PRINT10,UI,UO
 10   FORMAT('1','FLOW VELOCITY INSIDE THE SHELL=',F8.5/'0','FLOW
     &VELOCITY IN THE ANNULAR REGION=',F8.5)
       PRINT11
 11   FORMAT('-','THE FREQUENCIES ARE:')
       DO 20 I=1,6
       OMEGA=-EIGA(I)/EIGB(I)
 20    PRINT12,OMEGA
 12     FORMAT('0','(',2D24.16,1X,')')
      STOP
      END
C
C
C*********************************************************************
C     SUBROUTINE PREMAT                                              *
C*********************************************************************
      SUBROUTINE PREMAT
      IMPLICIT REAL*8(A-H,O-Z)
      COMPLEX*16 COE(2,9)
      REAL*8 NI,NO,NU
      COMMON/DATA1/NI,NO,SKI,SKO,CIG(3),P(3),N
      COMMON/DATA2/EI,EO,ER,HR,URR
      COMMON/COCE/COE
      J=0
       E=EI
      NU=NI
      SK=SKI
C ******************************************************************
C      FREE SHELL VIBRATION
C ********************************************************************
       X1=-3.1416D0
  12  JJ=J+1
      COE(JJ,1)=-X1**2*E**2+(NU-1)*(SK+1)*N**2/2
      COE(JJ,2)=-(1+NU)*N*X1*E/2
      COE(JJ,3)=-NU*X1*E+SK*(-E**3*X1**3+N**2*(1-NU)*(X1)*E/2)
      COE(JJ,4)=-(1+NU)*N*X1/2*E
      COE(JJ,5)=-N**2-(1+3*SK)*(1-NU)*E**2/2*X1**2
      COE(JJ,6)=-SK*(3-NU)*N*E**2*X1**2/2-N
      COE(JJ,7)=-NU*X1*E+SK*(-E**3*X1**3+N**2*(1-NU)*X1*E/2)
      COE(JJ,8)=-N-(3-NU)*SK*N*E**2*X1**2/2
      COE(JJ,9)=-SK*(E**4*X1**4+(N**2-1)**2)-2*SK*(N*E)
     #**2*X1**2-1.0D0
      RETURN
      END
C*********************************************************************
C     SUBROUTINE STFOR                                               *
C*********************************************************************
C        THE STEADY FORCES ARE CALCULATED UN THIS SUBROUTINE
```

```
C*************************************************************************
C
      SUBROUTINE STFOR(UI,UO,GM1)
      IMPLICIT REAL*8(A-H,O-Z)
      INTEGER DEL(3,3),W,V,HH,KK,N
      REAL*8 NU,NI,NO,X1
      COMPLEX*16 CCOE(2,9),KI,X(3),UO,I
      DIMENSION AK(3,3),BK(3,3)
      COMMON/DATA1/NI,NO,SKI,SKO,CIG(3),P(3),N
      COMMON/DATA2/EI,EO,ER,HR,URR
      COMMON/DATA3/ZI,ZO,USR,DSR
      COMMON/DATA5/PPI,PPO,PO(2),PL(2),RMS,DEN,DDI,DDO,VIS,CA,CB
      COMMON/CON1/A,B,D,DEL
      COMMON/CON2/SE,SF,G,H,SJ,SL
      COMMON/CCCE/CCOE
      FA(RR,RE)=DSQRT(0.0055*(1+(20000*RR+1.D6/RE)**(1./3.)))
      FW(RR,RE)=1/(-4*DLOG10(RR/3.7+2.51/RE/FA(RR,RE)))**2
C ---------------------------------------------------------------
C     DATA FOR STEADY FLOW
C ---------------------------------------------------------------
        I=(0.D0,1.0D0)
         DEN=998.6D0
      DDI=8.261D-7
      DDO=DDI/ER
      ALEN=1.0D0
      VIS=1.121D-6
      SU=5308.0D0
       X1=-3.1416D0*EI
       N=3
C ---------------------------------------------------
      RMS=(1-ER**2)/2/DLOG(1/ER)
      RM=DSQRT(RMS)
      UOM=UO*SU
      UIM=UI*SU
      RR=0.D0
      RO=UOM*2*(EO-EI)/VIS*ALEN
      RI=UIM*2*EI/VIS*ALEN
      IF(RI.EQ.0.D0) GO TO 10
      FI=FW(RR,RI)
      GO TO 11
   10 FI=0.D0
   11 IF(RO.EQ.0.D0) GO TO 12
      FO=FW(RR,RO)
      GO TO 13
   12 FO=0.D0
   13 PPI=DEN*FI*UIM**2/EI
      PPO=DEN*FO*UOM**2/(EO-EI)
      UTBS=(1-RMS)/2/(1-ER)*FO*UOM**2
      UTAS=(RMS-ER**2)/2/ER/(1-ER)*FO*UOM**2
      UTS=FI*UIM**2/4
      BI=UTS+UTAS
      CI=2*UTS/EI-2*UTBS/EO/(1-RMS)
      DI=(PPO-PPI)/DEN
      J=0
      E=EI
      NU=NI
      BB=BI
      CC=CI
```

```
      DD=DI
      BD=DDI
 14   GM1=-BB*BD/E
      GM2=-(NU*CC*BD+GM1)/2-NU*DD*BD
      GM3=BB*BD
      GM4=-CC*BD
      GM5=-DD*BD*.25D0
           WRITE(6,99) DDI,UIM,PPI,UTS
 99       FORMAT('0','DDI=(',D11.4,1X,')',2X,'UIM=(',D11.4,1X,')',
    &      2X,'PPI=(',D11.4,1X,')',2X,'UTS=(',D11.4,1X,')')
           WRITE(6,100) BB,CC,DD
 100       FORMAT('0','BB=(',D11.4,1X,')',2X,'CC=(',D11.4,1X,')',
    &      2X,'DD=(',D11.4,1X,')')
           WRITE(6,101) FI,RI
 101       FORMAT('0','FI=(',D11.4,1X,')',2X,'RI=(',D11.4,1X,')')
           WRITE(6,102) GM1,GM2,GM3
 102       FORMAT('0','GM1=(',D11.4,1X,')',2X,'GM2=(',D11.4,1X,')',
    &      2X,'GM3=(',D11.4,1X,')')
           WRITE(6,103) GM4,GM5,X1,N
 103       FORMAT('0','GM4=(',D11.4,1X,')',2X,'GM5=(',D11.4,1X,')',
    &      2X,'X1=(',D11.4,1X,')',1X,'N=(',I3,1X,')')
      JJ=J+1
      PO(JJ)=((NU*E*CC-BB)/2+NU*E*DD)*DEN
      PL(JJ)=((NU*E*CC+BB)/2+NU*E*DD)*DEN
       K=1
       M=1
      AK(1,1)=.5D0
      BK(1,1)=.25D0
      CCOE(JJ,1)=GM1*(-X1**2)*BK(K,M)+GM2*(-X1**2)*AK(K,M)-GM4*
     # N**2*BK(K,M)-GM5*N**2*AK(K,M)
      CCOE(JJ,2)=(0.D0,0.D0)
      CCOE(JJ,3)=+GM4*X1*BK(K,M)+GM5*X1*AK(K,M)
      CCOE(JJ,4)=GM3*N/I*AK(K,M)
      CCOE(JJ,5)=GM1*(-X1**2)*BK(K,M)+GM2*(-X1**2)*AK(K,M)-GM4*
     #N**2*BK(K,M)-GM5*N**2*AK(K,M)
      CCOE(JJ,6)=-GM4*N*BK(K,M)-GM5*N*AK(K,M)
      CCOE(JJ,7)=GM3/I*AK(K,M)-GM4*X1*BK(K,M)-GM5*X1*AK(K,M)
      CCOE(JJ,8)=-GM4*N*BK(K,M)-GM5*N*AK(K,M)
       CCOE(JJ,9)=(GM1*(-X1**2)*BK(K,M)+GM2*(-X1**2)*AK(K,M)-GM4*
     #N**2*BK(K,M)-GM5*N**2*AK(K,M))
          WRITE(6,621)
 621        FORMAT('0','CCOE')
          JJ=1
          DO 441 KK=1,9
               WRITE(6,455) CCOE(JJ,KK)
 455            FORMAT('0',2(D11.4,1X))
 441              CONTINUE
        RETURN
        END
C ********************************************************************
C     SUBROUTINE UNSFOR(QTETI)*
C********************************************************************
C    THIS PROGRAM IS TO CALCULATE THE UNSTEADY FORCES CAUSED BY*
C      THE PERTURBATIONS*
C********************************************************************
C
           SUBROUTINE UNSFO(UI,UO)
           IMPLICIT COMPLEX*16(A-Z)
```

```
      COMPLEX*16  MM(3,3),CC(3,3),KK(3,3)
      REAL*8 EI,EO,X1,CIG,P,PI,GAMA,UI,ZI,ZO,DSR,USR,HR,ER,URR
      REAL*8 NI,NO,SKI,SKO,SU,LEN,VIS,TEI1,TEI2
      INTEGER N,K,M,J,L,NN
      COMMON PI,GAMA
      COMMON/DATA1/NI,NO,SKI,SKO,CIG(3),P(3),N
      COMMON/DATA2/EI,EQ,ER,HR,URR
      COMMON/DATA3/ZI,ZO,USR,DSR
      COMMON/CLLE/QTRI1,QTRI2,QTRI3
        INP(Y)=(IN(Y,N-1)+IN(Y,N+1))/2
      KNP(Y)=-(KN(Y,N-1)+KN(Y,N+1))/2
      KNPP(Y)=(KN(Y,N-2)/2+KN(Y,N)+KN(Y,N+2)/2)/2
         GAMA=.577215664901161D0
         PI=3.14159265358979D0
      X1=-3.1416D0*EI
      ALP=-3.1416D0*EI
      M=N+1
       ALA=X1
       ER=EI/EO
       ALB=ALA/ER
      M=N+1
      INIA=IN(ALA,N)
      INPIA=INP(ALA)
      KNIA=KN(ALA,N)
      KNPIA=KNP(ALA)
C ---------------------------------
      INIB=IN(ALB,N)
      KNIB=KN(ALB,N)
      INPIB=INP(ALB)
      KNPIB=KNP(ALB)
C -----------------------------------------------------
C        POTENTIAL FLOW THEORY
C -------------------------------------------------------
         F11=INIA/ALA/INPIA
C        WRITE(6,119) ALA,F11
C119     FORMAT('0','ALA=(',2D11.4,1X,')',2X,'F11=(',2D11.4,1X,')')
              F2=(INIA*KNPIB-INPIB*KNIA)/(KNPIB*INPIA-INPIB*KNPIA)
          F3=-2*X1*UO*F2/ALA*ZI
C         F3=(0.D0,0.D0)
          F4=F2/ALA*ZI
          F5=X1**2*UO**2/ALA*F2*ZI
        QTRI1=F11*ZI-F4
        QTRI2=-2*X1*UI*ZI*F11-F3
       QTRI3=X1**2*UI**2*F11*ZI-F5
             RETURN
             END
C**********************************************************************
C    SUBPROGRAMS FOR CALCULATING THE BESSEL FUNCTIONS                 *
C**********************************************************************
      COMPLEX FUNCTION IN*16(X,N)
      IMPLICIT REAL*8(A-Z)
      COMPLEX*16 X,T,T1,T2,T3,T4,I,T5,XXX
      INTEGER K,N,M
      COMMON PI,GAMA
      I=(0.D0,1.D0)
      IF(CDABS(X).GE.15.D0) GO TO 10
      IN=(0.D0,0.D0)
      K=0
```

```
 11   T=(X/2)**(2*K)/FA(K)/FA(N+K)
      IF(CDABS(T).LT.1.D-12) GO TO 12
      IN=IN+T
      K=K+1
      GO TO 11
 12   IN=(X/2)**N*IN
      GO TO 36
 10   T2=(2.0D0/PI/X)
      T3=CDSQRT(T2)
        TEI1=X
         T5=-I*X
        TEI2=T5
        T1=(4*N**2-1)/(8*X*I)
        XXX=I*(TEI1-PI/4-N*PI/2)
         IN=T3*(1.0D0-T1)*CDEXP(XXX)
36     WRITE(6,52) IN
52    FORMAT('0','IN=(',2D11.4,1X,')')
      RETURN
      END
C ---------------------------------------------------------------------
      COMPLEX FUNCTION KN*16(X,N)
      IMPLICIT REAL*8(A-Z)
      COMPLEX*16 X,KN1,T,T1,T2,T3
      INTEGER N,ML,K,I
      COMMON PI,GAMA
         PI=3.1416D0
            GAMA=0.5772D0
      IF(CDABS(X).GE.15.D0) GO TO 40
      IF(N.EQ.0) GO TO 46
      KN=FA(N-1)*(2/X)**N
       IF(N.EQ.1) GO TO 45
      ML=N-1
       DO 41 I=1,ML
 41   KN=KN+(-1)**I*FA(N-I-1)/FA(I)*(2/X)**(N-2*I)
 45   KN=KN/2
      GO TO 47
 46   KN=(0.D0,0.D0)
 47   KN1=(0.D0,0.D0)
      K=0
 43   T=(X/2)**(N+2*K)/FA(K)/FA(N+K)*(CDLOG(X/2)-(F(K+1)+F(N+K+1))/2)
      IF(CDABS(T).LT.1.D-12) GO TO 42
      KN1=KN1+T
      K=K+1
      GO TO 43
 42   KN=KN+KN1*(-1)**(N+1)
      RETURN
 40   T1=(4*N**2-1)/8/X
      T2=T1*(4*N**2-9)/16/X
      T3=1.D0*CDSQRT(PI/2/X)
      KN=T3*(1+T1+T2)
      RETURN
      END
C
      DOUBLE PRECISION FUNCTION R(K)
      IMPLICIT REAL*8(A-Z)
      INTEGER K,I
      R=0.D0
      DO 40 I=1,K
```

```
   40  R=R+1.D0/I
       RETURN
       END
C
       DOUBLE PRECISION FUNCTION F(K)
       IMPLICIT REAL*8(A-Z)
       INTEGER K
       COMMON PI,GAMA
       IF(K.EQ.1) GO TO 50
       F=R(K-1)-GAMA
       RETURN
   50  F=-GAMA
       RETURN
       END
C
       DOUBLE PRECISION FUNCTION FA(K)
        IMPLICIT REAL*8(A-Z)
       INTEGER K,L
       FA=1.D0
       L=1
   21  FA=FA*L
       IF(L.GE.K) GO TO 22
       L=L+1
       GO TO 21
   22  CONTINUE
       RETURN
       END
C*********************************************************************
C*      MATRIX AAA**
C*
C*********************************************************************
C  THIS PART IS USED TO ASSEMBLE MATRIX AAA WHICH CONTAINS THE*
C  FREE VIBRATIONS TERMS COE,THE STEADY FORCES CCOE,AND THE UNSTEADY*
C  FORCES QTXI,...*
C**********************************************************************
       SUBROUTINE MATRA(MM,KK,CC,AA,BB)
       IMPLICIT REAL*8(A-H,O-Z)
       COMPLEX*16 AAA(3,3),AA(6,6),BB(6,6),MM(3,3),KK(3,3),CC(3,3),
      &COE(2,9),CCOE(2,9)
       COMPLEX*16 QTRI1,QTRI2,QTRI3
       INTEGER N,JL
       COMMON/DATA1/NI,NO,SKI,SKO,CIG(3),P(3),N
       COMMON/DATA2/EI,EO,ER,HR,URR
       COMMON/DATA3/ZI,ZO,USR,DSR
       COMMON/DATA5/PPI,PPO,PO(2),PL(2),RMS,DEN,DDI,DDO,VIS,CA,CB
       COMMON/COCE/COE
       COMMON/CCCE/CCOE
       COMMON/CLLE/QTRI1,QTRI2,QTRI3
             WRITE(6,166) QTRI1,QTRI2,QTRI3
  166       FORMAT('0','QTRI1=(',2D11.4,1X,')',2X,'QTRI2=(',2D11.4,1X,')
      &',2X,'QTRI3=(',2D11.4,1X,')')
             JJ=1
          KK(1,1)=COE(JJ,1)*.5D0+CCOE(JJ,1)
          KK(1,2)=COE(JJ,4)*.5D0+CCOE(JJ,4)
          KK(1,3)=COE(JJ,7)*.5D0+CCOE(JJ,7)
C
          KK(2,1)=COE(JJ,2)*.5D0+CCOE(JJ,2)
          KK(2,2)=COE(JJ,5)*.5D0+CCOE(JJ,5)
```

```
          KK(2,3)=COE(JJ,8)*.5D0+CCOE(JJ,8)
C
          KK(3,1)=COE(JJ,3)*.5D0+CCOE(JJ,3)
          KK(3,2)=COE(JJ,6)*.5D0+CCOE(JJ,6)
          KK(3,3)=(COE(JJ,9)+QTRI3)*.5D0+CCOE(JJ,9)
          CC(3,3)=QTRI2*.5D0
C
C          DO 11 J=1,2
C           MM(J,J)=(1.0D0,0.D0)
C11          CONTINUE
            MM(1,1)=(1.0D0,.0D0)*.5D0
            MM(2,2)=(1.0D0,.0D0)*.5D0
            MM(3,3)=((1.0D0,.0D0)+QTRI1)*.5D0
           DO 12 J=1,3
           AA(J,J+3)=(1.0D0,.0D0)
           BB(J,J)=(-1.0D0,0.D0)
 12        CONTINUE
             DO 13 J=1,3
             DO 13 K=1,3
            AA(3+J,K)=KK(J,K)
            AA(3+J,3+K)=CC(J,K)
            BB(3+J,3+K)=MM(J,K)
 13           CONTINUE
           DO 14 K=1,6
          WRITE(6,419) (AA(K,J),J=1,6)
 419       FORMAT('0',6(D11.4,1X))
 14      CONTINUE
           DO 114 K=1,6
          WRITE(6,319) (BB(K,J),J=1,6)
 319       FORMAT('0',6(D11.4,1X))
 114     CONTINUE
      RETURN
      END
```

APPENDIX L

PROGRAM FOR VISCOUS THEORY USING TRAVELLING WAVE SOLUTION

This program considers the full theory, the cases of internal and annular flow could be considered, the effects of unsteady and steady viscous forces could be investigated. The program calculates the dimensionless frequency Ω for each flow velocity.

<u>Program Structure</u>

MAIN PROGRAM

SUBROUTINE PREMAT

SUBROUTINE STFOR

SUBROUTINE UNSFOR

SUBROUTINE MATRA

COMPLEX FUNCTION FS

COMPLEX FUNCTION DET

COMPLEX FUNCTION IN

COMPLEX FUNCTION KN

DOUBLE PRECISION R

DOUBLE PRECISION F

DOUBLE PRECISION FA

```
C***********************************************************************
C     COMPUTER PROGRAM FOR THE CASE OF STEADY AND UNSTEADY VISCOUS     *
C                      THORY(FULL THEORY)                              *
C                      TRAVELLING WAVE SOLUTION                        *
C***********************************************************************
C
C***********************************************************************
C              THE FOLLOWING ARE INFORMATIONS TO HELP RUNNING THE
C                 PROGRAM PROPERLY
C   ---------------------------------------------------------------- ----
C              INTERNAL AND OR ANNULAR FLOW
C               (I)   UNSTEADY +STEADY
C               (II)  UNSTEADY
C               (III) STEADY
C          ---- SET KF=1 THIS LEAD TO INTERNAL FLOW ONLY IN UNSTEADY
C          ----  IF KF(NOT=TO 1) INTERNAL AND ANNULAR FLOW ARE CONSIDERED
C          ----  LL=0  CONSTANT VELOCITY POFILE INTERNAL FLOW
C          ----  LS=0  CONSTANT VELOCITY PROFILE ANNULAR FLOW
C          ------ IF CA1=CA2=0.D0, AND UB=UMAX THIS IS THE CASE OF CONST
C                   VELOCITY PROFILE
C             IN MATRIX AAA
C              -------------
C             IF QTRI=QTETI=QTXI=0       NO UNSTEADY FORCES
C             IF COE=0                   NO STEADY FORCES
C   *********************************************************************
C       MAIN PROGRAM
C   *********************************************************************
      IMPLICIT REAL*8(A-H,O-Z)
       COMPLEX*16 QTXI(6),QTETI(6),QTRI(6),AAA(3,3),XY(3)
     #,FS,UO,MIL,COE(2,9),CCOE(2,9)
      INTEGER INFER(3),MS,N
        EXTERNAL FS
      REAL*8 NI,NO,UI
      COMMON/DATA1/NI,NO,SKI,SKO,CIG(3),P(3),N
      COMMON/DATA2/EI,EO,ER,HR,URR
      COMMON/DATA3/ZI,ZO,USR,DSR
      COMMON/DATA7/UI,UO
      COMMON/AREA1/AAA
      COMMON/DATA5/PPI,PPO,PO(2),PL(2),RMS,DEN,DDI,DDO,VIS,CA,CB
      DATA EPS/1.D-10/,NSIG/8/,NGUESS/1/,ITMAX/10/,II/1/
      COMMON/COCE/COE
      COMMON/CRCE/CCOE
      COMMON/CLLE/QTXI,QTETI,QTRI
C --------------------------------
C      DATAS REQUIRED FOR SHELL
C --------------------------------
      PI=3.141617D0
C -----------------------------
C  STEEL WATER SHELL
C  ------------------------------
C ------------------------
C         GAP(0.1/10)WATER
C ------------------------------------
         EI=1/11.D0
       EO=1/10.0D0
        ER=EI/EO
       ZI=23.3D0
       SU=5308.D0
```

```
      NI=.3D0
      LEN=1.0D0
      SKI=(5.5D-3)**2/12
      N=3
C ---------------------------------------
       CALL PREMAT
C ---------------------------------------
      UI=0.04D0
      UO=(0.0D0,0.D0)
      MS=1
      NK=MS-1
      XY(1)=(-.619D-3,.171D-4)
C
      CALL ZANLYT(FS,EPS,NSIG,NK,NGUESS,II,XY,ITMAX,INFER,IER)
        CALL UNSFO(UI,UO,XY(1),MIL)
          CALL STFOR(UI,UO,GM1)
      CALL MATRA(XY(1),AAA)
      PRINT 111,XY(MS)
 111  FORMAT('-','FREQUENCY AT A SPECIFIC VELOCITY TO STUDY THE
     & INSTABILITY=(',2D11.4,1X,')')
            PRINT 155 ,INFER(1)
 155        FORMAT('0','NO.OF ITERATIONS REQUIRED=',I3/)
            PRINT30
 30           FORMAT('1')
      PRINT10,UI,UO
 10   FORMAT('1','FLOW VELOCITY INSIDE THE INNER CYLINDER=',F8.5/'0','FL
     #OW VELOCITY IN THE ANNULAR REGION=',F8.5)
      STOP
      END
C
C
C***********************************************************************
C     SUBROUTINE PREMAT                                                *
C***********************************************************************
      SUBROUTINE PREMAT
      IMPLICIT REAL*8(A-H,O-Z)
      COMPLEX*16 COE(2,9)
      REAL*8 NI,NO,NU
      COMMON/DATA1/NI,NO,SKI,SKO,CIG(3),P(3),N
      COMMON/DATA2/EI,EO,ER,HR,URR
      COMMON/COCE/COE
      J=0
      E=EI
      NU=NI
      SK=SKI
       X1=-3.1416D0*E
 12   JJ=J+1
      COE(JJ,1)=-X1**2+(NU-1)*(SK+1)*N**2/2
      COE(JJ,2)=-(1+NU)*N*X1/2
      COE(JJ,3)=-NU*X1+SK*(-X1**3+N**2*(1-NU)*(X1)/2)
      COE(JJ,4)=-(1+NU)*N*X1/2
      COE(JJ,5)=-N**2-(1+3*SK)*(1-NU)*X1**2/2
      COE(JJ,6)=-SK*(3-NU)*N*X1**2/2-N
      COE(JJ,7)=-NU*X1+SK*(-X1**3+N**2*(1-NU)*X1/2)
      COE(JJ,8)=-N-(3-NU)*SK*N*X1**2/2
      COE(JJ,9)=-SK*(X1**4+(N**2-1)**2)-2*SK*(N)
     #**2*X1**2-1.0D0
      RETURN
```

```
      END
C************************************************************************
C      COMPLEX FUNCTION FS                                              *
C************************************************************************
      COMPLEX FUNCTION FS*16(KI)
      IMPLICIT REAL*8(A-Z)
      COMPLEX*16 KI,AAA(3,3),DET,UO,MIL
      INTEGER L(3),M(3)
      COMMON/DATA7/UI,UO
      COMMON/AREA1/AAA
          CALL STFOR(UI,UO,GM1)
        CALL UNSFO(UI,UO,KI,MIL)
        CALL MATRA(KI,AAA)
              DO 320 K=1,3
            WRITE(6,319) (AAA(K,J),J=1,3)
 319        FORMAT('0',6(D11.4,1X))
 320      CONTINUE
      FS=DET(AAA,L,M,3)
          PRINT 11,FS
 11   FORMAT('0','FS=',2(D11.4,1X))
         PRINT 116,KI
 116  FORMAT('0','KI=',2(D11.4,1X))
      RETURN
      END
C
C************************************************************************
C      SUBROUTINE STFOR                                                 *
C************************************************************************
C        THE STEADY FORCES ARE CALCULATED UN THIS SUBROUTINE
C************************************************************************
C
       SUBROUTINE STFOR(UI,UO,GM1)
      IMPLICIT REAL*8(A-H,O-Z)
      INTEGER DEL(3,3),W,V,HH,KK,N
      REAL*8 NU,NI,NO,X1
      COMPLEX*16 CCOE(2,9),KI,X(3),UO,I
      DIMENSION AK(3,3),BK(3,3)
      COMMON/DATA1/NI,NO,SKI,SKO,CIG(3),P(3),N
      COMMON/DATA2/EI,EO,ER,HR,URR
      COMMON/DATA3/ZI,ZO,USR,DSR
      COMMON/DATA5/PPI,PPO,PO(2),PL(2),RMS,DEN,DDI,DDO,VIS,CA,CB
      COMMON/CON1/A,B,D,DEL
      COMMON/CON2/SE,SF,G,H,SJ,SL
      COMMON/CRCE/CCOE
      FA(RR,RE)=DSQRT(0.0055*(1+(20000*RR+1.D6/RE)**(1./3.)))
      FW(RR,RE)=1/(-4*DLOG10(RR/3.7+2.51/RE/FA(RR,RE)))**2
C  -------------------------------------------------------------
C     DATA FOR STEADY FLOW
C  ----------------------------------------------------------
         I=(0.D0,1.0D0)
           DEN=998.6D0
      DDI=8.261D-7
      DDO=DDI/ER
      VIS=1.121D-6
      SLEN=1.0D0
      SU=5308.0D0
       X1=-3.1416D0*EI
       N=3
```

```
C -------------------------------------
      RMS=(1-ER**2)/2/DLOG(1/ER)
      RM=DSQRT(RMS)
      RMA=RM/(RM-ER)
      LRA=DLOG(RM/ER)
      RMB=RM/(1-RM)
      LRB=DLOG(1/RM)
      CA=-0.7864D0-0.56*RMA+0.5064*RMA*LRA+0.56*RMA**2*LRA
      CB=0.7864D0-0.56*RMB-0.5064*RMB*LRB+0.56*RMB**2*LRB
      UOM=UO*SU
      UIM=UI*SU
      RR=0.D0
      RO=UOM*2*(EO-EI)/VIS*SLEN
      RI=UIM*2*EI/VIS*SLEN
      IF(RI.EQ.0.D0) GO TO 10
      FI=FW(RR,RI)
      GO TO 11
   10 FI=0.D0
   11 IF(RO.EQ.0.D0) GO TO 12
      FO=FW(RR,RO)
      GO TO 13
   12 FO=0.D0
   13 PPI=DEN*FI*UIM**2/EI
      PPO=DEN*FO*UOM**2/(EO-EI)
      UTBS=(1-RMS)/2/(1-ER)*FO*UOM**2
      UTAS=(RMS-ER**2)/2/ER/(1-ER)*FO*UOM**2
      UTS=FI*UIM**2/2
      BI=UTS+UTAS
      CI=2*UTS/EI-2*UTBS/EO/(1-RMS)
      DI=(PPO-PPI)/DEN
      BO=UTBS
      CO=2*UTBS/EO/(1-RMS)
      DO=-(CA*UTAS+CB*UTBS)-PPO/DEN
      J=0
      E=EI
      NU=NI
      BB=BI
      CC=CI
      DD=DI
      BD=DDI
   14 GM1=-BB*BD/E
      GM2=-(NU*CC*BD+GM1)/2-NU*DD*BD
      GM3=BB*BD
      GM4=-CC*BD
      GM5=-DD*BD
           WRITE(6,99) DDI,UIM,PPI,UTS
   99     FORMAT('0','DDI=(',D11.4,1X,')',2X,'UIM=(',D11.4,1X,')',
     &     2X,'PPI=(',D11.4,1X,')',2X,'UTS=(',D11.4,1X,')')
           WRITE(6,100) BB,CC,DD
  100      FORMAT('0','BB=(',D11.4,1X,')',2X,'CC=(',D11.4,1X,')',
     &     2X,'DD=(',D11.4,1X,')')
           WRITE(6,101) FI,RI
  101      FORMAT('0','FI=(',D11.4,1X,')',2X,'RI=(',D11.4,1X,')')
           WRITE(6,102) GM1,GM2,GM3
  102      FORMAT('0','GM1=(',D11.4,1X,')',2X,'GM2=(',D11.4,1X,')',
     &     2X,'GM3=(',D11.4,1X,')')
           WRITE(6,103) GM4,GM5,X1,N
  103      FORMAT('0','GM4=(',D11.4,1X,')',2X,'GM5=(',D11.4,1X,')',
```

```
     &     2X,'X1=(',D11.4,1X,')',1X,'N=(',I3,1X,')')
      JJ=J+1
      PO(JJ)=((NU*E*CC-BB)/2+NU*E*DD)*DEN
      PL(JJ)=((NU*E*CC+BB)/2+NU*E*DD)*DEN
       K=1
       M=1
      AK(1,1)=.5D0
      BK(1,1)=.25D0
      CCOE(JJ,1)=GM1*(-X1**2)*BK(K,M)+GM2*(-X1**2)*AK(K,M)-GM4*
     # N**2*BK(K,M)-GM5*N**2*AK(K,M)
      CCOE(JJ,2)=(0.D0,0.D0)
      CCOE(JJ,3)=+GM4*X1*BK(K,M)+GM5*X1*AK(K,M)
      CCOE(JJ,4)=GM3*N/I*AK(K,M)
      CCOE(JJ,5)=GM1*(-X1**2)*BK(K,M)+GM2*(-X1**2)*AK(K,M)-GM4*
     #N**2*BK(K,M)-GM5*N**2*AK(K,M)
      CCOE(JJ,6)=-GM4*N*BK(K,M)-GM5*N*AK(K,M)
      CCOE(JJ,7)=GM3/I*AK(K,M)-GM4*X1*BK(K,M)-GM5*X1*AK(K,M)
      CCOE(JJ,8)=-GM4*N*BK(K,M)-GM5*N*AK(K,M)
      CCOE(JJ,9)=GM1*(-X1**2)*BK(K,M)+GM2*(-X1**2)*BK(K,M)-GM4*
     #N**2*BK(K,M)-GM5*N**2*AK(K,M)
          WRITE(6,621)
621         FORMAT('0','CCOE')
          JJ=1
           DO 441 KK=1,9
               WRITE(6,455) CCOE(JJ,KK)
455             FORMAT('0',2(D11.4,1X))
441                CONTINUE
         RETURN
         END
C
C ********************************************************************
C     SUBROUTINE UNSFOR(QTETI)*
C*********************************************************************
C    THIS PROGRAM IS TO CALCULATE THE UNSTEADY FORCES CAUSED BY*
C      THE PERTURBATIONS*
C*********************************************************************
C
           SUBROUTINE UNSFO(UI,UO,KI,MIL)
           IMPLICIT COMPLEX*16(A-Z)
           COMPLEX*16  QTETI(3),QTRI(3),QTXI(3),A(4,4),B(4,4),WA(15)
           COMPLEX*16  AA(10,10),FTT(6,10),MIL,T(4,9),MEF,MEI,TT1,TT2,
     & TT3,TT4,FST(3,3),WK(3),C(6,6),D(6,6),TST(6,6),WWA(48),WWK(6)
           REAL*8 EI,EO,X1,CIG,P,PI,GAMA,UI,ZI,ZO,DSR,USR,HR,ER,URR
           REAL*8 NI,NO,SKI,SKO,SU,LEN,VIS,TEI1,TEI2,KMS,XX1,XX2
           REAL*8 NVISC,EX1,TEIA,TEIB,TEI3,TEI5,TEI6,DF,DG,TSS
           REAL*8 CA0,CA1,CA2,C1,C2,C3,R1,R2,Y1,Y2
           INTEGER N,K,M,J,L,NN,MM,IA,IB,IJOB,IER,LL,LM,IL,LS,LR
           INTEGER II,JJ,KK,KMF,KML,III,IIA,IIB,MMN,NNN,IIJOB,IIER
           COMMON PI,GAMA
           COMMON/DATA1/NI,NO,SKI,SKO,CIG(3),P(3),N
           COMMON/DATA2/EI,EO,ER,HR,URR
           COMMON/DATA3/ZI,ZO,USR,DSR
           COMMON/CLLE/QTXI,QTETI,QTRI
C           ---------------------------------------
C           MODIFIED BESSEL FUNCTION
C           ---------------------------------------
           INP(Y)=(IN(Y,N-1)+IN(Y,N+1))/2
           INF(Y)=(IN(Y,M-1)+IN(Y,M+1))/2
```

```
      INPP(Y)=(IN(Y,N-2)/2+IN(Y,N)+IN(Y,N+2)/2)/2
      INPF(Y)=(IN(Y,M-2)/2+IN(Y,M)+IN(Y,M+2)/2)/2
      KNP(Y)=-(KN(Y,N-1)+KN(Y,N+1))/2
      KNF(Y)=-(KN(Y,M-1)+KN(Y,M+1))/2
      KNPP(Y)=(KN(Y,N-2)/2+KN(Y,N)+KN(Y,N+2)/2)/2
      KNPF(Y)=(KN(Y,M-2)/2+KN(Y,M)+KN(Y,M+2)/2)/2
         GAMA=.5772156649011610D0
         PI=3.14159265358979D0
C     DATAS FOR VISCOUS FLUID AND SHELL DIMENSIONS
C ---------------------------------------------------------
C  ------------------------
C      WATER STEEL
C  -------------------------
       SU=5308.0D0
       LEN=1.0D0
         VIS=1.121D-6
       RFE=1.21D0/997.2D0
       RHE=1.0D0
C ---------------------------------------
      EPI=SU*LEN/VIS
      EPO=EPI
           ER=EI/EO
      URR=1.0D0
      HR=1.0D0
      X1=-3.1416D0*EI
      ALP=-3.1416D0*EI
      RHOE=RHE/EPO
C ***************************************
      M=N+1
      ALA=CDSQRT(ALP**2)
      ALB=ALA/ER
      X2=X1/ER
      I=(0.D0,1.D0)
      MEI=CDSQRT(I*EPI*(KI*EI)+X1**2)
      MEA=MEI
      MEB=MEI/ER
C     MEI=EI*MIL
C   ****************************************
C   INNE SHELL
C   ------------------------------------
      BXI1=IN(MEI,N)
      BXPI1=INP(MEI)
      BRI1=IN(MEI,M)
      BRPI1=INF(MEI)
      BRPPI1=INPF(MEI)
      BXPPI1=INPP(MEI)
C ---------------------------- --------
C     CONDITION AT R=A,ANNULAR
C ----------------------------------------
       INIA=IN(ALA,N)
       YNIA=KN(ALA,N)
       BXIA=IN(MEA,N)
       BRIA=IN(MEA,M)
       BXPIA=INP(MEA)
       BRPIA=INF(MEA)
       BXYA=KN(MEA,N)
       BRYA=KN(MEA,M)
       BXPYA=KNP(MEA)
```

```
            BRPYA=KNF(MEA)
            INPIA=INP(ALA)
            YNPIA=KNP(ALA)
            BRPPIA=INPF(MEA)
            BXPPIA=INPP(MEA)
            BRPPYA=KNPF(MEA)
            BXPPYA=KNPP(MEA)
            INPPIA=INPP(ALA)
            YNPPIA=KNPP(ALA)
C     CONDITION AT R=B,ANNULAR
C  ********************************************
            INIB=IN(ALB,N)
            YNIB=KN(ALB,N)
            BXIB=IN(MEB,N)
            BRIB=IN(MEB,M)
            BXPIB=INP(MEB)
            BRPIB=INF(MEB)
            BXYB=KN(MEB,N)
            BRYB=KN(MEB,M)
            BXPYB=KNP(MEB)
            BRPYB=KNF(MEB)
            INPIB=INP(ALB)
            YNPIB=KNP(ALB)
            LM=1
C ---------------------------------------------------
C       SOLUTION FOR BRI1 USING MODIFIED BESSEL FUNCTION
C  --------------------------------------------------
               WRITE(6,163) BRIA,MEI,M
  163          FORMAT('0','BRIA=(',2D11.4,1X,')',2X,'MEI=(',2D11.4,1X,')',
     &         2X,'M=',I5)
            WRITE(6,131) EI,EPI
 131        FORMAT('0','EI=(',D11.4,1X,')',2X,'EPI=(',D11.4,1X,')')
  9         WRITE(6,11) MEI,MIL
  11        FORMAT('0','MEI=(',2D11.4,1X,')',2X,'MIL=(',2D11.4,1X,')')
            WRITE(6,112) TEI1,TEI2
 112        FORMAT('0','TEI1=(',D11.4,1X,')',2X,'TEI2=(',D11.4,1X,')')
            WRITE(6,122) KNIA,KNPIA
 122        FORMAT('0','KNIA=(',2D11.4,1X,')',2X,'KNPIA=(',2D11.4,1X,')')
            WRITE(6,12) INIA,INPIA,INPPIA
  12        FORMAT('0','INIA=(',2D11.4,1X,')',2X,'INPIA=(',2D11.4,1X,')',
     & 2X,'INPPIA=(',2D11.4,1X,')')
            WRITE(6,192) TT1,TT2,TT3
  192       FORMAT('0','TT1=(',2D11.4,1X,')',2X,'TT2=(',2D11.4,1X,')',
     &      2X,'TT3=(',2D11.4,1X,')')
             WRITE(6,13) BRYA
   13        FORMAT('0','BRYA=(',2D11.4,1X,')')
             WRITE(6,14) BXYA
  14        FORMAT('0','BXYA=(',2D11.4,1X,')')
             WRITE(6,18) BXPYA,BRPYA
  18       FORMAT('0','BXPYA=(',2D11.4,1X,')',2X,'BRPYA=(',2D11.4,1X,')')
C ***************************************************
C   INVERSION OF MATRIX A,INNER FLOW
C ****************************************************
           A(1,1)=I*X1*INIA
            A(1,2)=(0.D0,0.D0)
             A(1,3)=(MEI*BRPI1+(N+1)*BRI1)
             A(2,1)=-N*INIA
              A(2,2)=(-MEI*BXPI1)
```

```
              A(2,3)=-X1*I*BRI1
              A(3,1)=ALA*INPIA
                 A(3,2)=(N*BXI1)
                  A(3,3)=-I*X1*BRI1
                   FSS1=DET(A,L,M,3)
               WRITE(6,77) FSS1
 77              FORMAT('0','FSS1=(',2D11.4,1X,')')
C ------------------------------------------------
                  WRITE(6,82) AKJ
 82             FORMAT('0','AKJ')
               DO 34 K=1,3
               WRITE(6,71) (A(K,J),J=1,3)
 71             FORMAT('0',6(D11.4,1X))
 34             CONTINUE
C
C SOLVING FOR C1I,C3I,C5I,AND PRINTING THE MATRIX B(K,J)
C
               DO 101 K=1,3
               DO 101 J=1,3
                    B(K,J)=(0.D0,0.D0)
                  IF(K.EQ.J) B(K,J)=(1.0D0,0.D0)
 101               CONTINUE
C -------------------------------------------------------------
                 DD=A(2,2)*(A(3,3)*A(1,1)-A(3,1)*A(1,3))-A(3,2)*(A(1,1)*
     &           A(2,3)-A(1,3)*A(2,1))
                 B(3,1)=(A(3,2)*A(2,1)-A(3,1)*A(2,2))/DD
                 B(3,2)=-A(3,2)*A(1,1)/DD
                 B(3,3)=A(2,2)*A(1,1)/DD
                 SS=A(1,1)*A(2,3)-A(1,3)*A(2,1)
                 B(2,1)=-(A(2,1)+SS*B(3,1))/A(1,1)/A(2,2)
                 B(2,2)=(A(1,1)-SS*B(3,2))/A(1,1)/A(2,2)
                 B(2,3)=-SS*B(3,3)/A(1,1)/A(2,2)
                 B(1,1)=(1-A(1,3)*B(3,1))/A(1,1)
                 B(1,2)=-A(1,3)*B(3,2)/A(1,1)
                 B(1,3)=-A(1,3)*B(3,3)/A(1,1)
                 WRITE(6,53) BKJ
 53              FORMAT('0','BKJ')
                DO 44 K=1,3
                WRITE(6,99) (B(K,J),J=1,3)
 99              FORMAT('0',6(D11.4,1X))
 44               CONTINUE
C   -----------------------------------------------------------
C       CHEK FOR CORRECT INVERSION IDENTITYMATRIX
C ------------------------------------------------------------
                      DO 61 II=1,3
                      DO 61 KK=1,3
                    FST(II,KK)=(0.D0,0.D0)
                       DO 61 JJ=1,3
                  FST(II,KK)=FST(II,KK)+A(II,JJ)*B(JJ,KK)
 61                   CONTINUE
                  WRITE(6,501) FSTKJ
 501              FORMAT('0','FSTKJ')
            DO 516 K=1,3
                  WRITE(6,517) (FST(K,J),J=1,3)
 517        FORMAT('0',6(D11.4,1X))
 516            CONTINUE
C  *************************************************************
C                 LL=1,VARIABLE VELOCITY PROFILE FOR INTENAL FLOW
```

```
C * *****************************************************************
C          DETERMINATION OF THE CONSTANTS
C ------------------------------------------------------------
               R1=.98D0
               R2=.7D0
               Y1=.7D0
               Y2=.89D0
               CA0=1.0D0
               CA2=((R2-R1)+R1*Y2-Y1*R2)/(R1*R2**2-R1**2*R2)
               CA1=(Y2-1-R2**2*CA2)/R2
                  WRITE(6,193) CA0,CA1,CA2
 193      FORMAT('0','CA0=(',D11.4,1X,')',2X,'CA1=(',D11.4,1X,')',1X,
    &    'CA2=('D11.4,1X,')')
C    ------------------------------------------------------------
          LR=0
          LL=0
                      IF(LR.EQ.1) GO TO 291
                      IF(LL.EQ.1) GO TO 135
C-------------------------------------------------------
C            PRESURE PERTURBATION U=U0
C -----------------------------------------------------
C              CONSTANT VELOCITY PROFILE
C -------------------------------------------------------
               IF(N.EQ.3) GO TO 153
               BX11=IN(MEA,1)
               TI2=INIA
               TI4=BX11/MEI
               TI6=BXI1-2*TI4
                 GO TO 291
 153             TI2=INIA
                 BX11=IN(MEA,1)
                 BX21=IN(MEA,2)
                 TI4=BX21/MEA-BX11/MEA**2
                 TI6=BXI1-3*TI4
                   GO TO 291
C ---------------------------------------------------
C                VARIABLE VELOCITY PROFILE
C  ********************************************************
C *******************************************************
 135            ALA1=.99D0*ALA
                MEI1=.99D0*MEI
                INN=IN(ALA1,N)
                BX1=IN(MEI1,1)
                BX0=IN(MEI1,0)
                BX2=IN(MEI1,2)
                BX3=IN(MEI1,3)
C ---------------------------------------------
                     IF(N.EQ.2) GO TO 5
C ---------------------------------------------
                    TI2=CA0*INN+CA1/ALA*(ALA1*INN-(ALA1**4/48/4+ALA1**6/
    & 768/6))+CA2/ALA**2*(ALA1**2*INN-(ALA1**5/48/5+ALA1**7/768/7))
                    TI4=CA0*(BX2/MEI1-BX1/MEI1**2)+CA1*(BX2-2*BX1/MEI1
    &               )/MEI+CA2*(BX2*MEI1-3*(BX1-BX1/MEI1))/MEI**2
                     TI6=CA0*(BX3-3*(BX2/MEI1-BX1/MEI1**2))+CA1*(BX3*MEI1
    &              -4*(BX2-2*BX1/MEI1))/MEI+CA2*(MEI1**2*BX3-5*(BX2*MEI1-3
    &             *(BX1-BX1/MEI1)))/MEI**2
                      GO TO 133
C ------------------------------------------------------------------
```

```
-5          TI2=CA0*IN2+CA1*(ALA1*IN2-(ALA1**3/24+ALA**5/96/5))/ALA+
     &      CA2*(ALA1**2*IN2-2*(ALA1**4/32-ALA1**6/96/6))/ALA**2
            TI4=CA0*(BX1/MEI1)+CA1*(BX1-BX1/MEI1)/MEI+CA2*(MEI1*BX1-2
     $        *BX0)/MEI**2
          TI6=CA0*(BX2-2*BX1/MEI1)+CA1*(MEI1*BX2-3*(BX1-BX1/MEI1))/MEI
     &      +CA2*(MEI1**2*BX2-4*(MEI1*BX1-2*BX0))/MEI**2
C ---------------------------------------------------------------------
  133       WRITE(6,102) TI2,TI4,TI6
  102       FORMAT('0','TI2=(',2D11.4,1X,')',2X,'TI4=(',2D11.4,1X,')',
     &      2X,'TI6=(',2D11.4,1X,')')
C    ----------------------------------------------------------
C     INNER SHELL
C -----------------------------------------------------
 291                T(1,1)=-(-2*I*X1*ALA*INPIA)/EPI/EI**2
                     T(1,2)=-(-I*N*X1*BXI1)/EPI/EI**2
                     T(1,3)=-((1-X1**2+N)*BRI1-MEI*(1+N)*BRPI1-MEI**2*
     &              BRPPI1)/EI**2/EPI
                      T(2,1)=-(2*N*INIA-2*N*ALA*INPIA)/EPI/EI**2
                    T(2,2)=-(MEI*BXPI1-N**2*BXI1-MEI**2*BXPPI1)/EPI/EI**2
                       T(2,3)=-((1+N)*I*X1*BRI1-I*X1*MEI*BRPI1)/EPI/EI**2
C- -------------------------------------------------------------------
C                        RADIAL STRESSES USING RADIAL DIRECTION
C ---------------------------------------------------------------------
       T(3,1)=-((I*KI*INIA+UI*(-I*X1)*TI2)/EI+2*ALA**2*INPPIA/EPI/EI**2)
          T(3,2)=-((-I*X1*N*UI*TI4)/EI+2*(MEI*N*BXPI1-N*BXI1)/EPI/EI**2)
         T(3,3)=-((-X1**2*UI*TI6)/EI/MEI+2*(-I*X1*MEI)/EPI/EI**2*BRPI1)
C * *******************************************************************
C              HERE IF WE WANT TO SOLVE FOR INNER SHELL ONLY
C                 THEN JUMP OVER THE ANNULAR FLOW
C              SET KF=1
C ---------------------------------------------------------------------
          KF=0
          IF(KF.EQ.1) GO TO 941
C ************************************************************
C SOLVING FOR L1O,L2O,L3O,L4O,L5O,L6O
C          MATRIX INVERSION ANNULAR FLOW
C ************************************************************
            TEIA=MEA
            TEIB=MEB
            TEI3=TEIA-TEIB
            IF(TEI3.GE.50.D0) GO TO 33
            EX1=DEXP(TEI3)
              GO TO 44
 33             EX1=.50D-30
C              EX1=1.0D0
 44         C(1,1)=I*X1*INIA
            C(1,2)=I*X1*YNIA
            C(1,3)=(0.D0,0.D0)
            C(1,4)=(0.D0,0.D0)
            C(1,5)=((1+N)*BRIA+MEA*BRPIA)*EX1
            C(1,6)=(1+N)*BRYA+MEA*BRPYA
CC ---------------------------------
            C(2,1)=-N*INIA
            C(2,2)=-N*YNIA
            C(2,3)=-MEA*BXPIA*EX1
            C(2,4)=-MEA*BXPYA
            C(2,5)=-I*X1*BRIA*EX1
            C(2,6)=-I*X1*BRYA
```

```
C  ------------------------------------
         C(3,1)=ALA*INPIA
         C(3,2)=ALA*YNPIA
         C(3,3)=N*BXIA*EX1
         C(3,4)=N*BXYA
         C(3,5)=-I*X1*BRIA*EX1
         C(3,6)=-I*X1*BRYA
C  ------------------------------------
         C(4,1)=I*X2*INIB
         C(4,2)=I*X2*YNIB
         C(4,3)=(0.D0,0.D0)
         C(4,4)=(0.D0,0.D0)
         C(4,5)=((1+N)*BRIB+MEB*BRPIB)
         C(4,6)=((1+N)*BRYB+MEB*BRPYB)*EX1
CC ------------------------------------
         C(5,1)=-N*INIB
         C(5,2)=-N*YNIB
         C(5,3)=-MEB*BXPIB
         C(5,4)=-MEB*BXPYB*EX1
         C(5,5)=-I*X2*BRIB
         C(5,6)=-I*X2*BRYB*EX1
C  ------------------------------------
         C(6,1)=ALB*INPIB
         C(6,2)=ALB*YNPIB
         C(6,3)=N*BXIB
         C(6,4)=N*BXYB*EX1
         C(6,5)=-I*X2*BRIB
         C(6,6)=-I*X2*BRYB*EX1
C ----------------------------------------------------
         PRINT363
363       FORMAT('0','CKJ')
         DO 164 K=1,6
         WRITE(6,165) (C(K,J),J=1,6)
165      FORMAT('0',10(D11.4,1X),//,2(D11.4,1X))
164      CONTINUE
         FSS=DET(C,L,M,6)
         WRITE(6,43) FSS
43       FORMAT('0','FSS=(',2D11.4,1X,')')
C ----------------------------------------------------
C        INVERSION OF THE MATRIX
C ----------------------------------------------------
            DO 211 K=1,6
            DO 211 J=1,6
                  D(K,J)=(0.D0,0.D0)
                IF(K.EQ.J) D(K,J)=(1.0D0,0.D0)
211               CONTINUE
             IIA=6
             IIB=6
              NNN=6
              MMN=6
              IIJOB=0
                 CALL LEQ2C(C,NNN,IIA,D,MMN,IIB,IIJOB,WWA,WWK,IIER)
C ----------------------------------------------------
C ----------------------------------------------------
         PRINT63
63       FORMAT('0','DKJ')
         DO 136 K=1,6
         WRITE(6,137) (D(K,J),J=1,6)
```

```
 137        FORMAT('0',10(D11.4,1X),//,2(D11.4,1X))
 136        CONTINUE
C  -----------------------------------------------------------------
C       CHEK FOR CORRECT INVERSION IDENTITY MATRIX
C ------------------------------------------------------------------
                        DO 31 II=1,6
                        DO 31 KK=1,6
                      TST(II,KK)=(0.D0,0.D0)
                         DO 31 JJ=1,6
                   TST(II,KK)=TST(II,KK)+C(II,JJ)*D(JJ,KK)
  31                    CONTINUE
                   WRITE(6,601) TSTKJ
 601              FORMAT('0','TSTKJ')
             DO 616 K=1,6
                   WRITE(6,617) (TST(K,J),J=1,6)
 617         FORMAT('0',10(D11.4,1X),//,2(D11.4,1X))
 616             CONTINUE
C * ******************************************************************
C                    FOR CONSTANT VELOCITY PROFILE,SET LS=0
C  ****************************************************************
                      LS=1
                     IF(LS.EQ.1) GO TO 212
C *******************************************************************
C                        CONSTANT VELOCITY PROFILE
C                          ANNULAR FLOW
C **********************************************************************
                       IF(N.EQ.3) GO TO 55
                        TI02=INIA
                        TY02=YNIA
                         BX11=IN(MEA,1)
                        BXY1=KN(MEA,1)
                        TI04=(BX11/MEA)
                        TY04=(-BXY1/MEA)
                        TI06=(BXIA-2*TI04)
                        TY06=(-BXYA+2*TY04)
                          GO TO 656
 55                     TI02=INIA
                        TY02=YNIA
                        BINA2=IN(MEA,2)
                        BINA1=IN(MEA,1)
                        TI04=BINA2/MEA
                        BKNA2=KN(MEA,2)
                        BKNA1=KN(MEA,1)
                        TY04=-BKNA2/MEA
                         BINAN=IN(MEA,N)
                         BKNAN=KN(MEA,N)
                        TI06=(BINAN-3*(BINA2/MEA-BINA1/MEA**2))
                        TY06=(-BKNAN+3*(-BKNA2/MEA-BKNA1/MEA**2))
                            GO TO 656
C -----------------------------------------------------------------------
C                  INTEGRATION,  ANNULAR ,ANALYTICAL
C -----------------------------------------------------------------------
 212                    ALA2=1.02D0*ALA
                        ALAM=1.317D0*ALA
                        MEI2=1.02D0*MEI
                        MEIM=1.317*MEI
                        INON=IN(ALA2,N)
             KN00=KN(ALA2,0)
```

```
      KN01=KN(ALA2,1)
      KN02=KN(ALA2,2)
      KN0N=KN(ALA2,N)
        BINA0=IN(MEI2,0)
        BINA1=IN(MEI2,1)
        BINA2=IN(MEI2,2)
        BINAN=IN(MEI2,N)
        BKNA0=KN(MEI2,0)
        BKNA1=KN(MEI2,1)
        BKNA2=KN(MEI2,2)
         BKNAN=KN(MEI2,N)
C ------------------------------------------------------------------
               PK=CDLOG(ALA2/2)
   PKK=(PK+.577D0)*(ALA2**3/24+ALA2**5/768)-(11*ALA2**3/288
 & +37*ALA2**5/2304)/2+(16/ALA2**3-2/ALA2+ALA2/4)/2
           YNN=KN(ALA2,3)
           INL=IN(ALA2,3)
           PKS=ALA2**3/48+ALA2**5/768
               PI0=ALA2**4/48/4+ALA2**6/768/65
               PI1=ALA2**5/48/5+ALA2**7/768/7
           P0K=(ALA2**4/192*(.5777D0+PK-1/4.D0)+ALA2**6/4608*
 $  (.577D0+PK-1/6.D0))-(ALA2**4/1152*11+37*ALA2**6/13824)/2
 & +(-8/ALA2**2-2*PK+ALA2**2/8)/2
           P1K=(ALA2**5/48/5*(.5777D0+PK-1/5.D0)+ALA2**7/768/7*
 $  (.577D0+PK-1/7.D0))-(ALA2**5*11/5/288+37*ALA2**7/7/2304)/2
 &  +(-16/ALA2-2*ALA2+ALA2**3/3/4)/2
C ---------------------------------------------------------------------
C              (RM-R)/(RM-R1)
C ------------------------------------------------------------------
          ALAX=ALAM-ALA2
          MEIX=MEIM-MEI2
         CF1=CA0+CA1*(ALAM/ALAX)+CA2*ALAM**2/ALAX**2
         CF2=CA0+CA1*(MEIM/MEIX)+CA2*MEIM**2/MEIX**2
    TI02=(CA0+CA1+CA2)*INON+CA1*PI0/(ALAM)+2*CA2*(ALAM*PI0-PI1)
 &/(ALAM)**2
    TY02=(CA0+CA1+CA2)*KN0N+CA1*P0K/(ALAM)+2*CA2*(ALAM*P0K-P1K)
 &/(ALAM)**2
    TI04=(CF2)*(BINA2/MEI2-BINA1/MEI2**2)
 &-(CA1/MEIX+2*CA2*MEIM/MEIX**2)*(BINA2-2*BINA1/MEI2)
 & +CA2*(MEI2*BINA2-3*(BINA1-BINA1/MEI2))/MEIX**2
    TY04=(CF2)*(-BKNA2/MEI2-BKNA1/MEI2**2)
 &   -(CA1/MEIX+2*CA2*MEIM/MEIX**2)*(-BKNA2-2*BKNA1/MEI2)
 &  +CA2*(-MEI2*BKNA2+3*(-BKNA1-BKNA1/MEI2))/MEIX**2
    TI06=(CF2)*(BINAN-3*(BINA2/MEI2-BINA1/MEI2**2))
 &-(CA1/MEIX+2*CA2*MEIM/MEIX**2)*(MEI2*BINAN-4*(BINA2-2*BINA1/MEI2))
 & +CA2*(MEI2**2*BINAN-5*(MEI2*BINA2-3*
 & (BINA1-BINA1/MEI2)))/MEIX**2
   TY06=(CF2)*(-BKNAN+3*(-BKNA2/MEI2-BKNA1/MEI2**2))
 &-(CA1/MEIX+2*CA2*MEIM/MEIX**2)*(-MEI2*BKNAN+4*(-BKNA2-2*BKNA1/MEI2
 &))+CA2*(-MEI2**2*BKNAN+5*(-MEI2*BINA2+3
 &*(-BKNA1-BKNA1/MEI2)))/MEIX**2
C ---------------------------------------------------------------------
656     WRITE(6,772) PI0,PI1
 772    FORMAT('0','PI0=(',2D11.4,1X,')',2X,'PI1=(',2D11.4,1X,')')
        WRITE(6,872) P0K,P1K
 872    FORMAT('0','P0K=(',2D11.4,1X,')',2X,'P1K=(',2D11.4,1X,')')
        WRITE(6,172) TI02,TY02
 172    FORMAT('0','TI02=(',2D11.4,1X,')',2X,'TY02=(',2D11.4,1X,')')
```

```
      WRITE(6,182) TI04,TY04,TI06,TY06
182   FORMAT('0','TI04=(',2D11.4,1X,')',2X,'TY04=(',2D11.4,1X,')',
     & 2X,'TI06=(',2D11.4,1X,')',2X,'TY06=(',2D11.4,1X,')')
C -------------------------------------------------------------------
              SEI=EI**2*EPI
               NVIS=EPO/EPI
              XTT=NVIS/SEI
               U01=UO
C -------------------------------------------------------------------
              T(1,4)=(-2*I*X1*ALA*INPIA)*XTT
              T(1,5)=(-2*I*X1*ALA*YNPIA)*XTT
              T(1,6)=(-I*N*X1*BXIA)*XTT*EX1
              T(1,7)=(-I*N*X1*BXYA)*XTT
              T(1,8)=((1-X1**2+N)*BRIA-MEA*(1+N)*BRPIA-MEA**2*
     &        BRPPIA)*XTT*EX1
              T(1,9)=((1-X1**2+N)*BRYA-MEA*(1+N)*BRPYA-MEA**2*
     &        BRPPYA)*XTT
               T(2,4)=(2*N*INIA-2*N*ALA*INPIA)*XTT
               T(2,5)=(2*N*YNIA-2*N*ALA*YNPIA)*XTT
            T(2,6)=(MEA*BXPIA-N**2*BXIA-MEA**2*BXPPIA)*XTT*EX1
            T(2,7)=(MEA*BXPYA-N**2*BXYA-MEA**2*BXPPYA)*XTT
               T(2,8)=((1+N)*I*X1*BRIA-I*X1*MEA*BRPIA*XTT)*EX1
               T(2,9)=((1+N)*I*X1*BRYA-I*X1*MEA*BRPYA)*XTT
      T(3,4)=((I*KI*INIA+U01*(-I*X1)*TI02)/EI+2*ALA**2*INPPIA*XTT)
      T(3,5)=((I*KI*YNIA+U01*(-I*X1)*TY02)/EI+2*ALA**2*YNPPIA*XTT)
        T(3,6)=((-I*X1*N*U01*TI04)/EI+2*(MEA*N*BXPIA-N*BXIA)*XTT)*EX1
        T(3,7)=((-I*X1*N*U01*TY04)/EI+2*(MEA*N*BXPYA-N*BXYA)*XTT)
       T(3,8)=((-X1**2*U01*TI06)/EI/MEA+2*(-I*X1*MEA)*XTT*BRPIA)*EX1
       T(3,9)=((-X1**2*U01*TY06)/EI/MEA+2*(-I*X1*MEA)*XTT*BRPYA)
C --------------------------------------------------------------------
941              WRITE(6,69) TKJ
 69             FORMAT('0','TKJ')
                   DO 254 K=1,3
                   WRITE(6,255) (T(K,J),J=1,9)
255             FORMAT('0',10(D11.4,1X),//,8(D11.4,1X))
254           CONTINUE
C ---------------------------------------------------------------
C          ASSEMBLING MATRIX AA(9,9).
C---------------------------------------------------------------
         DO 223 K=1,3
         DO 224 J=1,3
            AA(K,J)=B(K,J)
224           CONTINUE
223           CONTINUE
         DO 213 K=1,3
         DO 214 J=4,9
              AA(K,J)=(0.0D0,0.D0)
214       CONTINUE
213       CONTINUE
         DO 313 K=4,9
         DO 312 J=1,3
          AA(K,J)=(0.D0,0.D0)
312       CONTINUE
313       CONTINUE
          DO 411 K=4,9
          DO 412 J=4,9
CC       AA(K,J)=(0.D0,0.D0)
         AA(K,J)=D(K-3,J-3)
```

```
 412         CONTINUE
 411          CONTINUE
                      DO 90 II=1,3
                      DO 90 KK=1,9
                     FTT(II,KK)=(0.D0,0.D0)
                       DO 90 JJ=1,9
                  FTT(II,KK)=FTT(II,KK)+T(II,JJ)*AA(JJ,KK)
  90                  CONTINUE
                 WRITE(6,601) FTTKJ
 601            FORMAT('0','FTTKJ')
           DO 716 K=1,3
                 WRITE(6,717) (FTT(K,J),J=1,4)
 717       FORMAT('0',6(D11.4,1X))
 716           CONTINUE
C*********     AERODYNAMIC FORCES   *************
             RP1=(KI-X1*UI)
             RP2=(KI-X1*UO*.7D0)
              QTXI(1)=(FTT(1,1)*RP1+FTT(1,4)*RP2)*ZI/I*EI
              QTXI(2)=(FTT(1,2)*RP1+FTT(1,5)*RP2)*ZI*EI
              QTXI(3)=(FTT(1,3)*RP1+FTT(1,6)*RP2)*ZI*EI
C
              QTETI(1)=(FTT(2,1)*RP1+FTT(2,4)*RP2)*ZI*EI
              QTETI(2)=(FTT(2,2)*(I*RP1)+FTT(2,5)*I*RP2)*ZI*EI
           QTETI(3)=(FTT(2,3)*RP1+FTT(2,6)*RP2)*I*ZI*EI
C
              QTRI(1)=(FTT(3,1)*RP1+FTT(3,4)*RP2)*ZI*EI
              QTRI(2)=(FTT(3,2)*(I*RP1)+FTT(3,5)*RP2*I)*ZI*EI
           QTRI(3)=(FTT(3,3)*RP1+FTT(3,6)*RP2)*I*ZI*EI
C -------------------------------------------------------------
               DO 177 L=1,3
                WRITE(6,178) QTXI(L)
 178           FORMAT('0',2(D11.4,1X))
 177           CONTINUE
                DO 606 L=1,3
                  WRITE(6,607) QTETI(L)
 607              FORMAT('0',2(D11.4,1X))
 606           CONTINUE
                DO 608 L=1,3
                WRITE(6,609) QTRI(L)
 609             FORMAT('0',2(D11.4,1X))
 608            CONTINUE
 111             CONTINUE
                 RETURN
                  END
C ------ --------------------------------
      COMPLEX FUNCTION IN*16(X,N)
      IMPLICIT REAL*8(A-Z)
      COMPLEX*16 X,T,T1,T2,T3,T4,I,T5,XXX
      INTEGER K,N,M
      COMMON PI,GAMA
      I=(0.D0,1.D0)
      IF(CDABS(X).GE.15.D0) GO TO 10
      IN=(0.D0,0.D0)
      K=0
  11  T=(X/2)**(2*K)/FA(K)/FA(N+K)
      IF(CDABS(T).LT.1.D-12) GO TO 12
      IN=IN+T
      K=K+1
```

```
      GO TO 11
 12   IN=(X/2)**N*IN
      GO TO 36
 10   T2=(1.0D0/2.0D0/PI/X)
      T3=CDSQRT(T2)
        TEI1=X
         T5=-I*X
        TEI2=T5
        T1=(4*N**2-1)/(8*X)
        XXX=I*(TEI2+N+1/2)*PI
         IF(TEI1.GT.0.D0) GO TO 115
          XXX=I*TEI2
         IN=T3*(1.0D0-T1)*CDEXP(XXX)
          GO TO 36
115      IN=T3*(1+T1)*CDEXP(I*TEI2)
C 15      WRITE(6,51) T1,T2,T3,T4
C 51   FORMAT('0','T1=(',2D11.4,1X,')',2X,'T2=(',2D11.4,1X,')',2X,'T3=(
C    &',2D11.4,1X,')',2X,'T4=(',2D11.4,1X,')')
C36    WRITE(6,52) IN
C52   FORMAT('0','IN=(',2D11.4,1X,')')
 36   RETURN
      END
C ---------------------------------
      COMPLEX FUNCTION KN*16(X,N)
      IMPLICIT REAL*8(A-Z)
      COMPLEX*16 X,KN1,T,T1,T2,T3,T5,XXX,II
      INTEGER N,ML,K,I
      COMMON PI,GAMA
         PI=3.1416D0
            GAMA=0.5772D0
      IF(CDABS(X).GE.15.D0) GO TO 40
      IF(N.EQ.0) GO TO 46
      KN=FA(N-1)*(2/X)**N
       IF(N.EQ.1) GO TO 45
      ML=N-1
       DO 41 I=1,ML
 41   KN=KN+(-1)**I*FA(N-I-1)/FA(I)*(2/X)**(N-2*I)
 45   KN=KN/2
      GO TO 47
 46   KN=(0.D0,0.D0)
 47   KN1=(0.D0,0.D0)
      K=0
 43   T=(X/2)**(N+2*K)/FA(K)/FA(N+K)*(CDLOG(X/2)-(F(K+1)+F(N+K+1))/2)
      IF(CDABS(T).LT.1.D-12) GO TO 42
      KN1=KN1+T
      K=K+1
      GO TO 43
 42   KN=KN+KN1*(-1)**(N+1)
      RETURN
 40   T1=(4*N**2-1)/8/X
      T2=T1*(4*N**2-9)/16/X
      T3=1.D0*CDSQRT(PI/2/X)
        II=(0.D0,1.0D0)
        TEI1=X
        T5=-II*X
        TEI2=T5
        XXX=II*TEI2
      KN=T3*(1+T1+T2)*CDEXP(-XXX)
```

```
      RETURN
      END
C
      DOUBLE PRECISION FUNCTION R(K)
      IMPLICIT REAL*8(A-Z)
      INTEGER K,I
      R=0.D0
      DO 40 I=1,K
   40 R=R+1.D0/I
      RETURN
      END
C
      DOUBLE PRECISION FUNCTION F(K)
      IMPLICIT REAL*8(A-Z)
      INTEGER K
      COMMON PI,GAMA
      IF(K.EQ.1) GO TO 50
      F=R(K-1)-GAMA
      RETURN
   50 F=-GAMA
      RETURN
      END
C
      DOUBLE PRECISION FUNCTION FA(K)
       IMPLICIT REAL*8(A-Z)
      INTEGER K,L
      FA=1.D0
      L=1
   21 FA=FA*L
      IF(L.GE.K) GO TO 22
      L=L+1
      GO TO 21
   22 CONTINUE
      RETURN
      END
C*********************************************************************
C*     MATRIX AAA**
C*
C*********************************************************************
C  THIS PART IS USED TO ASSEMBLE MATRIX AAA WHICH CONTAINS THE*
C  FREE VIBRATIONS TERMS COE,THE STEADY FORCES CCOE,AND THE UNSTEADY*
C  FORCES QTXI,...*
C**********************************************************************
      SUBROUTINE MATRA(KI,AAA)
      IMPLICIT REAL*8(A-H,O-Z)
      COMPLEX*16 AAA(3,3),QTXI(3),CKMN(36)
     &,QTETI(3),QTRI(3),KI,UO,COE(2,9),CCOE(2,9)
      DIMENSION AK(3,3),BK(3,3)
      INTEGER N,JL
      COMMON/DATA1/NI,NO,SKI,SKO,CIG(3),P(3),N
      COMMON/DATA2/EI,EO,ER,HR,URR
      COMMON/DATA3/ZI,ZO,USR,DSR
      COMMON/DATA5/PPI,PPO,PO(2),PL(2),RMS,DEN,DDI,DDO,VIS,CA,CB
      COMMON/COCE/COE
      COMMON/CRCE/CCOE
      COMMON/CLLE/QTXI,QTETI,QTRI
           AK(1,1)=.5D0
           BK(1,1)=.25D0
```

```
          JJ=1
          CKMN(1)=(COE(JJ,1)
     &    +QTXI(1)+KI**2)*AK(1,1)+CCOE(JJ,1)
          CKMN(2)=(COE(JJ,4)+QTXI(2))*AK(1,1)+CCOE(JJ,4)
          CKMN(3)=(COE(JJ,7)+QTXI(3))*AK(1,1)+CCOE(JJ,7)
C
          CKMN(7)=(COE(JJ,2)+QTETI(1))*AK(1,1)+CCOE(JJ,2)
          CKMN(8)=(COE(JJ,5)+
     &    QTETI(2)+KI**2)*AK(1,1)+CCOE(JJ,5)
          CKMN(9)=(COE(JJ,8)+QTETI(3))*AK(1,1)+CCOE(JJ,8)
C
          CKMN(13)=(COE(JJ,3)+QTRI(1))*AK(1,1)+CCOE(JJ,3)
          CKMN(14)=(COE(JJ,6)+QTRI(2))*AK(1,1)+CCOE(JJ,6)
          CKMN(15)=(COE(JJ,9)+
     &    QTRI(3)+KI**2)*AK(1,1)+CCOE(JJ,9)
C
          AAA(1,1)=CKMN(1)
          AAA(1,2)=CKMN(2)
          AAA(1,3)=CKMN(3)
            AAA(2,1)=CKMN(7)
            AAA(2,2)=CKMN(8)
            AAA(2,3)=CKMN(9)
            AAA(3,1)=CKMN(13)
            AAA(3,2)=CKMN(14)
            AAA(3,3)=CKMN(15)
             DO 420 K=1,3
           WRITE(6,419) (AAA(K,J),J=1,3)
 419        FORMAT('0',6(D11.4,1X))
 420       CONTINUE
      RETURN
      END
C***********************************************************************
C     COMPLEX FUNCTION DET                                             *
C***********************************************************************
      COMPLEX FUNCTION DET*16(A,L,M,N)
      DIMENSION A(N,N),L(N),M(N)
      COMPLEX*16 A,PIVOT,HOLD
      INTEGER END,ROW,COL,PIVROW,PIVCOL
      END=N-1
      DET=(1.D0,0.D0)
      DO 10 I=1,N
      L(I)=I
   10 M(I)=I
      DO 100 LMNT=1,END
      PIVOT=(0.D0,0.D0)
      DO 20 I=LMNT,N
      ROW=L(I)
      DO 20 J=LMNT,N
      COL=M(J)
      IF(CDABS(PIVOT).GE.CDABS(A(ROW,COL))) GO TO 20
      PIVROW=I
      PIVCOL=J
      PIVOT=A(ROW,COL)
   20 CONTINUE
      IF(PIVROW.EQ.LMNT) GO TO 22
      DET=-DET
      KEEP=L(PIVROW)
      L(PIVROW)=L(LMNT)
```

```
      L(LMNT)=KEEP
   22 IF(PIVCOL.EQ.LMNT) GO TO 26
      DET=-DET
      KEEP=M(PIVCOL)
      M(PIVCOL)=M(LMNT)
      M(LMNT)=KEEP
   26 DET=DET*PIVOT
      IF(CDABS(PIVOT).EQ.0.D0) GO TO 333
      JAUG=LMNT+1
      PIVROW=L(LMNT)
      PIVCOL=M(LMNT)
      DO 100 I=JAUG,N
      ROW=L(I)
      HOLD=A(ROW,PIVCOL)/PIVOT
      DO 100 J=JAUG,N
      COL=M(J)
  100 A(ROW,COL)=A(ROW,COL)-HOLD*A(PIVROW,COL)
      DET=DET*A(ROW,COL)
  333 RETURN
      END
```

APPENDIX M

PROGRAM FOR VISCOUS THEORY USING FOURIER TRANSFORM METHOD

This program considers only internal flow with unsteady viscous forces. The program calculates Ω for variable $\bar{U}_i$. The shell could be clamped or pinned at both ends.

Program Structure

MAIN PROGRAM

SUBROUTINE POLEMAT

SUBROUTINE ZANLYT

SUBROUTINE UNSFOR

SUBROUTINE MATRA

COMPLEX FUNCTION HXX

COMPLEX FUNCTION DET

COMPLEX FUNCTION IW

DOUBLE PRECISION FUNCTION R

DOUBLE PRECISION FUNCTION F

DOUBLE PRECISION FUNCTION FA

```
C*********************************************************************
C     COMPUTER PROGRAM FOR THE CASE OF UNSTEADY VISCOUS FORCES        *
C     USING FOURIER TRANSFORM METHOD                                  *
C                        CLAMPED-CLAMPED SHELL
C*********************************************************************
C
C*********************************************************************
C     MAIN PROGRAM                                                    *
C*********************************************************************
      IMPLICIT REAL*8(A-H,O-Z)
       COMPLEX*16 QQTXI(6,3,3),QQTETI(6,3,3),QQTRI(6,3,3),QQTXO(6,3,
     #3),QQTETO(6,3,3),QQTRO(6,3,3),AAA(9,9),COEM(3,3,3),XY(3),
     #B(8),UN[illegible],FS,UO,MIL,COE(2,9,3,3),CCOE(2,9,3,3)
      INTEGER IJ,K,M,INFER(3),J,MS,N
        EXTERNAL FS
      REAL*8 NI,NO,WA(8),UI
      COMMON/DATA1/NI,NO,SKI,SKO,CIG(3),P(3),N
      COMMON/DATA2/EI,EO,ER,HR,URR
      COMMON/DATA3/ZI,ZO,USR,DSR
      COMMON/DATA7/UI,UO
      COMMON/AREA1/AAA
      COMMON/DATA5/PPI,PPO,PO(2),PL(2),RMS,DEN,DDI,DDO,VIS,CA,CB
      DATA EPS/1.D-10/,NSIG/5/,NGUESS/1/,ITMAX/12/,II/1/
      DATA IA/8/,IB/8/,NN/8/,IJOB/0/,IZ/36/
      COMMON/COCE/COE
      COMMON/COEF/CCOE
      COMMON/CLLE/QQTXI,QQTETI,QQTRI,QQTXO,QQTETO,QQTRO
      PI=3.141617D0
      CIG(1)=0.98250221457623D0
      CIG(2)=1.00077731190727D0
      CIG(3)=0.99996645012540D0
      P(1)=4.7300407448627D0
      P(2)=7.85320462409584D0
      P(3)=10.99560783800167D0
C         ----------------------------
C              WATER STEEL
C ---------------------------------
      EI=1/11.D0
      EO=1/10.D0
      HR=1.0D0
      URR=1.0D0
      ER=EI/EO
      NI=0.3D0
      SKI=(5.5D-3)**2/12
      ZI=23.3D0
      DSR=1.D0
      USR=1.D0
      N=3
      DEN=998.0D0
C -------------------------------------------
         CALL CONT(CIG,P)
         CALL PREMAT(COEM)
      UI=0.02D0
      UO=(0.00D0,0.D0)
       MS=1
       NK=MS-1
      XY(1)=(.418D-5,-.135D-3)
C
```

```
      CALL ZANLYT(FS,EPS,NSIG,NK,NGUESS,II,XY,ITMAX,INFER,IER)
            CALL UNSFO(UI,UO,XY(1),MIL)
      CALL MATRA(UI,UO,XY(1),AAA)
CC
      PRINT 111,XY(MS)
 111  FORMAT('-','FREQUENCY AT A SPECIFIC VELOCITY TO STUDY THE
     & INSTABILITY=(',2D11.4,1X,')')
         PRINT 155,INFER(1)
 155        FORMAT('0','NO.OF ITERATIONS REQUIRED=',I3/)
            PRINT30
 30           FORMAT('1')
      PRINT10,UI,UO
  10  FORMAT('1','FLOW VELOCITY INSIDE THE INNER CYLINDER=',F8.5/'0','FL
     #OW VELOCITY IN THE ANNULAR REGION=',F8.5)
      STOP
      END
C*********************************************************************
C     SUBROUTINE CONT                                                *
C*********************************************************************
      SUBROUTINE CONT(CIG,P)
      IMPLICIT REAL*8(A-H,O-Z)
      DIMENSION A(3,3),B(3,3),CIG(3),D(3,3),SE(3,3),SF(3,3),G(3,3),
     #H(3,3),SJ(3,3),SL(3,3),DEL(3,3),P(3)
      INTEGER DEL
      COMMON/CON1/A,B,D,DEL
      COMMON/CON2/SE,SF,G,H,SJ,SL
      DO 3 K=1,3
      DO 3 M=1,3
      IF(K.EQ.M) GO TO 1
      DEM=P(M)**4-P(K)**4
      PC=P(M)*CIG(M)-P(K)*CIG(K)
      PWR=(-1)**(K+M)
      PMKS=P(M)**2*P(K)**2
      A(K,M)=-4*PMKS*(PWR+1)*PC/DEM
      B(K,M)=0.D0
      D(K,M)=-A(K,M)
      SE(K,M)=4*(3*P(M)**4+P(K)**4)*PMKS*P(M)*P(K)*(1-PWR)/DEM**2
      SF(K,M)=4*PMKS*(1-PWR)/DEM
      G(K,M)=-4*PWR*PMKS*PC/DEM-2*(P(M)**4+P(K)**4)*SF(K,M)/DEM
      SL(K,M)=-SF(K,M)
      H(K,M)=4*PWR*PMKS*PC/DEM-(3*P(M)**4+P(K)**4)*SL(K,M)/DEM
      SJ(K,M)=16*PMKS*P(M)*P(K)*CIG(M)*CIG(K)*(PWR-1)/DEM**2
      DEL(K,M)=0
      GO TO 3
  1   A(K,K)=P(K)*CIG(K)*(P(K)*CIG(K)-2)
      B(K,K)=-P(K)**4
      D(K,K)=-A(K,K)
      SE(K,K)=-B(K,K)/2
      SF(K,K)=0:D0
      G(K,K)=A(K,K)/2
      H(K,K)=-G(K,K)
      SJ(K,K)=0.5D0
      SL(K,K)=0.D0
      DEL(K,K)=1
  3   CONTINUE
      RETURN
      END
C
```

```
C*************************************************************************
C      SUBROUTINE PREMAT                                                  *
C*************************************************************************
       SUBROUTINE PREMAT(COEM)
       IMPLICIT REAL*8(A-H,O-Z)
       DIMENSION A(3,3),B(3,3),D(3,3),DEL(3,3)
       COMPLEX*16 COE(2,9,3,3),COEM(3,3,3)
       REAL*8 NI,NO,NU
       INTEGER R,Q,W,V,H,KK,IJ
       COMMON/DATA1/NI,NO,SKI,SKO,CIG(3),P(3),N
       COMMON/DATA2/EI,EO,ER,HR,URR
       COMMON/CON1/A,B,D,DEL
       COMMON/COCE/COE
       DO 3 K=1,3
       DO 3 M=1,3
       COEM(1,K,M)=A(K,M)
       COEM(2,K,M)=DEL(K,M)
   3   COEM(3,K,M)=DEL(K,M)
       J=0
       E=EI
       NU=NI
       SK=SKI
  12   JJ=J+1
       DO 4 K=1,3
       DO 4 M=1,3
       COE(JJ,1,K,M)=(E**2*B(K,M)+(NU-1)*(SK+1)*N**2*A(K,M)/2)
       COE(JJ,2,K,M)=-(1+NU)*N*E**2*D(K,M)/2
       COE(JJ,3,K,M)=(P(M)*E)**4*SK*DEL(K,M)-(2*NU-SK*(1-NU)*N**2)
      C*E**2*D(K,M)/2
       COE(JJ,4,K,M)=(1+NU)*N*A(K,M)/2
       COE(JJ,5,K,M)=-N**2*DEL(K,M)+(1+3*SK)*(1-NU)*E**2*D(K,M)/2
       COE(JJ,6,K,M)=SK*(3-NU)*N*E**2*D(K,M)/2-N*DEL(K,M)
       COE(JJ,7,K,M)=((NU+(NU-1)*SK*N**2/2)*A(K,M)-SK*E**2*B(K,M))
       COE(JJ,8,K,M)=-N*DEL(K,M)+(3-NU)*SK*N*E**2*D(K,M)/2
       COE(JJ,9,K,M)=-SK*(((P(M)*E)**4+(N**2-1)**2)*DEL(K,M)-2*(N*E)
      #**2*D(K,M))-DEL(K,M)
   4   CONTINUE
          DO 444 KK=1,9
           DO 444 K=1,3
           DO 444 M=1,3
                WRITE(6,445) COE(IJ,KK,K,M)
 445             FORMAT('0',2(D11.4,1X))
 444                CONTINUE
       RETURN
       END
C*************************************************************************
C      COMPLEX FUNCTION FS                                                *
C*************************************************************************
       COMPLEX FUNCTION FS*16(KI)
       IMPLICIT REAL*8(A-Z)
       COMPLEX*16 KI,RES,QB(3,3),AAA(9,9),DET,UO,MIL
       INTEGER L(9),M(9),K,J
       COMMON/DATA7/UI,UO
       COMMON/AREA1/AAA
          CALL UNSFO(UI,UO,KI,MIL)
         CALL MATRA(UI,UO,KI,AAA)
       FS=DET(AAA,L,M,9)
          PRINT 11,FS
```

```
11    FORMAT('0','FS=',2(D11.4,1X))
        PRINT 116,KI
116   FORMAT('0','KI=',2(D11.4,1X))
      RETURN
      END
C
C ******************************************************************
C     SUBROUTINE UNSFOR(QTETI)*
C*******************************************************************
C    THIS PROGRAM IS TO CALCULATE THE UNSTEADY FORCES CAUSED BY*
C      THE PERTURBATIONS*
C*******************************************************************
C
           SUBROUTINE UNSFO(UI,UO,KI,MIL)
           IMPLICIT COMPLEX*16(A-Z)
           COMPLEX*16  A(3,3),B(3,3),D(6,6),T(6,10),QTXI(6,3,3),ST(4,4)
         COMPLEX*16 'QTETI(6,3,3),QTRI(6,3,3),QTXO(6,3,3),QTETO(6,3,3)
     &,QTRO(6,3,3),QQTETI(6,3,3),QQTRI(6,3,3),QQTXI(6,3,3),QTRI1(6,3,3),
     &QQTETO(6,3,3),QQTRO(6,3,3),QQTXO(6,3,3),QTXXI(6,3,3),QTRO1(6,3,3),
     &QTRRI(6,3,3),QTETTI(6,3,3),QTXXO(6,3,3),QTETTO(6,3,3),QTRRO(6,3,3)
           COMPLEX*16  C(6,6),E(6,6),AA(10,10),FTT(6,10),MIL
           REAL*8 EI,EO,X1,X2,CIG,P,PI,GAMA,UI,ZI,ZO,DSR,USR,HR,ER,URR
           REAL*8 WK(3),WF(6),NI,NO,SKI,SKO,SU,LEN,VIS
           INTEGER N,K,L,M,NN,MM,IB,IA,IJOB,IER,IL,IS,IM,NF,NM,J
           INTEGER LL,MS,NB,IC,K1,M2,M1,II,JJ,KK,IJ,LI,JK
           COMMON PI,GAMA
           COMMON/DATA1/NI,NO,SKI,SKO,CIG(3),P(3),N
           COMMON/DATA2/EI,EO,ER,HR,URR
           COMMON/DATA3/ZI,ZO,USR,DSR
           COMMON/CLLE/QQTXI,QQTETI,QQTRI,QQTXO,QQTETO,QQTRO
           INP(Y)=(IN(Y,N-1)+IN(Y,N+1))/2
           INF(Y)=(IN(Y,M-1)+IN(Y,M+1))/2
           INPP(Y)=(IN(Y,N-2)/2+IN(Y,N)+IN(Y,N+2)/2)/2
           INFF(Y)=(IN(Y,M-2)/2+IN(Y,M)+IN(Y,M+2)/2)/2
              GAMA=.5772156649011G1D0
              PI=3.14159265358979D0
C ------------------------------------------
C             WATER-STEEL
C ------------------------------------------
            SU=5308.0D0
            LEN=1.0D0
            VIS=1.121D-06
C -------------------------
           EPI=SU*LEN/VIS
           EPO=EPI
           UAVI=UI*.8D0
           UAVO=UO*.8D0
            RFE=1.D0
           RHE=1.D0
           RHOE=RHE/EPO
           M=N+1
           DT=2,D0
           X1=-20+DT/2*(1-DSQRT(1/3.D0))
           X2=-20+DT/2*(1+DSQRT(1/3.D0))
           DO 955 IJ=1,3
           DO 955 K=1,3
           DO 955 M2=1,3
              QTXXI(IJ,K,M2)=(0.D0,0.D0)
```

```
          QTRRI(IJ,K,M2)=(0.D0,0.D0)
          QTETTI(IJ,K,M2)=(0.D0,0.D0)
955         CONTINUE
         DO 737 LI=1,41
       S1=X1
      ALA=S1*EI
      ALB=S1*EO
      I=(0.D0,1.D0)
      MIL=CDSQRT(KI/EI*EPI*I+X1**2)
      MEI=EI*MIL
      M=N+1
C ---------------------------------------------------
C            INTERNAL FLOW R=A
C ---------------------------------------------------
      INIA=IN(ALA,N)
      INPIA=INP(ALA)
      INPPIA=INPP(ALA)
      BRI1=IN(MEI,M)
      BXI1=IN(MEI,N)
      BXPI1=INP(MEI)
      BRPI1=INF(MEI)
      BXPPI1=INPP(MEI)
      BRPPI1=INFF(MEI)
C ---------------------------------------------------------
  9     PRINT11,MEI,MEA,MEO
  11    FORMAT('0','MEI=(',2D11.4,1X,')',2X,'MEA=(',2D11.4,1X,')'
     & ,2X,'MEO=(',2D11.4,1X,')')
      PRINT12,INIA,INPIA
 12   FORMAT('0','INIA=(',2D11.4,1X,')',2X,'INPIA=(',2D11.4,1X,')')
     PRINT13,BRI1
 13   FORMAT('0','BRI1=(',2D11.4,1X,')')
      PRINT14,BXI1
 14   FORMAT('0','BXI1=(',2D11.4,1X,')')
C ---------------------------------------------
C   INVERSION OF MATRIX A
C ---------------------------------------------------
195   A(1,1)=-I*X1*EI*INIA
      A(1,2)=(0.D0,0.D0)
       A(1,3)=-(MEI*BRPI1+(N+1)*BRI1)
       A(2,1)=-N*INIA
        A(2,2)=(-MEI*BXPI1)
        A(2,3)=-X1*EI*I*BRI1
        A(3,1)=ALA*INPIA
           A(3,2)=(N*BXI1)
            A(3,3)=-I*X1*EI*BRI1
C ---------------------------------------------
            WRITE(6,82) AKJ
 82          FORMAT('0','AKJ')
           DO 34 K=1,3
           WRITE(6,71) (A(K,J),J=1,3)
 71         FORMAT('0',6(D11.4,1X))
 34         CONTINUE
C ---------------------------------------------------------
            DD=A(2,2)*(A(3,3)*A(1,1)-A(3,1)*A(1,3))-A(3,2)*(A(1,1)*
     &      A(2,3)-A(1,3)*A(2,1))
            B(3,1)=(A(3,2)*A(2,1)-A(3,1)*A(2,2))/DD
            B(3,2)=-A(3,2)*A(1,1)/DD
```

```
               B(3,3)=A(2,2)*A(1,1)/DD
               SS=A(1,1)*A(2,3)-A(1,3)*A(2,1)
               B(2,1)=-(A(2,1)+SS*B(3,1))/A(1,1)/A(2,2)
               B(2,2)=(A(1,1)-SS*B(3,2))/A(1,1)/A(2,2)
               B(2,3)=-SS*B(3,3)/A(1,1)/A(2,2)
               B(1,1)=(1-A(1,3)*B(3,1))/A(1,1)
               B(1,2)=-A(1,3)*B(3,2)/A(1,1)
               B(1,3)=-A(1,3)*B(3,3)/A(1,1)
               WRITE(6,53) BKJ
 53            FORMAT('0','BKJ')
              DO 44 K=1,3
              WRITE(6,99) (B(K,J),J=1,3)
 99            FORMAT('0',6(D11.4,1X))
 44             CONTINUE
                    DO 61 II=1,3
                    DO 61 KK=1,3
                   ST(II,KK)=(0.D0,0.D0)
                     DO 61 JJ=1,3
                 ST(II,KK)=ST(II,KK)+A(II,JJ)*B(JJ,KK)
 61                 CONTINUE
                WRITE(6,501) STKJ
 501            FORMAT('0','STKJ')
          DO 516 K=1,3
                WRITE(6,517) (ST(K,J),J=1,3)
 517      FORMAT('0',6(D11.4,1X))
 516          CONTINUE
C ---------------------------------------------------------------------
            IF(N.EQ.3) GO TO 36
            TI2=INIA
            TI4=-BXI1/MEI
            TI6=-BXI1+2*TI4
             GO TO 136
 36          TI2=INIA
             BX11=IN(MEI,1)
             BX21=IN(MEI,2)
             TI4=BX21/MEI-BX11/MEI**2
             TI6=BXI1-3*TI4
 136                T(1,1)=-(-2*I*X1*S1*INPIA)/EPI
                   T(1,2)=-(-I*N*X1*BXI1)/EPI/EI
     T(1,3)=-((1/EI**2-X1**2+N/EI**2)*BRI1-MIL*(1+N)*BRPI1/EI-MIL**2*
    &              BRPPI1)/EPI
                   T(1,4)=(0.D0,0.D0)
                    T(2,1)=-(2*N*INIA/EI**2-2*N*S1*INPIA/EI)/EPI
      T(2,2)=-(MIL/EI*BXPI1-N**2/EI**2*BXI1-MIL**2*BXPPI1)/EPI
         T(2,3)=-((1+N)*I*X1/EI*BRI1-I*X1*MIL*BRPI1)/EPI
                     T(2,4)=(0.D0,0.D0)
     T(3,1)=-((I*KI/EI*INIA+UI*(-I*X1)*TI2)+2*S1**2*INPPIA/EPI)
        T(3,2)=-((-I*X1*N*UI*TI4)+2*(MIL*N*BXPI1/EI-N*BXI1/EI**2)/EPI)
      T(3,3)=-((-X1**2*UI*TI6)/MIL+2*(-I*X1*MIL)/EPI*BRPI1)
                     T(3,4)=(0.D0,0.D0)
                      WRITE(6,69) TKJ
 69                FORMAT('0','TKJ')
                      DO 254 K=1,3
                      WRITE(6,255) (T(K,J),J=1,4)
 255              FORMAT('0',8(D11.4,1X))
 254            CONTINUE
                DO 223 K=1,3
                  DO 224 J=1,3
```

```
                 AA(K,J)=B(K,J)
  224         CONTINUE
  223         CONTINUE
              DO 213 K=1,3
                 AA(K,4)=(0.D0,0.D0)
  213            CONTINUE
                 DO 312 J=1,3
                AA(4,J)=(0.D0,0.D0)
  312            CONTINUE
                  AA(4,4)=(0.D0,0.D0)
 C                AA(4,4)=1/(X1*KNPIA)
                    DO 90 II=1,3
                    DO 90 KK=1,4
                   FTT(II,KK)=(0.D0,0.D0)
                     DO 90 JJ=1,4
                FTT(II,KK)=FTT(II,KK)+T(II,JJ)*AA(JJ,KK)
  90                CONTINUE
               WRITE(6,601) FTTKJ
  601          FORMAT('0','FTTKJ')
         DO 716 K=1,3
               WRITE(6,717) (FTT(K,J),J=1,4)
  717    FORMAT('0',6(D11.4,1X))
  716        CONTINUE
 C
                DO 797 K1=1,3
               DO 797 M2=1,3
              HKM=HXX(X1,K1,M2)
              GKM=I*X1*HKM
 C
 C*********    AERODYNAMIC FORCES  *************
             UAVI=UI
             RP1=(X1*KI/EI-X1**2*UAVI)*EI**2
             RP2=I*(KI/EI-X1*UAVI)*EI
 C
            QTXI(1,K1,M2)=FTT(1,1)*RP1*GKM
            QTXI(2,K1,M2)=FTT(1,2)*RP2*GKM
            QTXI(3,K1,M2)=(FTT(1,3)+FTT(1,4))*RP2*GKM
 C
            QTETI(1,K1,M2)=FTT(2,1)*RP1*HKM
            QTETI(2,K1,M2)=FTT(2,2)*RP2*HKM
            QTETI(3,K1,M2)=(FTT(2,3)+FTT(2,4))*RP2*HKM
 C
            QTRI(1,K1,M2)=FTT(3,1)*RP1*HKM
            QTRI(2,K1,M2)=FTT(3,2)*RP2*HKM
            QTRI(3,K1,M2)=(FTT(3,3)+FTT(3,4))*RP2*HKM
 C
 C
              DO 966 IJ=1,3
                   QTXXI(IJ,K1,M2)=QTXXI(IJ,K1,M2)+QTXI(IJ,K1,M2)
                   QTRRI(IJ,K1,M2)=QTRRI(IJ,K1,M2)+QTRI(IJ,K1,M2)
                   QTETTI(IJ,K1,M2)=QTETTI(IJ,K1,M2)+QTETI(IJ,K1,M2)
  966              CONTINUE
  797               CONTINUE
                   X1=X1+DT
                       IF(LI.EQ.21) X1=X2
  737             CONTINUE
        DO 301 IJ=1,3
        DO 301 K=1,3
```

```
      DO 301 M=1,3
          QQTXI(IJ,K,M)=ZI*QTXXI(IJ,K,M)/2/PI
301       CONTINUE
      DO 305 IJ=1,3
      DO 305 K=1,3
      DO 305 M=1,3
           QQTETI(IJ,K,M)=ZI*EI*QTETTI(IJ,K,M)/2/PI
           QQTRI(IJ,K,M)=ZI*EI*QTRRI(IJ,K,M)/2/PI
305         CONTINUE
299            RETURN
               END
C ----------------------------------------------
      COMPLEX FUNCTION HXX*16(AB,K1,M2)
      IMPLICIT COMPLEX*16(A-Z)
      REAL*8 AB,CIG,P,AB1,NI,NO,SKI,SKO
      INTEGER K1,M2,J,M1,N
      COMMON/DATA1/NI,NO,SKI,SKO,CIG(3),P(3),N
      CIG(1)=0.98250221457623D0
      CIG(2)=1.00077731190727D0
      CIG(3)=0.99996645012540D0
      P(1)=4.7300407448627D0
      P(2)=7.85320462409584D0
      P(3)=10.99560783800167D0
      HXX=(1.D0,0.D0)
      I=(0.D0,1.D0)
      AB1=AB
      M1=M2
      DO 1 J=1,2
      IF(DABS(AB).EQ.M1) GO TO 10
      A=2*CIG(M1)*P(M1)**3
      B=I*2*P(M1)**2
      E1=(-1)**(M1+1)*CDEXP(I*AB1)+1
      E2=E1-B
      IM=(A*E1-B*AB1*E2)/(AB1**4-P(M1)**4)
      GO TO 11
 10   IF(J.EQ.2) GO TO 20
      IM=((I*CIG(M1)*P(M1)**3-I*P(M1)**2+AB*P(M1)**2)*(-1)**(M1+1)*
     #CDEXP(I*AB)+I*P(M1)**2)/(-2*AB**3)
      GO TO 11
 20   IM=((-I*CIG(M1)*P(M1)**3+I*P(M1)**2+AB*P(M1)**2)*(-1)**(M1+1)*
     #CDEXP(-I*AB)-I*2*P(M1)**2)/(-2*AB**3)
 11   HXX=HXX*IM
      M1=K1
      AB1=-AB
 1    CONTINUE
      RETURN
      END
C*****************************************************************
C     SUBPROGRAMS FOR CALCULATING THE BESSEL FUNCTIONS           *
C*****************************************************************
      COMPLEX FUNCTION IN*16(X,N)
      IMPLICIT REAL*8(A-Z)
      COMPLEX*16 X,T,T1,T2,T3,T4,I,T5,XXX
      INTEGER K,N,M
      COMMON PI,GAMA
      I=(0.D0,1.D0)
      IF(CDABS(X).GE.15.D0) GO TO 10
      IN=(0.D0,0.D0)
```

```
      K=0
   11 T=(X/2)**(2*K)/FA(K)/FA(N+K)
      IF(CDABS(T).LT.1.D-12) GO TO 12
      IN=IN+T
      K=K+1
      GO TO 11
   12 IN=(X/2)**N*IN
      GO TO 36
   10 T2=(1.0D0/2.0D0/PI/X)
      T3=CDSQRT(T2)
        TEI1=X
         T5=-I*X
        TEI2=T5
        T1=(4*N**2-1)/(8*X)
        XXX=I*(TEI2+N+1/2)*PI
         IF(TEI1.GT.0.D0) GO TO 115
          XXX=I*(TEI2+N+1/2)*PI
         IN=T3*(1.0D0-T1)*CDEXP(XXX)
          GO TO 36
  115    IN=T3*(1+T1)*CDEXP(I*TEI2)
  36  RETURN
      END
C
      DOUBLE PRECISION FUNCTION R(K)
      IMPLICIT REAL*8(A-Z)
      INTEGER K,I
      R=0.D0
      DO 40 I=1,K
   40 R=R+1.D0/I
      RETURN
      END
C
      DOUBLE PRECISION FUNCTION F(K)
      IMPLICIT REAL*8(A-Z)
      INTEGER K
      COMMON PI,GAMA
      IF(K.EQ.1) GO TO 50
      F=R(K-1)-GAMA
      RETURN
   50 F=-GAMA
      RETURN
      END
C
      DOUBLE PRECISION FUNCTION FA(K)
       IMPLICIT REAL*8(A-Z)
      INTEGER K,L
      FA=1.D0
      L=1
   21 FA=FA*L
      IF(L.GE.K) GO TO 22
      L=L+1
      GO TO 21
   22 CONTINUE
      RETURN
      END
C*********************************************************************
C*********************************************************************
C*      MATRIX AAA**
```

```
C*
C*************************************************************************
C  THIS PART IS USED TO ASSEMBLE MATRIX AAA WHICH CONTAINS THE*
C  FREE VIBRATIONS TERMS COE,THE STEADY FORCES CCOE,AND THE UNSTEADY*
C  FORCES QTXI,...*
C*************************************************************************
      SUBROUTINE MATRA(UI,UO,KI,AAA)
      IMPLICIT REAL*8(A-H,O-Z)
      COMPLEX*16 AAA(9,9),CK(2,3,3),QTXI(6,3,3),QQTXI(6,3,3),
     $QTETI(6,3,3),QQTETI(6,3,3),QTRI(6,3,3),QQTRI(6,3,3),AA(18,18)
     &,QTXO(6,3,3),QQTXO(6,3,3),QTETO(6,3,3),QQTETO(6,3,3),CKMN(36,3,3)
     &,QTRO(6,3,3),QQTRO(6,3,3),KI,UO,CCOE(2,9,3,3),COE(2,9,3,3)
      INTEGER W,V,HH,N
      REAL*8 NU,NI,NO
      DIMENSION A(3,3),B(3,3),D(3,3),SE(3,3),SF(3,3),G(3,3),H(3,3),
     #SJ(3,3),SL(3,3),DEL(3,3)
      COMMON/DATA1/NI,NO,SKI,SKO,CIG(3),P(3),N
      COMMON/DATA2/EI,EO,ER,HR,URR
      COMMON/DATA3/ZI,ZO,USR,DSR
      COMMON/DATA5/PPI,PPO,PO(2),PL(2),RMS,DEN,DDI,DDO,VIS,CA,CB
      COMMON/CON1/A,B,D,DEL
      COMMON/COEF/CCOE
      COMMON/COCE/COE
      COMMON/CLLE/QQTXI,QQTETI,QQTRI,QQTXO,QQTETO,QQTRO
             JJ=1
               DO 331 K=1,3
               DO 331 M=1,3
          CKMN(1,K,M)=CCOE(JJ,1,K,M)+COE(JJ,1,K,M)
     &    +QQTXI(1,K,M)+KI**2*A(K,M)
          CKMN(2,K,M)=CCOE(JJ,4,K,M)+COE(JJ,4,K,M)+QQTXI(2,K,M)
          CKMN(3,K,M)=CCOE(JJ,7,K,M)+COE(JJ,7,K,M)+QQTXI(3,K,M)
C
          CKMN(7,K,M)=CCOE(JJ,2,K,M)+COE(JJ,2,K,M)+QQTETI(1,K,M)
          CKMN(8,K,M)=CCOE(JJ,5,K,M)+COE(JJ,5,K,M)+
     &    QQTETI(2,K,M)+KI**2*DEL(K,M)
          CKMN(9,K,M)=CCOE(JJ,8,K,M)+COE(JJ,8,K,M)+QQTETI(3,K,M)
C
          CKMN(13,K,M)=CCOE(JJ,3,K,M)+COE(JJ,3,K,M)+QQTRI(1,K,M)
          CKMN(14,K,M)=CCOE(JJ,6,K,M)+COE(JJ,6,K,M)+QQTRI(2,K,M)
          CKMN(15,K,M)=CCOE(JJ,9,K,M)+COE(JJ,9,K,M)+
     &    QQTRI(3,K,M)+KI**2*DEL(K,M)
 331       CONTINUE
C
          K=1
          IL=1
  175     NL=1
            JL=0
            DO 318 NS=1,3
             L=NL*NS
              DO 341 M=1,3
              AAA(IL,JL+M)=CKMN(L,K,M)
  341           CONTINUE
              JL=JL+3
  318          CONTINUE
           DO 313 NL=6,12,6
               IL=IL+1
           JL=0
           DO 314 NS=1,3
```

```
               L=NL+NS
             DO 311 M=1,3
              AAA(IL,JL+M)=CKMN(L,K,M)
 311            CONTINUE
              JL=JL+3
 314             CONTINUE
 313                CONTINUE
                   IF(K.EQ.3) GO TO 176
                    K=K+1
                    IL=IL+1
                   GO TO 175
 176   RETURN
       END
C************************************************************************
C      COMPLEX FUNCTION DET                                             *
C************************************************************************
       COMPLEX FUNCTION DET*16(A,L,M,N)
       DIMENSION A(N,N),L(N),M(N)
       COMPLEX*16 A,PIVOT,HOLD
       INTEGER END,ROW,COL,PIVROW,PIVCOL
       END=N-1
       DET=(1.D0,0.D0)
       DO 10 I=1,N
       L(I)=I
  10   M(I)=I
       DO 100 LMNT=1,END
       PIVOT=(0.D0,0.D0)
       DO 20 I=LMNT,N
       ROW=L(I)
       DO 20 J=LMNT,N
       COL=M(J)
       IF(CDABS(PIVOT).GE.CDABS(A(ROW,COL))) GO TO 20
       PIVROW=I
       PIVCOL=J
       PIVOT=A(ROW,COL)
  20   CONTINUE
       IF(PIVROW.EQ.LMNT) GO TO 22
       DET=-DET
       KEEP=L(PIVROW)
       L(PIVROW)=L(LMNT)
       L(LMNT)=KEEP
  22   IF(PIVCOL.EQ.LMNT) GO TO 26
       DET=-DET
       KEEP=M(PIVCOL)
       M(PIVCOL)=M(LMNT)
       M(LMNT)=KEEP
  26   DET=DET*PIVOT
       IF(CDABS(PIVOT).EQ.0.D0) GO TO 333
       JAUG=LMNT+1
       PIVROW=L(LMNT)
       PIVCOL=M(LMNT)
       DO 100 I=JAUG,N
       ROW=L(I)
       HOLD=A(ROW,PIVCOL)/PIVOT
       DO 100 J=JAUG,N
       COL=M(J)
 100   A(ROW,COL)=A(ROW,COL)-HOLD*A(PIVROW,COL)
       DET=DET*A(ROW,COL)
```

```
333 RETURN
    END
```

```
C***********************************************************************
C      COMPUTER PROGRAM FOR THE CASE OF UNSTEADY VISCOUS FORCES        *
C      USING FOURIER TRANSFORM METHOD                                  *
C                             PINNED-PINNED SHELL                      *
C***********************************************************************
C
C***********************************************************************
C      MAIN PROGRAM                                                    *
C***********************************************************************
       IMPLICIT REAL*8(A-H,O-Z)
        COMPLEX*16 QQTXI(6,3,3),QQTETI(6,3,3),QQTRI(6,3,3),QQTXO(6,3,
      #3),QQTETO(6,3,3),QQTRO(6,3,3),AAA(9,9),COEM(3,3,3),XY(3),
      #B(8),UNIT,FS,UO,MIL,COE(2,9,3,3),CCOE(2,9,3,3)
       INTEGER IJ,K,M,INFER(3),J,MS,N
         EXTERNAL FS
       REAL*8 NI,NO,WA(8),UI
       COMMON/DATA1/NI,NO,SKI,SKO,CIG(3),P(3),N
       COMMON/DATA2/EI,EO,ER,HR,URR
       COMMON/DATA3/ZI,ZO,USR,DSR
       COMMON/DATA7/UI,UO
       COMMON/AREA1/AAA
       COMMON/DATA5/PPI,PPO,PO(2),PL(2),RMS,DEN,DDI,DDO,VIS,CA,CB
       DATA EPS/1.D-10/,NSIG/5/,NGUESS/1/,ITMAX/12/,II/1/
       DATA IA/8/,IB/8/,NN/8/,IJOB/0/,IZ/36/
       COMMON/COCE/COE
       COMMON/COEF/CCOE
       COMMON/CLLE/QQTXI,QQTETI,QQTRI,QQTXO,QQTETO,QQTRO
       PI=3.141617D0
       P(1)=3.1416D0
       P(2)=6.2832D0
       P(3)=9.4248D0
C         ----------------------------
C             WATER STEEL
C ---------------------------------
       EI=1/11.D0
       EO=1/10.D0
       HR=1.0D0
       URR=1.0D0
       ER=EI/EO
       NI=0.3D0
       SKI=(5.5D-3)**2/12
       ZI=23.3D0
       DSR=1.D0
       USR=1.D0
       N=3
       DEN=998.0D0
C --------------------------------------------
          CALL CONT(CIG,P)
          CALL PREMAT(COEM)
       UI=0.02D0
       UO=(0.00D0,0.D0)
        MS=1
        NK=MS-1
       XY(1)=(.418D-5,-.135D-3)
C
        CALL ZANLYT(FS,EPS,NSIG,NK,NGUESS,II,XY,ITMAX,INFER,IER)
              CALL UNSFO(UI,UO,XY(1),MIL)
       CALL MATRA(UI,UO,XY(1),AAA)
```

```
CC
      PRINT 111,XY(MS)
 111  FORMAT('-','FREQUENCY AT A SPECIFIC VELOCITY TO STUDY THE
     & INSTABILITY=(',2D11.4,1X,')')
         PRINT 155,INFER(1)
 155         FORMAT('0','NO.OF ITERATIONS REQUIRED=',I3/)
             PRINT30
 30            FORMAT('1')
      PRINT10,UI,UO
  10  FORMAT('1','FLOW VELOCITY INSIDE THE INNER CYLINDER=',F8.5/'0','FL
     #OW VELOCITY IN THE ANNULAR REGION=',F8.5)
      STOP
      END
C**********************************************************************
C     SUBROUTINE CONT                                                  *
C**********************************************************************
      SUBROUTINE CONT(C,P)
      IMPLICIT REAL*8(A-H,O-Z)
      DIMENSION A(3,3),B(3,3),C(3),D(3,3),SE(3,3),SF(3,3),G(3,3),H(3,3),
     #SJ(3,3),SL(3,3),DEL(3,3),P(3)
      COMMON/CON1/A,B,D,DEL
      COMMON/CON2/SE,SF,G,H,SJ,SL
       PI=3.1416D0
      DO 3 K=1,3
      DO 3 M=1,3
      IF(K.EQ.M) GO TO 1
      A(K,M)=0.D0
      B(K,M)=0.D0
      D(K,M)=-A(K,M)
      GO TO 3
   1  A(K,K)=P(K)**2/2
      B(K,K)=-P(K)**4/2
      D(K,K)=-A(K,K)
      DEL(K,K)=.5D0
   3  CONTINUE
      RETURN
      END
C
C**********************************************************************
C     SUBROUTINE PREMAT                                                *
C**********************************************************************
      SUBROUTINE PREMAT(COEM)
      IMPLICIT REAL*8(A-H,O-Z)
      DIMENSION A(3,3),B(3,3),D(3,3),DEL(3,3)
      COMPLEX*16 COE(2,9,3,3),COEM(3,3,3)
      REAL*8 NI,NO,NU
      INTEGER R,Q,W,V,H,KK,IJ
      COMMON/DATA1/NI,NO,SKI,SKO,CIG(3),P(3),N
      COMMON/DATA2/EI,EO,ER,HR,URR
      COMMON/CON1/A,B,D,DEL
      COMMON/COCE/COE
      DO 3 K=1,3
      DO 3 M=1,3
      COEM(1,K,M)=A(K,M)
      COEM(2,K,M)=DEL(K,M)
   3  COEM(3,K,M)=DEL(K,M)
      J=0
      E=EI
```

```
      NU=NI
      SK=SKI
 12   JJ=J+1
      DO 4 K=1,3
      DO 4 M=1,3
      COE(JJ,1,K,M)=(E**2*B(K,M)+(NU-1)*(SK+1)*N**2*A(K,M)/2)
      COE(JJ,2,K,M)=-(1+NU)*N*E**2*D(K,M)/2
      COE(JJ,3,K,M)=(P(M)*E)**4*SK*DEL(K,M)-(2*NU-SK*(1-NU)*N**2)
     C*E**2*D(K,M)/2
      COE(JJ,4,K,M)=(1+NU)*N*A(K,M)/2
      COE(JJ,5,K,M)=-N**2*DEL(K,M)+(1+3*SK)*(1-NU)*E**2*D(K,M)/2
      COE(JJ,6,K,M)=SK*(3-NU)*N*E**2*D(K,M)/2-N*DEL(K,M)
      COE(JJ,7,K,M)=((NU+(NU-1)*SK*N**2/2)*A(K,M)-SK*E**2*B(K,M))
      COE(JJ,8,K,M)=-N*DEL(K,M)+(3-NU)*SK*N*E**2*D(K,M)/2
      COE(JJ,9,K,M)=-SK*(((P(M)*E)**4+(N**2-1)**2)*DEL(K,M)-2*(N*E)
     #**2*D(K,M))-DEL(K,M)
  4   CONTINUE
         DO 444 KK=1,9
          DO 444 K=1,3
          DO 444 M=1,3
               WRITE(6,445) COE(IJ,KK,K,M)
445             FORMAT('0',2(D11.4,1X))
444                CONTINUE
      RETURN
      END
C*********************************************************************
C     COMPLEX FUNCTION FS                                            *
C*********************************************************************
      COMPLEX FUNCTION FS*16(KI)
      IMPLICIT REAL*8(A-Z)
      COMPLEX*16 KI,RES,QB(3,3),AAA(9,9),DET,UO,MIL
      INTEGER L(9),M(9),K,J
      COMMON/DATA7/UI,UO
      COMMON/AREA1/AAA
         CALL UNSFO(UI,UO,KI,MIL)
        CALL MATRA(UI,UO,KI,AAA)
      FS=DET(AAA,L,M,9)
         PRINT 11,FS
 11   FORMAT('0','FS=',2(D11.4,1X))
         PRINT 116,KI
 116  FORMAT('0','KI=',2(D11.4,1X))
      RETURN
      END
C
C *****************************************************************
C     SUBROUTINE UNSFOR(QTETI)*
C******************************************************************
C    THIS PROGRAM IS TO CALCULATE THE UNSTEADY FORCES CAUSED BY*
C      THE PERTURBATIONS*
C******************************************************************
C
           SUBROUTINE UNSFO(UI,UO,KI,MIL)
           IMPLICIT COMPLEX*16(A-Z)
           COMPLEX*16  A(3,3),B(3,3),D(6,6),T(6,10),QTXI(6,3,3),ST(4,4)
         COMPLEX*16  QTETI(6,3,3),QTRI(6,3,3),QTXO(6,3,3),QTETO(6,3,3)
     &,QTRO(6,3,3),QQTETI(6,3,3),QQTRI(6,3,3),QQTXI(6,3,3),QTRI1(6,3,3),
     &QQTETO(6,3,3),QQTRO(6,3,3),QQTXO(6,3,3),QTXXI(6,3,3),QTRO1(6,3,3),
     &QTRRI(6,3,3),QTETTI(6,3,3),QTXXO(6,3,3),QTETTO(6,3,3),QTRRO(6,3,3)
```

```
      COMPLEX*16  C(6,6),E(6,6),AA(10,10),FTT(6,10),MIL
      REAL*8 EI,EO,X1,X2,CIG,P,PI,GAMA,UI,ZI,ZO,DSR,USR,HR,ER,URR
      REAL*8 WK(3),WF(6),NI,NO,SKI,SKO,SU,LEN,VIS
      INTEGER N,K,L,M,NN,MM,IB,IA,IJOB,IER,IL,IS,IM,NF,NM,J
      INTEGER LL,MS,NB,IC,K1,M2,M1,II,JJ,KK,IJ,LI,JK
      COMMON PI,GAMA
      COMMON/DATA1/NI,NO,SKI,SKO,CIG(3),P(3),N
      COMMON/DATA2/EI,EO,ER,HR,URR
      COMMON/DATA3/ZI,ZO,USR,DSR
      COMMON/CLLE/QQTXI,QQTETI,QQTRI,QQTXO,QQTETO,QQTRO
      INP(Y)=(IN(Y,N-1)+IN(Y,N+1))/2
      INF(Y)=(IN(Y,M-1)+IN(Y,M+1))/2
      INPP(Y)=(IN(Y,N-2)/2+IN(Y,N)+IN(Y,N+2)/2)/2
      INFF(Y)=(IN(Y,M-2)/2+IN(Y,M)+IN(Y,M+2)/2)/2
         GAMA=.5772156649011610D0
         PI=3.14159265358979D0
C ------------------------------------------
C           WATER-STEEL
C ------------------------------------------
       SU=5308.0D0
       LEN=1.0D0
       VIS=1.121D-06
C ---------------------------
       EPI=SU*LEN/VIS
       EPO=EPI
       UAVI=UI*.8D0
       UAVO=UO*.8D0
        RFE=1.D0
       RHE=1.D0
       RHOE=RHE/EPO
       M=N+1
       DT=2.D0
       X1=-20+DT/2*(1-DSQRT(1/3.D0))
       X2=-20+DT/2*(1+DSQRT(1/3.D0))
       DO 955 IJ=1,3
       DO 955 K=1,3
       DO 955 M2=1,3
           QTXXI(IJ,K,M2)=(0.D0,0.D0)
           QTRRI(IJ,K,M2)=(0.D0,0.D0)
           QTETTI(IJ,K,M2)=(0.D0,0.D0)
955          CONTINUE
          DO 737 LI=1,41
        S1=X1
       ALA=S1*EI
       ALB=S1*EO
       I=(0.D0,1.D0)
       MIL=CDSQRT(KI/EI*EPI*I+X1**2)
       MEI=EI*MIL
       M=N+1
C ------------------------------------------------
C            INTERNAL FLOW R=A
C ------------------------------------------------
       INIA=IN(ALA,N)
       INPIA=INP(ALA)
       INPPIA=INPP(ALA)
       BRI1=IN(MEI,M)
       BXI1=IN(MEI,N)
       BXPI1=INP(MEI)
```

```
      BRPI1=INF(MEI)
      BXPPI1=INPP(MEI)
      BRPPI1=INFF(MEI)
C ---------------------------------------------------------------
 9     PRINT11,MEI,MEA,MEO
 11    FORMAT('0','MEI=(',2D11.4,1X,')',2X,'MEA=(',2D11.4,1X,')'
     & ,2X,'MEO=(',2D11.4,1X,')')
      PRINT12,INIA,INPIA
 12   FORMAT('0','INIA=(',2D11.4,1X,')',2X,'INPIA=(',2D11.4,1X,')')
      PRINT13,BRI1
 13   FORMAT('0','BRI1=(',2D11.4,1X,')')
      PRINT14,BXI1
 14   FORMAT('0','BXI1=(',2D11.4,1X,')')
C ---------------------------------------------------------
C   INVERSION OF MATRIX A
C ---------------------------------------------------------------
 195   A(1,1)=-I*X1*EI*INIA
       A(1,2)=(0.D0,0.D0)
       A(1,3)=-(MEI*BRPI1+(N+1)*BRI1)
       A(2,1)=-N*INIA
       A(2,2)=(-MEI*BXPI1)
       A(2,3)=-X1*EI*I*BRI1
       A(3,1)=ALA*INPIA
       A(3,2)=(N*BXI1)
       A(3,3)=-I*X1*EI*BRI1
C -----------------------------------------------------------
        WRITE(6,82) AKJ
 82     FORMAT('0','AKJ')
        DO 34 K=1,3
        WRITE(6,71) (A(K,J),J=1,3)
 71     FORMAT('0',6(D11.4,1X))
 34     CONTINUE

C -----------------------------------------------------------------------
         DD=A(2,2)*(A(3,3)*A(1,1)-A(3,1)*A(1,3))-A(3,2)*(A(1,1)*
     &   A(2,3)-A(1,3)*A(2,1))
         B(3,1)=(A(3,2)*A(2,1)-A(3,1)*A(2,2))/DD
         B(3,2)=-A(3,2)*A(1,1)/DD
         B(3,3)=A(2,2)*A(1,1)/DD
         SS=A(1,1)*A(2,3)-A(1,3)*A(2,1)
         B(2,1)=-(A(2,1)+SS*B(3,1))/A(1,1)/A(2,2)
         B(2,2)=(A(1,1)-SS*B(3,2))/A(1,1)/A(2,2)
         B(2,3)=-SS*B(3,3)/A(1,1)/A(2,2)
         B(1,1)=(1-A(1,3)*B(3,1))/A(1,1)
         B(1,2)=-A(1,3)*B(3,2)/A(1,1)
         B(1,3)=-A(1,3)*B(3,3)/A(1,1)
         WRITE(6,53) BKJ
 53      FORMAT('0','BKJ')
        DO 44 K=1,3
        WRITE(6,99) (B(K,J),J=1,3)
 99      FORMAT('0',6(D11.4,1X))
 44       CONTINUE
              DO 61 II=1,3
              DO 61 KK=1,3
             ST(II,KK)=(0.D0,0.D0)
               DO 61 JJ=1,3
          ST(II,KK)=ST(II,KK)+A(II,JJ)*B(JJ,KK)
 61           CONTINUE
```

```
            WRITE(6,501) STKJ
 501        FORMAT('0','STKJ')
      DO 516 K=1,3
            WRITE(6,517) (ST(K,J),J=1,3)
 517  FORMAT('0',6(D11.4,1X))
 516        CONTINUE
C -----------------------------------------------------------------------
         IF(N.EQ.3) GO TO 36
         TI2=INIA
         TI4=-BX11/MEI
         TI6=-BXI1+2*TI4
          GO TO 136
 36       TI2=INIA
          BX11=IN(MEI,1)
          BX21=IN(MEI,2)
          TI4=BX21/MEI-BX11/MEI**2
          TI6=BXI1-3*TI4
 136            T(1,1)=-(-2*I*X1*S1*INPIA)/EPI
               T(1,2)=-(-I*N*X1*BXI1)/EPI/EI
 T(1,3)=-((1/EI**2-X1**2+N/EI**2)*BRI1-MIL*(1+N)*BRPI1/EI-MIL**2*
     &         BRPPI1)/EPI
               T(1,4)=(0.D0,0.D0)
                T(2,1)=-(2*N*INIA/EI**2-2*N*S1*INPIA/EI)/EPI
   T(2,2)=-(MIL/EI*BXPI1-N**2/EI**2*BXI1-MIL**2*BXPPI1)/EPI
      T(2,3)=-((1+N)*I*X1/EI*BRI1-I*X1*MIL*BRPI1)/EPI
                 T(2,4)=(0.D0,0.D0)
 T(3,1)=-((I*KI/EI*INIA+UI*(-I*X1)*TI2)+2*S1**2*INPPIA/EPI)
    T(3,2)=-((-I*X1*N*UI*TI4)+2*(MIL*N*BXPI1/EI-N*BXI1/EI**2)/EPI)
   T(3,3)=-((-X1**2*UI*TI6)/MIL+2*(-I*X1*MIL)/EPI*BRPI1)
                 T(3,4)=(0.D0,0.D0)
                  WRITE(6,69) TKJ
 69             FORMAT('0','TKJ')
                   DO 254 K=1,3
                   WRITE(6,255) (T(K,J),J=1,4)
 255           FORMAT('0',8(D11.4,1X))
 254         CONTINUE
             DO 223 K=1,3
               DO 224 J=1,3
                  AA(K,J)=B(K,J)
 224        CONTINUE
 223        CONTINUE
            DO 213 K=1,3
               AA(K,4)=(0.D0,0.D0)
 213           CONTINUE
               DO 312 J=1,3
              AA(4,J)=(0.D0,0.D0)
 312           CONTINUE
                AA(4,4)=(0.D0,0.D0)
C               AA(4,4)=1/(X1*KNPIA)
                  DO 90 II=1,3
                  DO 90 KK=1,4
                 FTT(II,KK)=(0.D0,0.D0)
                   DO 90 JJ=1,4
              FTT(II,KK)=FTT(II,KK)+T(II,JJ)*AA(JJ,KK)
 90               CONTINUE
             WRITE(6,601) FTTKJ
 601         FORMAT('0','FTTKJ')
       DO 716 K=1,3
```

```
                 WRITE(6,717) (FTT(K,J),J=1,4)
 717         FORMAT('0',6(D11.4,1X))
 716             CONTINUE
C
                  DO 797 K1=1,3
                 DO 797 M2=1,3
                    F1=CDEXP(-I*X1)
                    F2=CDEXP(I*X1)
                HKM=(F1*(-1)**K1-1)*(F2*(-1)**M2-1)*M2*K1*PI**2/(-X1**2+
     &   M2**2*PI**2)/(-X1**2+K1**2*PI**2)
                 GKM=I*X1*HKM
C
C*********     AERODYNAMIC FORCES   *************
                UAVI=UI
                RP1=(X1*KI/EI-X1**2*UAVI)*EI**2
                RP2=I*(KI/EI-X1*UAVI)*EI
C
               QTXI(1,K1,M2)=FTT(1,1)*RP1*GKM
               QTXI(2,K1,M2)=FTT(1,2)*RP2*GKM
               QTXI(3,K1,M2)=(FTT(1,3)+FTT(1,4))*RP2*GKM
C
               QTETI(1,K1,M2)=FTT(2,1)*RP1*HKM
               QTETI(2,K1,M2)=FTT(2,2)*RP2*HKM
               QTETI(3,K1,M2)=(FTT(2,3)+FTT(2,4))*RP2*HKM
C
               QTRI(1,K1,M2)=FTT(3,1)*RP1*HKM
               QTRI(2,K1,M2)=FTT(3,2)*RP2*HKM
               QTRI(3,K1,M2)=(FTT(3,3)+FTT(3,4))*RP2*HKM
C
C
                DO 966 IJ=1,3
                    QTXXI(IJ,K1,M2)=QTXXI(IJ,K1,M2)+QTXI(IJ,K1,M2)
                    QTRRI(IJ,K1,M2)=QTRRI(IJ,K1,M2)+QTRI(IJ,K1,M2)
                    QTETTI(IJ,K1,M2)=QTETTI(IJ,K1,M2)+QTETI(IJ,K1,M2)
 966                CONTINUE
 797                 CONTINUE
                    X1=X1+DT
                       IF(LI.EQ.21) X1=X2
 737               CONTINUE
           DO 301 IJ=1,3
           DO 301 K=1,3
           DO 301 M=1,3
              QQTXI(IJ,K,M)=ZI*QTXXI(IJ,K,M)/2/PI
 301          CONTINUE
           DO 305 IJ=1,3
           DO 305 K=1,3
           DO 305 M=1,3
               QQTETI(IJ,K,M)=ZI*EI*QTETTI(IJ,K,M)/2/PI
               QQTRI(IJ,K,M)=ZI*EI*QTRRI(IJ,K,M)/2/PI
 305            CONTINUE
 299               RETURN
                   END
C***********************************************************************
C     SUBPROGRAMS FOR CALCULATING THE BESSEL FUNCTIONS                 *
C***********************************************************************
      COMPLEX FUNCTION IN*16(X,N)
      IMPLICIT REAL*8(A-Z)
      COMPLEX*16 X,T,T1,T2,T3,T4,I,T5,XXX
```

```
      INTEGER K,N,M
      COMMON PI,GAMA
      I=(0.D0,1.D0)
      IF(CDABS(X).GE.15.D0) GO TO 10
      IN=(0.D0,0.D0)
      K=0
 11   T=(X/2)**(2*K)/FA(K)/FA(N+K)
      IF(CDABS(T).LT.1.D-12) GO TO 12
      IN=IN+T
      K=K+1
      GO TO 11
 12   IN=(X/2)**N*IN
      GO TO 36
 10   T2=(1.0D0/2.0D0/PI/X)
      T3=CDSQRT(T2)
        TEI1=X
         T5=-I*X
        TEI2=T5
        T1=(4*N**2-1)/(8*X)
        XXX=I*(TEI2+N+1/2)*PI
         IF(TEI1.GT.0.D0) GO TO 115
          XXX=I*(TEI2+N+1/2)*PI
         IN=T3*(1.0D0-T1)*CDEXP(XXX)
          GO TO 36
115      IN=T3*(1+T1)*CDEXP(I*TEI2)
 36   RETURN
      END
C
      DOUBLE PRECISION FUNCTION R(K)
      IMPLICIT REAL*8(A-Z)
      INTEGER K,I
      R=0.D0
      DO 40 I=1,K
 40   R=R+1.D0/I
      RETURN
      END
C
      DOUBLE PRECISION FUNCTION F(K)
      IMPLICIT REAL*8(A-Z)
      INTEGER K
      COMMON PI,GAMA
      IF(K.EQ.1) GO TO 50
      F=R(K-1)-GAMA
      RETURN
 50   F=-GAMA
      RETURN
      END
C
      DOUBLE PRECISION FUNCTION FA(K)
       IMPLICIT REAL*8(A-Z)
      INTEGER K,L
      FA=1.D0
      L=1
 21   FA=FA*L
      IF(L.GE.K) GO TO 22
      L=L+1
      GO TO 21
 22   CONTINUE
```

```
      RETURN
      END
C*********************************************************************
C*********************************************************************
C*     MATRIX AAA**
C*
C*********************************************************************
C  THIS PART IS USED TO ASSEMBLE MATRIX AAA WHICH CONTAINS THE*
C  FREE VIBRATIONS TERMS COE,THE STEADY FORCES CCOE,AND THE UNSTEADY*
C  FORCES QTXI,...*
C**********************************************************************
      SUBROUTINE MATRA(UI,UO,KI,AAA)
      IMPLICIT REAL*8(A-H,O-Z)
      COMPLEX*16 AAA(9,9),CK(2,3,3),QTXI(6,3,3),QQTXI(6,3,3),
     $QTETI(6,3,3),QQTETI(6,3,3),QTRI(6,3,3),QQTRI(6,3,3),AA(18,18)
     &,QTXO(6,3,3),QQTXO(6,3,3),QTETO(6,3,3),QQTETO(6,3,3),CKMN(36,3,3)
     &,QTRO(6,3,3),QQTRO(6,3,3),KI,UO,CCOE(2,9,3,3),COE(2,9,3,3)
      INTEGER W,V,HH,N
      REAL*8 NU,NI,NO
      DIMENSION A(3,3),B(3,3),D(3,3),SE(3,3),SF(3,3),G(3,3),H(3,3),
     #SJ(3,3),SL(3,3),DEL(3,3)
      COMMON/DATA1/NI,NO,SKI,SKO,CIG(3),P(3),N
      COMMON/DATA2/EI,EO,ER,HR,URR
      COMMON/DATA3/ZI,ZO,USR,DSR
      COMMON/DATA5/PPI,PPO,PO(2),PL(2),RMS,DEN,DDI,DDO,VIS,CA,CB
      COMMON/CON1/A,B,D,DEL
      COMMON/COEF/CCOE
      COMMON/COCE/COE
      COMMON/CLLE/QQTXI,QQTETI,QQTRI,QQTXO,QQTETO,QQTRO
             JJ=1
               DO 331 K=1,3
               DO 331 M=1,3
          CKMN(1,K,M)=CCOE(JJ,1,K,M)+COE(JJ,1,K,M)
     &    +QQTXI(1,K,M)+KI**2*A(K,M)
          CKMN(2,K,M)=CCOE(JJ,4,K,M)+COE(JJ,4,K,M)+QQTXI(2,K,M)
          CKMN(3,K,M)=CCOE(JJ,7,K,M)+COE(JJ,7,K,M)+QQTXI(3,K,M)
C
          CKMN(7,K,M)=CCOE(JJ,2,K,M)+COE(JJ,2,K,M)+QQTETI(1,K,M)
          CKMN(8,K,M)=CCOE(JJ,5,K,M)+COE(JJ,5,K,M)+
     &    QQTETI(2,K,M)+KI**2*DEL(K,M)
          CKMN(9,K,M)=CCOE(JJ,8,K,M)+COE(JJ,8,K,M)+QQTETI(3,K,M)
C
          CKMN(13,K,M)=CCOE(JJ,3,K,M)+COE(JJ,3,K,M)+QQTRI(1,K,M)
          CKMN(14,K,M)=CCOE(JJ,6,K,M)+COE(JJ,6,K,M)+QQTRI(2,K,M)
          CKMN(15,K,M)=CCOE(JJ,9,K,M)+COE(JJ,9,K,M)+
     &    QQTRI(3,K,M)+KI**2*DEL(K,M)
 331       CONTINUE
C
          K=1
          IL=1
 175      NL=1
            JL=0
            DO 318 NS=1,3
             L=NL*NS
              DO 341 M=1,3
              AAA(IL,JL+M)=CKMN(L,K,M)
 341            CONTINUE
              JL=JL+3
```

```
 318          CONTINUE
        DO 313 NL=6,12,6
           IL=IL+1
        JL=0
        DO 314 NS=1,3
          L=NL+NS
        DO 311 M=1,3
         AAA(IL,JL+M)=CKMN(L,K,M)
 311       CONTINUE
         JL=JL+3
 314        CONTINUE
 313           CONTINUE
              IF(K.EQ.3) GO TO 176
               K=K+1
               IL=IL+1
              GO TO 175
 176  RETURN
      END
C***********************************************************************
C     COMPLEX FUNCTION DET                                             *
C***********************************************************************
      COMPLEX FUNCTION DET*16(A,L,M,N)
      DIMENSION A(N,N),L(N),M(N)
      COMPLEX*16 A,PIVOT,HOLD
      INTEGER END,ROW,COL,PIVROW,PIVCOL
      END=N-1
      DET=(1.D0,0.D0)
      DO 10 I=1,N
      L(I)=I
 10   M(I)=I
      DO 100 LMNT=1,END
      PIVOT=(0.D0,0.D0)
      DO 20 I=LMNT,N
      ROW=L(I)
      DO 20 J=LMNT,N
      COL=M(J)
      IF(CDABS(PIVOT).GE.CDABS(A(ROW,COL))) GO TO 20
      PIVROW=I
      PIVCOL=J
      PIVOT=A(ROW,COL)
 20   CONTINUE
      IF(PIVROW.EQ.LMNT) GO TO 22
      DET=-DET
      KEEP=L(PIVROW)
      L(PIVROW)=L(LMNT)
      L(LMNT)=KEEP
 22   IF(PIVCOL.EQ.LMNT) GO TO 26
      DET=-DET
      KEEP=M(PIVCOL)
      M(PIVCOL)=M(LMNT)
      M(LMNT)=KEEP
 26   DET=DET*PIVOT
      IF(CDABS(PIVOT).EQ.0.D0) GO TO 333
      JAUG=LMNT+1
      PIVROW=L(LMNT)
      PIVCOL=M(LMNT)
      DO 100 I=JAUG,N
      ROW=L(I)
```

```
      HOLD=A(ROW,PIVCOL)/PIVOT
      DO 100 J=JAUG,N
      COL=M(J)
  100 A(ROW,COL)=A(ROW,COL)-HOLD*A(PIVROW,COL)
      DET=DET*A(ROW,COL)
  333 RETURN
      END
```